UNIVERSITÉ DE STRASBOURG

UNIVERSITÉ DE STRASBOURG

EDSC
École Doctorale des
Sciences Chimiques

ÉCOLE DOCTORALE DES SCIENCES CHIMIQUES ED222
Institut Charles Sadron

THÈSE présentée par :

Sansanee SRICHAN

soutenue le : **04 février 2015**

pour obtenir le grade de : **Docteur de l'université de Strasbourg**

Spécialité : Chimie des Polymères

Synthesis of sequence-controlled polymers by copolymerization of *para*-substituted styrenic derivatives and *N*-substituted maleimides

THÈSE dirigée par :
M. Jean-François LUTZ   Directeur de Recherche CNRS, ICS, Strasbourg

RAPPORTEURS :
M. Julien NICOLAS   Chargé de Recherche CNRS, Institut Galien Paris-Sud, Paris
M. Franck D´AGOSTO   Directeur de Recherche CNRS, C2P2, Lyon

EXAMINATEURS :
Mme Jannick DUCHET-RUMEAU   Professeur, INSA, Lyon
M. Olivier FELIX   Chargé de Recherche CNRS, ICS, Strasbourg
M. Vincent ROUCOULES   Professeur, IS2M, Mulhouse

To my parents

REMERCIEMENTS

sentir pas trop dangereux de travailler dans cet endroit. Je peux dire que jusqu'à présent le labo CMP est le meilleur du labo dans lequel j'ai travaillé. Merci aussi pour vos conseils techniques dans le labo que je penserai adapter dans ma future carrière.

Plusieurs personnes ont également participé à cette thèse, je remercie Mélanie, Catherine, Odile et Julie, les personnes de SEC sans eux mes polymères n'ont pas pu charteriser. Je remercie ainsi Cathy pour l'analyse de DSC. Je remercie par la suite Bernard Lotz pour les études de TEM de l'un de mes polymères, merci pour vos explications lesquelles vous avez faites avec gentillesse et jamais agacé quand je n'ai pas compris des choses.

Pendant les trois années de thèse bien sûr je n'ai pas fait que travailler, pas mal du temps j'ai utilisé pour profiter la vie. Je remercie à tout le monde de l'ICS que je ne peux pas tous nommer ici pour le bon accueil, pour des belles rencontres hors des heures du travail.

Ce paragraphe, je voudrais remercier toutes les personnes formidables que j'ai rencontrées lors d'un séjour en France. Je commence par ma grand sœur, Mirela Zamfir, ma première encadrant laquelle me fait rentrer dans le monde de polymère, je ne l'ai pas classé dans la catégorie de professionnelle car elle est plus que ça, merci pour notre amitié que tu gardes jusqu'à aujourd'hui. Merci Hatice Mutlu, I can say that you are also like my « family », thanks for all of your helps, your precious advice, thanks for the travel, all discussions that we have together. Sometime I recieved the direct comment from you but I know well that it comes from your heart and you know it helps me a lot. La suite, Madame anushka « ma chère Anna » tu es une amie magnifique, quand j'ai besoin de relaxer je viens vers toi et ça marche! Merci d'ouvrir tout le temps la porte de ta maison pour m'accueillir et de me ramener à la maison même après trois heures du matin bien sûr je parle aussi de Romain. Ma jumelle, Tam, je ne sais pas combien de conversation qu'on a fait par jour, je peux discuter avec toi de tous les sujets commence par la vie quotidien jusqu'à la miss universe et ça va continuerai comme ça ma chère. Merci pour la correction de faute française que j'ai fait chaque fois, je te promets que je ne vais pas oublier je t'avais dit que j'ai ramené le grand dictionnaire avec moi tu me diras après un an si ça aide ou pas. Je remercie toi aussi Maxime, le deuxième français à qui je permets de me conduire à la maison. J'espèrerai vous conduire aussi jusqu'à la porte de chez moi en Thaïlande. Ma Olinga, tout au début ton accent anglais m'as posé de problème mais maintenant on peut sortir, discuter, parler, rigoler y a aucun soucis. J'espère que la

Thaïlande sera un des pays dans ton plan d'aventure et on se retrouvera un jour. Aziz, mon frère en France, j'ai appris plein chose de toi pendant le déjeuner, le café et des fois dans le bus. Comme tu es une bonne personne généreuse je te souhaite une bonne chance pour ta future professionnelle, attention je te suivrai. Raj, I want to thank also for your help. Don't forget Gargnano, the place that we have the very nice memory together with Sarmistha and hope to see you in Japan. Je n'ai pas encore fini! Merci Dalila qui est maintenant devenue une grande conférencière et ma belle Meryem, tu es une fille drôle, tu m'as toujours fait rire, je penserai à ça quand je serai de mauvaise humeur. Merci également à Nathalie pour le partage de produit quelque fois, Chloé une collègue sympa dans mon bureau, ainsi tous les amis qui ont passé le temps à la cantine avec moi. Enfin je ne peux pas tous lister les noms de personne que je voudrais remercier.

Quand on vit dans un endroit étrange, on connait personne c'est vraiment difficile d'avoir le courage, mais moi non je ne suis pas dans ce cas. Merci ma petite famille thaïlandaise en France pour tous les aides, P'tom, P'yim, P'pim, P'nan, P'oum, P'imm et P'paul. Merci P'pek, Peaw, N'tum, N'taddy et Tul, de tous les temps m'écouter quand j'ai eu des problèmes ou même quand je suis trop stressée pendant la rédaction grâce à eux je suis passée. Merci énormément à Sae, mon meilleur ami, tu m'as vraiment beaucoup aidé, merci beaucoup de m'encourager. Je peux dire que sans toi c'est difficile, voilà merci pour tous.

Enfin, je voudrais remercier mille fois mes amis et ma famille en Thaïlande pour tous les supports. Ça fait longtemps que j'ai quitté mes parents mais ils sont toujours à côte, ils sont toujours me supporter, me donner le courage, ils font tous pour que sa fille soit réussir. Le décalage du 6h n'est pas le souci pour nous. Je donne ce diplôme de doctorat sans doute à mes super parents et maintenant ils sont super contente que je vais rentrer à la maison voilà c'est le temps de récompenser avec eux.

Avant de terminer, je n'oublie sûrement pas de remercier moi-même d'être forte et merci de ramener toi-même dans la bonne direction depuis début jusqu'à la fin de ton parcours.

Fair
No pressure, no diamonds
Thomas Carlyle

TABLE OF CONTENTS

PUBLICATIONS

- ✓ <u>Sansanee Srichan</u>, Laurence Oswald, Mirela Zamfir, and Jean-François Lutz, **Precision polyelectrolytes**, *Chem. Commun.*, **2012**, 48, 1517-1519.

- ✓ <u>Sansanee Srichan</u>, Delphine Chan-Seng, and Jean-François Lutz, **Influence of Strong Electron-Donor Monomers in Sequence-Controlled Polymerization**, *ACS macro Lett.*, **2012**, 1, 589-592.

- ✓ <u>Sansanee Srichan</u>, Hatice Mutlu, and Jean-François Lutz, **On the synthesis of sequence-controlled poly(vinyl benzyl amine-*co*-*N*-substituted maleimides) copolymers**, *Eur. Polym. J.*, available online, DOI: 10.1016/j.eurpolymj.2014.09.002

- ✓ <u>Sansanee Srichan</u>, Hatice Mutlu, Nezha Badi, and Jean-François Lutz, **Precision PEGylated Polymers Obtained by Sequence-controlled Copolymerization and Postpolymerization Modification**, *Angew. Chem. Int. Ed.*, **2014**, 53, 9231-9235.

- ✓ <u>Sansanee Srichan</u>, Navaphun Kayunkid, Laurence Oswald, Bernard Lotz, and Jean-François Lutz, **Synthesis and Characterization of Sequence-controlled Semicrystalline Comb Copolymers : Influence of Primary Structure on Materials Properties**, *Macromolecules*, **2014**, 47, 1570-1577.

- ✓ Nathalie Baradel, Olga Shishkan, <u>Sansanee Srichan,</u> and Jean-François Lutz, **Synthesis of sequence-controlled copolymers using time-regulated additions of *N*-substituted maleimides in styrenic radical polymerizations**, ACS Symposium Series; American Chemical Society: Washington, DC, **2014**. Chapter 8, pp 119-131.

ABBREVIATIONS

AA	acrylic acid
AM	acrylamide
AN	acrylonitrile
ARGET ATRP	activator regenerated by electron-transfer for atom transfer radical polymerization
ATA	atropic acid
ATRP	atom-transfer radical polymerization
tBA	*tert*-butylacrylate
dNBipy	4,4′-di(5-nonyl)-2,2′-bipyridine
Boc	*tert*-butyloxycarbonyl
BzMI	*N*-benzyl maleimide
BPO	benzoyl peroxide
BTA	benzene-1,3,5-tricarboxamide
t-BuVBA	*tert*-butyl vinylbenzoate
CH_2Cl_2	dichloromethane
$CHCl_3$	chloroform
Con A	concanavalin A
CPMI	*N*-(4-carboxyphenyl)maleimide
CRC	cysteine-arginine-cysteine
CRP	controlled radical polymerization
CuAAC	copper-catalyzed azide-alkyne cycloaddition
CuBr	copper (I) bromide
DTBN	di-*tert*-butyl nitroxide
DBU	1,8-diazabicyclo [5.4.0] undec-7-ene
DCP	dicumyl peroxide
DEF	diethylfumarate
DMF	dimethylformamide
DMSO	dimethylsulfoxide
DNA	deoxyribonucleic acid
DPS	diphenylphosphinostyrene
DSC	differential scanning calorimetry

EASC	ethylaluminium sesquichloride
Et_2AlCl	diethylaluminiumchloride
Fe_3O_4	iron (II, III) oxide
Fmoc	fluorenylmethyloxycarbonyl chloride
FN	fumaronitrile
FT-IR	Fourier transform infrared spectroscopy
HEMI	*N*-(2-hydroxyethyl)maleimide
HPMI	*N*-(4-hydroxyphenyl)maleimide
K_2CO_3	potassium carbonate
KPS	potassium persulfate
MAA	methacrylic acid
MAc	maleic acid
MAh	maleic anhydride
MALDI-TOF	matrix-assisted laser desorption/ionization mass spectroscopy
MBA	*N*,*N*´-methylenebisacrylamide
MBP	methyl 2-bromopropinate
MeCN	acetonitrile
MIs	*N*-substituted maleimides
MMA	methyl methacrylate
MMI	*N*-methylol maleimide
NMR	nuclear magnetic resonance
NMP	nitroxide-mediated polymerization
MeOH	methanol
NSGs	*N*-substituted glycine
NVC	*N*-vinylcarbazole
OEG	oligo(ethylene glycol)
PCF	pair correlation function
PCR	polymerase chain reaction
PEG	poly(ethylene glycol)
PFP-MI	pentafluorophenyl maleimides
PHS	poly(4-hydroxystyrene)
PLGA	poly(lactid acid-co-gycolic acid)
PrMI	*N*-propyl maleimide

PNA	peanut agglutinin
Poly(NMEP-*co*-FPHPMA)	poly(*N*-(2-methacryloxyethyl)pyrrolidone-*co*-1,3-(4-formylphenoxy)-2-hydroxy propylmethacrylate)
Poly(VP-*co*-HEMA)	poly(*N*-vinyl-z-pyrrolidone-*co*-2-hydroxyethylmethacrylate)
PSt	polystyrene
PVBAm	poly(vinyl benzyl amine)
QCM-D	quartz microbalance with dissipation monitoring
RAFT	reversible addition fragmentation chain transfer
R_g	radius of gyration
RNA	ribonucleic acid
SASA	solvent-accessible surface area
$SnCl_4$	tin (IV) chloride
SCPs	sequence-controlled polymers
SCPN	single chain polymeric nanoparticle
SEC	size exclusion chromatography
SET-LRP	single-electron transfer living radical polymerization
SFRP	stable free radical polymerization
SG1	*N*-tert-butyl-*N*-(1-diethylphosphono-2,2-dimethylpropyl)
SPPS	solid-phase peptide synthesis
St	styrene
T_m	melting temperature
T_c	crystallization temperature
TBAF	tetra-*n*-butylammonium fluoride
TEM	transmission electron microscopy
TEMPO	2,2,6,6-tetramethyl-1-piperidinyl-*N*-oxy
TEMPO-TMS	trans-2,6-diethyl-2,6-bis(1-trimethylsilanoxyethyl)-1-(1-phenylethoxy)piperidine-N-oxyl)
TES-MI	triethylsilyl protected *N*-propagylmaleimide
TFA	trifluoroacetic acid
TFMPMI	*N*-[3,5-bis(trifluoromethyl)phenyl]maleimide
THF	tetrahydrofuran
TIPS-MI	triisopropylsilyl protected *N*-propagylmaleimide
TMS-MI	trimethylsilyl protected *N*-propargylmaleimide

UPy	2-ureidopyrimidinine
VBP	N-(p-vinyl benzyl)phthalimide
VCZ	N-vinylcarbazole
WGA	wheat germ agglutinin
ZnCl$_2$	zinc chloride

LIST OF FIGURES

LIST OF TABLES

LIST OF SCHEMES

General Introduction

INTRODUCTION GENERALE

En raison du besoin constant de nouveaux matériaux de plus en plus élaborés, la production de macromolécules synthétiques ayant des propriétés et des microstructures bien contrôlées est devenue en quelques années un sujet crucial. Malgré les différents paramètres pouvant être ajustés par les chimistes des polymères, le contrôle de la structure et en particulier le contrôle des séquences de (co)monomères a été pendant longtemps sous-estimé. Des polymères présentant un très haut niveau de contrôle des séquences de monomères se trouvent dans la nature, c'est notamment le cas des protéines ou de l'ADN [1,2]. Par exemple, le simple fait de relier entre eux les vingt acides aminés naturels par des liaisons amides, conduit à un arrangement de séquences de protéine qui permet d'accéder à des structures plus complexes responsables des propriétés de la matière vivante. Les propriétés physiques et chimiques des macromolécules dépendent de la séquence d'unités monomère le long de la chaîne de polymère. Par conséquent, la régulation de ces séquences de monomères est devenue un sujet de première importance en science des matériaux [3]. En particulier, la capacité de reproduire un certain niveau de contrôle par des polymères synthétiques est devenue un défi d'un grand intérêt au cours des dernières années.
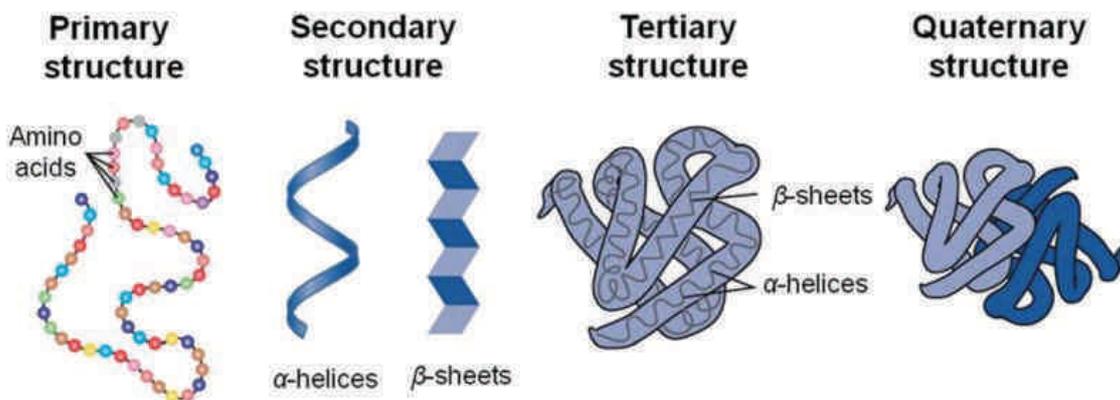
Figure 1. Influence des séquences de comonomères sur la structure des protéines. Réimprimé avec la permission de référence [4].

Au cours des dernières décennies, plusieurs approches ont été proposées afin de préparer des macromolécules synthétiques à séquences contrôlées. Par exemple, la structure primaire des macromolécules peut être régulée en utilisant les voies de synthèse biologiques telles que la réaction en chaînes par polymérase (PCR), des techniques d'ingénierie de

protéines [5,6], ou soit par des procédés chimiques [7,8]. Ces derniers offrent certains avantages par rapport aux procédés biologiques en raison de la disponibilité d'un grand nombre de blocs de construction. Au cours des dernières années, plusieurs méthodes chimiques ont été suggérées pour la préparation de macromolécules avec des architectures et des compositions contrôlées. Par exemple, l'approche itérative dans laquelle les monomères s'attachent à un support-solide un par un. Cependant, cette procédure est longue et une purification est nécessaire à chaque étape. Par conséquent, il est préférable d'utiliser une procédure plus simple afin d'élaborer des matériaux à séquences contrôlées. La polymérisation radicalaire est une autre méthode permettant la production de polymères synthétiques parce qu'elle est connue pour sa mise en œuvre facile. En particulier, les polymérisations radicalaires contrôlées (CRPs), telles que la polymérisation radicalaire contrôlée par les nitroxydes (NMP) [9-11], la polymérisation radicalaire contrôlée par transfert d'atomes (ATRP) [12-14] et la polymérisation radicalaire contrôlée par transfert de chaine réversible par addition-fragmentation (RAFT) [15] ont été introduites il y a une vingtaine d'années. Ces méthodes permettent de contrôler précisément l'architecture de polymères synthétiques (copolymères à blocs, polymères greffés ou copolymères branchés). Toutefois, la microstructure obtenue par cette procédure est mal contrôlée. En effet, les polymères obtenus par CRP sont en générales atactiques et possèdent dans la plupart des cas des séquences statistiques.

Néanmoins, dans certains cas particuliers, des séquences de comonomère peuvent être régulées par copolymérisation radicalaire. Par exemple, la polarité des doubles liaisons de monomères est un facteur important. En effet, lorsque le styrène est copolymérisé avec l'anhydride maléique dans des conditions stoichiométriques, des copolymères alternés sont obtenus [16]. Ce comportement peut être expliqué par le fait que les valeurs du facteur de polarité (e) de ces deux monomères sont très différentes [17]. Donc, quand ces deux monomères réagissent l'un sur l'autre, la propagation croisée est favorisée par rapport à l'homopolymérisation. Plusieurs études décrivant la préparation de polymères alternés en utilisant la copolymérisation de monomères donneur et accepteur, en quantité stœchiométrique, ont été publiées ces dernières années [18,19]. Cependant, la copolymérisation d'une quantité non-stœchiométrique de monomères a récemment gagner de intérêt parce qu'elle permet de préparer des polymères à séquences contrôlées possédants des microstructures inédites. Par exemple, notre groupe a décrit une nouvelle approche permettant

de préparer des polymères à séquences contrôlées en utilisant le contrôle des temps d'addition d'une petite quantité de maléimides *N*-substitués (MIs) au cours de la polymérisation d'un grand excès de styrène [20]. Cette méthode permet de placer un monomère accepteur à des positions précises dans la chaine de polystyrène (**Figure 2**). Dans ce concept, les MIs ont été utilisés comme monomères accepteurs d'électrons à la place de l'anhydride maléique parce qu'ils présentent une large gamme de fonctionnalité sur la position *N*. L'utilisation de cette stratégie simple permet de préparer des polymères à séquences contrôlées intéressants tels que des polymères hydrosolubles [21], des polymères aux propriétés similaires à des biopuces [22] ou des polymères ayant des conformations compactes bien définies [23-25].
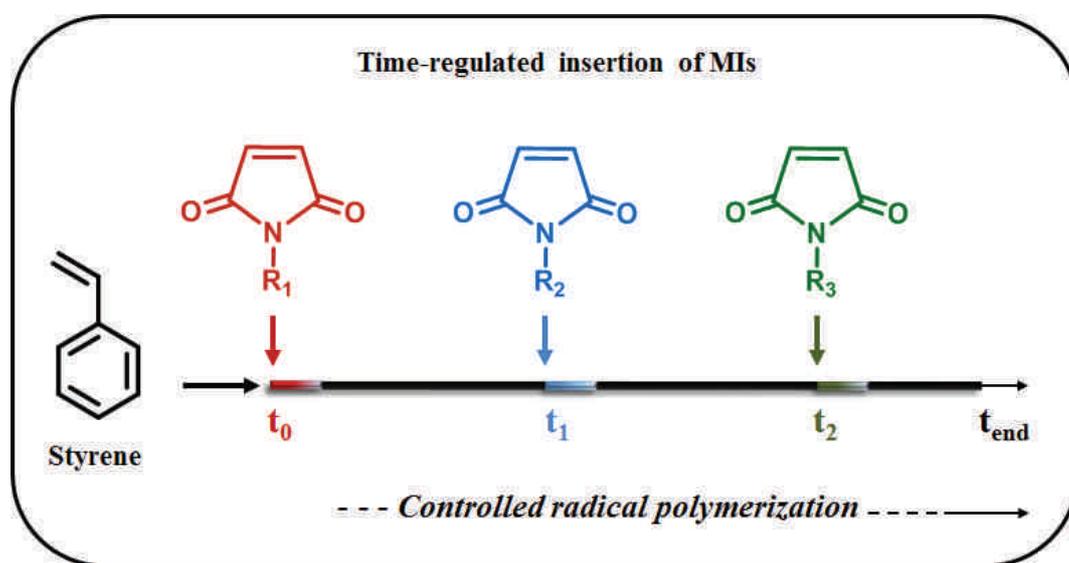
Figure 2. Concept général pour la synthèse de polymères à séquences contrôlées par la cinétique et régulés par l'insertion d'une faible quantité de maléimides *N*-substitués (MIs) au cours de la polymérisation d'un grand excès de styrène.

Jusqu'à présent, seul le styrène a été testé comme monomère donneur dans le concept de copolymérisations contrôlées de monomères donneur et accepteur. Toutefois, d'autres monomères donneurs peuvent être également utilisés. La première étude qui a confirmé la possibilité d'utiliser les autres dérivés du styrène dans ce concept a été effectuée pendant mon stage de master avec l'utilisation de monomère de type 4-*tert*-butyl benzoate de *vinyle* (*t*-BuVBA) [21] (**Figure 3**, bleue). Ce monomère a été étudié car il s'agit d'un précurseur protégé de l'acide vinyle benzoïque qui permet la synthèse de polyélectrolytes à séquences contrôlées. L'étude a bien montré que la copolymérisation de ce monomère avec le maléimide s'effectue de manière bien contrôlée. Cependant, le rapport d'activité mesuré indique que la

microstructure du polymère préparé avec un monomère de type benzyle maleimide est moins précise que celle préparée avec du styrène.
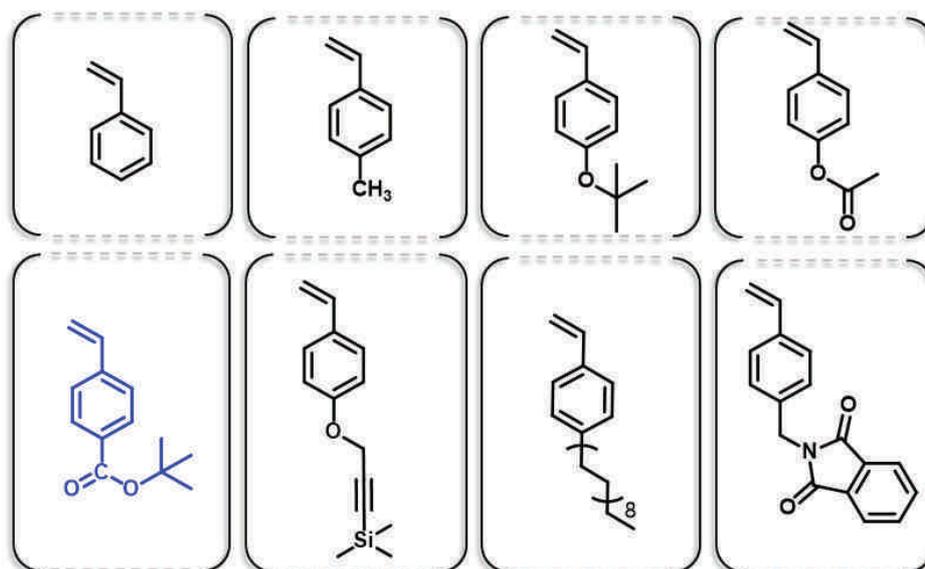
Figure 3. Structures de monomères donneurs testés dans des copolymérisations avec des maleimides. La structure dessinée en bleu a été étudiée pendant la recherche de mon master.

Dans ce travail de thèse, des copolymères ont été synthétisés par la technique de NMP, bien que d'autres techniques comme l'ATRP puissent être également utilisées dans ce concept de copolymérisation de monomères donneurs et accepteurs. La NMP a été sélectionnée car elle permet un excellent contrôle des polymérisations de dérivés de styrène. L'alcoxyamine BlocBuilder® MA a été utilisée afin d'amorcer et de contrôler la polymérisation. Le choix d'utiliser divers dérivés de styrène a été motivé par le souhait de préparer des nouveaux polymères fonctionnels à séquences contrôlées comme illustrés sur la **Figure 4**. Par exemple, des polymères polyélectrolytes, des polymères pégylés et des polymères semi-cristallins ont été élaborés dans cette thèse. Notre objectif est de faire varier les propriétés physiques-chimiques et mécaniques de ces polymères par le contrôle de leurs structures.
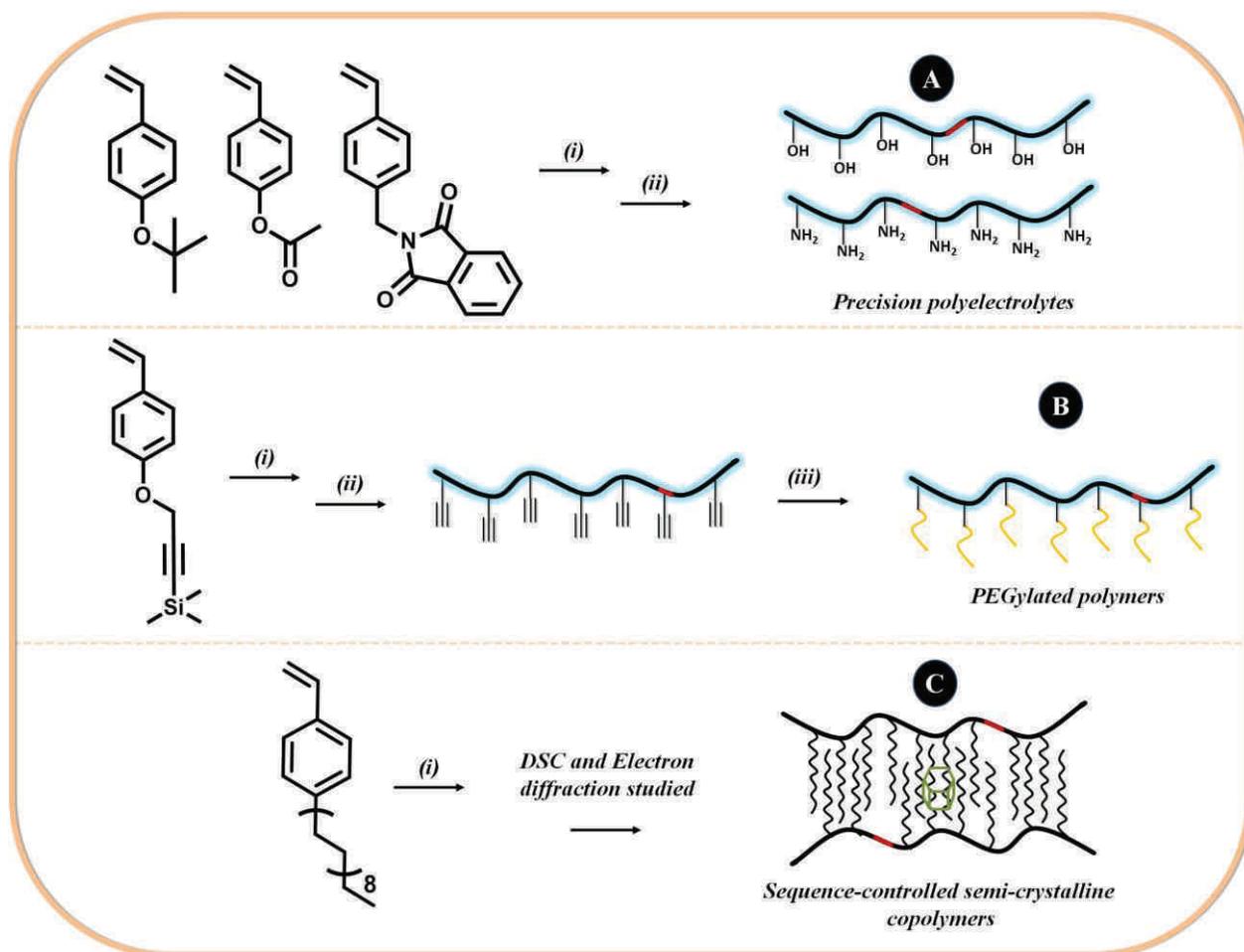
Figure 4. Différents types de copolymères à séquences contrôlées élaborés dans cette thèse. (A) des polyélectrolytes. (B) Des polymères pégylés ayant une microstructure bien contrôlée obtenus par l'approche de post-modification. (C) Des copolymères semi-cristallins à séquences contrôlées. Condition: (i) NMP de dérivés de styrène avec l'insertion locale de MIs, (ii) la déprotection et (iii) la réaction de CuAAC.

Cette thèse inclut les articles qui ont été publiés pendant les trois années de thèse et est organisée en cinq chapitres.

Le **premier chapitre** de cette thèse fournit un aperçu sur les polymères à séquences contrôlées. Les approches synthétiques employées afin de contrôler la structure primaire des polymères telles que l'utilisation des modèles de polymérisation et la synthèse itérative y sont décrites brièvement. Par ailleurs, la copolymérisation radicalaire de monomères donneurs et accepteurs a également été abordée dans ce chapitre. La polymérisation radicalaire contrôlée en particulier la technique de NMP qui a été effectuée tout au long de ce travail de thèse a été discutée. Des exemples de copolymérisation utilisant des monomères donneur et accepteur en

quantités stœchiométriques et non stœchiométriques ont été illustrés. De plus, ce chapitre comprend les derniers progrès dans la préparation de polymères à séquences contrôlées en utilisant la technique basée sur le positionnement précis d'une petite quantité de maléimides *N*-substitués dans la chaine de polystyrène. La fin de ce chapitre met en évidence quelques exemples de l'influence de la séquence de monomères sur leurs propriétés telles que les propriétés mécaniques, l'influence sur les conformations de polymères et leur capacité à se replier en solution.

Les **chapitres deux** et **trois** concernent principalement la synthèse de polyélectrolytes à séquences contrôlées y compris à partir de poly(4-hydroxystyrène)s et poly(vinyle benzyle amine)s. Puisque les 4-hydroxystyrènes et les vinyles benzyles amines ne sont pas des monomères idéaux pour la CRP, des précurseurs protégés ont été utilisés comme illustrés sur la **Figure 4**. L'influence des substituants en position *para* de monomères donneurs sur la cinétique de la polymérisation ont été étudiée dans le deuxième chapitre. Des homo- et copolymérisations radicalaires contrôlées par les nitroxydes de ces monomères donneurs protégés a été effectuées en présence d'une petite quantité de maleimides *N*-substitués. La cinétique des copolymérisations a été étudiée par résonance magnétique nucléaire (RMN). Ces études conduisent à la synthèse de polymères qui sont solubles dans des solutions aqueuses mais uniquement en conditions acides ou basiques.

Le **quatrième chapitre** a été consacré à la préparation de copolymères pégylés biocompatibles à séquences contrôlées qui sont solubles dans l'eau neutre. Dans cette partie du travail, des monomères donneurs portant les fonctions alcynes protégées ont été utilisés et copolymérisés avec une petite quantité de maléimides *N*-substitués. Après la suppression de ces groupes protecteurs, des composés fonctionnalisés avec un groupement azoture tels que des poly(éthylène glycol)s (PEG) ont été greffés sur des copolymères en utilisant la réaction de cycloaddition entre les fonctions azoture et alcyne catalysée par le cuivre (CuAAC) [27]. Des copolymères à séquences contrôlées solubles dans une solution aqueuse neutre ont été obtenus.

Enfin, le **chapitre cinq** est dédié à la synthèse de copolymères à séquences contrôlées possédant des caractères semi-cristallins. Ces macromolécules ont été obtenues par la copolymérisation en condition non stœchiométrique d'un monomère donneur portant de

longues chaines alkyles sur la chaîne latérale avec des maléimides *N*-substitués. L'influence de la microstructure de ces polymères sur leurs propriétés, et plus précisément leurs comportements de cristallisation ont été étudiés. Les propriétés semi-cristallines et la structure cristalline des polymères ont été examinées par des mesures de calorimétrie différentielle à balayage (DSC) et par microscopie électronique à transmission (TEM) respectivement.

GENERAL INTRODUCTION

Due to the constant need for new materials in our modern age, the production of synthetic macromolecules with controlled molecular structures and properties is a topic of prime importance. Among the different molecular parameters that can be adjusted by polymer chemists, the control of microstructure, and in particular of comonomer sequences, has been long underestimated. Polymers exhibiting a very high level of control of their monomer sequences such as proteins and DNA [1,2] are found in the nature. For instance, using twenty natural amino acids linked together by amide bonds, the sequence of proteins provides access to complex structures which are responsible for the properties of living matter. Both physical and chemical properties of macromolecules depend on the sequence of monomer units along the chain. Therefore, monomer sequence regulation has recently become an important topic in materials science [3]. In particular, the ability to reproduce some level of control in synthetic polymers has become a challenge of high interest within the last few years.
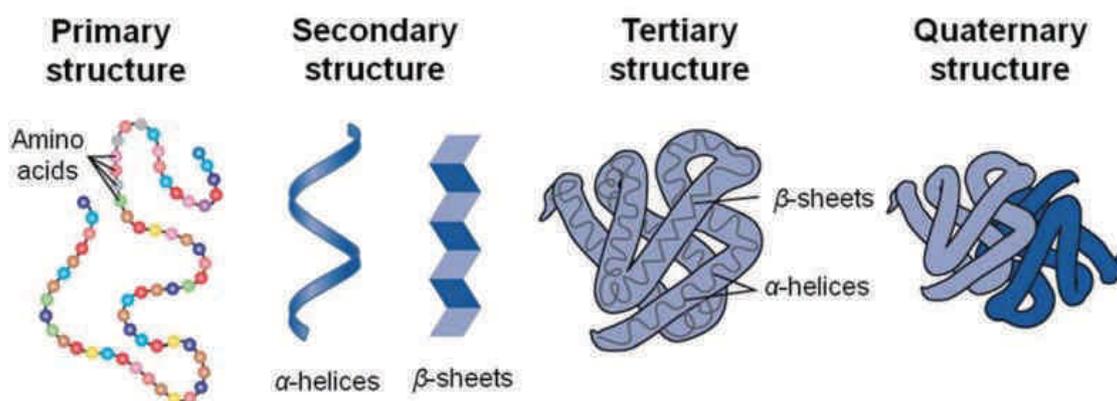
Figure 5. Influence of comonomer sequences on protein structure. Reprinted with permission from reference [4].

Different approaches have been proposed to prepare synthetic sequence-controlled macromolecules during the last decades. For instance, the primary structure of macromolecules can be regulated using biological methodologies, such as the polymerase chain reactions (PCR) or protein engineering [5,6], or chemical processes [7,8]. The latter could provide some advantages over biological approaches due to the availability of a wide range of building-blocks. Several chemical methods have been proposed to prepare

macromolecules with controlled sequences over the last years. For example, iterative strategies, in which monomers are connected one by one to a solid-support, are very powerful. However, this process is time-consuming and purification is required at each step. Thus, it would be relevant to use simpler polymerization processes to prepare sequence-controlled polymers. For instance, radical polymerization is a facile and popular method for preparing synthetic polymers. In particular, interesting controlled radical polymerizations (CRPs), such as nitroxide-mediated polymerization (NMP) [9-11], atom transfer radical polymerization (ATRP) [12-14] and reversible addition-fragmentation chain transfer (RAFT) polymerization [15], have been introduced about twenty years ago. These methods permit to control precisely the architecture of synthetic polymers (e.g.; to synthesize block, graft or brushes copolymers). However, microstructure is usually poorly controlled in these processes. Indeed, CRP-made copolymers are usually atactic and exhibit in most cases statistical sequences.

However, in some particular cases, comonomer sequences can be regulated in radical copolymerizations. For instance, the polarity of the double bond of monomers is an important factor in radical polymerization. For example, when a stoichiometric amount of styrene is copolymerized with maleic anhydride, an alternating copolymers is formed [16]. This behavior can be explained by the fact that the values of the polar factor (*e*) of these two monomers are very different [17]. Thus, when these two monomers react with each other, the cross-propagation is favored as compared to homopolymerization. Many studies describing the preparation of alternating copolymers by copolymerization of donor and acceptor comonomers used in stoichiometric amounts have been published in the past decades [18,19]. However, the CRP copolymerization of non-stoichiometric amounts of donor-acceptor comonomer pairs has recently gained interest because it allows preparation of sequence-controlled polymers with unprecedented microstructures. For instance, our group has described a new approach to prepare sequence-controlled polymers using time-controlled addition of small amount of *N*-substituted maleimides (MIs) during the CRP of a large excess of styrene [20]. This process allows the placement of the acceptor monomer at desired positions in the polystyrene chains (**Figure 6**). MIs are used as acceptors comonomers in this concept instead of maleic anhydride because they can bear a wide range of functional groups on their *N*-position. It was shown that this simple copolymerization strategy allows design of interesting sequence-controlled polymers such as water soluble polymers [21], single–chain bio-arrays [22] or well-defined foldable polymers [23-25] were elaborated using this concept.
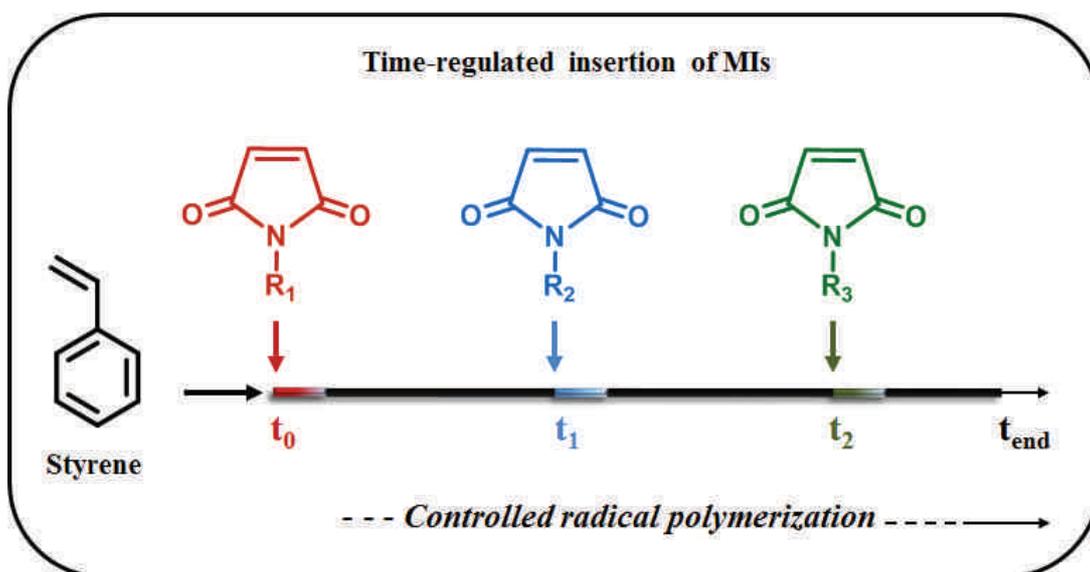
Figure 6. General concept for the CRP synthesis of sequence-controlled polymers using a time-regulated insertion of a discrete amount of *N*-substituted maleimide (MI) during the polymerization of a large excess of styrene.

Prior to this thesis, only styrene was tested as a donor monomer in these sequence-controlled donor/acceptor copolymerizations. However, many other donor monomers can be potentially utilized in this concept. The first study that confirmed the possibility of using other styrenic derivatives in this strategy was reported during my master research with the use of *tert*-butyl 4-vinyl benzoate (*t*-BuVBA) as a donor monomer [21] (**Figure 7**, blue color). This monomer was studied because it is a protected precursor of vinyl benzoic acid and it therefore allows synthesis of sequence-controlled polyelectrolytes. It was found that the copolymerization of *t*-BuVBA and MIs proceeds in a sequence-controlled fashion. Nevertheless, the reactivity ratios measured for these experiments indicated that the microstructure of the polymers prepared with *t*-BuVBA are less precisely-controlled than the one made with styrene. This is probably due to the electron-withdrawing character of the substituent in *para*-position of *t*-BuVBA. Based on these first observations, other donor monomers have been investigated in this thesis. As shown in **Figure 7**, different styrenic derivatives have been tested in sequence-controlled polymerizations with MIs.
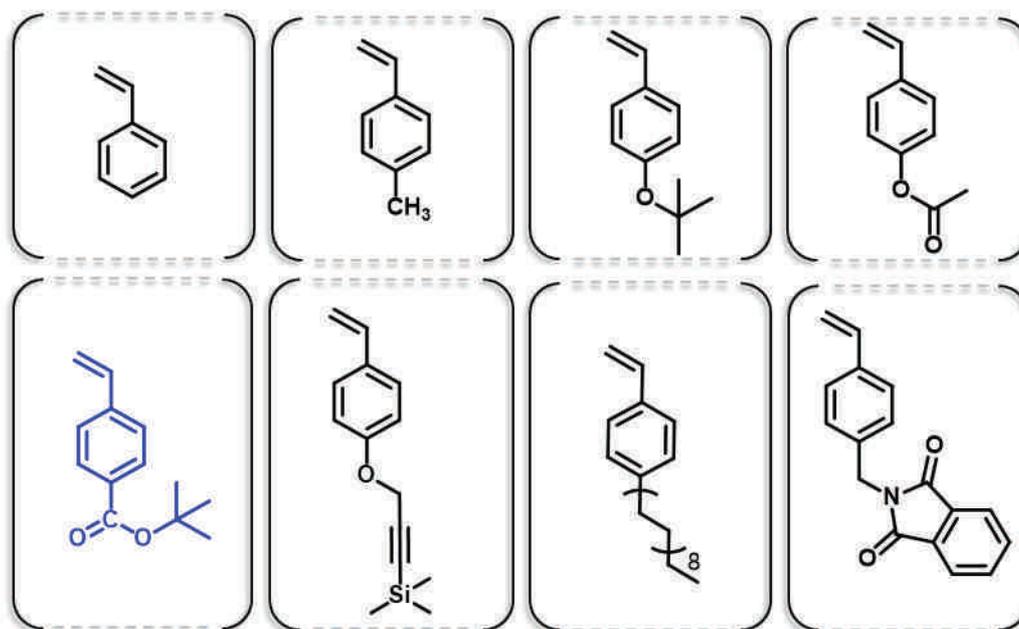
Figure 7. Structure of the donor monomers tested in this thesis in sequence-controlled copolymerizations with MIs. The structure displayed in blue was studied during my master thesis and is just displayed for reader's information.

In this thesis, all the copolymers were prepared by nitroxide-mediated polymerization (NMP). Although different type of CRPs (e.g. ATRP) can be used in our donor-acceptor copolymerization concept, NMP was selected because it allows an excellent control of the polymerization of styrenic derivatives. The commercial alkoxyamine BlocBuilder® MA was used to initiate and control the polymerization. The motivation of using diverse styrenic derivatives was to prepare new sequence-controlled polymers and materials as illustrated in **Figure 8**. For instance, polyelectrolytes, biocompatible PEGylated polymers and semi-crystalline polymers were investigated in this thesis. Our objective was to tune the physic-chemical and mechanical properties of these important types of polymers by controlling their microstructures.
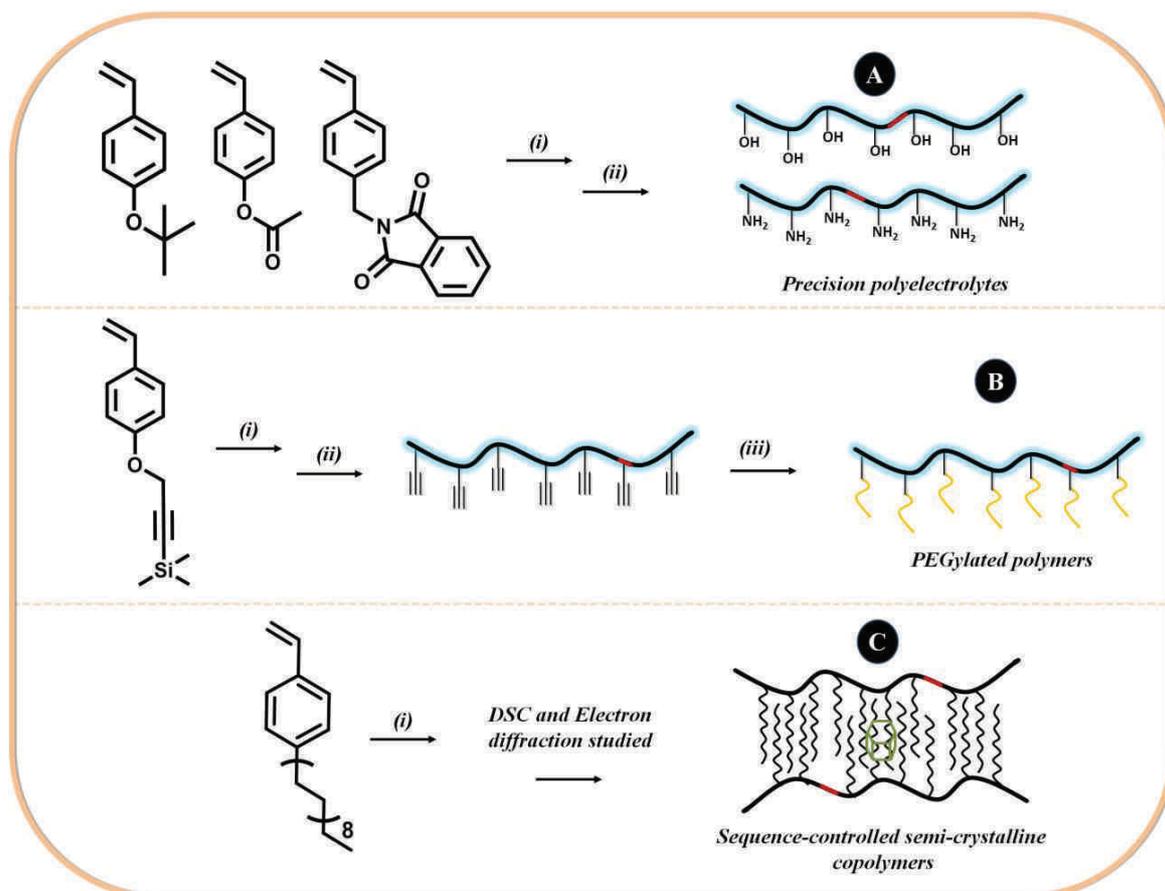
Figure 8. Different types of sequence-controlled copolymers investigated in this thesis. (A) Precision polyelectrolytes. (B) PEGylated polymers with controlled microstructures obtained by a post-modification approach. (C) Sequence-controlled semi-crystalline copolymers. (i): NMP of styrenic derivatives monomers with local insertion of small amounts of MIs, (ii): deprotection and (iii) CuAAC reaction.

This manuscript includes the articles that were published during the three years of doctoral research and is divided into five main chapters as follow:

The **first chapter** of this thesis provides an overview on sequence-controlled polymers. The synthetic approaches employed to control the primary structure of polymers such as template and iterative syntheses are briefly described. Whilst the emphasis of this chapter will be put on the radical copolymerization of donor and acceptor comonomers, the controlled radical polymerization techniques especially NMP process which was used along this thesis research are discussed. The examples of copolymerization in stoichiometric and non-stoichiometric quantities of donor-acceptor comonomer pairs are illustrated. Besides, this

chapter includes the advances on the preparation of sequence-controlled polymers using precise positioning of a discrete amount of *N*-substituted maleimides in a polystyrene backbone technique. The end of this chapter highlights some examples of the influence of monomer sequences on polymer properties such as mechanic properties, the influence on the polymer conformations and the ability to induce folding on single polymer chains.

The **second** and **third chapters** focus on the synthesis of sequence-controlled polyelectrolytes including poly(4-hydroxystyrene)s and poly(vinyl benzyl amine)s. Since 4-hydroxystyrene and *N*-(*p*-vinyl benzyl amine) are not ideal monomers for CRP, protected precursors were used as shown in **Figure 8**. The influence of these *para*-substituents on the copolymerization kinetics was studied in the second chapter. Nitroxide-mediated homo- and copolymerization of these protected donor monomers was investigated in the presence of small quantities of *N*-substituted maleimides. The kinetics of copolymerization were examined by nuclear magnetic resonance (NMR). These studies led to the synthesis of polymers which are soluble in acidic or basic aqueous solutions.

The **fourth chapter** is devoted to the preparation of sequence-controlled biocompatible PEGylated water soluble copolymers. In this part of the work, donor monomers bearing protected alkyne functionalities were used and copolymerized with discrete amount of *N*-substituted maleimides. After removal of the protecting groups on the alkyne functions, azido-functionalized poly(ethylene glycol)s (PEG)s were grafted on the copolymers using copper-catalyzed alkyne-azide cycloaddition (CuAAC) chemistry [26] leading to sequence-controlled copolymers that are soluble in a neutral water.

Finally, **chapter five** investigates the preparation of semi-crystalline sequence-controlled copolymers. These macromolecules were obtained by copolymerization of a donor monomer with a long alkyl side chain with non-stoichiometric amount of MIs. The influence of the microstructure of the polymers on their properties and more precisely their crystallization behaviors were studied. The semi-crystalline properties and the crystalline structure were examined by differential scanning calorimetry (DSC) measurement and transmission electronic microscopy (TEM) technique respectively.

References

[1]. Badi, N.; Lutz, J.-F., *Chem. Soc. Rev.,* **2009**, *38*, 3383-3390.

[2]. Börner, H. G., *Macromol. Rapid Commun.,* **2011**, *32*, 115-126.

[3]. Lutz, J.-F.; Ouchi, M.; Liu, D. R.; Sawamoto, M., *Science,* **2013**, *341*, 1238149.

[4]. Silva, N. H. C. S.; Vilela, C.; Marrucho, I. M.; Freire, C. S. R.; Pascoal Neto, C.; Silvestre, A. J. D., *J. Mater. Chem. B,* **2014**, *2*, 3715-3740.

[5]. McGrath, K. P.; Fournier, M. J.; Mason, T. L.; Tirrell, D. A., *J. Am. Chem. Soc.,* **1992**, *114*, 727-733.

[6]. Saiki, R.; Gelfand, D.; Stoffel, S.; Scharf, S.; Higuchi, R.; Horn, G.; Mullis, K.; Erlich, H., *Science,* **1988**, *239*, 487-491.

[7]. McHale, R.; Patterson, J. P.; Zetterlund, P. B.; O'Reilly, R. K., *Nat. Chem,* **2012**, *4*, 491-497.

[8]. Pfeifer, S.; Zarafshani, Z.; Badi, N.; Lutz, J.-F., *J. Am. Chem. Soc.,* **2009**, *131*, 9195-9197.

[9]. Hawker, C. J.; Bosman, A. W.; Harth, E., *Chem. Rev.,* **2001**, *101*, 3661-3688.

[10]. Nicolas, J.; Guillaneuf, Y.; Lefay, C.; Bertin, D.; Gigmes, D.; Charleux, B., *Prog. Polym. Sci.,* **2013**, *38*, 63-235.

[11]. Tebben, L.; Studer, A., *Angew. Chem. Int. Ed.,* **2011**, *50*, 5034-5068.

[12]. Braunecker, W. A.; Matyjaszewski, K., *Prog. Polym. Sci.,* **2007**, *32*, 93-146.

[13]. Matyjaszewski, K.; Tsarevsky, N. V., *J. Am. Chem. Soc.,* **2014**, *136*, 6513-6533.

[14]. Wang, J.-S.; Matyjaszewski, K., *J. Am. Chem. Soc.,* **1995**, *117*, 5614-5615.

[15]. Moad, G.; Rizzardo, E.; Thang, S. H., *Polymer,* **2008**, *49*, 1079-1131.

[16]. Baldwin, M. G., *J. Polym. Sci., Part A: Gen. Pap.,* **1965**, *3*, 703-710.

[17]. Alfrey, T.; Price, C. C., *J. Polym. Sci.,* **1947**, *2*, 101-106.

[18]. Coleman, L. E.; Conrady, J. A., *J. Polym. Sci.,* **1959**, *38*, 241-245.

[19]. Oishi, T.; Iwahara, M.; Fujimoto, M., *Polym. J.,* **1991**, *23*, 1409-1417.

[20]. Pfeifer, S.; Lutz, J.-F., *J. Am. Chem. Soc.,* **2007**, *129*, 9542-9543.

[21]. Srichan, S.; Oswald, L.; Zamfir, M.; Lutz, J.-F., *Chem. Commun.,* **2012**, *48*, 1517-1519.

[22]. Baradel, N.; Fort, S.; Halila, S.; Badi, N.; Lutz, J.-F., *Angew. Chem. Int. Ed.,* **2013**, *52*, 2335-2339.

[23]. Schmidt, B. V.; Fechler, N.; Falkenhagen, J.; Lutz, J. F., *Nat. Chem.,* **2011**, *3*, 234-38.

[24]. Shishkan, O.; Zamfir, M.; Gauthier, M. A.; Börner, H. G.; Lutz, J.-F., *Chem. Commun.,* **2014**, *50*, 1570-1572.

[25]. Zamfir, M.; Theato, P.; Lutz, J.-F., *Polym. Chem.,* **2012**, *3*, 1796-1802.

[26]. Hein, J. E.; Fokin, V. V., *Chem. Soc. Rev.,* **2010**, *39*, 1302-1315.

Chapter I

An Introduction to Sequence-Controlled Polymers (SCPs)

I.1. General Overview

Sequence-controlled polymers (SCPs) are polymers that have ordered arrangement of their monomer units along the chain [1]. The most known examples of SCPs which exhibit a very high level of monomer sequence control are biopolymers, such as DNA [2] and proteins [3]. Proteins are based on 20 natural amino acids that are linked together by amide bonds. These amino acid residues can be considered as the letters of an alphabet which are used to write the information on a linear polypeptide chain and each letter of this alphabet provides a specific contribution. Generally, the sequence of these amino acids provides access to four main protein structures: primary, secondary, tertiary and quaternary structures as shown in **Figure 9** [4-6]. Regarding DNA, a double-stranded molecule held together by hydrogen bonds between pairs of nucleotides, the organization of four nucleotide monomer units, namely cytosine, guanine, adenine, and thymine, can be found in an ordered sequence [7]. It is important to note that the highly ordered monomer sequences of these biopolymers are largely responsible for the most important properties of living matter.
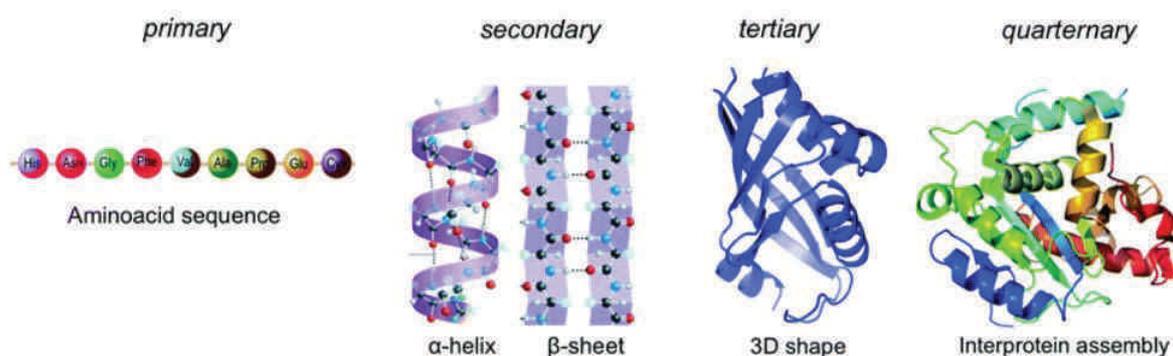
Figure 9. Levels of structural complexity of proteins. Adapted with permission from reference [5].

Recently, polymer chemists have tried to improve the complexity of synthetic polymers in order to access structurally more diverse materials and obtain new properties comparable to those of natural polymers. However, the control over the microstructure of theses macromolecules is still having some limitations and is still far from what nature is able to engineer. However, in recent years, many studies have focused on the synthesis of macromolecules with precise control of their monomer sequences [8,9]. These new developments will be discussed in this chapter.
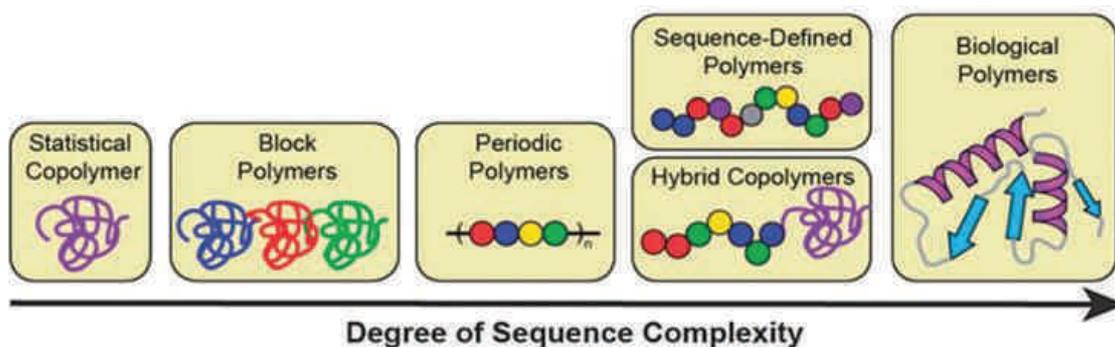
Figure 10. Degree of sequence-controlled complexity ranging from synthetic to biological polymers. Reprinted with permission from reference [10].

I.2. Synthetic chemical process for controlling monomer sequences

Over the last years, different methods have been introduced to control monomer sequences in synthetic polymers. Both chemical and biological approaches have been described in the literature. The latter approaches are in general restricted to the synthesis of sequence-controlled polymers with natural backbones (e.g. artificial proteins, nucleic acids), even though non-canonical monomers can be used. Chemical approaches could provide some advantages over biological methods because of the broad range of chemical structures available. These promising methodologies are described in details in the following sections.

I.2.1. Template approach

Template synthesis has been studied by many authors and may provide opportunities to synthesize new sequence-defined molecular structures [11-13]. In such approaches, the monomer units are linked to a preformed macromolecule and polymerized. Very different polymerization mechanisms can be used to synthesize the polymers on the template [14]. For instance, O'Reilly and coworkers [15] demonstrated the preparation of two sequence-controlled decamers containing two- and four-monomer repeat units by using DNA-templated synthesis. The two macromolecules can be obtained by the sequential coupling of reactive monomers to the oligonucleotide adapters and at the end the growing product chain was cleaved from its DNA adapter via Wittig reaction (**Figure 11**). This method is easy and

versatile because the product can be obtained without intermediate purification steps and no protecting groups are needed.

Figure 11. DNA-templated synthesis mechanism for the synthesis of decamers. Reprinted with permission from reference [15].

Radical polymerization can also be used to synthesize a polymer on a template, even though only a few reports can be found in the literature. For instance, template-assisted sequence-controlled radical polymerization has been recently studied by Sawamoto and coworkers [16-18] (**Figure 12** (a)).
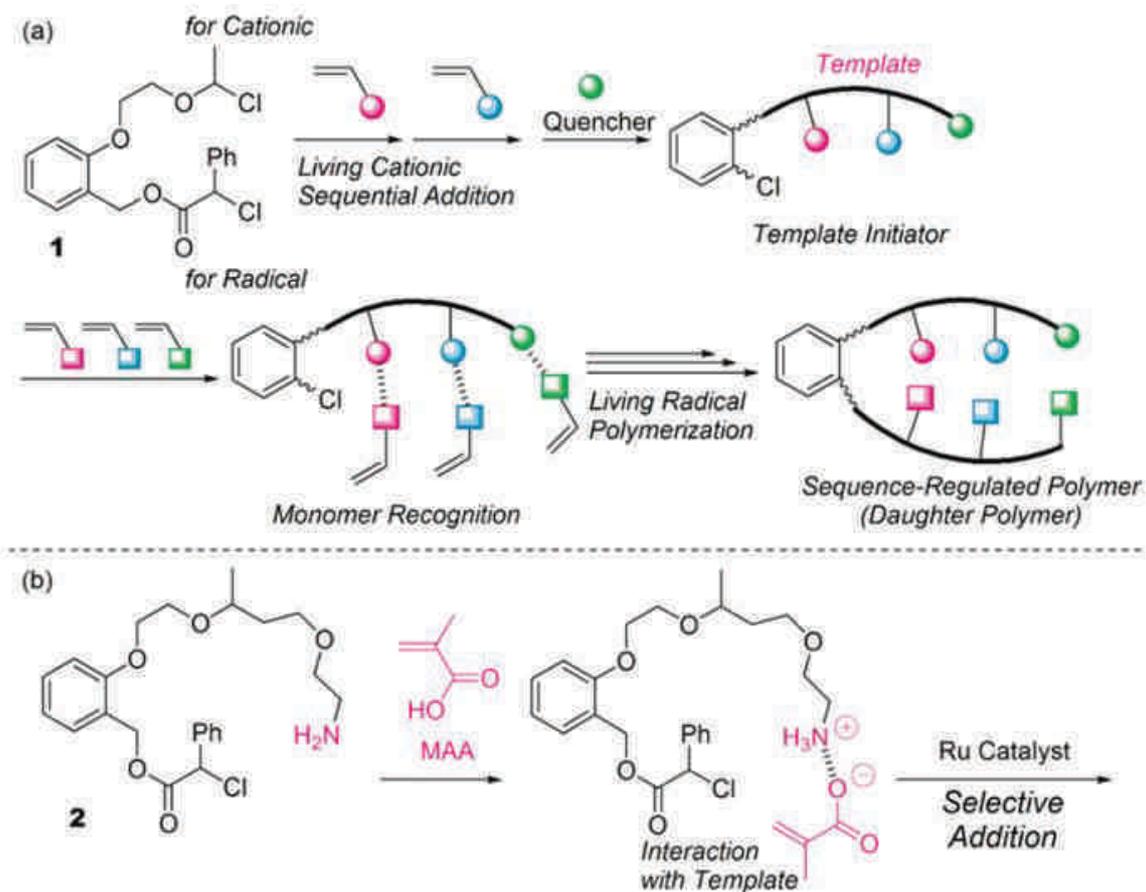
Figure 12. a) Sequence-regulated polymer obtained by living radical polymerization of heterobifunctional initiator. b) Template-assisted radical addition of MAA. Reprinted with permission from reference [16].

So far, these authors have just developed small models to mimic more complex template polymerizations. In particular, they synthesized a new heterobifunctional halide **1**, which is bearing two different sites: a haloether and a haloester. After that, a template initiator was prepared by living cationic polymerization [19] starting from the haloether site. The obtained cationic intermediate was then quenched with LiBH$_4$ followed by cleavage of the *tert*-butyloxycarbonyl (Boc) protecting group yielding the amino-functionalized targeted template initiator **2**. Subsequently, in a living radical polymerization process, methacrylic acid

(MAA) was added to the template initiator and ruthenium complex catalyst was used to assist in the regulation of haloester site and neighboring template. Due to the amino functional groups present on the template and the presence of the carboxylic acid function of MAA, this monomer was then recognized via ionic interaction ((**Figure 12** (b)) [18]. Thus, monomer-specific polymerization could be achieved on this model template.

I.2.2. Iterative approach

The iterative strategy (i.e. sequential attachment of comonomers) is also a very robust approach to prepare sequence-controlled polymers. This method was first developed for the synthesis of peptides. In 1901, the synthesis of the first dipeptide obtained by partial hydrolysis of the diketopiperazine of glycine has been reported by Fischer and the term "peptide" was introduced to refer to a polymer of amino acids [20]. Nevertheless, this process was time-consuming. Moreover, the afforded products were impure and most of them obtained in poor yields. A rapid, simplified, and effective strategy to prepare peptides was reported in 1963 by Merrifield [21]. In this strategy, a peptide chain is formed by iterative attachment of amino-acids on a solid support (i.e. a cross-linked microgel bead swollen by an organic solvent) [22]. The synthesis of peptides could be achieved efficiently by this approach because the purification of the peptide intermediates was greatly simplified by the use of a solid-support.

The general scheme for the solid-phase synthesis using iterative approach is shown in **Figure 13**. The process can be explained by the fact that the monomer unit (M) can be attached to the functionalized support by the reaction between the reactive end groups (Y) of the monomer and functional groups of the support (X). It should be noted that one of the two reactive end groups of the monomer has to be protected (X in grey), while the other end functionality can be used for coupling. Following the addition of the monomer, the protecting group is then removed to generate a new reactive end-group. The coupling-deprotection cycle is repeated a certain number of times until the desired entire sequence is obtained. At the end, the covalent bond connecting the support to the polymer chain is cleaved together with the side chains protecting groups. Isolation of the polymer from the solid support is then accomplished by simple filtration of the solid support.
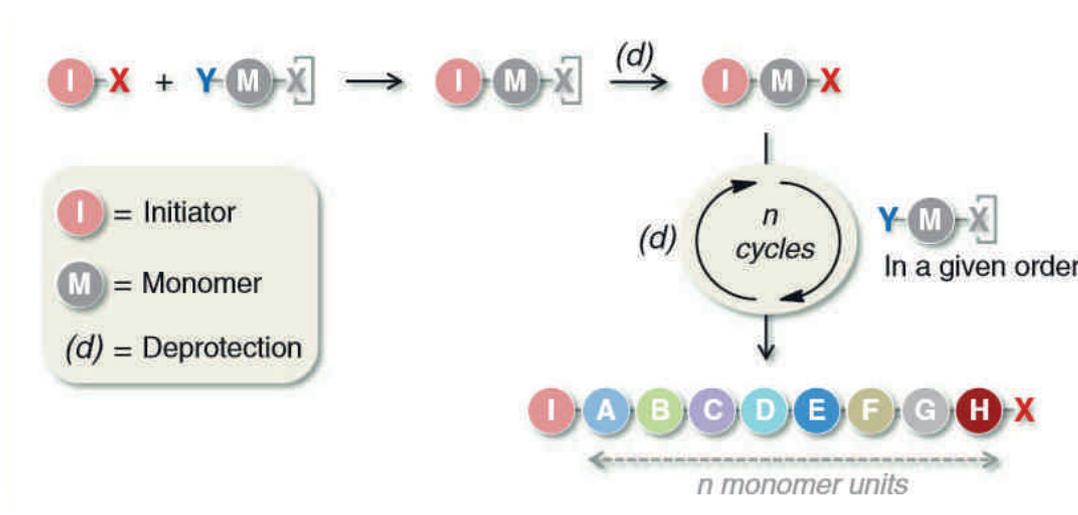
Figure 13. General strategy for iterative attachment of monomers. Reprinted with permission from reference [1].

Besides solid-supports, soluble supports can also be used for iterative synthesis. Such supports are soluble polymer chains that can be recycled by precipitation in a non-solvent. A large number of examples have been reported in the literature [23-25]. For instance, our group has recently investigated the liquid-phase synthesis of peptide-polymer conjugates [26]. In this study, the hexapeptide GKYGKY was chosen as a model and three different supports were compared (**Figure 14**) including well-defined polystyrene soluble supports with (a) and without (b) cleavable sites. These two supports were prepared by ATRP polymerization from a functional initiator. In addition, commercial Wang solid support (c) was also used to compare the structure of the obtained peptides on soluble and solid supports. When the sequences were constructed on linear polystyrene support, the synthesized compound could be collected due to the possibility to isolate the support by precipitation in methanol. In accordance with the matrix-assisted laser desorption/ionization mass spectroscopy (MALDI-TOF-MS) results, well-defined oligopeptides were obtained through approaches (a), (b) and (c) exhibiting very similar MS spectra. This study indicates that soluble supports are interesting to prepare bio-hybrid polymers.

In a more recent study, it was shown that soluble polymer supports are very useful for peptide PEGylation (**Figure 15**) [27]. In this study, the polystyrene soluble support was prepared by ATRP using a functional initiator. Model peptides (Tyr-Lys-Tyr-Lys-Gly) were synthesized by sequential Fmoc-amino acid coupling followed by removal of Fmoc protecting

group under appropriate conditions. mPEG-COOH was then coupled to the *N*-terminal amino groups attached on the support and the formed PEG-peptide conjugate was cleaved from the support. The authors concluded that soluble supports allowed the synthesis of *N*-terminal PEGylated polymers.
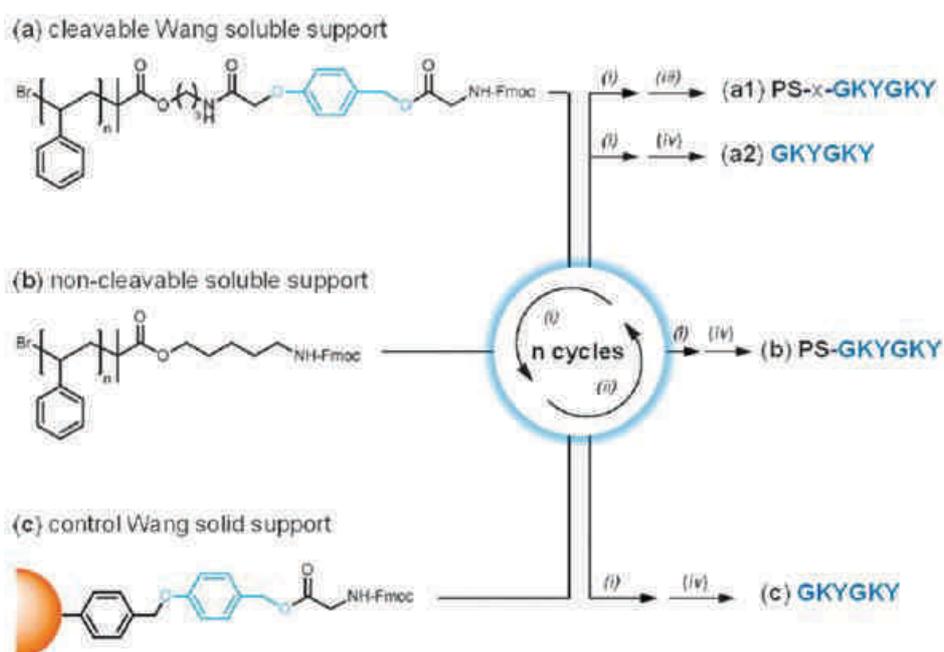
Figure 14. General strategy for synthesizing peptide-polymer conjugates. Reprinted with permission from reference [26].
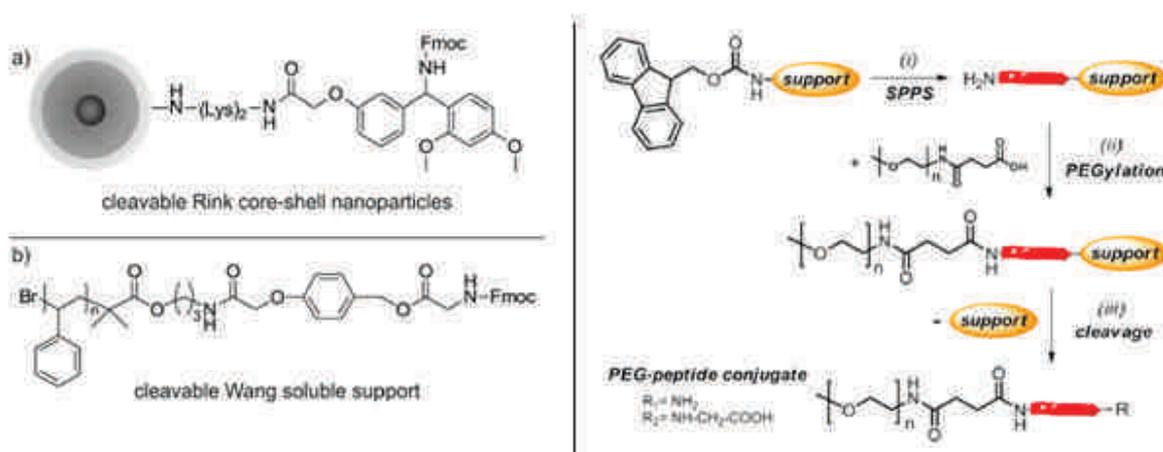
Figure 15. Two different supports used to synthesize PEG-peptide conjugates (left) and strategy for the synthesis (right). Reprinted with permission from reference [27].

Besides peptide synthesis, iterative approaches on solid or soluble supports can be used to synthesize other types of natural and non-natural sequence-controlled polymers. Numerous examples have been reported in the literature. For instance, in 1992, Zuckermann and coworker have described the preparation of so-called peptoid oligomers by solid-phase synthesis [28]. However, a disadvantage of this approach is the necessity of preparing suitable quantities of a diverse set of protected *N*-substituted glycine monomers. Afterwards, the authors developed the solid-phase submonomer method [29,30] in which the protection of the end functionalities of the monomer was not required. In the submonomer method, each cycle of monomer addition involved two steps consisting in an acylation of the amine present at the surface of the resin with a haloacetic acid, followed by a displacement with an excess of primary amine (**Figure 16**). The submonomer method is considered as more efficient because it is very easy to perform since the displacement reaction in the second step is sensitive neither to the air nor to the moisture and no heating is typically required [31]. In addition, many submonomers are in general commercially available thus leading to a diversity of sequences in peptoid polymer chain peptides with high coupling efficiency, corresponding to about 40 % conversion.
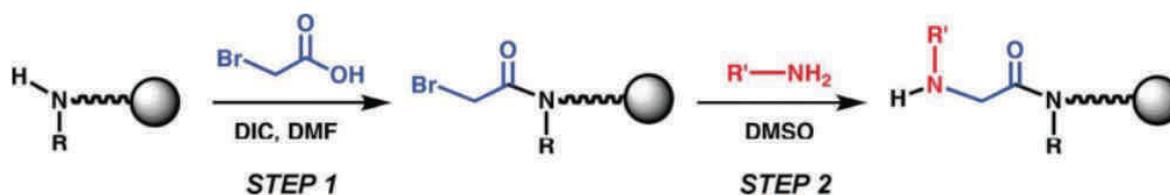
Figure 16. Solid-phase assembly of *N*-substituted glycine from two submonomers. Reprinted with permission from reference [30].

Several other examples of non-natural sequence-defined oligomers prepared by solid phase chemistry have been reported. For example, Rose and coworkers [32] and Hartmann and coworkers [33] have described the synthesis of sequence-defined unnatural polyamides by using non-protected diacids and diamines on a solid-support.

Hartmann and coworkers have also recently reported the synthesis of sequence-defined oligomers containing sugar functionalities [34,35] (**Figure 17**). In this study the multivalent mannose ligands have been attached to an alkyne moiety present on a building block via 1,3 dipolar cycloaddition. The sequence-defined monodisperse oligomers were later

obtained after cleavage from the solid support. The mannose structure was further recognized by Con A lectin binding.
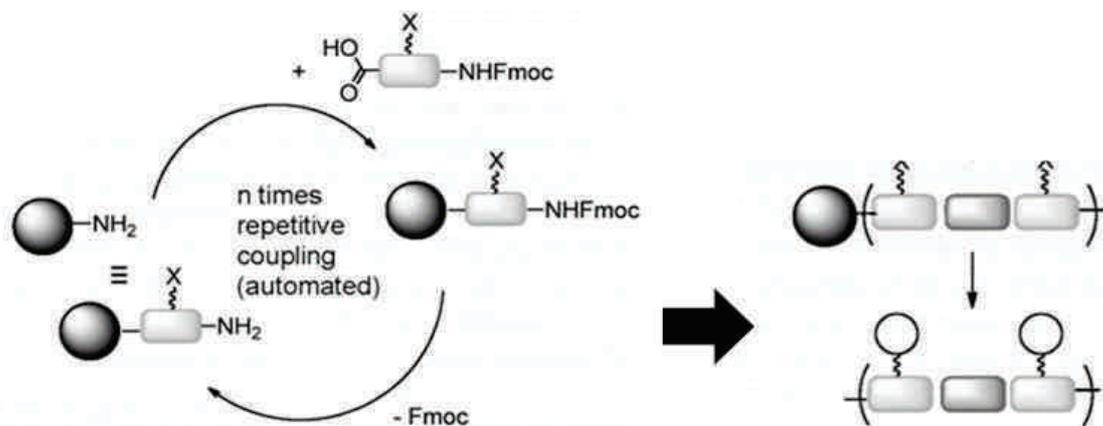
Figure 17. The solid-phase synthesis of building block followed by the side-chain functionalities introducing sugar ligands *via* click chemistry. Reproduced with permission from reference [35].

Our group has also proposed an "AB+CD" iterative approach to synthesize unnatural sequence-defined macromolecules [36]. In this approach, two successive chemoselective chemical reactions are used to build the oligomers, namely the 1,3-dipolar cycloaddition reaction of terminal alkynes (A) with azides (D) and the amidification reaction of carboxylic acids (B) with primary amines (C). 6-Heptynoic acid and 11-azido-3,6,9-trioxaundecan-1-amine were used as AB and CD blocks respectively (**Figure 18**). Well-defined polystyrene synthesized by ATRP was used as soluble support and the formed oligomer was isolated by cleavage using a TFA/CH$_2$Cl$_2$ mixture. The polystyrene support was eliminated by precipitation in methanol while oligomers remained in the methanol solution. The solution was concentrated yielding the monodisperse oligomers. When compared to preparation of these oligomers using a modified Wang resin support, both techniques showed the formation of well-defined oligomers.

It was later shown that the "AB+CD" approach can be used to prepare information-containing macromolecules [37]. In this study, 4-pentynoic acid (0) and 2-methyl-4-pentynoic acid (1) were used as coded AB building-blocks and 1-amino-11-azido-3,6,9-trioxaundecane was used as a CD spacer. These building blocks were used to build oligomers from a Wang resin support (**Figure 19**). Binary encoding was obtained by using either the monomer 0 and 1

as AB monomer in the amidification step. A series of encoded pentamers constituted of three AB and two CD building blocks was synthesized and characterized in this work.
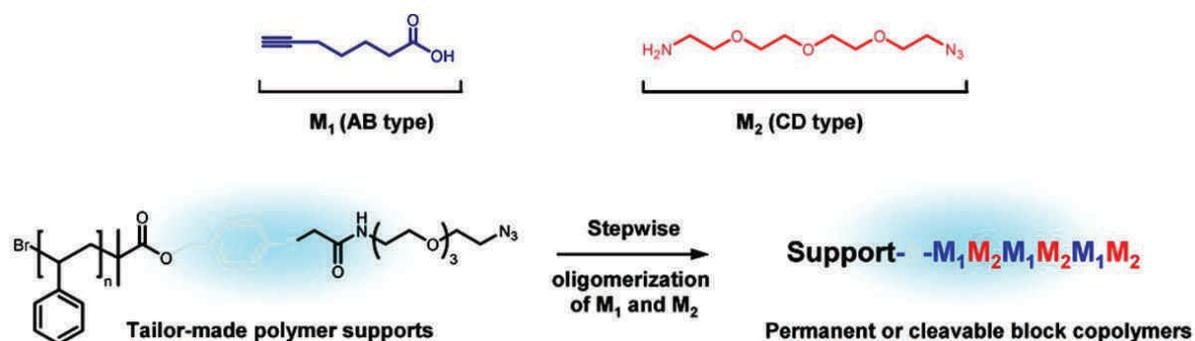
Figure 18. Liquid-phase synthesis of block copolymers containing sequence-ordered segments. Reprinted with permission from reference [36].
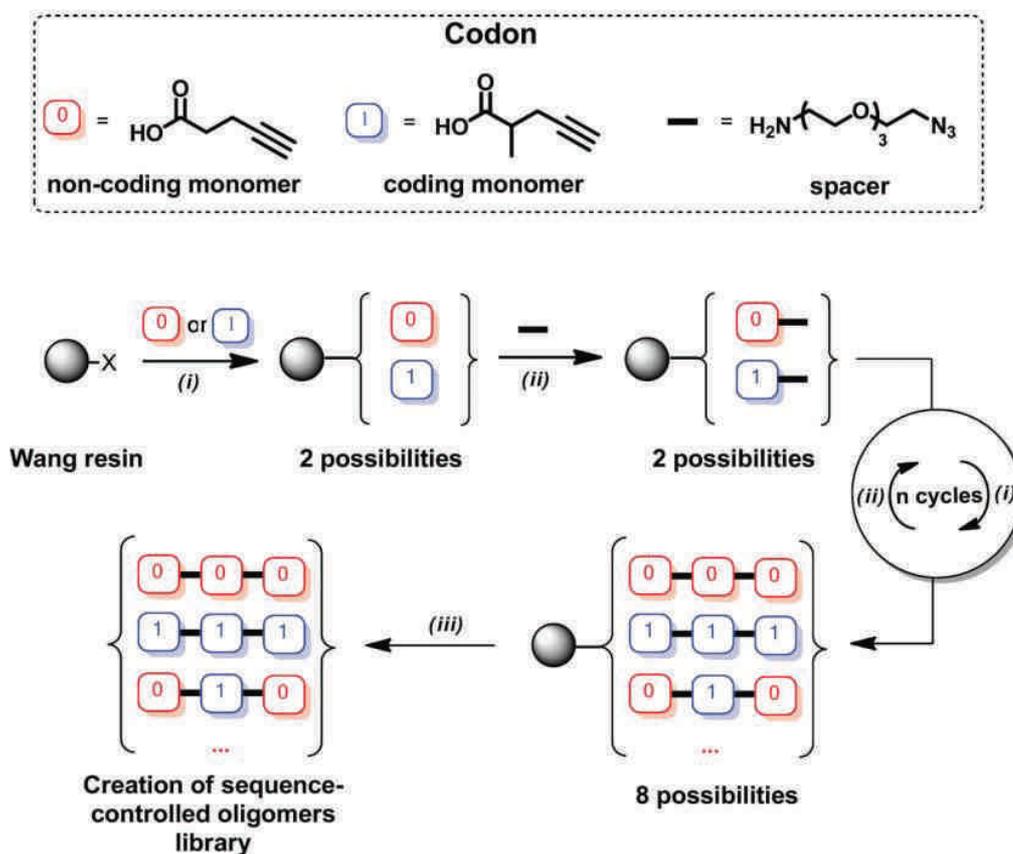
Figure 19. General strategy for synthesizing sequence-defined oligomer via "AB+CD" iterative approach. Reprinted with permission from reference [37].

I.3. Sequence-controlled polymers (SCPs) in radical polymerization

As described in the previous paragraph, iterative synthesis is often used to synthesize sequence-controlled polymers. However, a growing interest to use more conventional polymerization techniques to prepare sequence-controlled polymers is noticeable. The two main polymerization mechanisms are step-growth and chain-growth polymerization. In chain-growth mechanism, and in particular in radical polymerization, the comonomer sequences are in general poorly controlled (e.g. statistical). However, some concepts for controlling sequences in radical polymerizations have been recently reported [38]. These approaches are described in details in this section. First, some generalities about conventional and controlled radical polymerization will be presented. Afterwards, sequence-controlled radical copolymerization will be discussed.

I.3.1. Controlled radical polymerization techniques

I.3.1.1. Generalities

Radical polymerization is a chain-growth process, in which polymer grows by successive insertion of monomer units through their double bond. It involves three fundamental steps: initiation, propagation and termination. Conventional radical polymerization is a facile process that can be applied to various monomers but that yield macromolecules with ill-defined molecular structures (e.g. architecture, molecular weight, molecular weight distribution). In comparison, anionic polymerization, which is also a chain-growth mechanism, leads in general to much better defined polymers. In 1956, the term "living" polymerization was introduced by Szwarc [39,40] to describe anionic polymerizations. This method allows for the preparation of well-defined macromolecules with control molecular weight and molecular weight distribution. However, anionic polymerization has also some drawbacks. For instance, it needs to be free of moisture and impurities, thus laboratory implementation is quite difficult. In the mid-1990's, new methods called "controlled/living" radical polymerizations (CRP) that combine the advantages of conventional radical polymerization and living polymerizations have been introduced [41-44]. These novel techniques allows synthesis of macromolecules with complex topologies such as

block copolymers, graft copolymers or multifunctional stars (e.g. miktoarm stars) [45]. In addition, different types of copolymer microstructures can be created [9] (**Figure 20**).
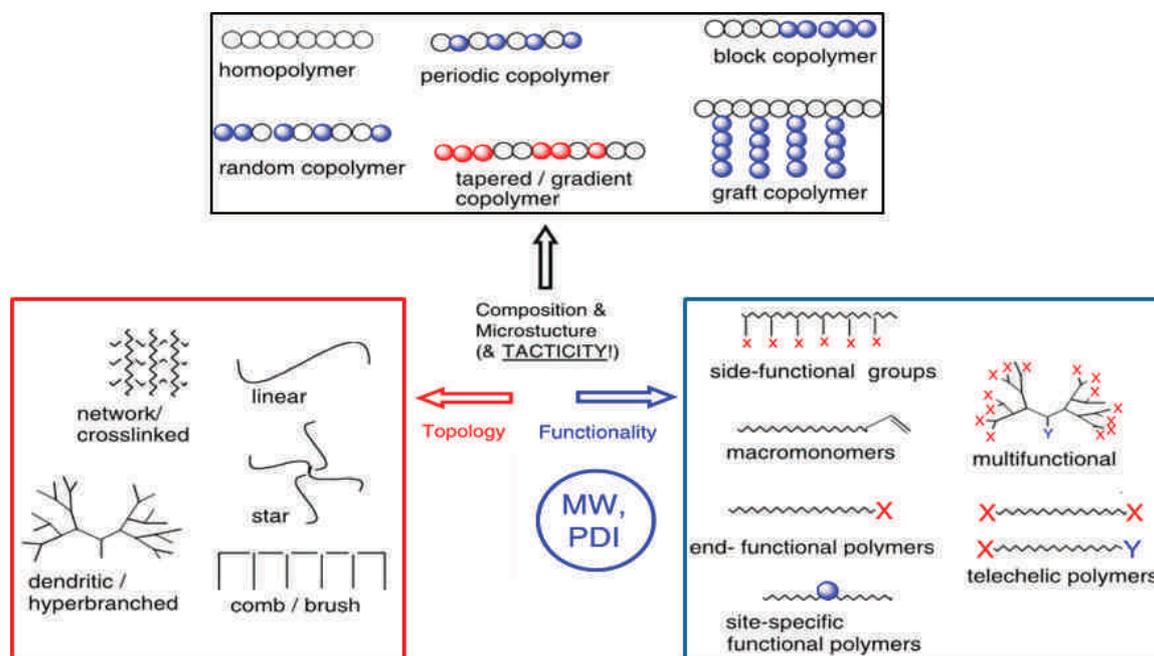
Figure 20. Example of molecular structure that can be obtained by CRP. Adapted with permission from reference [9].

The three notable controlled radical polymerization methods found in the literature which have been used to prepare macromolecules with controlled molecular weight and narrow molecular weight distribution are stable free radical polymerization (SFRP), also known as nitroxide-mediated polymerization (NMP) [46-51], atom transfer radical polymerization (ATRP) [52-55] and reversible addition-fragmentation chain transfer (RAFT) polymerization [56-60]. All these controlled/living radical polymerization techniques are complementary in their overall scope for macromolecular engineering.

The mechanism of CRP is based on the existence of a dynamic equilibrium between the formed dormant and active species as illustrated in **Scheme 1**. In general, this equilibrium should be fast enough as compared to the propagation rate to minimize the concentration of growing radical species in order to give a nearly equal chance for all polymer chains to grow leading to the formation of polymers with narrow molecular weight distribution. The radical bimolecular termination is also limited in such a process due to the lower concentration of active species.

a) NMP

$$P_n\text{-}T \underset{k_{deact}}{\overset{k_{act}}{\rightleftharpoons}} P_n^\bullet + T^\bullet$$

k_p Monomer k_t

b) ATRP

$$P_n\text{-}X + Mt^n/L \underset{k_{deact}}{\overset{k_{act}}{\rightleftharpoons}} P_n^\bullet + X\text{-}Mt^{n+1}/L$$

k_p Monomer k_t

c) RAFT

$$P_n^\bullet + P_m\text{-}X \overset{k_{exch}}{\rightleftharpoons} P_n\text{-}X + P_m^\bullet$$

k_p Monomer k_t k_t k_p Monomer
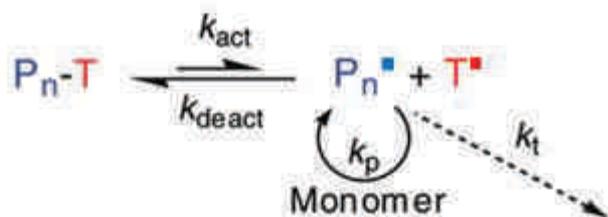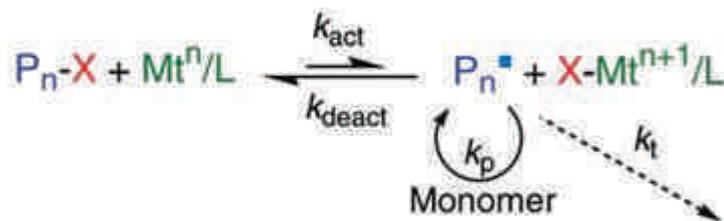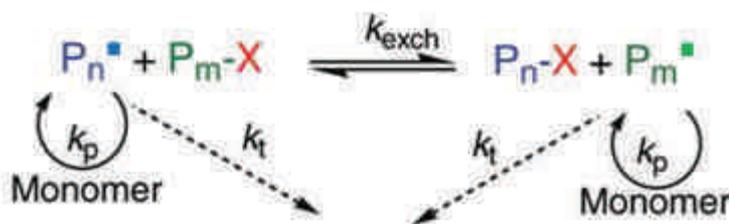
Scheme 1. A dynamic equilibrium between dormant and active species of the main three different CRPs methods. Reproduced with permission from reference [41].

Each CRP technique has different advantages and limitations which affect its applicability and suitability for specific applications. NMP is a very attractive CRP system because it is metal free thus the removal of transition metal catalyst is not required. However, this technique is mostly efficient for controlling the polymerization of styrene [61-63] and acrylates. It is difficult to control the polymerization of methacrylates, although interesting copolymerization concepts have been reported [64-66]. The ATRP method proposed by Sawamoto and Matyjaszewski has been successfully applied to a wide variety of monomers, including styrenics, acrylates, methacrylates and acrylonitrile. The significant advantage of ATRP is that the polymerization rates in ATRP can be easily adjusted through a wide variety of metal complexes and ligands [54]. Moreover, the broad choice of initiators and all reagents used in ATRP are generally commercially available. Nevertheless, purification after

polymerization is required due to the use of transition metals. RAFT is a successful CRP process due to its applicability to a wide range of monomers. This technique is also highly suitable for polymerization in aqueous and physiological media [67,68]. Among these three CRP techniques, NMP still attracts much interest because the process is experimentally simpler than ATRP and RAFT. Moreover, this technique is probably one of the most suitable for controlling the radical polymerization of styrene derivatives. Since *para-* substituted styrene derivatives were studied in this thesis (see general introduction), NMP was chosen as a CRP method. Thus, this technique will be described in more details in the following section.

I.3.1.2. Nitroxide-mediated polymerization (NMP)

I.3.1.2.1. Background

SFRP has gained interest due to the simplicity and robustness of the polymerization system to prepare well-defined polymers. In 1982, Otsu and coworkers were the first to use stable free radicals as mediators in radical polymerization. However, the polymer obtained did not exhibit well-controlled characteristics because the thiocarbamate radicals used in the system reacted directly with monomers to form polydisperse polymers with uncontrolled molecular weight [69,70]. Various systems have been developed regarding the use of stable free radicals as controlling agents for controlled radical polymerization such as nitroxide, triazolinyl [71-73] and verdazyl [74-76]. The most widely used one is nitroxide and has been first reported by Solomon and coworkers [46,47]. In their first investigation nitroxide worked very well but the resulting alkoxyamine was too stable when the polymerization was conducted at low temperature (60 °C) [77,78].

In 1993, Georges et al. [79] successfully demonstrated the controlled polymerization of styrene using a bimolecular initiating system in the presence of benzoyl peroxide (BPO) and the mediating stable free radical TEMPO (2,2,6,6-tetramethyl-1-piperidynyl-*N*-oxy). Molecular weights as high as 150000 g·mol^{-1} were observed and the obtained polystyrene exhibited polydispersity indices which were below 1.3. Moreover the molecular weights of the polymers increased linearly with conversion indicating a constant propagating radical concentration.

I.3.1.2.2. Basic mechanism: reversible termination processes in NMP

The typical mechanism of nitroxide-mediated controlled polymerization of styrene is illustrated in **Scheme 2** where the system is initiated with benzoyl peroxide (BPO).

$$K = k_d/k_c$$
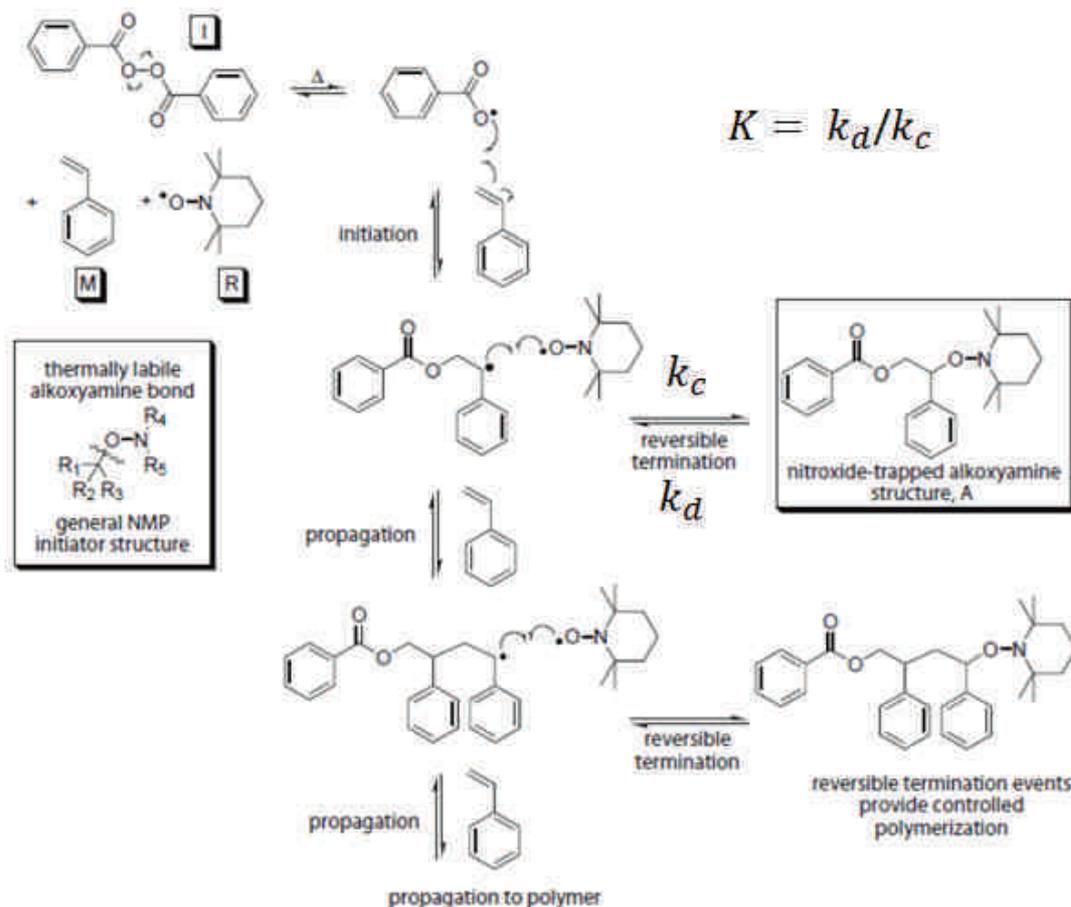
Scheme 2. Controlled polymerization of styrene using benzoyl peroxide (BPO) as an initiator and TEMPO as the mediating radical reported by Georges. Adapted with permission from reference [80].

The reaction starts with the formation of benzoyloxy primary radicals that initiate the polymerization of styrene [77]. The polystyrene radical is rapidly trapped by a nitroxide (TEMPO) but the formed C-O bond between styryl and TEMPO is thermolabile and reversible. Thus, the formed alkoxyamine bond dissociates into TEMPO and a macroradical which can react with additional monomers before being trapped again by TEMPO. The control in this system is essentially provided by the reversible termination reaction between dormant and active species. In fact, the trapping of the propagating chain by the stable nitroxide ensure the decrease in concentration of the propagating macroradicals.

Consequently, the termination by coupling or other side reactions is reduced, thus allowing the preparation of polymers with controlled molecular weight and narrow molecular weight distribution, while maintaining living alkoxyamine chain ends. In NMP processes, the values of the equilibrium constant K (k_d/k_c) are low meaning that a living chain spends most of its polymerization time in the dormant state. Actually, the exchange process between dormant and active species during the polymerization time should be fast compared to the propagation step in order to maintain the concentration in radicals in the polymerization medium low thus all living chains growth at the same rate and will have similar molecular weights resulting in narrow molecular weight distributions. On the other hand, if the exchange process is very slow, the polymers with broad molecular weights distributions can be obtained [81].

The kinetics of NMP were explained by the persistent radical effect (PRE) which was introduced by Fischer [82-84]. A typical example of the reaction governed by the persistent radical effect is the reversible homolysis of the alkoxyamine which is the key step in NMP. Indeed, the persistent radical effect was involved when alkoxyamine generated the persistent (nitroxide) and transient radical (growing radical) with equal or similar rate. The transient radical can react with itself by radical coupling, whereas the persistent radical cannot. As a consequence, the concentration of the transient radical decreases progressively by irreversible termination with themselves while the concentration of the persistent radical increases [85].

I.3.1.2.3. Mediating species and initiating systems

In early studies [79,86,87], TEMPO was used as a stable nitroxide to prepare polystyrenes with high molecular weights and narrow molecular weight distributions. Fukuda et al. proposed a direct method to determine k_d based on the use of SEC observation at the early stage of the polymerization of a PSt-TEMPO system at 125 °C [88]. The value of k_d was found to be 1.6 x 10^{-3} s^{-1} and when using the measured value of K reported in their previous work [89], thus k_c was given as 7.6 x 10^7 M^{-1} s^{-1}. Due to its low dissociation rate constant, TEMPO can only be used for the polymerization of styrene-based monomers at relatively high temperature (120 °C). TEMPO was found to be not sufficient to mediate the polymerization of acrylates and methacrylates due to their high activation-deactivation equilibrium constant. Moreover, in the case of NMP polymerization of methacrylate the β-hydrogen transfer from the propagating radical to the nitroxide occurs [90]. This side reaction

can be explained by the fact that at the beginning of the polymerization of MMA initiated by TEMPO the irreversible termination between two propagating radicals is predominant leading to an increase in nitroxide concentration hence the possibility to transfer β-hydrogen of the propagating MMA radical to nitroxide becomes higher. For these reasons, many other contributions have been made to develop new nitroxides for the controlled polymerization of non styrenic monomers. Some commonly used nitroxides are illustrated in **Figure 21**.
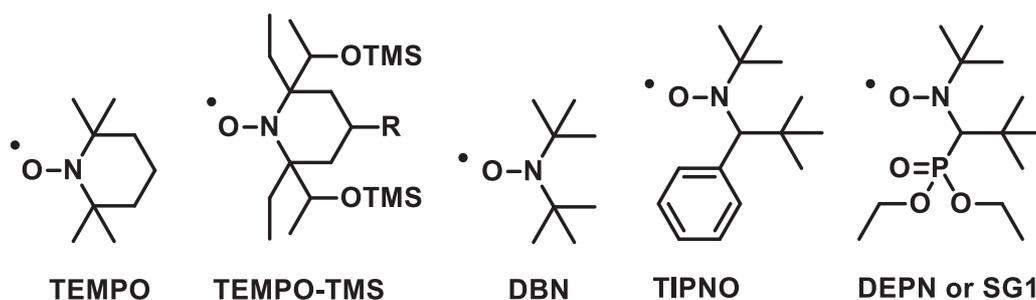
Figure 21. Exemples of nitroxides.

For instance, TEMPO-TMS was successfully used to mediate polymerization of butyl acrylate at 70 °C [91]. Using this steric nitroxide, the bond dissociation energy of the formed alkoxyamine was found to decrease [92,93]. Fukada and coworkers studied the polymerization of *tert*-butylacrylate (*t*BA) mediated by di-*tert*-butyl nitroxide (DTBN) [94]. Actually, the polymerization of *t*BA was already attempted with TEMPO at 120 °C but the obtained polymer exhibited very broad molecular weight distribution. Regarding the *t*BA-DTBN system, the obtained polydispersity was not as low as compared to PSt-TEMPO this may due to the larger rate constant of decomposition in the former system. However, the use of the nitroxide DTBN with the addition of a small amount of dicumyl peroxide (DCP) radical initiator allows the control of *t*BA polymerization at 120 °C. In fact the loss of growing radical through termination occurred in the polymerization of *t*BA initiated by BS-DBN (benzoyloxy 1-phenyl ethyl-DTBN). The addition of small amount of DCP initiator helped to generate a new growing radical and handle the rate of polymerization without affecting the polydispersity.

The development of bulkier nitroxides which contain hydrogen atom in α position of nitroxide NO moiety including TIPNO (2,2,5-tri-methyl-4-phenyl-3-azahexane-3-nitroxide) [95] and DEPN (*N-tert*-butyl-*N*-(1-diethylphosphono-2,2-dimethylpropyl)) [96-99] facilitated

the control of a broad range of monomers such as acrylates and acrylamides . These nitroxides were in general unstable and the NO-C bond supposed to decompose at lower temperatures. TIPNO [100,101] was found to be efficient to mediate the polymerization of styrene and *n*-butyl acrylate (*n*BA). DEPN was synthesized and successfully tested in bulk controlled radical polymerizations of styrene and *n*-butyl acrylate. This new type of nitroxide allows faster polymerization and the polymerization can be controlled at lower temperature than TEMPO mediated polymerization. Benoit et al. determined K of the system of DEPN-mediated polymerization of styrene at 120 °C as 6.0 X 10^{-9} M which is larger than that of the TEMPO system [97]. To conclude, the efficiency of polymerization increased with increased steric bulk of the nitroxide. Furthermore, bulkier nitroxides has a large effect on k_c as well as k_d, it can decrease the bond dissociation energy of C-O bond formed during polymerization which facilitated C-O homolysis at lower temperature. All of the studies indicated that the nitroxide structure play a crucial role in the success of controlled polymerization of acrylates and acrylamides.

Both bimolecular and unimolecular initiator systems can be used in NMP. Unimolecular initiators are alkoxyamine derivatives that decompose into an initiating radical and a nitroxide. These systems are more efficient for initiating radical polymerization because they are less subject to the solvent cage effect than classical thermal initiators. Their C-O bond decomposes upon heating to release the initiating species and the nitroxide in a 1:1 molar ratio thus the initiator efficiency is almost 1 [102]. Moreover, well-defined structure of the chain end could be obtained due to the attachment of initiating species and nitroxide at the α-chain end and ω-chain end respectively. For instance, Hawker and coworkers [103] reported that a TEMPO-based alkoxyamine gave a better control at higher molecular weight and narrow molecular weight distribution compared to corresponding bimolecular initiator. Unimolecular system is simply based on the alkoxyamine presented at the chain end of dormant species formed during the NMP polymerization. Rizzardo and Moad [104] investigated the polymerization mediated by different type of alkoxyamines, the results showed that the alkoxyamine homolysis rates increased with the size of the substituents and the radical stability of the alkoxyamine and additionally the steric and polar factors were considered important to determine the C-O bond homolysis. In recent years, Arkema commercializes a SG1-based alkoxyamine derived from BlocBuilder to control radical polymerization. This new alkoxyamine consists of an initiating species and a nitroxide

controlling agent in one molecule. As illustrated in **Figure 22**, upon heat treatment, the alkoxyamine generates by homolytic cleavage, a methacrylic acid radical that initiates the polymerization and *N*-tert-butyl-*N*-(1-diethylphosphono-2,2-dimethylpropyl) nitroxide (DEPN), so-called SG1, that controls the polymer chain growth.
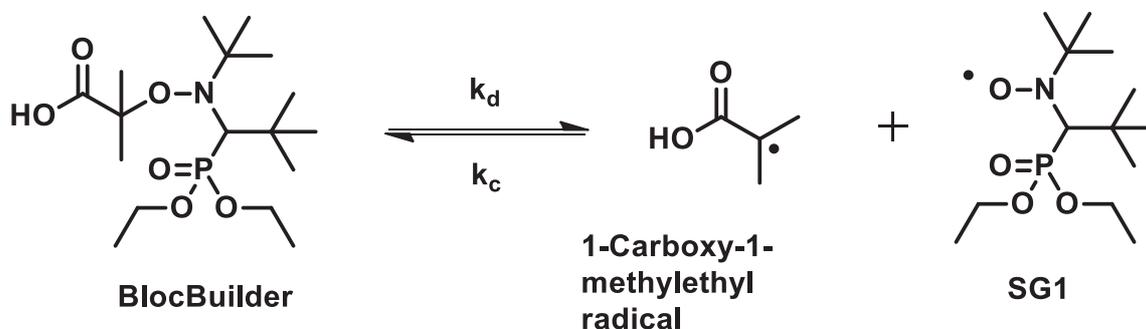
Figure 22. Decomposition of BlocBuilder mono-alkoxyamine.

Nicolas and coworkers [64] have reported the use of SG1-based alkoxyamine to control the polymerization of MMA at low temperature (90 °C). The polymerization was successfully controlled by introducing a small amount of styrene (8.8 mol %). This addition of comonomer may help to reduce the activation-deactivation equilibrium constant of the system. Later, well-defined poly(MMA) was successfully prepared by bulk NMP polymerization in the presence of 2.2–8.8 mol % of acrylonitrile (AN) using BlocBuilder alkoxyamine [105]. The authors demonstrated the poly(MMA-*co*-AN) exhibited controlled characteristics when the polymerization was performed at relatively low temperature (90-99 °C). The first order kinetics of the system was observed and the obtained polymers possessed low polydispersities. Moreover well-defined block copolymers could be envisaged due to the high degree of livingness of the chain-end functionality of polymers.

I.3.2. Copolymers in radical polymerization

Different types of copolymers can be obtained in conventional and controlled radical polymerizations depending on the reactivity of the comonomers used. Monomer reactivity in radical polymerization has been described by Alfrey et al. [106]. The authors reported that in a copolymerization process, the propagation step depends on the monomer species therefore each propagating chain has two possibilities to grow by reacting either with the same kind of

molecule or with another. Hereby, four separate propagation steps are considered and each propagation step has its own rate constant. For instance, for the copolymerization of two monomers, *A* and *B*, [107] four competing propagation steps of this copolymerization process are expected as shown in **Scheme 3**. During the course of the polymerization, propagating chains with a terminal active units either *A* or *B* designated as $A^\cdot$ and $B^\cdot$ respectively are present and able to add either monomer *A* or monomer *B* leading to four possible propagating reactions. When a propagating chain has the tendency to react with the same kind of monomer, the propagation is called self-propagating as illustrated in reactions (1) and (4) in **Scheme 3**. On the other hand, as clearly showed in reactions (2) and (3), a propagating chain can grow by addition of the other monomer, thus the propagation in this case is termed cross-propagation. The rate constant of this propagation step is represented as k_{AA} for a propagating chain $A^\cdot$ adding to monomer *A* and k_{AB} for a propagating chain $A^\cdot$ adding to monomer *B*, and so on.
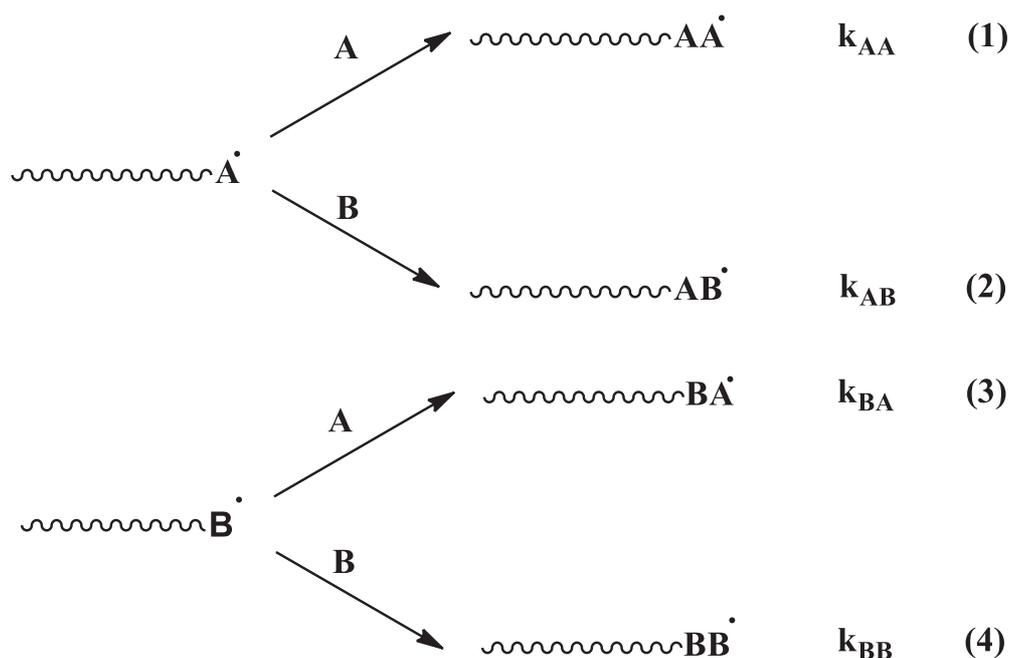
Scheme 3. Four propagating reactions occurring during a free radical copolymerization of monomer A with monomer B.

It is important to note that during a copolymerization process, since the two monomers (i.e. *A* and *B*) are consumed at different rates, the composition in the two monomers of the copolymer formed will relatively change over time. Therefore, the separate rate of

disappearance of each monomer can be given as illustrated in the equations (5) and (6). The behavior of monomers when entering to a copolymerization was derived in equation (7) by Mayo and Lewis [106].

$$-\frac{d[A]}{dt} = k_{AA}[A^\cdot][A] + k_{BA}[B^\cdot][A] \quad (5)$$

$$-\frac{d[B]}{dt} = k_{AB}[A^\cdot][B] + k_{BB}[B^\cdot][B] \quad (6)$$

$$-\frac{d[A]}{d[B]} = \frac{k_{AA}[A^\cdot][A] + k_{BA}[B^\cdot][A]}{k_{AB}[A^\cdot][B] + k_{BB}[B^\cdot][B]} \quad (7)$$

These rate constants could be used actually to determine the monomer reactivity ratio of the corresponding monomer. The monomer reactivity ratio (r) defined as the ratio of the propagation rate constant for a propagating chain adding to the same kind of monomer to the propagation rate constant for its addition to the other monomer. For example, reactivity ratio of monomer A (r_A) and monomer B (r_B) are represented as:

$$r_A = \frac{k_{AA}}{k_{AB}} \text{ and } r_B = \frac{k_{BB}}{k_{BA}}$$

In the copolymerization process, the reactivity of each monomer represents its tendency to copolymerize and the value is in general between zero and unity. In the case where r_A value is greater than unity, it means that the propagating chain $A^\cdot$ prefers the addition of monomer A than monomer B, thus the tendency would be to form a block copolymer. In contrast, if the value of r_A is less than unity the propagating chain $A^\cdot$ will preferentially add to monomer B. Additionally, if both reactivity ratios are equal to unity, each monomer does not have a preference to add either A and B to the propagating chain resulting in random structures. Moreover, when the product of the reactivity ratios of both monomers ($r_A r_B$) is zero or close to zero, it means that the two monomers prefer to adds to other monomer (i.e. $A^\cdot$ adds only to B and $B^\cdot$ adds only to A) thus copolymers with alternating monomer sequence will be formed (**Figure 23**).
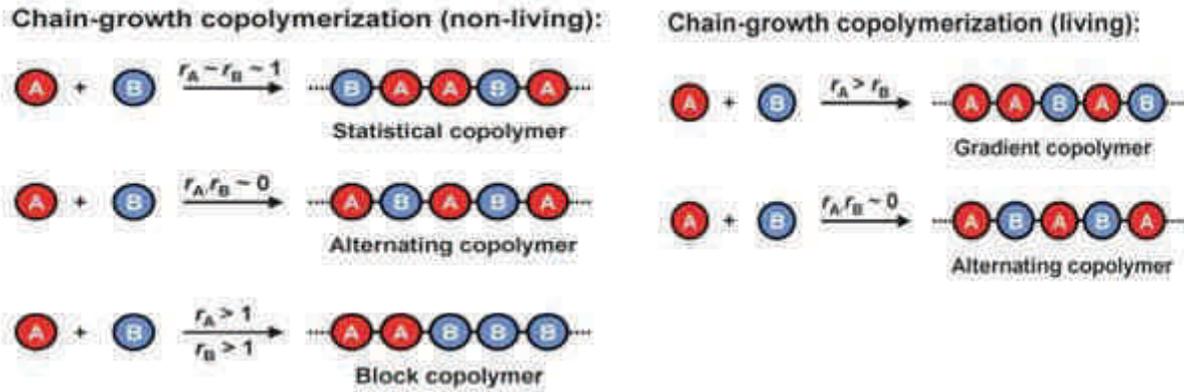
Figure 23. Microstructures attainable in free radical polymerization and controlled/living polymerization. Reprinted with permission from reference [108].

If we considered a steady-state approximation in the copolymerization the concentration of the intermediate active growing chains $A^{\cdot}$ and $B^{\cdot}$ remains constant. Thus their rates of cross-propagation must be equal as illustrated in equation (8). By applying the equation (8) to (7) and by introducing the monomer reactivity ratio terms, the copolymer composition equation has been established as in equation (9) [106].

$$k_{AB}\,[A^{\cdot}][B] = \; k_{BA}\,[B^{\cdot}][A] \quad (8)$$

$$\frac{d[A]}{d[B]} \; = \; \frac{[A]}{[B]}\,\frac{r_A\,[A] + [B]}{[A] + \, r_B\,[B]} \quad (9)$$

In fact, this copolymer composition depends on the concentration and the reactivity of the two monomers. In addition, at a given concentration, the mole fraction of monomer in the feed (f) and in the copolymer (F) could be determined as indicated below (equations 10 and 11). If the mole fraction of two monomers in the feed was known the mole fraction of monomers in the copolymer can be expressed as in equation (12).

$$f_A \; = 1 - f_B \; = \; \frac{[A]}{[A] + [B]} \quad (10)$$

$$F_A \; = 1 - F_B \; = \; \frac{d[A]}{d[A] + d[B]} \quad (11)$$

$$F_A \; = \; \frac{r_A f_A^2 \; + \; f_A f_B}{r_A f_A^2 \; + \; 2 f_A f_B \; + \; r_B\,f_B^2} \quad (12)$$

The determination of the monomer reactivity ratios have been reported in the literature [109-111]. For example, Minoura and coworkers [112] studied the copolymerization of St and maleic acid (MAc) in an emulsion system (benzene/water mixture) at 40 °C using potassium persulfate (KPS) as initiator. Since styrene, maleic acid and KPS were not present in the same phase hence the addition of a chiral catalyst lecithin was needed to emulsify the system. The results showed that the monomer reactivity in oil/water interfacial system depend on the amount of lecithin. For example, when the lecithin was added in too large quantities, a wall of micelle was formed. Consequently, the rate of polymerization decreased due to this formation preventing the monomers to come close to each other. However, when the reaction was performed in solution in THF, the addition of lecithin did not influence the rate of polymerization because the degree of asymmetric induction in the homogeneous system is much lower than that in the emulsion system. Additionally, the observed apparent monomer reactivity ratios of styrene and maleic acid in the THF solution system were 0.25 and 0.1 respectively. Moreover, using different initiators, various monomer compositions in the polymer chain could be obtained. When the copolymerization was initiated by KPS, styrene was not present in the copolymer. The composition of styrene was observed to be richer in the system initiated by azobisisobutyronitrile (AIBN) or benzoyl peroxide (BPO). This difference in styrene composition was explained by the fact that styrene, AIBN and BPO are soluble in benzene whilst KPS is not.

Lately, Ponratnam and Kapur [113] have reported the reactivity ratios of acid and basic comonomers such as acrylic acid (AA) and acrylamide (AM). The copolymerization system was conducted in aqueous solution with different values of pH. The monomer reactivity ratios were observed for a copolymerization system at pH = 2 as 0.92 and 0.25 for AA and AM, respectively. When the pH of the medium was changed for example, at pH = 9, the new values of reactivity ratios were determined as 0.3 and 0.95 for AA and AM respectively. The authors explained that at high pH the formed acrylate anion has the tendency to copolymerize with the propagating radical of acrylamide monomer resulting in a decrease in the monomer reactivity ratio value. The reactivity ratios of these two monomers were also determined in other different pH [114] and they obtained the similar results.

In 1979, Ledwith et al. [115] reported the monomer reactivity ratio of MMA and *N*-vinylcarbazole (VCZ). The radical copolymerization was performed in methanol solution at 55 °C using AIBN to initiate the system. The reactivity ratio values of 0.57 and 0.75 were determined for MMA and VCZ, respectively. On the other hand, another monomer reactivity ratio values were observed when the copolymerization was performed in benzene (1.80 for MMA and 0.06 for VCZ). The authors explained that the increase in VCZ monomer reactivity ratio value in methanol arises from the fact that VCZ is not soluble in methanol so it forms a microphase containing the growing copolymer chains in which VCZ is preferentially partitioned. Different solvents such as acetone and isopropanol were used in order to examine the polarity effect. It has been shown in these investigations that the polarity has no effect on monomer reactivity ratio because when the copolymerization of VCZ and MMA was performed in acetone and benzene, similar values were observed while the polarities of benzene and acetone are much different. However, the effect of polarity of the solvent on the monomer reactivity ratio has been studied later. For instance, Boudevska and Todorova investigated the free radical copolymerization of MAh with St. The copolymerizations were performed in different solvents [116]. They showed that the obtained monomer reactivity ratios of MA and St were different in each experiment. For example, when the copolymerizations were performed in chloroform and acetonitrile, the reactivity ratios of MAh were determined as 0.51 and 0.06 respectively. They concluded that the interaction between the carboxylate species of MA and the solvent maybe occurred and cause the monomer reactivity ratio. In this case, the reactivity of MA decreased when increasing the polarity of the solvent system. In contrast, the monomer reactivity ratio of nonpolar monomers such as St increased when the polarity of the solvent increased (0.08 and 0.29 in chloroform and acetonitrile respectively).

Müller and coworkers have determined the monomer reactivity ratio of *n*BuA and MMA by investigation the ATRP polymerization in ethyl acetate at 90 °C using methyl 2-bromopropionate (MBP) as initiator, CuBr as metal catalyst, and 4,4′-di(5-nonyl)-2,2′-bipyridine (d*N*Bipy) as ligand [117]. The reactivity ratios of these comonomer pairs were determined by the Jaacks [118] and Kelen-Tüdös method [119]. It was found that, the reactivity ratios of *n*BuA and MMA obtained from these two methods led to similar results (r_{nBuA}= 0.39 and 0.36, r_{MMA} = 2.19 and 2.07, determined by Jaacks and Tüdös methods respectively.

Some of the monomer reactivity ratios of common comonomer pairs are listed as examples in **Table 1**.

Table 1. Monomer reactivity ratio of common comonomer pairs in free radical polymerization [120].

Monomer 1	r_1	Monomer 2	r_2
Ethylene	0.130	Vinyl acetate	1.230
Styrene	0.290	Acrylonitrile	0.020
	0.097	Maleic anhydride	0.001
	0.057	Maleimide	0.088
	0.585	Methyl methacrylate	0.478
	0.820	Butadiene	1.380
	1.7	Vinylidene chloride	0.110
	0.282	Vinylbenzoic acid	1.029
Maleic anhydride	0	Acrylonitrile	6
	0.012	Methyl acrylate	2.788
	0.02	Methyl methacrylate	5.2
Vinyl acetate	0.018	Butyl acrylate	3.480
Vinyl chloride	0.040	Butadiene	8.8
	0.160	Styrene	23.920

In 1947, Alfrey and Price [121] developed the $Q - e$ scheme (equations 12 and 13) to predict the propagation rate of the reaction and particularly the reactivity of comonomer pairs that have not yet been copolymerized. Three interesting parameters presented in the scheme are the intrinsic reactivity of the propagating chain A (P_A), the intrinsic reactivity of monomer A (Q_A), and the polar factor of monomer A (e_A). From this correlation between intrinsic reactivity and monomer structure, the monomer reactivity ratio can be obtained according to equation (14).

$$k_{AA} = P_A Q_A \exp(-e_A^2) \qquad (12)$$

$$k_{AB} = P_A Q_B \exp(-e_A e_B) \qquad (13)$$

$$r_A = \frac{k_{AA}}{k_{AB}} = \frac{Q_A}{Q_B} \exp(-e_A(e_A - e_B)) \qquad (14)$$

As evidently showed in $Q - e$ scheme the reactivity ratio of monomer is related actually to their structure. Hence three important factors have been considered:

1) <u>Steric effect</u>: the monomer reactivity with their radical may depends on the steric hindrance as illustrated by the work of Dawson [122]. They showed that *trans* isomer of 1,2-dichloroethylene was more reactive than the *cis* structure due to the inability of the latter to achieve the coplanar conformation in the transition state. Moreover, the reactivity of di-, tri-, and tetrasubstituted ethylene has been studied. The disubstituted ethylene was found to be less reactive than vinyl chloride due to steric hindrance.

2) <u>Resonance stabilization effect</u>: monomers exhibiting substituted unsaturation can stabilize the derived radical because of the delocalization of their π-electron leading to radical with a relatively lower reactivity but in other word the monomer itself is more reactive.

3) <u>Polar effect</u>: the reactivity of the monomer increases when two comonomer pairs have a larger difference in polarity.

Especially in radical polymerization, the polarity of the double bond is considered as an important parameter. For instance, when two monomers possessing different polarities, i.e. one has an electron rich double bond and one has an electron poor double bond, react together, the attraction of the different charges facilitates cross-propagation. Notable examples of electron-acceptor are maleic anhydride and maleimides. These electron acceptor monomers have no tendency to homopolymerize but are able to form alternating copolymers with electron donor monomers such as styrene [123]. It should be noted that the substituent on the monomer can influence the polarity of the double bond of the monomer. However, it is possible to use the $Q - e$ scheme to predict the behavior of the copolymer. For example, the tendency toward alternation is greater for monomers having more or less the same Q values with high e values of opposite sign. This latter requirement is due to the possibility to have a strong interaction between electron acceptor monomer and electron donor radical and vice versa resulting in a decrease in the activation energy for cross-propagation as evidently seen by *e* value of styrene and maleic anhydride. The notable values of Q and e corresponding to specific monomers are shown in **Table 2**

Table 2. Q-e values of common monomers [124].

Monomer	Q	e
Styrene	1	-0.8
Maleic anhydride	0.86	3.69
Methyl methacrylate	0.78	0.40
Methacrylic acid	0.98	0.62
Ethylene	0.016	0.05
Butadiene	1.70	-0.50
Vinyl chloride	0.056	0.16
Maleimide	0.94	2.86
Acrylamide	0.23	0.54

I.3.2.1. Alternating copolymers based on donor-acceptor radical copolymerization in stoichiometric conditions

In the past years, many works based on donor-acceptor copolymerizations which allow the preparation of alternating copolymers using radical polymerization methods have been published [125-128]. In particular, the copolymerizations of the common system such as styrene (St) and maleic anhydride (MAh) have been studied in the literature. It was reported that the homopolymer of MAh can be obtained only in very low polymerization degree. This observation simply indicated that this monomer preferred to copolymerize with other monomers especially donor monomers of vinyl type such as St. For instance, Alfrey and coworkers published at the early 1940's the work on the copolymerization of St and MAh [128]. In this study, the polymerization was investigated in benzene solution and the system was initiated by BPO. The monomer feeds in each experiment were varied in order to determine the copolymer compositions. It was found that the mole fraction of these two monomers in the copolymers were unimolar ($\approx$ 1:1) until the ratio of the initial feeding of St and MAh was up to 5:1. Nevertheless, the mole fraction of MAh was decreased when the initial feed of St increased to 20. Similar results have been reported later in the literature [129,130]. Pan and coworkers have lately prepared the controlled alternating copolymer (St-

alt-MAh) in the presence of dibenzyl trithiocarbonate (DBTTC) [131]. The controlled fashion of this copolymerization was evidenced by the linear evolution of ln([M]$_0$/[M]) versus time and the narrow molecular weight distribution of the obtained copolymers ($\approx$ 1.19-1.3).

There are not only the MAh comonomer that can formed alternating copolymers with St [132]. The use of *N*-maleimides (MIs) as acceptor monomers has been successfully demonstrated since the last decades. For instance, In 1959, Coleman and Conrady [133] prepared alternating copolymers by copolymerization of *N*-butyl and *N*-dodecyl maleimide with either styrene or methyl methacrylate using AIBN as initiator. They found that the ratio of molar fraction in copolymer of *N*-butyl maleimides and styrene was 1 in all cases. On the other hand, a ratio of 3 was obtained in the case of copolymerization of *N*-butyl maleimides and methyl methacrylate. Yamada et al. investigated [134] later the copolymerization of St with three different *N*-substituted maleimides such as *N*-methylol maleimide (MMI), *N*-2-hydroxyethyl-maleimide (HEMI) and *N*-4-hydroxyphenyl maleimide (HPMI) [135]. Alternating copolymers were obtained in all cases. Li and coworkers have successfully synthesized the alternating copolymer of *N*-(2-acetoxy-ethyl)maleimide (AEMI) and *N*-phenylmaleimide (PhMI) using ATRP method. The 1:1 alternating copolymers were obtained with narrow molecular weight distribution.

Other donor-acceptor comonomers pairs have been also used to form alternating copolymers. For example, Mikava and coworkers [136] reported the copolymerization of *N*-vinylcarbazole (VCZ) with electron acceptor monomers such as fumaronitrile (FN) and diethyl fumarate (DEF) in benzene solution using AIBN as an initiator. The copolymer composition of these comonomers was determined as 1:1 in both cases even if the monomer feed ratio of VCZ was varied. These results confirmed the formation of alternating copolymers between VCZ and FN or DEF monomers. Matyjaszewski and coworkers studied alternating RAFT polymerization of MMA with St in the presence of a Lewis acid at 60 °C [137]. During the propagation step, the complex between MMA monomer and diethylaluminum chloride (Et$_2$AlCl) used as Lewis acid was formed. The methacrylic radical is therefore unable to self-propagate but strongly enhances the cross-propagation. The use of a Lewis acid in a RAFT process allows synthesizing sequence-controlled alternating copolymers with predetermined molecular weights and narrow molecular weight distributions (M_w/M_n < 1.4). Nevertheless, alternating copolymers with high molecular weight cannot be

obtained due to the decomposition of dithioesters by side reactions with this Lewis acid. Consequently, RAFT polymerizations using other Lewis acids [138] such as tin (IV) chloride (SnCl₄), zinc chloride (ZnCl₂), or ethylaluminum sesquichloride (EASC) were studied. The authors reported that in the case of strong acids such as $SnCl_4$ and $ZnCl_2$ no control of the radical copolymerization was observed as evidenced by getting a very broad molecular weight distribution (the value was 3.74 when $ZnCl_2$ was used). On the other hand, in the presence of EASC, MMA and St were copolymerized in a controlled manner. The addition of a Lewis acid enhanced the electron donor character of the monomer by complexion to the lone electron pairs of the acceptor monomer leading to the decrease of the electron density of the acceptor monomer double bond. Furthermore, Lewis acid can be added to other kind of copolymerization such as styrene with acrylonitrile [139], styrene with methyl methacrylate [140], and isobutene with acrylonitrile [141] resulting in alternating copolymers.

I.3.2.2. Sequence-controlled polymers based on radical copolymerization in non-stoichiometric conditions

As described above, alternating copolymers can be synthesized by the copolymerization of donor-acceptor comonomers. Nevertheless, non-equimolar copolymerization was also interesting since it allows preparing polymers with controlled primary structure. For example, Hawker and coworkers [142] studied the NMP copolymerization using nine equivalents of styrene (St) and one equivalent of maleic anhydride (MAh). At the early stage of the polymerization, the rapid incorporation of maleic anhydride on the growing polystyrene chain occurred, and upon the complete consumption of maleic anhydride, styrene was purely homopolymerized yielding finally functionalized block copolymers with low polydispersity. Lately, the radical addition-fragmentation chain transfer (RAFT) copolymerization of St and MAh with a molar feed of 9:1 was examined by Li and coworkers [143]. Kinetics followed by gas chromatography showed that the conversion of MAh apparently increased faster than those observed for St. After MAh was completely consumed, the unreacted styrene continually propagated forming a block copolymer. Additionally, as proved by atomic force microscopy (AFM), the amphiphilic block copolymer was obtained due to the hydrolysis of poly(MAh-*alt*-St) segment of the block copolymer. Instead of maleic anhydride, *N*-substituted maleimides (MIs) can also be used as acceptor

monomers. For instance, a new approach for preparing sequence-controlled polymers using sequential addition was proposed by our group (**Figure 24**) [38].
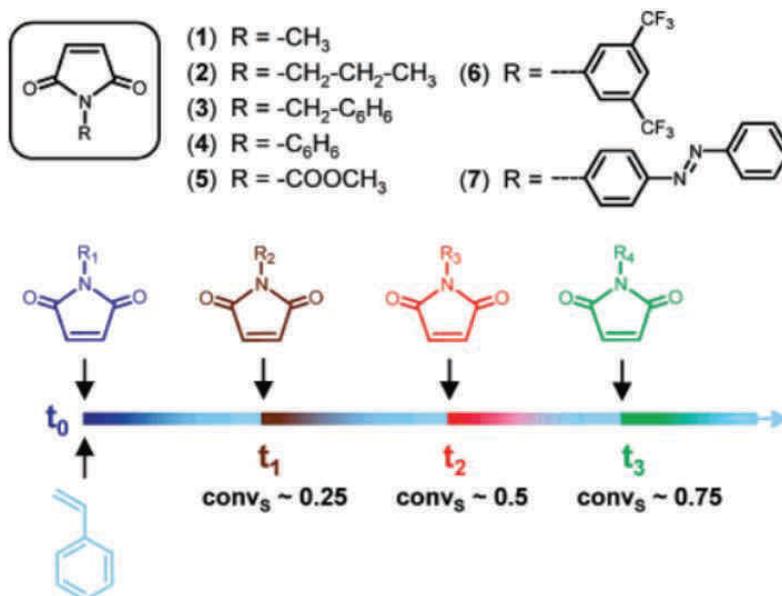
Figure 24. Concept of the sequential addition of various functional *N*-substituted maleimides during radical polymerization of styrene. Reprinted with permission from reference [38].

The concept is based on the atom transfer radical polymerization (ATRP) of a large excess of styrene in the presence of discrete amounts of four *N*-substituted maleimides, *N*-propyl maleimide (PrMI), *N*-benzyl maleimide (BzMI), *N*-methyl maleimide (MMI) and *N*-[3,5-bis(trifluoromethyl)phenyl] maleimide (TFMPMI) (**Figure 24**). The fast incorporation of small amounts of maleimide in the growing polystyrene chain can be explained by the fact that maleimides have a very low tendency for homopolymerization hence the cross-propagation with styrene was favorable. However, these polymerization procedures may have some limitations when more than four different maleimides were needed. Therefore, Chan-Seng et al. proposed later an automated polymerization protocol to overcome this limit [144].

The model used in this study still relied on the copolymerization of St with MIs but the polymerization technique was changed from ATRP to NMP polymerization technique using an automated platform. They demonstrated that up to eight BzMI can be added on polystyrene chains with a DP 100 and according to this process, similar kinetic behaviors of the automated and manual polymerizations were obtained. Moreover, different kind of maleimides can be potentially placed on the polystyrene chain using this automated platform

(**Figure 25**). For example, four different maleimides such as BzMI, PrMI, pentafluorophenyl 4-maleimidobenzoate (PFP-MI) and triisopropylsilyl protected *N*-propargylmaleimide (TIPS-MI) were precisely added at different places into the polystyrene backbone (**Figure 25**c). The obtained well-defined copolymers confirmed the viability of this robotic tool.
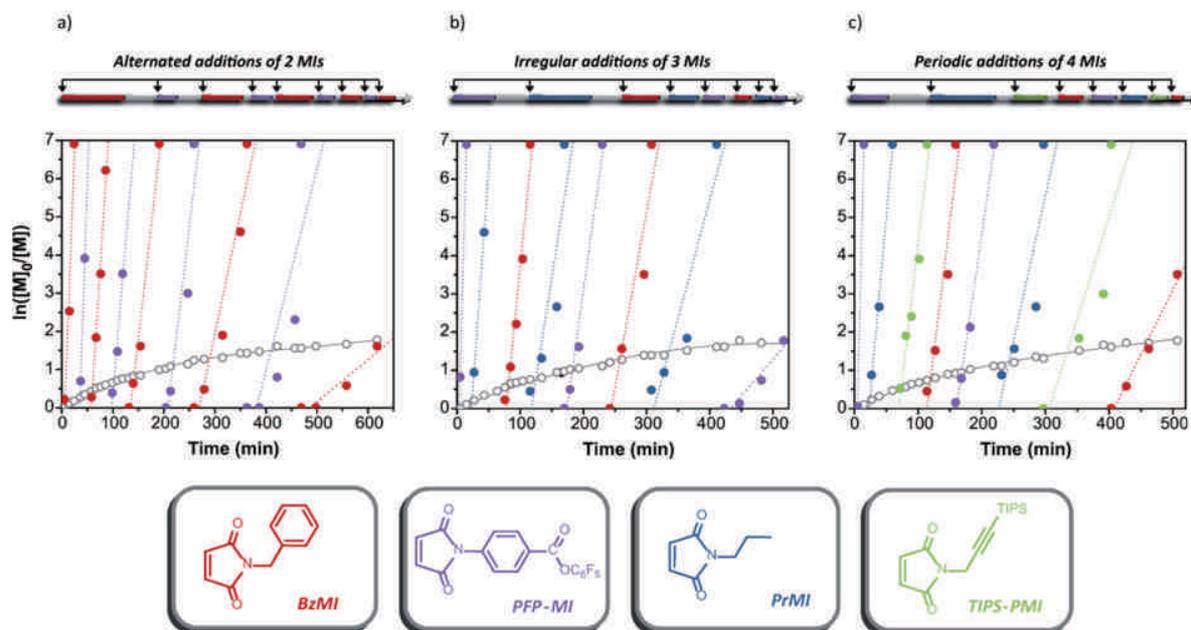
Figure 25. Automated preparation of complex monomer sequence patterns. Reprinted with permission from reference [144].

Although, the concept of precise positioning of monomers on synthetic polystyrene chains was successfully used, sequence defects are still present in these polymers. Some optimized conditions were therefore described to reduce these defects [145]. Firstly, the conditions which led to an ultra-precise incorporation of a single MI unit on a polystyrene chain were determined. As illustrated in **Figure 22**, 1 eq of PrMI was added at different places on the growing polystyrene chain. The situation (d) clearly showed that when PrMI was added near the end of the polymerization process, the insertion of the maleimide on a narrow area of the polymer chain is obtained. This phenomenon can be explained by the fact that for a non-equimolar feed mixture of donor and acceptor monomers, the tendency of AB alternation is always occurring in the early stages of the reaction thus the broad sequence distribution was formed. In contrast, when small amount of maleimide was added at almost the end of the reaction where the comonomer ratio of St and maleimide is very low, the precise incorporation could be obtained.
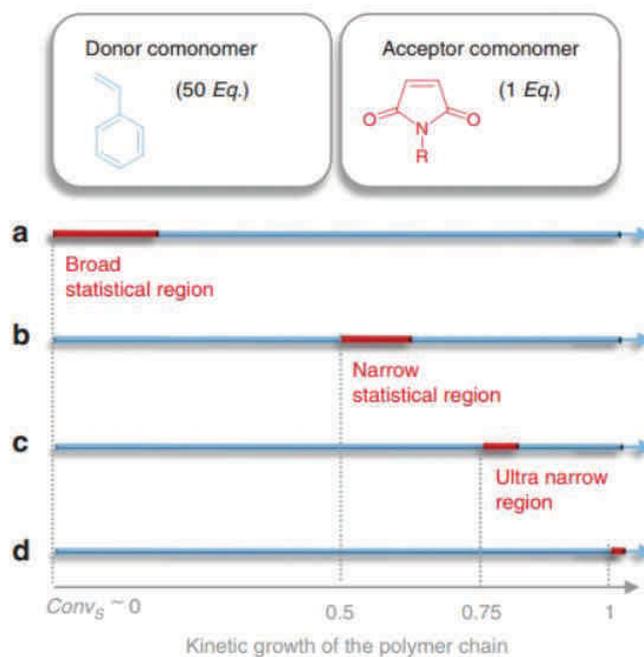
Figure 26. The obtained related microstructures for sequence-regulated polymers by controlled/living radical copolymerization of a large excess of styrene and *N*-substituted maleimide. Reprinted with permission from reference [145].

Combining the living polymerization mechanism with the optimized conditions identified above, various functional *N*-substituted maleimides can be added with ultra-precise insertion on the polymer chain (**Figure 27**). To achieve this goal, MI was added when the styrene is almost consumed. Afterwards, styrene was newly fed into the reaction, the growing polymer chain can be again reactivated due to the living character of the propagating chain and the second feed of MI can be done one more time near the end of the polymerization. Successive feeds of donor and acceptor monomers were indeed used in this study to keep ultra-narrow insertion of the latter. Actually, this process can be repeated several times for example, in this study, different MIs can be successively added up to three times per one polystyrene chain. Moreover, the second generation of controlled radical polymerizations such activators regenerated by electron transfer for atom transfer radical polymerization (ARGET ATRP) and single-electron transfer living radical polymerization (SET-LRP) was able to prepare ultra-precise sequence-controlled polymers using this approach.
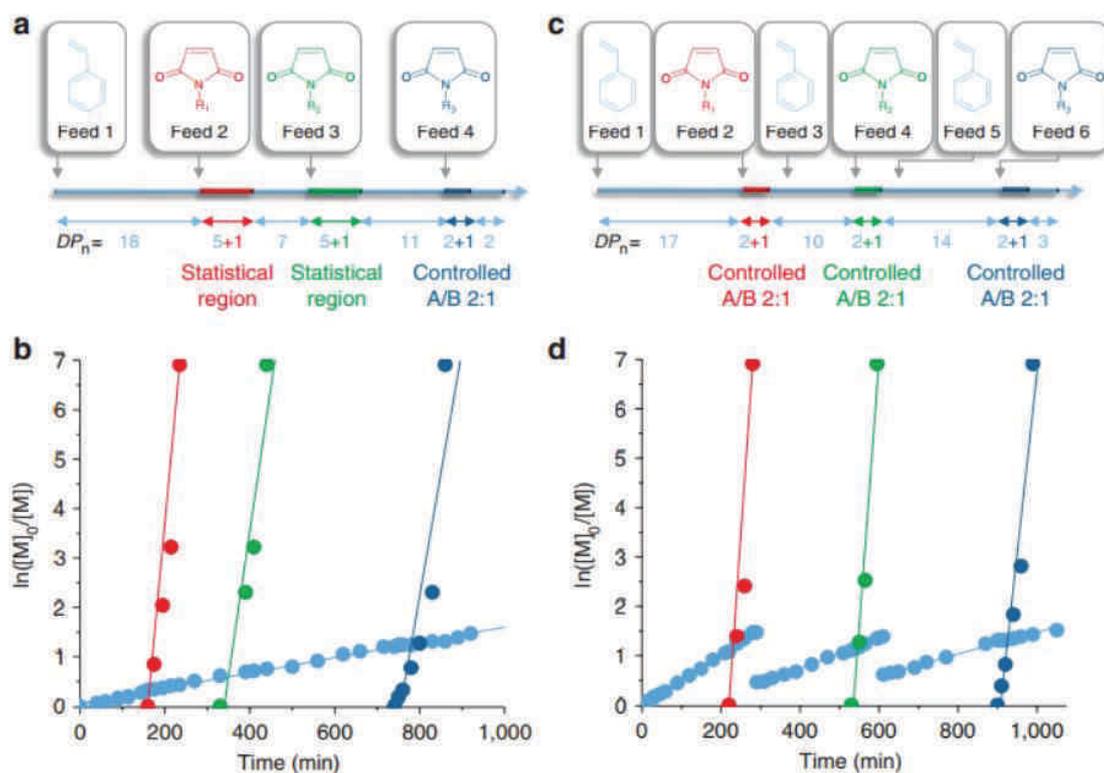
Figure 27. The conventional and ultra-precise synthesis of sequence-controlled polymers containing three different MIs by SET-LRP. Reprinted with permission from reference [145].

The sequence-controlled copolymerization of styrene and *N*-substituted maleimides was also used to prepare complex multifunctional polymers. For instance, our group has shown [146] that recognition biomolecules could be positioned on polystyrene chains using controlled radical polymerization techniques (**Figure 28**). First of all, polystyrene chains containing precise specific sites of three different protected *N*-substituted maleimides (MIs) were prepared by NMP process. Triisopropylsilyl protected *N*-propagylmaleimide (TIPS-MI) was firstly added at the beginning of the polymerization due to its high stability. After 50 % of styrene conversion triethylsilyl protected *N*-propagylmaleimide (TES-MI) was added, while trimethylsilyl protected *N*-propagylmaleimide (TMS-MI) was incorporated to the end of the polymer chain because among the three protecting groups TMS was the most labile. Next, the most labile protecting group, TMS, was first removed by treatment with K_2CO_3 in a methanol/water/THF mixture. Subsequently, mannose derivative reacted with the deprotected alkyne site by copper-catalyzed azide–alkyne cycloaddition (CuAAC) [147-150]. The next two selective deprotections of TES and TIPS and the attachment of galactose and

glucosamine were then carry out as illustrated in **Figure 28**. Quartz microbalance with dissipation monitoring (QCM-D) has been employed to recognize the sugars moiety of the copolymer with specific binding proteins (concanavalin A, Con A) for mannose, peanut agglutinin (PNA) for galactose and wheat-germ agglutinin (WGA) for *N*-acetylglucosamin. The result clearly confirmed that the biological activity of these three hexoses remained after polymer attachment.
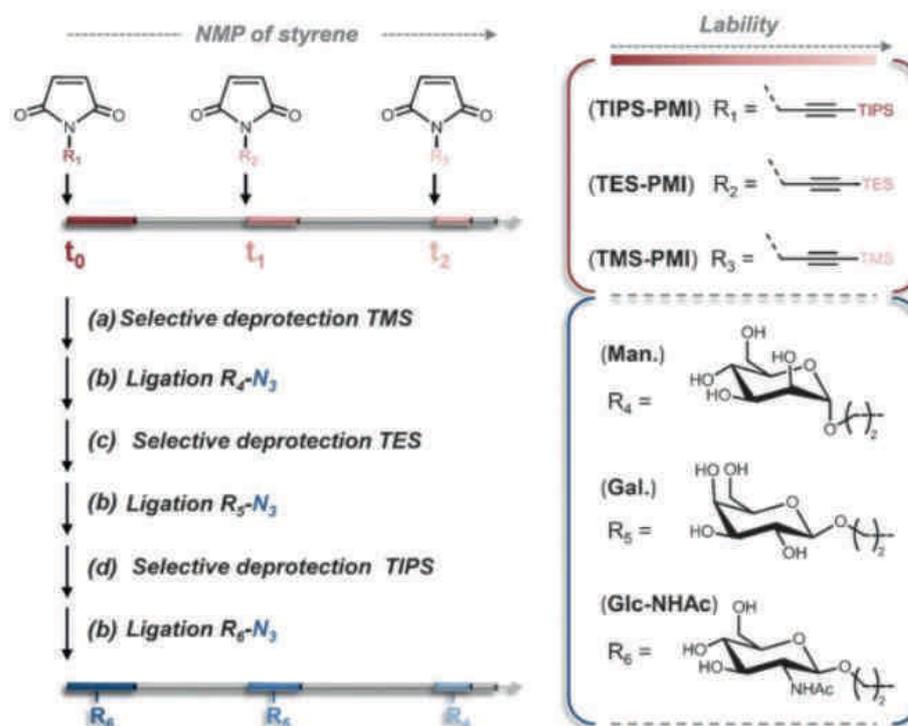
Figure 28. General strategy for the synthesis of single-chain sugar arrays. Reprinted with permission from reference [146].

To date, a diverse array of nanomaterials has been under development for biomedical applications such as water-soluble polymers and dendritic polymer architectures, especially dendritic architectures [151] which are one of the most pervasive topologies observed in nature at the macro- and microdimensional-length. Numerous synthetic strategies have been reported in the past years for the preparation of these materials which has led to a broad range of dendritic synthetic structures. For instance, a sequential monomer addition methodology proposed by our group was used to prepare sequence-controlled dendritic macromonomers [152]. The concept is still based on the copolymerization particularly using the NMP process of a large excess of styrene with a discrete amount of *N*-substituted maleimides. Especifically,

the maleimides used to be incorporated into the polymer backbone in this present study were substituted by a bulky functional dendron unit such as acetal-protected dendrons (D1-D3), alcohol dendron (D4-D5) and alkene dendron (D6) of various generations [153-156] (**Figure 29**). In this report two different models of copolymerization have been studied, in the first model the dendron was added at the beginning of the polymerization reaction and in the second model the dendron was added during the course of the polymerization. In all cases, dendron-substituted MIs were consumed after 20 min of the addition time. As evidenced by SEC characterization, these dendron-modified polystyrenes exhibited controlled molecular weight and narrow molecular weight distribution. Moreover, these local functional clusters can be modified using robust post-polymerization modification approaches.
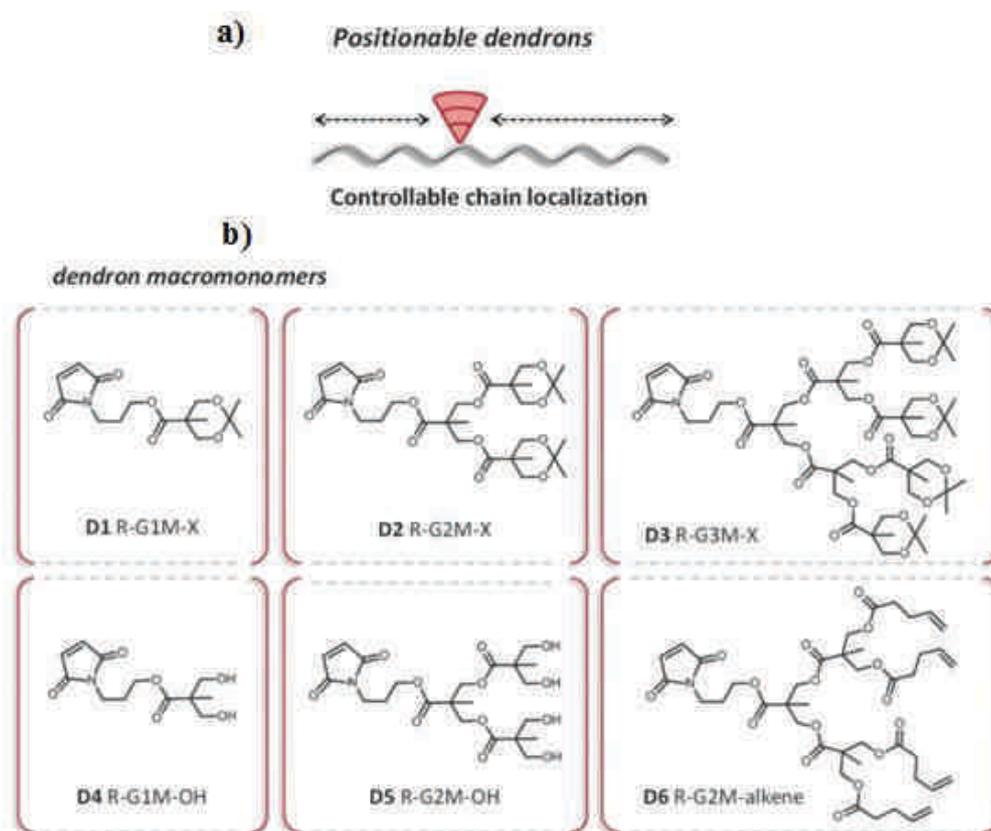
Figure 29. a) Strategies studied for the local incorporation of dendron-substituted MIs in polystyrene chains and b) Molecular structures of the dendron-substituted MIs used in the present study. Reprinted with permission from reference [152].

I.4. Influence of sequence control on polymer properties

The control of comonomer sequences is an interesting strategy for controlling the properties of synthetic copolymers. For instance, physico-chemical and mechanical properties can be adjusted by comonomer sequence regulation. In addition, sequence-controlled copolymers can fold into precise nano-objects that may exhibit properties comparable to those of biopolymers. During the last few years, many research groups have examined the properties of sequence-controlled copolymers. Some of these examples are described in the following section.

I.4.1. Influence of sequence control on physical and mechanical properties

Sequence control has been found to strongly affect physical and mechanical properties of macromolecules. Particularly, in the biomedical field, the control over monomer sequence is becoming more interesting because their physical properties can be regulated by the microstructural distribution of the monomer units along the copolymer chains. For example, Jang and coworkers [157] have demonstrated that the monomer sequence has an effect on mechanical properties of hydrogels network. Their study was focused particularly on two different structural forms of poly(*N*-vinyl-2-pyrrolidone-*co*-2-hydroxyethyl methacrylate) that can simply be abbreviated as poly(VP-*co*-HEMA).

(a) Random poly(VP-co-HEMA) (DR= 1.170)

(b) Blocky poly(VP-co-HEMA) (DR= 0.104)

Figure 30. a) Random structural form and b) Blocky structural form of poly(VP-*co*-HEMA). Reprinted with permission from reference [157].

As illustrated in **Figure 30**, the authors have considered a random structure (a) where HEMA monomers are randomly distributed along the polymer chain and a blocky structure (b) where HEMA monomers are gathered at one chain end. These two different structures have been simulated for the same degree of polymerization (DP=50) and the same composition of VP and HEMA (37:13) using atomistic molecular dynamics (MD) with 0 and 10 wt % of water content. A cross-linker molecule (*N*,*N*'-methylenebisacrylamide (MBA)) has been introduced at one end of each polymer chain then all chains arranged themselves to participate in the network leading to a three-dimensional network structure. From this study, the authors have shown that the properties of poly(VP-*co*-HEMA) such as density and mechanical strength are directly affected by the monomer sequence of the copolymer. For instance, the random sequence network has been observed to be denser than the blocky sequence system which has been explained by the difference in expansion of chain conformation and restricted conformational relaxation. Regarding mechanical properties, monomer sequence exhibited an important role in chain deformation. In fact, in the presence of water molecules, the random distribution of HEMA monomer along the polymer chain led to a compressive deformation whereas no deformation is observed in the blocky structure.

These authors reported later [158] that the monomer sequence of poly(VP-*co*-HEMA) could also affect the transport properties of the polymer, especially at a molecular level. The two different structures described in their previous work have been used as polymer models. Two guest molecules with similar sizes and atomic constituents such as D-glucose and ascorbic acid have been selected because they present an essential role in our body. This study focused on the interaction between the guest molecules and the hydrogel polymers in the presence of various water contents. To illustrate the dispersity of the monomer units along the polymer chain, a simulation at 80 % water content was performed and the results have shown that random poly(VP-*co*-HEMA) hydrogels were observed to be highly dispersed in solution. In contrast, the blocky poly(VP-*co*-HEMA) hydrogels had a more clearly segregated structure. The distribution of the guest molecules in the polymer network hydrogel has been then determined by the pair correlation function (PCF) between the guests and hydrogels. It was found that in both random and blocky structures, guest molecules associated more with the VP units due to their hydrophilic compatibility. These results have been confirmed indeed by the calculation of solvent-accessible surface area (SASA) for blocky sequence hydrogel containing 20 % water. SASA has been reported as 29–37 % for VP units and 4–15 % for

HEMA units. Additionally, the calculated SASA for both VP and HEMA units in a blocky structure was larger than those calculated for random copolymers. Concerning the diffusion of the guest molecules within the hydrogels in the presence of 20 % water content, ascorbic acid and D-glucose diffused with a diffusion coefficient two times lower in blocky sequence hydrogel than in random sequence hydrogel because the guest molecules preferred to interact more with the block of VP units in the blocky sequence hydrogel. When the water content increased, the diffusion of the guest molecules was similar in both structures due to the increase in channel size in hydrogels where guest molecules can diffuse so the monomer sequence effect is decreased.
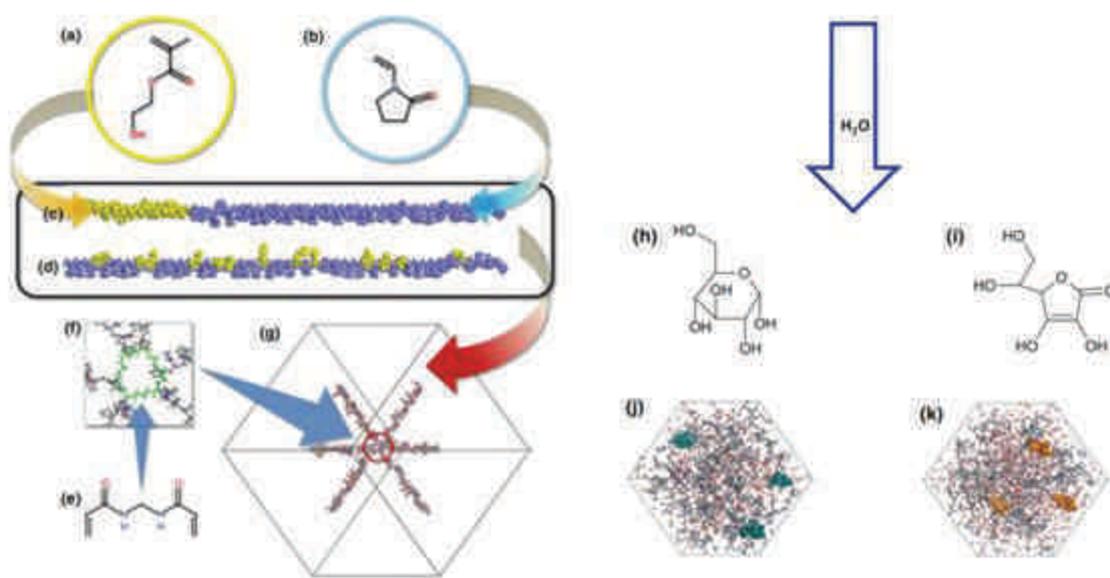
Figure 31. Preparation of poly(VP-*co*-HEMA) hydrogels. (a) HEMA. (b) VP. (c) Block sequence with DP = 50. (d) Random sequence with DP = 50. (e) MBA. (f) Configuration of the cross-linking point. (g) Extended network with periodic boundary condition. (h) D-glucose. (i) Ascorbic acid equilibrated structure of the hydrogels with (j) D-glucose and with (k) ascorbic acid. Adapted with permission from reference [158].

Another report realized by Meyer and coworkers [159,160] described the influence of the monomer sequence on the degradation properties of poly(lactic acid-*co*-glycolic acid) (PLGA). Here, the study was focused on the rate of degradation of PLGAs, one of the most widely employed biodegradable and bioassimilable polymers [161]. Four copolymers containing the same composition of lactic acid (L) and glycolic acid (G) repeat units were

prepared: two repeating sequence polyLGs with different molecular weights synthesized by using a segmer assembly polymerization method, and two random copolymers PLGAs (one prepared by ring-opening polymerization and other synthesized by condensation reaction of the dimeric precursors).
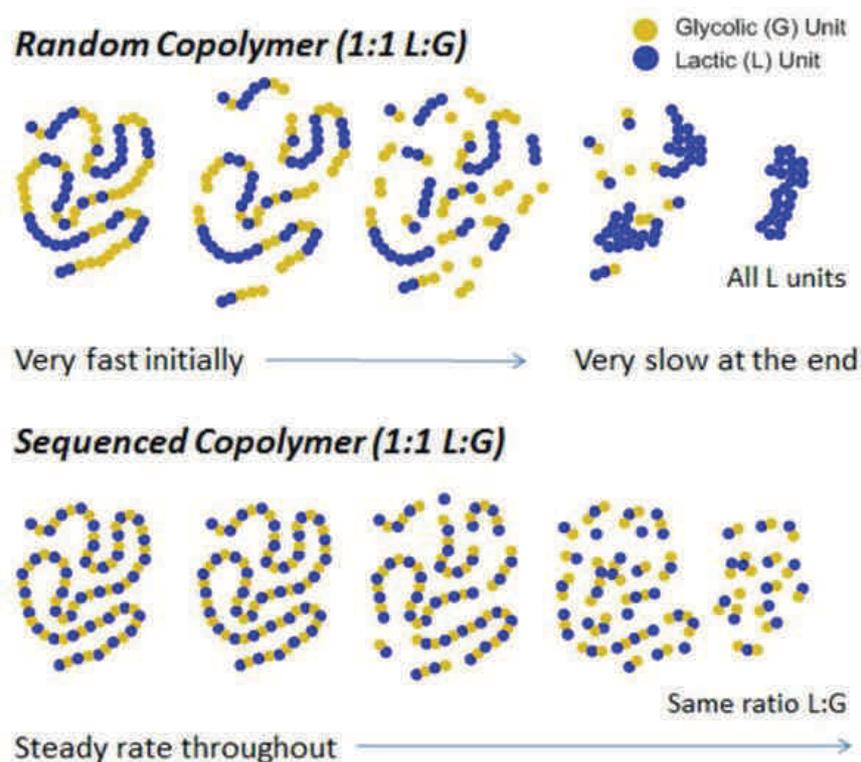
Figure 32. Difference hydrolysis patterns for random and sequenced PLGA copolymers with the same L:G ratio. Reprinted with permission from reference [160].

The hydrolytic degradation behavior of the four copolymers which have approximately the same molecular weight has been studied. The microparticles of these copolymers used in this study were prepared with sizes ranging from 2 to 4 μm. By using size exclusion chromatography (SEC) method to characterize the copolymers, the authors observed that the initial weight loss of random copolymers is bigger than those observed for the two sequenced PLGs copolymers. It means that the copolymers with random structures degraded more rapidly while the two sequenced copolymers exhibited a tardy decrease in molecular weight. Moreover, the degradation of sequenced and random copolymers had also different thermal behavior as proved by differential scanning calorimetry (DSC) technique. For example, at high temperature, random copolymers exhibited multiple melting transitions,

whilst the thermal behavior of the sequenced copolymers presented an unique melting transition. In conclusion, this observation could be explained by the fact that G-G connections would cleave more quickly than G-L/L-G, which should cleave more quickly than the hydrophobic L-L connections (**Figure 32**). This is the reason why the uniformity of the degradation was obtained in the case of the sequenced polymers. This phenomenon has been also observed by others who clearly demonstrated that glycolic units which have a hydrophilic behavior are hydrolyzed 1.3 times faster than lactic units [162].

These successful researches on the effect of monomer sequence on degradation behavior of copolymers has led to the development of biomedical applications, in which the controlled release of small molecules are needed to act as drug delivery platform [163].

I.4.2. Influence of sequence control on intramolecular and folded conformations

The folding of sequence-controlled copolymers plays an important role in Nature. For instance, sequence-controlled proteins fold into precise secondary, tertiary and quaternary structures (**Figure 5**) [6]. Through hydrogen bonds between two linear sequence backbones, secondary structure is mainly formed as α-helices and β-sheets, and the packing of these latter structures forms a tertiary structure. The quaternary structure describes the spatial organization of the chains in the case there is more than one polypeptide chain present in the protein complex [164]. It should be noted that the self-assembly and organization of this natural polymers are usually performed at the molecular level and have been shown as a principal key to achieve advanced functional control.

It is well-known that the hydrophobicity of proteins has shown a strong effect on protein folding, but in a real situation, the effect of different forces can be involved. To simplify this complicated system, the scientists have studied only the simulation of the coil-to-globule transitions which depend on hydrophobic interactions to try to understand the forces that influence molecular assembly. For example, Khokhlov and Khalatur [165] have used in 1999 Monte Carlo simulations to generate special primary structures in AB copolymers. At first, a dense parent globular conformation of a homopolymer chain was prepared by switching on strong attraction between monomeric units (**Figure 33**, (a)). The hydrophilic globular units present at the surface (assigned as A) and the hydrophobic core

(assigned as B) have been attributed to different colors (b). The last step, after removing the uniform strong attraction of monomeric units, protein-like copolymer was obtained in a coil state (c). They have studied the average energy of attraction and the kinetics of the coil-globule transition and concluded that there are many properties of protein-like and random copolymers which are different. In term of the coil-to-globule transitions, the transition at a high temperature of protein-like molecules was found to be sharper than those observed for molecules with random sequences. Moreover, AB sequence can be generated from the parent conformation of a polymer chain displaying a primary structure that can induce certain functions to the copolymers. In 2006, Semler and Genser [166] published a work based on the original idea proposed by Khokhlov and Khalatur. In this study, Monte Carlo simulation was used to model the formation of random copolymers with tunable monomer sequence distributions. The results were similar to ones obtained by Khokhlov and Khalatur.
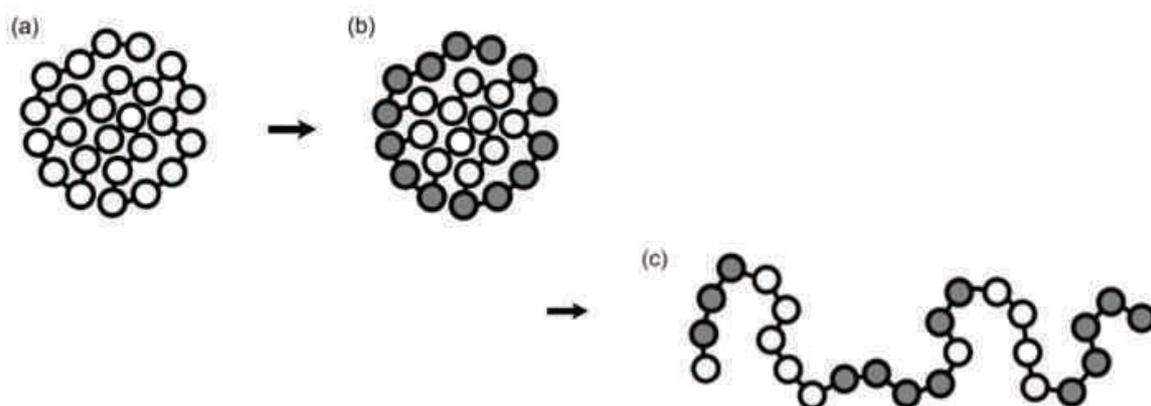
Figure 33. Main steps of the sequence design scheme for protein-like copolymers: (a) homopolymer globule. (b) The same globule after the coloring procedure. (c) Protein-like copolymer in the coil state. Reprinted with permission from reference [165].

Recently, the study of the effect of hydrophobicity on the coil-to-globule collapse of polypeptoids have been reported by Zuckermann and coworkers [167]. Two HP models (hydrophobic and polar monomers), protein-like and repeating sequences containing the same composition of hydrophobic *N*-methylglycine (H) and polar *N*-(2-carboxyethyl)glycine (P) monomers have been generated using synthesis and theoretical computational methods. First of all, the protein-like and repeating sequence chains containing 80 % of hydrophobic monomer (H) and 20 % of polar monomer (P) were prepared. The coloring was applied to target a protein-like H/P sequence, the macromolecule underwent then a coil-to-globule

transition in solution. They reported that after several refolding the globule collapsing behavior of the polymer was certainly different depending on how monomer sequences were distributed along the chain. As evidenced by small-angle X-ray scattering, dynamic light scattering, and probing with environmentally sensitive fluorophores studies, a designed protein-like sequence collapsed into a more compact globule in aqueous solution.

During the past, the chemists have tried to synthesize synthetic polymers backbones which can be able to fold into well-defined conformations. Therefore, the field of foldamers has been developing rapidly. However, it should be mentioned that the term of foldamers which was introduced by Gellman in 1996 [168] is described generally in the literature for sequence-defined biopolymers and not for synthetic polymers because the monomer sequences in the latter are difficult to control [169]. In addition, synthetic polymers are different from proteins because chain disorders can be produced [170] and most of them display an amorphous structure in this way the folding into secondary structure is not possible. Nevertheless, due to the development of synthetic chemical concepts, polymeric materials with crystalline arrangements can be obtained [171].

Palmans and Meijer [172,173] used some years ago a metal-catalyzed system to induce chain folding in polymers (**Figure 34**). First of all, amphiphilic copolymers comprising poly(ethylene glycol) (PEG), benzene-1,3,5-tricarboxamide (BTA) and diphenylphosphinostyrene (DPS) as hydrophilic, hydrophobic and ligand units respectively have been prepared by reversible addition-fragmentation chain transfer (RAFT) polymerization process. Ru-catalytic sites were then solubilized in toluene and incorporated into the controlled copolymers via the syringe technique. A two-state folding process of the single chain was then observed due to ligand exchange [174]. Single chain polymeric nanoparticles (SCPN) were subsequently formed and the transfer hydrogenation of ketones in water occurred [175]. Similar work was published later by the same authors where they concluded that a two-step folding process could also occur for a block copolymer containing a BTA block and a photocleavable protecting group 2-ureidopyrimidinone (UPy) block [176].
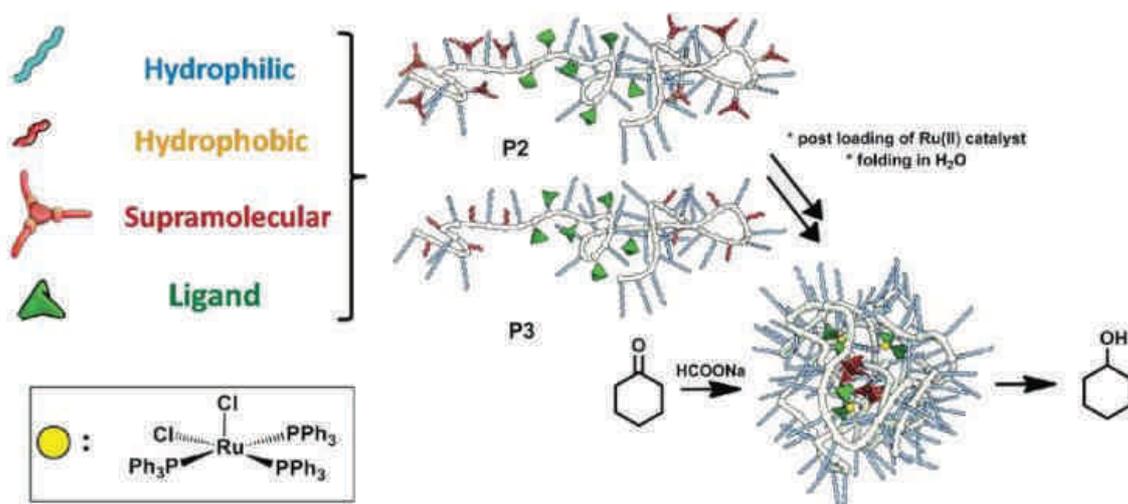
Figure 34. Design of catalytically active SCPNs for transfer hydrogenation of ketones in water. Reprinted with permission from reference [172].

On the other side, as inspired by nature, the protein chains can be directly cross-linked between them due to the presence of thiol groups from cysteine amino acids. Proteins folding could be further stabilized by disulfide bridges [177]. Hereby, our group took advantage of it to propose a new versatile approach towards intramolecular covalent folding of atactic synthetic polymers [169]. This purpose could be achieved by preparing first the well-defined polymers with controlled microstructure using a bulk atom transfer radical polymerization (ATRP) technique. The preparation of these precursors is based on the addition of discrete amounts of ultrareactive N-substituted maleimides (MIs) bearing propargylic moieties into the growing polystyrene chain [38]. Since, the unprotected N-propargyl maleimides provides the undesirable side reactions during the radical polymerization process hence the propargylic function was protected either with a trimethylsilyl (TMS) or a triisopropylsilyl (TIPS) protecting groups. The foldable polymers were prepared first by the copolymerization of St and MIs. Subsequently, the bromine presents at the end of polymer chain was transformed into an azide function and the deprotection of MI was performed resulting in alkyne functions. The folding of this polymer occurred in dilute solution by intramolecular copper-catalyzed azide–alkyne cycloaddition (CuAAC) reaction. It should be mentioned that the reactive monomers could be added at difference places on the growing polystyrene chains leading to different types of covalently folded polymer chains (**Figure 35**). For example, a pseudocyclic macromolecules (**Figure 35**b, Q-shape) could be obtained if one unit of MI was introduced at

the beginning of the polymerization, while bicyclic molecules (**Figure 35**c, 8-shape) could be formed using a bifunctional initiator to prepare the polymer and inserting MI units from the start of the polymerization.
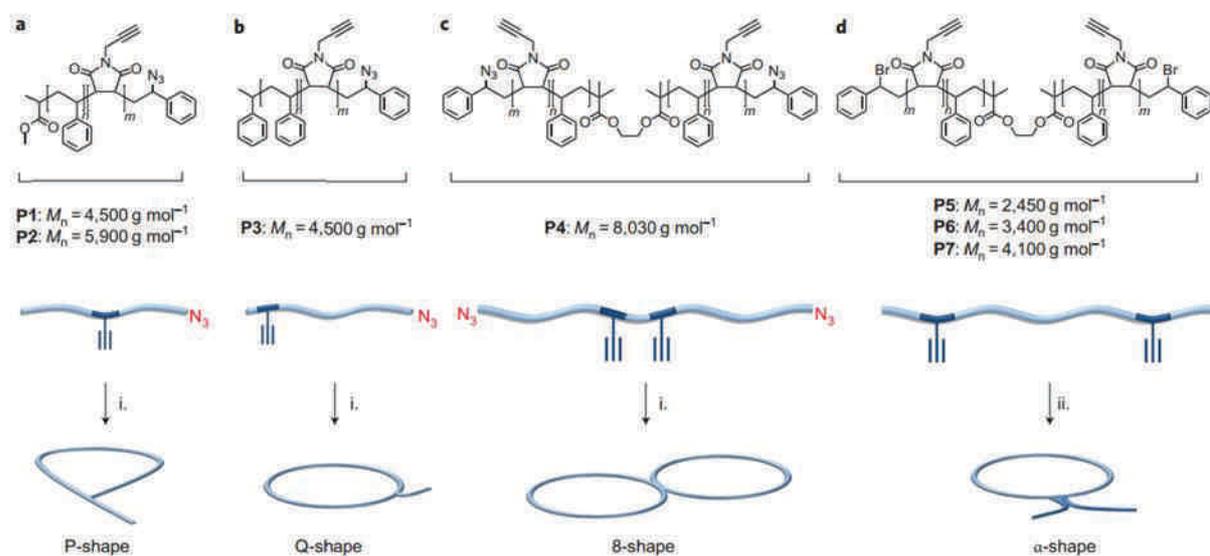
Figure 35. Covalent folding of linear synthetic polymer chains. Reprinted with permission from reference [169].

Moreover, sequence-controlled nitroxide-mediated polymerization (NMP) process can be successfully used to prepare α-shape asymmetric covalent bridges by using efficient chemical steps [178]. The asymmetric covalent bridge was formed by the fact that two different MIs, TIPS-PMI and PFP-MI, were added at different places into the growing polystyrene chain. The latter was first reacted ith a primary amine functionalized linker bearing at the other extremity an azide. Afterward the TIPS protecting group was removed providing access to alkyne functions in the polymer chains. The polymer was then folded in a dimethylformamide (DMF) solution through a CuAAC reaction as described above. The general strategy is represented in **Figure 36**.
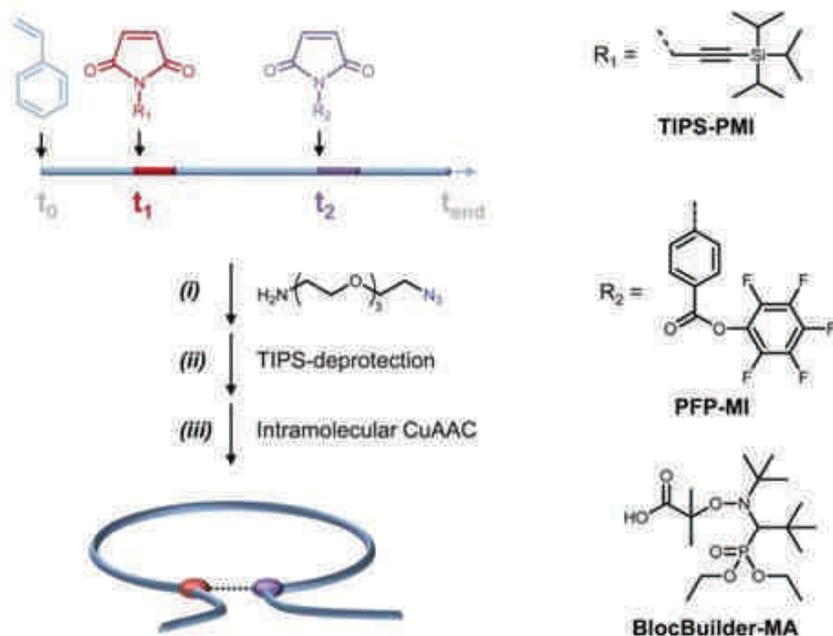
Figure 36. General strategy studied for folding polystyrene chains using asymmetric covalent bridges. Reprinted with permission from reference [178].

More recently, our group has successfully prepared the bicyclic covalent folding of linear synthetic polymer chains with more complex topology via intramolecular twin disulfide bridge formation [179]. In this study, oligomers containing cysteine–arginine–cysteine (CRC) sequences were used to form intramolecular bridges. The preparation of bi-cyclic covalent bridge is principally achieved in four steps as shown in **Figure 37**. First, NMP of St was performed with the introduction of PFP-MI at two precise locations on the polymer chain, one was added at the beginning of the polymerization and second approximately added after 55-65 % of styrene monomer conversion. The sequence-controlled polymers containing activated ester functional sites were then reacted with protected CRC tripeptide derivative possessing a terminal primary amine (**3**) followed by the removal of the protecting group of the CRC sequence resulting in free thiol groups. The intramolecular oxidation of two CXC motifs in dilute *N*-methyl-2-pyrrolidone solution led to the formation of a twin disulfide cyclic dimer. Nevertheless, the authors pointed out that some chains can be experimentally mono-functionalized and thus may not be able to fold.
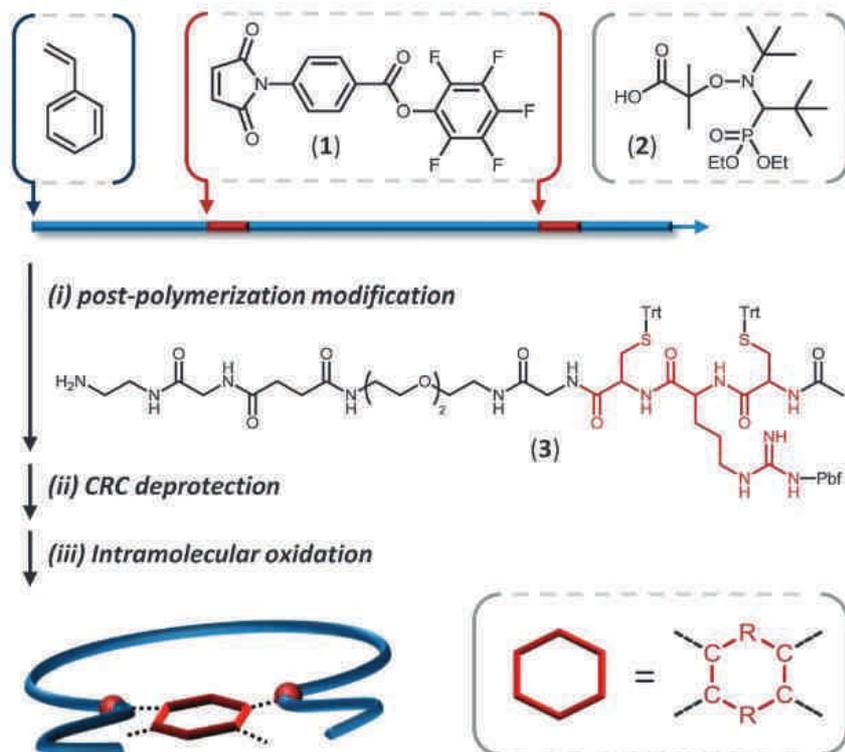
Figure 37. General strategy to prepare defined bicyclic topologies. Reprinted with permission from reference [179].

The effect of monomer sequences on the conformation has been continually studied. For instance, Jayaraman and coworkers [180] studied the interaction between copolymer grafted nanoparticles using monomer sequence to tune the grafted chain conformation. This work was inspired by the folding of proteins and the use of this latter for guiding the assembly of nanoparticles. Nevertheless, this study was focused only on the simple AB copolymer chains including alternating, multiblock and diblock copolymers grafted on spherical nanoparticles (**Figure 38**). Monte Carlo simulation has shown that alternating copolymers compactly aggregated to bring attractive monomers together when the grafted copolymers was placed in small molecule solvent resulting in lower radius of gyration (R_g) while diblock copolymers have the highest R_g. This highest value was due to the fact that the grafted diblock copolymers exhibited both intra- and interchain attractive monomer aggregation. Concerning multiblock copolymers, -(A_3B_3)-sequence rearranged as purely intrachain contacts because the number of favorable contacts and R_g possessed the lowest value as compared to alternating copolymers, whilst -(A_6B_6)-sequence has a higher value for both R_g and number of contacts because the attractive monomers were placed closer to each other than in the case of

-(A_3B_3)-sequence. The different conformation such as purely intrachain or combination of intra- and interchain monomer contacts is actually dependent on the placement and number of the grafts and especially the sequence of attractive monomers along the copolymer chain.
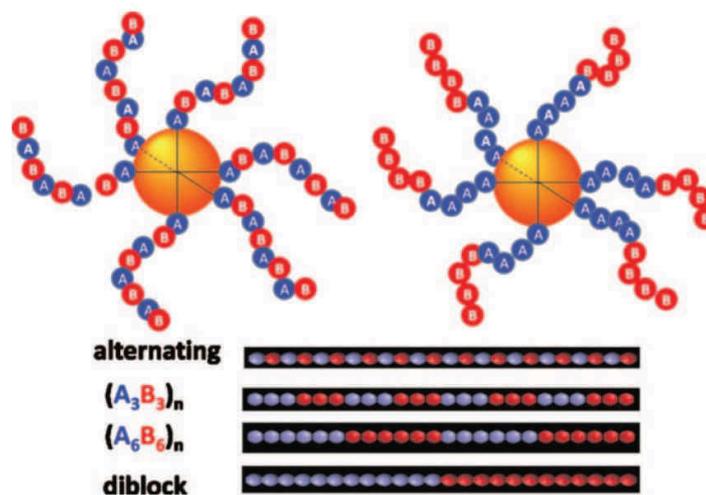
Figure 38. A schematic of model AB copolymer grafted particles with alternating and diblock sequences. Reprinted with permission from reference [180].

The works outlined in this bibliography research part illustrated some examples of the progress in the field of sequence-controlled polymers. Numerous research works described how the control over monomer sequences of synthetic macromolecules can be controlled and also showed the influence of these sequence-controlled polymers on their properties. As evidenced in this chapter, several approaches can be used to prepare such sequence-controlled materials including a facile and versatile procedure consisting in the copolymerization of donor-acceptor comonomers in non-stoichiometric conditions. Therefore, this technique has been used here to prepare a variety of sequence-controlled macromolecules that will be described in the following chapters of this thesis.

References

[1]. Lutz, J.-F.; Ouchi, M.; Liu, D. R.; Sawamoto, M., *Science,* **2013**, *341*, 1238149.

[2]. Badi, N.; Lutz, J.-F., *Chem. Soc. Rev.,* **2009**, *38*, 3383-3390.

[3]. Börner, H. G., *Macromol. Rapid Commun.,* **2011**, *32*, 115-126.

[4]. Lodish H, B. A., Zipursky SL, et al., Molecular Cell Biology,. 4th edition ed.; **2000**.

[5]. Allendorf, M. D.; Stavila, V., *CrystEngComm,* **2015**, Advance Article, DOI: 10.1039/C4CE01693A

[6]. Anfinsen, C. B., *Science,* **1973**, *181*, 223-230.

[7]. Berg, J. M.; Tymoczko, J. L.; Stryer, L., Biochemistry,. 5th ed.; W H Freeman; : New York, **2002.**

[8]. Aldaye, F. A.; Palmer, A. L.; Sleiman, H. F., *Science,* **2008**, *321*, 1795-1799.

[9]. Matyjaszewski, K., *Prog. Polym. Sci.,* **2005**, *30*, 858-875.

[10]. Rosales, A. M.; Segalman, R. A.; Zuckermann, R. N., *Soft Matter,* **2013**, *9*, 8400-8414.

[11]. Hoss, R.; Vögtle, F., *Angew. Chem. Int. Ed. Engl.,* **1994**, *33*, 375-384.

[12]. Suzuki, K.; Sato, S.; Fujita, M., *Nat. Chem.,* **2010**, *2*, 25-29.

[13]. McKee, M. L.; Milnes, P. J.; Bath, J.; Stulz, E.; Turberfield, A. J.; O'Reilly, R. K., *Angew. Chem. Int. Ed.,* **2010**, *49*, 7948-7951.

[14]. Raid Banat, T. T., Khaldoun Al-Sou'od; Aldaye, F. A., *Jordan J. Chem.,* **2012**, *7*, 267-278.

[15]. Milnes, P. J.; McKee, M. L.; Bath, J.; Song, L.; Stulz, E.; Turberfield, A. J.; O'Reilly, R. K., *Chem. Commun.,* **2012**, *48*, 5614-5616.

[16]. Ida, S.; Ouchi, M.; Sawamoto, M., *J. Am. Chem. Soc.,* **2010**, *132*, 14748-14750.

[17]. Ida, S.; Ouchi, M.; Sawamoto, M., *Macromol. Rapid Commun.,* **2011**, *32*, 209-214.

[18]. Ida, S.; Terashima, T.; Ouchi, M.; Sawamoto, M., *J. Am. Chem. Soc.,* **2009**, *131*, 10808-10809.

[19]. Minoda, M.; Sawamoto, M.; Higashimura, T., *Macromolecules,* **1990**, *23*, 4889-4895.

[20]. Dunn, M. S.; Butler, A. W.; Deakers, T., *J. Biol. Chem.,* **1932**, *99*, 217-220.

[21]. Merrifield, R. B., *Angew. Chem. Int. Ed. Engl.,* **1985**, *24*, 799-810.

[22]. Merrifield, R. B., *J. Am. Chem. Soc.,* **1963**, *85*, 2149-2154.

[23]. Dickerson, T. J.; Reed, N. N.; Janda, K. D., *Chem. Rev.,* **2002**, *102*, 3325-3344.

[24]. Gravert, D. J.; Janda, K. D., *Chem. Rev.,* **1997**, *97*, 489-510.

[25]. Toy, P. H.; Janda, K. D., *Acc. Chem. Res.,* **2000**, *33*, 546-554.

[26]. Meszynska, A.; Badi, N.; Börner, H. G.; Lutz, J.-F., *Chem. Commun.,* **2012**, *48*, 3887-3889.

[27]. Stutz, C.; Meszynska, A.; Lutz, J.-F.; Börner, H. G., *ACS Macro Lett.,* **2013**, *2*, 641-644.

[28]. Simon, R. J.; Kania, R. S.; Zuckermann, R. N.; Huebner, V. D.; Jewell, D. A.; Banville, S.; Ng, S.; Wang, L.; Rosenberg, S.; Marlowe, C. K., *Proc. Natl. Acad. Sci.,* **1992**, *89*, 9367-9371.

[29]. Zuckermann, R. N.; Kerr, J. M.; Kent, S. B. H.; Moos, W. H., *J. Am. Chem. Soc.,* **1992**, *114*, 10646-10647.

[30]. Zuckermann, R. N., *Biopolymers,* **2011**, *96*, 545-55.

[31]. Sun, J.; Zuckermann, R. N., *ACS Nano,* **2013**, *7*, 4715-4732.

[32]. Rose, K.; Vizzavona, J., *J. Am. Chem. Soc.,* **1999**, *121*, 7034-7038.

[33]. Hartmann, L.; Krause, E.; Antonietti, M.; Börner, H. G., *Biomacromolecules,* **2006**, *7*, 1239-1244.

[34]. Ponader, D.; Maffre, P.; Aretz, J.; Pussak, D.; Ninnemann, N. M.; Schmidt, S.; Seeberger, P. H.; Rademacher, C.; Nienhaus, G. U.; Hartmann, L., *J. Am. Chem. Soc.,* **2014**, *136*, 2008-2016.

[35]. Ponader, D.; Wojcik, F.; Beceren-Braun, F.; Dernedde, J.; Hartmann, L., *Biomacromolecules,* **2012**, *13*, 1845-1852.

[36]. Pfeifer, S.; Zarafshani, Z.; Badi, N.; Lutz, J.-F., *J. Am. Chem. Soc.,* **2009**, *131*, 9195-9197.

[37]. Trinh, T. T.; Oswald, L.; Chan-Seng, D.; Lutz, J.-F., *Macromol. Rapid Commun.,* **2014**, *35*, 141-145.

[38]. Pfeifer, S.; Lutz, J.-F., *J. Am. Chem. Soc.,* **2007**, *129*, 9542-9543.

[39]. Smid, J.; Van Beylen, M.; Hogen-Esch, T. E., *Prog. Polym. Sci.,* **2006**, *31*, 1041-1067.

[40]. Szwarc, M., *Nature,* **1956**, *178*, 1168-1169.

[41]. Matyjaszewski, K.; Spanswick, J., *Materials Today,* **2005**, *8*, 26-33.

[42]. Veregin, R. P. N.; Georges, M. K.; Hamer, G. K.; Kazmaier, P. M., *Macromolecules,* **1995**, *28*, 4391-4398.

[43]. Grishin, D. F.; Grishin, I. D., *Russ J Appl Chem,* **2011**, *84*, 2021-2028.

[44]. Krzysztof, M., *Controlled/Living Radical Polymerization*. American Chemical Society: **2000**; Vol. 768, p 500.

[45]. Hadjichristidis, N.; Pitsikalis, M.; Pispas, S.; Iatrou, H., *Chem. Rev.,* **2001**, *101*, 3747-3792.

[46]. Solomon, D. H.; Rizzardo, E.; Cacioli, P., Polymerization process and polymers produced thereby. US Patents. 4581429 A: **1986**.

[47]. Hawker, C. J.; Bosman, A. W.; Harth, E., *Chem. Rev.,* **2001**, *101*, 3661-3688.

[48]. Nicolas, J.; Guillaneuf, Y.; Bertin, D.; Gigmes, D.; Charleux, B., Nitroxide-Mediated Polymerization. In *Polymer Science: A Comprehensive Reference*, Möller, K. M., Ed. Elsevier: Amsterdam, **2012**; pp 277-350.

[49]. Nicolas, J.; Guillaneuf, Y.; Lefay, C.; Bertin, D.; Gigmes, D.; Charleux, B., *Prog. Polym. Sci.,* **2013**, *38*, 63-235.

[50]. Tebben, L.; Studer, A., *Angew. Chem. Int. Ed.,* **2011**, *50*, 5034-5068.

[51]. Sciannamea, V.; Jérôme, R.; Detrembleur, C., *Chem. Rev.,* **2008**, *108*, 1104-1126.

[52]. Wang, J.-S.; Matyjaszewski, K., *J. Am. Chem. Soc.,* **1995**, *117*, 5614-5615.

[53]. Wang, J.-S.; Matyjaszewski, K., *Macromolecules,* **1995**, *28*, 7901-7910.

[54]. Matyjaszewski, K.; Xia, J., *Chem. Rev.,* **2001**, *101*, 2921-2990.

[55]. Matyjaszewski, K.; Tsarevsky, N. V., *J. Am. Chem. Soc.,* **2014**, *136*, 6513-6533.

[56]. Chiefari, J.; Chong, Y. K.; Ercole, F.; Krstina, J.; Jeffery, J.; Le, T. P. T.; Mayadunne, R. T. A.; Meijs, G. F.; Moad, C. L.; Moad, G.; Rizzardo, E.; Thang, S. H., *Macromolecules,* **1998**, *31*, 5559-5562.

[57]. Moad, G.; Rizzardo, E.; Thang, S. H., *Aust. J. Chem.,* **2005**, *58*, 379-410.

[58]. Chong, Y. K.; Le, T. P. T.; Moad, G.; Rizzardo, E.; Thang, S. H., *Macromolecules,* **1999**, *32*, 2071-2074.

[59]. Moad, G.; Rizzardo, E.; Thang, S. H., *Polymer,* **2008**, *49*, 1079-1131.

[60]. Ezio, R.; John, C.; Roshan, T. A. M.; Graeme, M.; San, H. T., Synthesis of Defined Polymers by Reversible Addition-Fragmentation Chain Transfer: The RAFT Process. In *Controlled/Living Radical Polymerization*, American Chemical Society: **2000**; Vol. 768, pp 278-296.

[61]. W. Ma, J.; A. Smith, J.; B. McAuley, K.; F. Cunningham, M.; Keoshkerian, B.; K. Georges, M., *Chem. Eng. Sci,,* **2003**, *58*, 1163-1176.

[62]. Detrembleur, C.; Clément, J.-L.; Sciannaméa, V.; Jérôme, C.; Catala, J.-M.; Gigmes, D.; Autissier, L.; Botek, E.; Zarycz, N.; Champagne, B., *J. Polym. Sci., Part A-1: Polym. Chem.,* **2013**, *51*, 1786-1795.

[63]. Nicolas, J.; Charleux, B.; Guerret, O.; Magnet, S., *Angew. Chem. Int. Ed.,* **2004**, *43*, 6186-6189.

[64]. Nicolas, J.; Dire, C.; Mueller, L.; Belleney, J.; Charleux, B.; Marque, S. R. A.; Bertin, D.; Magnet, S.; Couvreur, L., *Macromolecules,* **2006**, *39*, 8274-8282.

[65]. Nicolas, J.; Mueller, L.; Dire, C.; Matyjaszewski, K.; Charleux, B., *Macromolecules,* **2009**, *42*, 4470-4478.

[66]. Grignard, B.; Phan, T.; Bertin, D.; Gigmes, D.; Jerome, C.; Detrembleur, C., *Polym. Chem.,* **2010**, *1*, 837-840.

[67]. Vasilieva, Y. A.; Scales, C. W.; Thomas, D. B.; Ezell, R. G.; Lowe, A. B.; Ayres, N.; McCormick, C. L., *J. Polym. Sci., Part A-1: Polym. Chem.,* **2005**, *43*, 3141-3152.

[68]. Rodriguez-Emmenegger, C.; Schmidt, B. V. K. J.; Sedlakova, Z.; Šubr, V.; Alles, A. B.; Brynda, E.; Barner-Kowollik, C., *Macromol. Rapid Commun.,* **2011**, *32*, 958-965.

[69]. Otsu, T.; Yoshida, M., *Makromol. Chem., Rapid Commun.,* **1982**, *3*, 127-132.

[70]. Otsu, T.; Yoshida, M.; Tazaki, T., *Makromol. Chem., Rapid Commun.,* **1982**, *3*, 133-140.

[71]. Colombani, D.; Steenbock, M.; Klapper, M.; Müllen, K., *Macromol. Rapid Commun.,* **1997**, *18*, 243-251.

[72]. Steenbock, M.; Klapper, M.; Müllen, K., *Macromol. Chem. Phys.,* **1998**, *199*, 763-769.

[73]. Steenbock, M.; Klapper, M.; Müllen, K.; Bauer, C.; Hubrich, M., *Macromolecules,* **1998**, *31*, 5223-5228.

[74]. Yamada, B.; Nobukane, Y.; Miura, Y., *Polym. Bull.,* **1998**, *41*, 539-544.

[75]. Chen, E. K. Y.; Teertstra, S. J.; Chan-Seng, D.; Otieno, P. O.; Hicks, R. G.; Georges, M. K., *Macromolecules,* **2007**, *40*, 8609-8616.

[76]. Rayner, G.; Smith, T.; Barton, W.; Newton, M.; Deeth, R. J.; Prokes, I.; Clarkson, G. J.; Haddleton, D. M., *Polym. Chem.,* **2012**, *3*, 2254-2260.

[77]. Moad, G.; Rizzardo, E.; Solomon, D. H., *Macromolecules,* **1982**, *15*, 909-914.

[78]. Rizzardo, E.; Solomon, D., *Polym. Bull.,* **1979**, *1*, 529-534.

[79]. Georges, M. K.; Veregin, R. P. N.; Kazmaier, P. M.; Hamer, G. K., *Macromolecules,* **1993**, *26*, 2987-2988.

[80]. Lee, N. S.; Wooley, K. L., *Mater. Matters,* **2010**, *5.1*, 9.

[81]. Litvinenko, G.; Müller, A. H. E., *Macromolecules,* **1997**, *30*, 1253-1266.

[82]. Fischer, H., *Macromolecules,* **1997**, *30*, 5666-5672.

[83]. Kothe, T.; Marque, S.; Martschke, R.; Popov, M.; Fischer, H., *J. Chem. Soc., Perkin Trans. 2,* **1998**, 1553-1560.

[84]. Focsaneanu, K.-S.; Scaiano, J. C., *Helv. Chimi. Acta,* **2006**, *89*, 2473-2482.

[85]. Gryn'ova, G.; Lin, C. Y.; Coote, M. L., *Polym. Chem.,* **2013**, *4*, 3744-3754.

[86]. Nabifar, A.; McManus, N. T.; Vivaldo-Lima, E.; Lona, L. M. F.; Penlidis, A., *Chem. Eng. Sci.,* **2009**, *64*, 304-312.

[87]. Cunningham, M. F.; Ng, D. C. T.; Milton, S. G.; Keoshkerian, B., *J. Polym. Sci., Part A-1: Polym. Chem.,* **2006**, *44*, 232-242.

[88]. Goto, A.; Terauchi, T.; Fukuda, T.; Miyamoto, T., *Macromol. Rapid Commun.,* **1997**, *18*, 673-681.

[89]. Fukuda, T.; Terauchi, T.; Goto, A.; Ohno, K.; Tsujii, Y.; Miyamoto, T.; Kobatake, S.; Yamada, B., *Macromolecules,* **1996**, *29*, 6393-6398.

[90]. Dire, C.; Belleney, J.; Nicolas, J.; Bertin, D.; Magnet, S.; Charleux, B., *J. Polym. Sci., Part A-1: Polym. Chem.,* **2008**, *46*, 6333-6345.

[91]. Braunecker, W. A.; Matyjaszewski, K., *Prog. Polym. Sci.,* **2007**, *32*, 93-146.

[92]. Studer, A.; Harms, K.; Knoop, C.; Müller, C.; Schulte, T., *Macromolecules,* **2003**, *37*, 27-34.

[93]. Studer, A.; Schulte, T., *Chem. Rec.,* **2005**, *5*, 27-35.

[94]. Goto, A.; Fukuda, T., *Macromolecules,* **1999**, *32*, 618-623.

[95]. Benoit, D.; Chaplinski, V.; Braslau, R.; Hawker, C. J., *J. Am. Chem. Soc.,* **1999**, *121*, 3904-3920.

[96]. Bertin, D.; Chauvin, F.; Marque, S.; Tordo, P., *Macromolecules,* **2002**, *35*, 3790-3791.

[97]. Benoit, D.; Grimaldi, S.; Robin, S.; Finet, J.-P.; Tordo, P.; Gnanou, Y., *J. Am. Chem. Soc.,* **2000**, *122*, 5929-5939.

[98]. Didier, G.; Jerôme, V.; Nelly, C.; Catherine, L.; Trang, N. T. P.; Thomas, T.; Pierre-Emmanuel, D.; Yohann, G.; Géraldine, C.; François, B.; Denis, B., SG1 and BLOCBUILDER technology: a versatile toolbox for the elaboration of complex macromolecular architectures. In *Controlled/Living Radical Polymerization: Progress in RAFT, DT, NMP & OMRP*, American Chemical Society: **2009**; Vol. 1024, pp 245-262.

[99]. Gigmes, D.; Dufils, P.-E.; Gle, D.; Bertin, D.; Lefay, C.; Guillaneuf, Y., *Polym. Chem.,* **2011**, *2*, 1624-1631.

[100]. Souchal, P.; Roels, T.; Hémery, P.; Marx, L., *J. Polym. Sci., Part A-1: Polym. Chem.,* **2012**, *50*, 4073-4084.

[101]. Marx, L.; Hemery, P., *Polymer,* **2009**, *50*, 2752-2761.

[102]. Sciannamea, V.; Jérôme, R.; Detrembleur, C., *Chem. Rev.,* **2008**, *108*, 1104-1126.

[103]. Hawker, C. J.; Barclay, G. G.; Orellana, A.; Dao, J.; Devonport, W., *Macromolecules,* **1996**, *29*, 5245-5254.

[104]. Moad, G.; Rizzardo, E., *Macromolecules,* **1995**, *28*, 8722-8728.

[105]. Nicolas, J.; Brusseau, S.; Charleux, B., *J. Polym. Sci., Part A-1: Polym. Chem.,* **2010**, *48*, 34-47.

[106]. Mayo, F. R.; Lewis, F. M., *J. Am. Chem. Soc.,* **1944**, *66*, 1594-1601.

[107]. Price, C. C., *J. Polym. Sci.,* **1946**, *1*, 83-89.

[108]. Lutz, J.-F., *Polym. Chem.,* **2010**, *1*, 55-62.

[109]. Greenley, R. Z., Free Radical Copolymerization Reactivity Ratios. In *The Wiley Database of Polymer Properties*, John Wiley & Sons, Inc.: **2003**.

[110]. Chujo, R.; Ubara, H.; Nishioka, A., *Polym. J.,* **1972**, *3*, 670-674.

[111]. Fineman, M.; Ross, S. D., *J. Polym. Sci.,* **1950**, *5*, 259-262.

[112]. Doiuchi, T.; Minoura, Y., *Macromolecules,* **1977**, *10*, 260-265.

[113]. Ponratnam, S.; Kapur, S. L., *Makromol. Chem.,* **1977**, *178*, 1029-1038.

[114]. Paril, A.; Alb, A. M.; Giz, A. T.; Çatalgil-Giz, H., *J. Appl. Polym. Sci.,* **2007**, *103*, 968-974.

[115]. Ledwith, A.; Galli, G.; Chiellini, E.; Solaro, R., *Polym. Bull.,* **1979**, *1*, 491-499.

[116]. Boudevska, H.; Todorova, O., *Makromol. Chem.,* **1985**, *186*, 1711-1720.

[117]. Roos, S. G.; Müller, A. H. E.; Matyjaszewski, K., *Macromolecules,* **1999**, *32*, 8331-8335.

[118]. Jaacks, V., *Makromol. Chem.,* **1972**, *161*, 161-172.

[119]. Kelen, T.; Tüdöus, F.; Turcsányi, B.; Kennedy, J. P., *J. Polym. Sci., Polym. Chem. Ed.,* **1977**, *15*, 3047-3074.

[120]. Brandrup, J. I., H., *Polymer Handbook*, 3rd ed.; A Wiley-Interscience publication, Canada: **1989**; pp 153-251.

[121]. Alfrey, T.; Price, C. C., *J. Polym. Sci.,* **1947**, *2*, 101-106.

[122]. Dawson, T. L.; Lundberg, R. D.; Welch, F. J., *J. Polym. Sci., Part A-1: Polym. Chem.,* **1969**, *7*, 173-181.

[123]. Baldwin, M. G., *J. Polym. Sci., Part A: Gen. Pap.,* **1965**, *3*, 703-710.

[124]. Brandrup, J. I., H., *Polymer Handbook*, 3rd ed.; A Wiley-Interscience publication, Canada: **1989**; pp 268-274.

[125]. Lessard, B. t.; Marić, M., *Macromolecules,* **2009**, *43*, 879-885.

[126]. Yabuuchi, H.; Hirooka, M.; Kaetsu, I., *Polym. J.,* **1995**, *27*, 1021-1024.

[127]. Shahab, Y.; Mohamed, A.; Khettab, A.; Siddiq, A., *Eur. Polym. J.,* **1991**, *27*, 227-229.

[128]. Alfrey, T.; Lavin, E., *J. Am. Chem. Soc.,* **1945**, *67*, 2044-2045.

[129]. Baruah, S. D.; Laskar, N. C., *J. Appl. Polym. Sci.,* **1996**, *60*, 649-656.

[130]. Sadhir, R. K.; Smith, J. D. B.; Castle, P. M., *J. Polym. Sci., Polym. Chem. Ed.,* **1983**, *21*, 1315-1329.

[131]. You, Y.-Z.; Hong, C.-Y.; Pan, C.-Y., *Eur. Polym. J.,* **2002**, *38*, 1289-1295.

[132]. Pfeifer, S.; Lutz, J.-F., *Chemistry (Weinheim an der Bergstrasse, Germany),* **2008**, *14*, 10949-10957.

[133]. Coleman, L. E.; Conrady, J. A., *J. Polym. Sci.,* **1959**, *38*, 241-245.

[134]. Yamada, M.; Takase, I.; Tsukano, T.; Ueda, Y.; Koutou, N., *Kobunshi Kagaku,* **1969**, *26*, 593-601.

[135]. Rao, B. S.; Sireesha, R.; Pasala, A. R., *Polym. Int.,* **2005**, *54*, 1103-1109.

[136]. Shirota, Y.; Yoshimura, M.; Matsumoto, A.; Mikawa, H., *Macromolecules,* **1974**, *7*, 4-11.

[137]. Kirci, B.; Lutz, J.-F.; Matyjaszewski, K., *Macromolecules,* **2002**, *35*, 2448-2451.

[138]. Lutz, J.-F.; Kirci, B.; Matyjaszewski, K., *Macromolecules,* **2003**, *36*, 3136-3145.

[139]. Yabumoto, S.; Ishii, K.; Kawamori, M.; Arita, K.; Yano, H., *J. Polym. Sci., Part A-1: Polym. Chem.,* **1969**, *7*, 1683-1696.

[140]. Hirai, H., *J. Macromol. Sci., Chem.,* **1975**, *9*, 883-897.

[141]. Mashita, K.; Yasui, S.; Hirooka, M., *Polymer,* **1995**, *36*, 2973-2982.

[142]. Benoit, D.; Hawker, C. J.; Huang, E. E.; Lin, Z.; Russell, T. P., *Macromolecules,* **2000**, *33*, 1505-1507.

[143]. Zhu, M.-Q.; Wei, L.-H.; Li, M.; Jiang, L.; Du, F.-S.; Li, Z.-C.; Li, F.-M., *Chem. Commun.,* **2001**, 365-366.

[144]. Chan-Seng, D.; Zamfir, M.; Lutz, J.-F., *Angew. Chem. Int. Ed.,* **2012**, *51*, 12254-12257.

[145]. Zamfir, M.; Lutz, J.-F., *Nat. Commun.,* **2012**, 1138.

[146]. Baradel, N.; Fort, S.; Halila, S.; Badi, N.; Lutz, J.-F., *Angew. Chem. Int. Ed.,* **2013**, *52*, 2335-2339.

[147]. Hein, J. E.; Fokin, V. V., *Chem. Soc. Rev.,* **2010**, *39*, 1302-1315.

[148]. Schulze, B.; Schubert, U. S., *Chem. Soc. Rev.,* **2014**, *43*, 2522-2571.

[149]. Moses, J. E.; Moorhouse, A. D., *Chem. Soc. Rev.,* **2007**, *36*, 1249-1262.

[150]. Meldal, M., *Macromol. Rapid Commun.,* **2008**, *29*, 1016-1051.

[151]. Tomalia, D. A., *Aldrichimica Acta,* **2004**, *2*, 39-57.

[152]. Baradel, N.; Gok, O.; Zamfir, M.; Sanyal, A.; Lutz, J.-F., *Chem. Commun.,* **2013**, *49*, 7280-7282.

[153]. Ihre, H.; Hult, A.; Fréchet, J. M. J.; Gitsov, I., *Macromolecules,* **1998**, *31*, 4061-4068.

[154]. Malkoch, M.; Malmström, E.; Hult, A., *Macromolecules,* **2002**, *35*, 8307-8314.

[155]. Kose, M. M.; Onbulak, S.; Yilmaz, I. I.; Sanyal, A., *Macromolecules,* **2011**, *44*, 2707-2714.

[156]. Kose, M. M.; Yesilbag, G.; Sanyal, A., *Org. Lett.,* **2008**, *10*, 2353-2356.

[157]. Lee, S. G.; Brunello, G. F.; Jang, S. S.; Lee, J. H.; Bucknall, D. G., *J. Phys. Chem. B,* **2009**, *113*, 6604-6612.

[158]. Lee, S.; Koh, W.; Brunello, G.; Choi, J.; Bucknall, D.; Jang, S., *Theor. Chem. Acc.,* **2012**, *131*, 1-16.

[159]. Li, J.; Stayshich, R. M.; Meyer, T. Y., *J. Am. Chem. Soc.,* **2011**, *133*, 6910-6913.

[160]. Li, J.; Rothstein, S. N.; Little, S. R.; Edenborn, H. M.; Meyer, T. Y., *J. Am. Chem. Soc.,* **2012**, *134*, 16352-16359.

[161]. Campolongo, M. J.; Luo, D., *Nat Mater,* **2009**, *8*, 447-448.

[162]. Vey, E.; Rodger, C.; Booth, J.; Claybourn, M.; Miller, A. F.; Saiani, A., *Polym. Degrad. Stab.,* **2011**, *96*, 1882-1889.

[163]. Tiwari, G.; Tiwari, R.; Sriwastawa, B.; Bhati, L.; Pandey, S.; Pandey, P.; Bannerjee, S., *Int. J. Pharm. Investig.,* **2012**, *2*, 2-11.

[164]. Baddeley, D.; Chagin, V. O.; Schermelleh, L.; Martin, S.; Pombo, A.; Carlton, P. M.; Gahl, A.; Domaing, P.; Birk, U.; Leonhardt, H.; Cremer, C.; Cardoso, M. C., *Nucleic Acids Res.,* **2010**, *38*, e8.

[165]. Khokhlov, A. R.; Khalatur, P. G., *Phys. Rev. Lett.,* **1999**, *82*, 3456-3459.

[166]. Semler, J. J.; Genzer, J., *Chem. Phys.,* **2006**, *125*, 014902.

[167]. Murnen, H. K.; Khokhlov, A. R.; Khalatur, P. G.; Segalman, R. A.; Zuckermann, R. N., *Macromolecules,* **2012**, *45*, 5229-5236.

[168]. Appella, D. H.; Christianson, L. A.; Klein, D. A.; Powell, D. R.; Huang, X.; Barchi, J. J.; Gellman, S. H., *Nature,* **1997**, *387*, 381-384.

[169]. Schmidt, B. V. K. J.; Fechler, N.; Falkenhagen, J.; Lutz, J.-F., *Nat. Chem.,* **2011**, *3*, 234-238.

[170]. De Rosa, C., Chain Conformation, Crystal Structures, and Structural Disorder in Stereoregular Polymers. In *Materials-Chirality*, John Wiley & Sons, Inc.: **2004**; pp 71-155.

[171]. Distefano, G.; Suzuki, H.; Tsujimoto, M.; Isoda, S.; Bracco, S.; Comotti, A.; Sozzani, P.; Uemura, T.; Kitagawa, S., *Nat. Chem.,* **2013**, *5*, 335-341.

[172]. Artar, M.; Terashima, T.; Sawamoto, M.; Meijer, E. W.; Palmans, A. R. A., *J. Polym. Sci., Part A-1: Polym. Chem.,* **2014**, *52*, 12-20.

[173]. Terashima, T.; Mes, T.; De Greef, T. F. A.; Gillissen, M. A. J.; Besenius, P.; Palmans, A. R. A.; Meijer, E. W., *J. Am. Chem. Soc.,* **2011**, *133*, 4742-4745.

[174]. Mes, T.; Van der Weegen, R.; Palmans, A. R. A.; Meijer, E. W., *Angew. Chem. Int. Ed.,* **2011**, *50*, 5085-5089.

[175]. Nieto, I.; Livings, M. S.; Sacci, J. B.; Reuther, L. E.; Zeller, M.; Papish, E. T., *Organometallics,* **2011**, *30*, 6339-6342.

[176]. Hosono, N.; Gillissen, M. A. J.; Li, Y.; Sheiko, S. S.; Palmans, A. R. A.; Meijer, E. W., *J. Am. Chem. Soc.,* **2012**, *135*, 501-510.

[177]. Bulaj, G., *Biotechnol. Adv.,* **2005**, *23*, 87-92.

[178]. Zamfir, M.; Theato, P.; Lutz, J.-F., *Polym. Chem.,* **2012**, *3*, 1796-1802.

[179]. Shishkan, O.; Zamfir, M.; Gauthier, M. A.; Börner, H. G.; Lutz, J.-F., *Chem. Commun.,* **2014**, *50*, 1570-1572.

[180]. Seifpour, A.; Spicer, P.; Nair, N.; Jayaraman, A., *J. Chem. Phys.,* **2010**, *132*, 164901.

Chapter II

Influence of Strong Electron-Donor Monomers in Sequence-Controlled Polymerizations

This chapter was published as:

*Sansanee Srichan et al. ACS macro Lett. **2012**, 1, 589-592.*

*Adapted with permission from "ACS macro Lett. **2012**, 1, 589-592. Copyright 2012 American Chemical Society."*

Abstract

A series of styrenic monomers containing strong donor substituents (i.e. 4-methylstyrene, 4-acetoxystyrene and 4-*tert*-butoxystyrene) were tested in sequence-controlled radical copolymerizations in the presence of acceptor comonomers (i.e. *N*-substituted maleimide). The copolymers were synthesized by nitroxide-mediated polymerization using the commercially available alkoxyamine BlocBuilder® MA. This technique allowed synthesis of copolymers with controlled molecular weights and molecular weight distributions for all monomers. Moreover, a beneficial effect of the donor substituents on the sequence-controlled copolymerization was noted. Indeed, all studied styrenic derivatives led to a very precise incorporation of functional *N*-substituted maleimides in the copolymer chains. The most favorable donor-acceptor copolymerization was observed with 4-*tert*-butoxystyrene. This particular monomer was therefore tested in the presence of various functional *N*-substituted maleimides (i.e. *N*-benzyl maleimide, 4-(-*N*-maleimido) azobenzene), *N*-(1-pyrenyl)maleimide, and *N*-(2-(amino Boc)ethylene)maleimide). In all cases, sequence-controlled microstructures were obtained and characterized. Moreover, the formed copolymers were hydrolyzed into poly(4-hydroxystyrene-*co*-*N*-substituted maleimide) derivatives. In all cases, it was verified that the sequence-controlled microstructure of the copolymers was preserved after hydrolysis.

Keywords: Donor-acceptor copolymerization, strong donor substituent, sequence-controlled microstructure, hydrolysis.

II.1 Introduction

Sequence-controlled polymers constitute a new class of macromolecules that holds promises in various technological areas such as catalysis, molecular recognition or biodegradable materials [1-5]. Various strategies for preparing sequence-controlled macromolecules have been reported during the last five years [6-16]. For example, our group has studied the sequence-controlled copolymerization of large excesses of styrene (i.e. an electron-donor monomer) with small amounts of *N*-substituted maleimides (i.e. strong electron-acceptor monomers) [8,17]. This peculiar copolymerization system allows the design of synthetic macromolecules with tailored microstructures [18]. For instance, single-chain functional arrays [8], periodic microstructures [19] and complex macromolecular origamis [20,21] can be created using this approach.

In such sequence-controlled copolymerizations, the donor monomer is the main building block of the chain, while the acceptor comonomers constitute a molecular alphabet, which allows writing of local information in the chain [17,22]. Thus, the donor monomer determines the gross properties of the copolymer (e.g. polarity, solubility, stiffness), whereas the acceptor comonomers induce local properties. In our earlier works, styrene was selected as a donor monomer, thus leading to the formation of apolar hydrophobic sequence-controlled copolymers. However, we have recently shown that other donor building blocks can be used. For instance, sequence-controlled polymers were constructed by copolymerization of *t*-butyl 4-vinyl benzoate (*t*-BuVBA) with various *N*-substituted maleimides [23]. After synthesis, the *t*-butyl esters functions were hydrolyzed, thus leading to the formation of sequence-controlled water-soluble polymers. Although this concept worked relatively well, it was observed that the 4-substituent of the styrenic derivative influences the copolymerization kinetics. For instance, a reactivity ratio of 0.14 was measured for the *t*-BuVBA/*N*-benzyl maleimide comonomer pair. Such a value is higher than those observed for styrene/MIs pairs (i.e. in the range 0.01-0.05) [18] and therefore probably the upper limit for an efficient sequence-controlled copolymerization. These experimental results are probably the consequence of the electron acceptor behavior of *t*-butyl ester function in *t*-BuVBA, which enhances the rate of propagation of this monomer as compared to styrene.

In the present work, we investigated a series of styrenic derivatives bearing electron donor substituents on the *para* position of their aromatic ring (**Scheme 4**). Such strong electron-donor monomers should exhibit moderate rates of propagation [24,25] and therefore lead to efficient sequence-controlled copolymerizations kinetics in the presence of MIs. Moreover, some of these building blocks are precursors of interesting functional polymers. For instance polymers derived from **c** and **d** can be deprotected into poly(4-hydroxystyrene) (**Scheme 4**) using chemical or irradiation protocols [26-30]. This polymer is water soluble in alkaline conditions and has been extensively used in the past years for the preparation of photoresists [31,32]. Herein, we report the sequence-controlled copolymerizations of donor monomers **a-d** with the model MIs **1-4**.
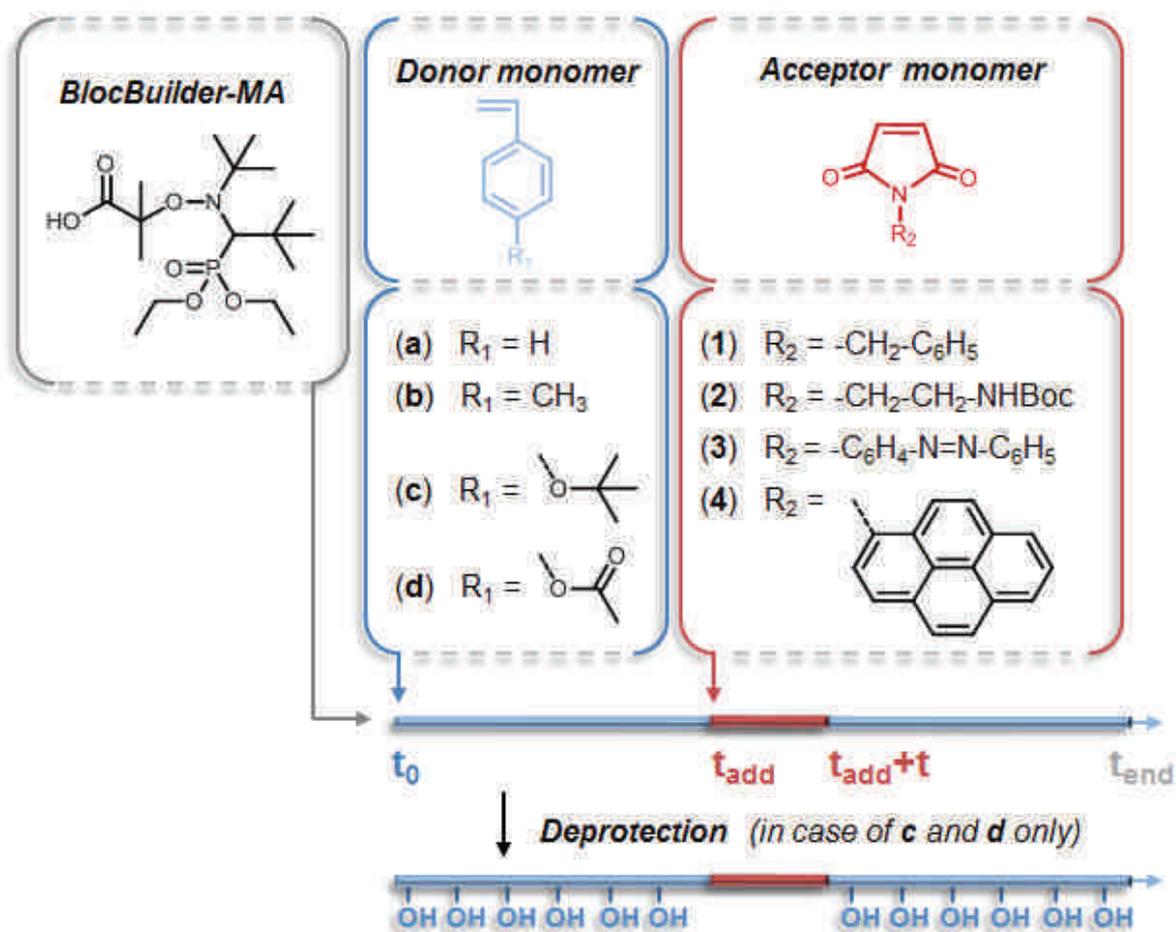
Scheme 4. General strategy studied in the present work. It should be noted that the red section represents the probable zone in which *N*-substituted maleimides are most likely located.

II.2 Results and discussion

The study started with the homopolymerization of the styrenic monomers **a-d**. The polymerization was performed under nitroxide-mediated polymerization (NMP) in anisole at 105 °C and 115 °C using the commercially available alkoxyamine initiator BlocBuilder® MA. The polymers obtained were well-defined with controlled molecular weights and narrow molecular weight distributions in all cases, as shown in **Table 3 .** It is noteworthy to mention that the *para*-substituted styrenic derivatives presented a slower apparent rate of polymerization as compared to styrene (**Figure 39**).

Table 3. Properties of homopolymers of **a**, **b**, **c** and **d** prepared by nitroxide-mediated polymerization.

M [eq.]	[BlocBuilder]	T [°C][a]	t_{end} [min][b]	Conv.[c]	M_n [g·mol^{-1}][d]	$M_{n,th}$[e]	M_w/M_n[d]
1 **a** 100 eq.	1 eq.	105	300	0.66	7900	7250	1.11
2 **b** 100 eq.	1 eq.	105	300	0.48	7900	6060	1.15
3 **c** 100 eq.	1 eq.	105	300	0.52	12500	9550	1.14
4 **d** 100 eq.	1 eq.	105	300	0.50	11300	8500	1.16
5 **c** 50 eq.	1 eq.	105	300	0.58	5800	5500	1.13
6 **c** 20 eq.	1 eq.	105	300	0.58	2500	2430	1.17
7 **a** 100 eq.	1 eq.	115	300	0.80	10600	8700	1.15
8 **b** 100 eq.	1 eq.	115	300	0.74	12000	9100	1.30
9 **c** 100 eq.	1 eq.	115	300	0.73	17200	13200	1.30
10 **d** 100 eq.	1 eq.	115	300	0.73	16200	12200	1.40

[a] Denotes the temperature of the reaction. [b] t_{end} denotes the final polymerization time. [c] Conversion of **a**, **b**, **c** or **d** calculated from ^{1}H NMR spectra in CDCl$_3$. [d] Number average molecular weight and molecular weight distribution of polymers determined by SEC in THF using a calibration based on polystyrene standards. [e] $M_{n,th} = M_M \cdot conv._M \cdot [M]/[BlocBuilder] + M_{BlocBuilder}$.
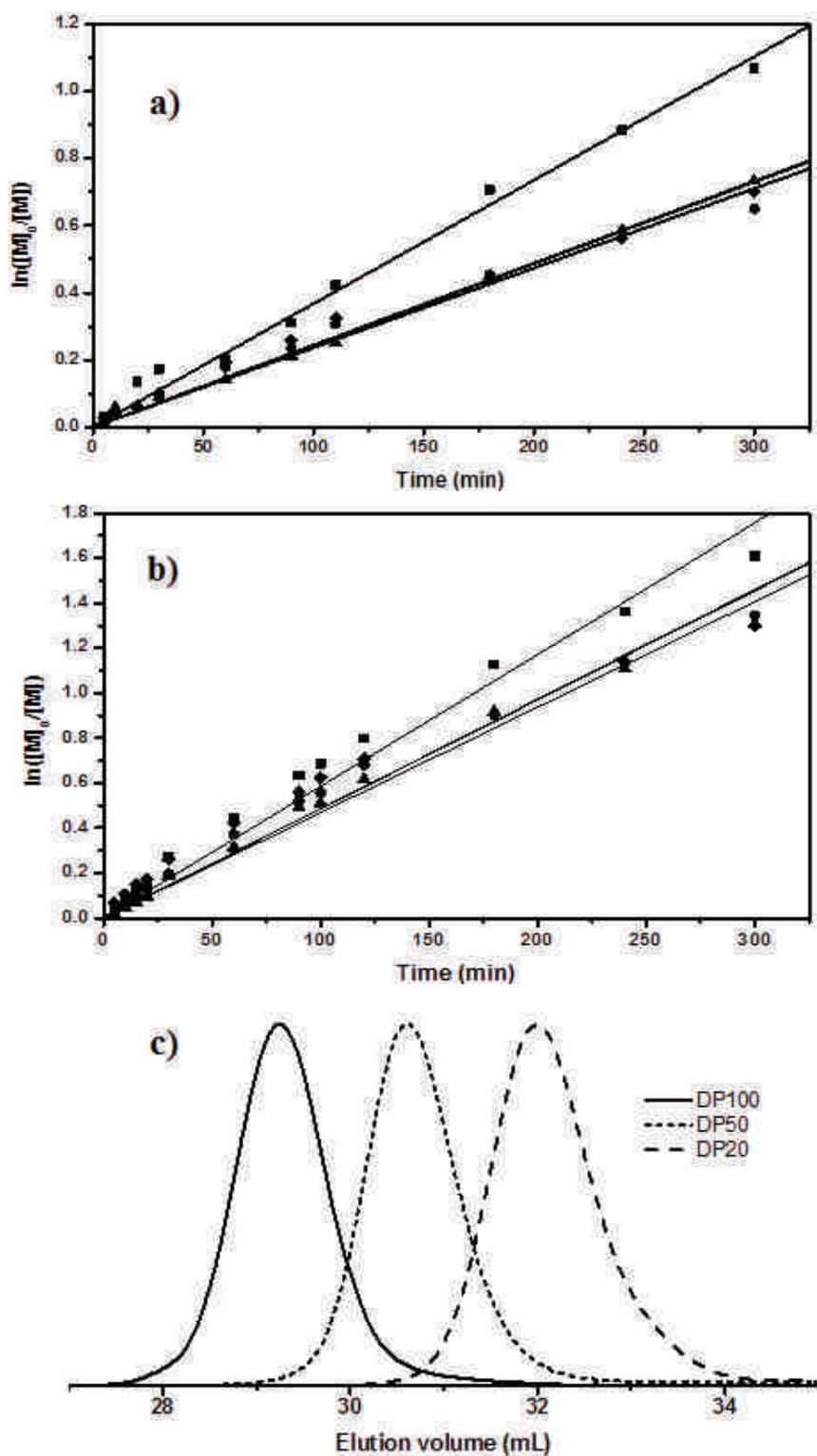
Figure 39. a) Semi-logarithmic plot of monomer conversion versus time for the homopolymerization of **a** (squares), **b** (circles), **c** (triangles) and **d** (diamonds) at 105 °C (Entries 1-4, **Table 3**). b) At 115 °C (Entries 7-10, **Table 3**). c) Chromatograms recorded in THF for homopolymers of **c** synthesized by NMP in anisole (Entries 3, 5 and 6, **Table 3**).

With the confirmation that all the homopolymerizations of the styrenic derivatives **a-d** are well-controlled, NMP of these monomers was performed in similar way in anisole at 115 °C in the presence of a small amount of *N*-benzyl maleimide (**1**) (**Table 4**).

Table 4. Experimental conditions and molecular weight characterization of the polymers obtained by copolymerization of styrenic monomers (**S**) a-d and *N*-substituted maleimides (**MI**) 1-4.[a]

	S	MI	t_{add}[b] [min]	Conv.s[c]	M_n[d]	$M_{n,th}$[e] [g·mol⁻¹]	M_w/M_n[d]
1	a	1	0	0.90	6000	5700	1.20
2	b	1	0	0.89	6600	6200	1.24
3	c	1	0	0.87	10300	8600	1.15
4	d	1	0	0.93	8700	8500	1.32
5	a	1	100	0.90	6900	5600	1.17
6	b	1	100	0.88	6500	6100	1.20
7	c	1	100	0.90	10000	8900	1.13
8	d	1	100	0.96	11200	8700	1.27
9	c	2	0	0.88	10200	8900	1.15
10	c	3	0	0.86	9400	8800	1.25
11	c	4	0	0.89	8900	8200	1.19

[a] Experiments performed in anisole (1:1 v/v relative to **S**) at 115 °C for 5 h using **S** (50 eq.), BlocBuilder® MA (1 eq.) and **MI** (3 eq.). [b] t_{add} denotes the time at which the **MI** was added to the polymerization mixture. [c] Conversion of **S** calculated from ¹H NMR spectra in CDCl₃. [d] Number average molecular weight and molecular weight distribution of polymers determined by SEC in THF using a calibration based on polystyrene standards. [e] $M_{n,th}$ = M_S·conv.$_S$·[**S**]/[BlocBuilder] + M_{MI}·conv.$_{MI}$· [**MI**]/[BlocBuilder] + $M_{BlocBuilder}$.

In the first experiments, **1** was introduced at the beginning of the polymerization at the same time as the styrenic monomer. The polymerization proceeded well, as illustrated in **Figure 40a** and **36b** with an increase of the molecular weight over time while maintaining narrow molecular weight distributions.
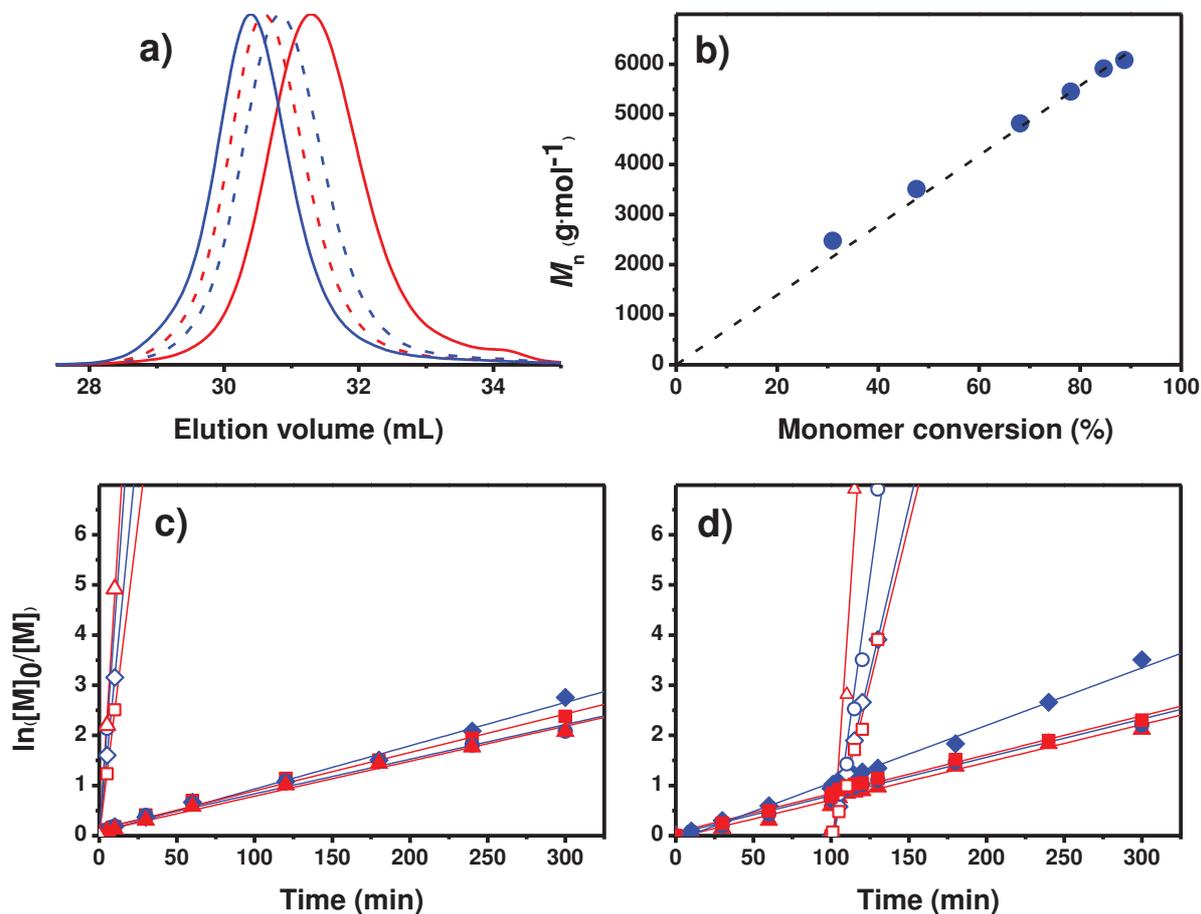
Figure 40. Sequence-controlled NMP of styrenic monomers a-d in the presence of a small amount of **1**. a) SEC traces of aliquots taken during the polymerization of **b** and **1** (Entry 2, **Table 4**) after 60 (full red line), 120 (dotted blue line), 180 (dotted red line) and 300 (full blue line) minutes. b) Plots of experimental (full blue circles) and theoretical M_n (dotted line) versus monomer conversion for the same experiment. c) Semi-logarithmic plot of monomer conversion versus time for the copolymerization of **a** (full red squares), **b** (full blue circles), **c** (full red triangles) and **d** (full blue diamonds) with **1** (corresponding open symbols) (Entries 1-4, **Table 4**). d) Same graph (same symbol/color code as in graph (c)) for the experiments in which **1** was added after 100 minutes of polymerization (Entries 5-8, **Table 4**).

Furthermore, as expected **1** was fully consumed extremely fast (**Figure 40c**), while the conversion of the styrenic comonomer remained comparatively low during the same time interval. In particular, a very fast consumption of **1** was observed in the presence of 4-*tert*-butoxystyrene (**c**). Overall, these kinetics data of copolymerization confirm the local and precise incorporation of **1** on the polymer backbone. As shown in **Table 4**, the *N*-substituted maleimide (**1**) can be added at the beginning of the polymerization but also at any time point of the reaction. Here, **1** was added 100 min after the polymerization of the styrenic monomer started (Entries 5-8, **Table 4**). The kinetic results obtained (**Figure 40d**) demonstrated that the *N*-substituted maleimide can be localized at any position along the polymer backbone without affecting the control of the polymerization. Again, a particularly fast incorporation of **1** was observed in the presence of **c**.

The study was extended to other *N*-substituted maleimides **2**-**4** introduced at the beginning of the polymerization when polymerizing **c** (Entries 9-11, **Table 4**). The polymerizations proceeded in a controlled fashion and yielded to well-defined macromolecules with sequence-controlled microstructures (**Table 4** and **Figure 41**).
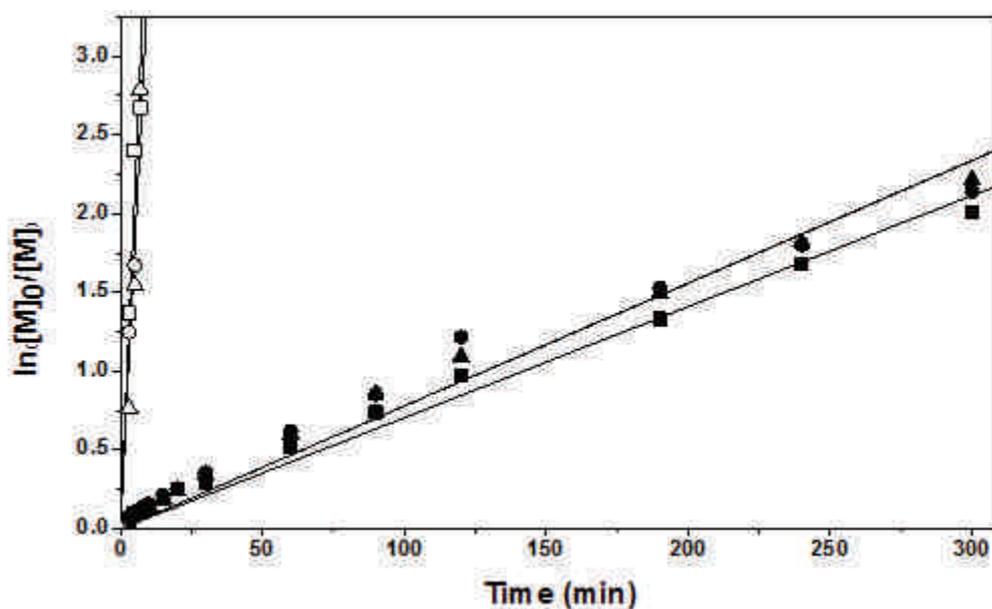
Figure 41. Semi-logarithmic of monomer conversion versus time for the copolymerization of **c** with **2** (open circles), **3** (open squares) and **4** (open triangles) (Entries 9-11, **Table 4**). The full symbols used for **c** in each experiment correspond to those used for the MIs.

The reactivity ratios r_{S-MI} for the copolymerization of the various styrenic monomers with **1** were determined by drawing the Jaacks plots for each comonomer pairs (**Table 5**). The values of r_{S-MI} suggested a strong alternating behavior between all the styrenic monomers and **1**. When the styrenic monomer employed was **c**, r_{c-1} was lower (0.028) compared to the other r_{S-1} confirming a higher precision of the incorporation of **1** on the polymer backbone.

Table 5. Reactivity ratios of the styrenic monomer (**S**, **a-d**) determined from the Jaacks plot in the presence of various *N*-substituted maleimides (**MIs**, **1-4**).

	1	2	3	4
a	0.041	-	-	-
b	0.045	-	-	-
c	0.028	0.062	0.040	0.039
d	0.059	-	-	-

The choice of 4-*tert*-butoxystyrene (**c**) and 4-acetoxystyrene (**d**) as styrenic monomer in the presence of a *N*-substituted maleimide allowed the preparation of a sequence-controlled hydrophobic precursor for the elaboration of locally functionalized poly (4-hydroxystyrene). The deprotection of repeat units based on **c** was performed using HCl in dioxane, while the conditions used to cleave the acetoxy group from **d** were H_2SO_4 in water/dioxane.

Figure 42 showed the ^{1}H NMR spectra of the sequence-controlled copolymer prepared from **c** in the presence of 4-(*N*-maleimido)azobenzene) (**3**) before and after deprotection. The quantitative hydrolysis of the *tert*-butoxy groups was confirmed without interference with the maleimides present on the polymer backbone. For instance, the disappearance of the *tert*-butoxy groups was observed at 1-1.5 ppm, while the characteristic peak of **3** at 7.5 and 7.9 ppm remained unchanged. Similarly while performing the deprotection on the sequence-controlled polymers based on **d**, the peaks at 2-2.5 ppm from the acetoxy groups vanished (**Figure 43**). It is noteworthy to mention that these sequence-controlled deprotected polymers were soluble in basic aqueous solutions.
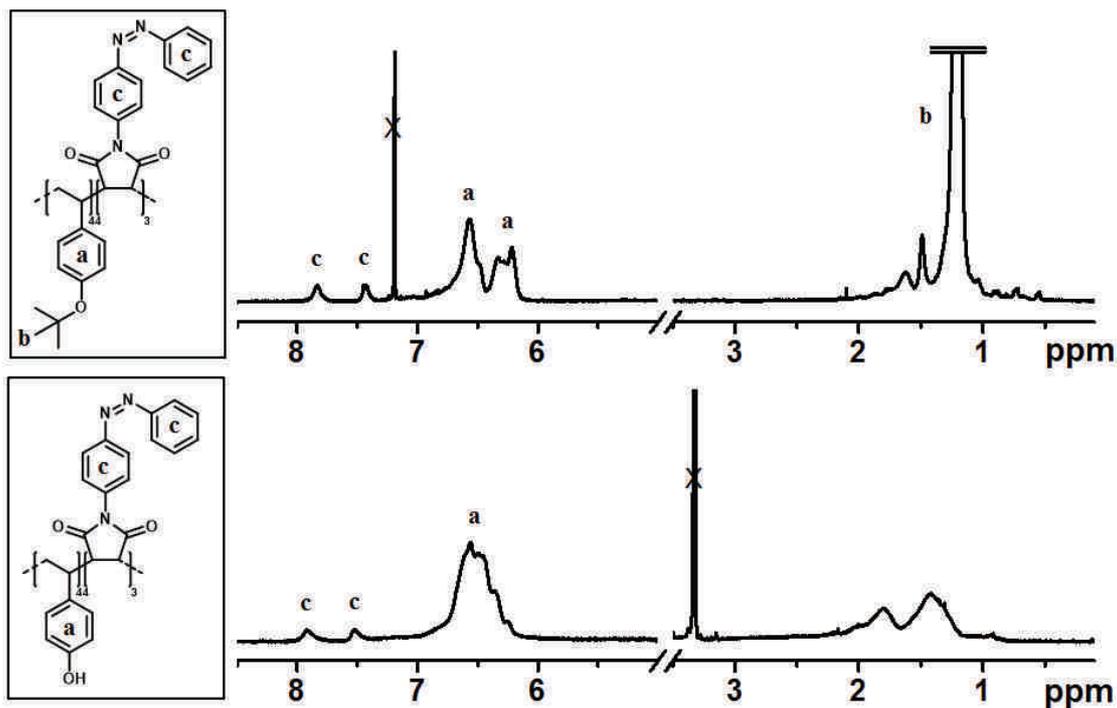
Figure 42. ^{1}H NMR spectra of the polymer obtained by NMP of **c** in the presence of a small amount of **3** introduced at the beginning of the polymerization (Entry 10, **Table 4**) before (top, CDCl$_3$) and after (bottom, CD$_3$OD) acidic treatment. Note that the azobenzene moieties are shown in cis configuration here for aesthetic reasons only.
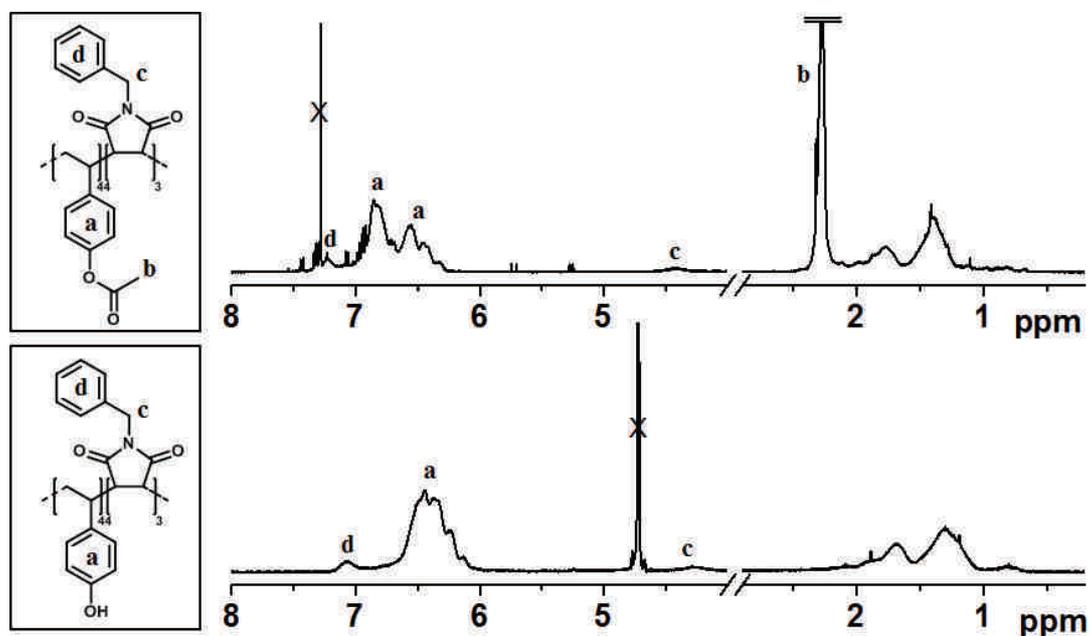
Figure 43. ^{1}H NMR spectra measured for a well-defined copolymer of **d** with **1** (Entry 4, **Table 4**) before (top) and after (bottom) hydrolytic deprotection in acidic conditions. The top and bottom spectra were recorded in CDCl$_3$ and CD$_3$OD, respectively.

The copolymers of **c** with MIs **1**, **2** and **4** were also hydrolyzed (**Figure 44**-**Figure 46**).
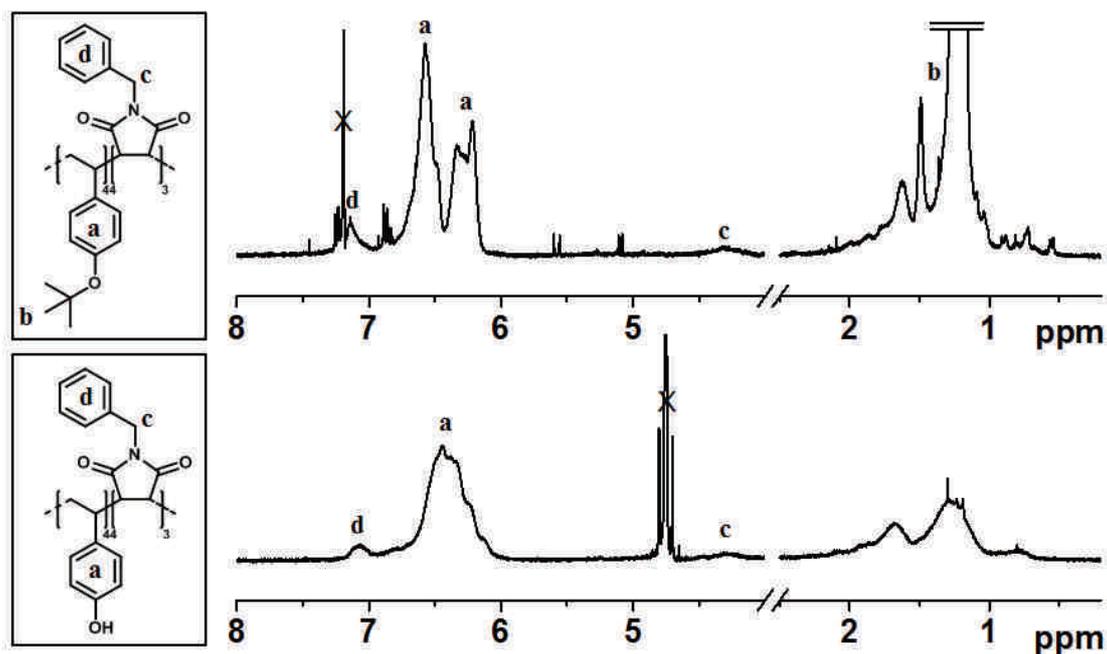
Figure 44. ¹H NMR spectra measured for a well-defined copolymer of **c** with **1** (Entry 3, **Table 4**) before (top) and after (bottom) hydrolytic deprotection in acidic conditions. The top and bottom spectra were recorded in CDCl₃ and CD₃OD, respectively.
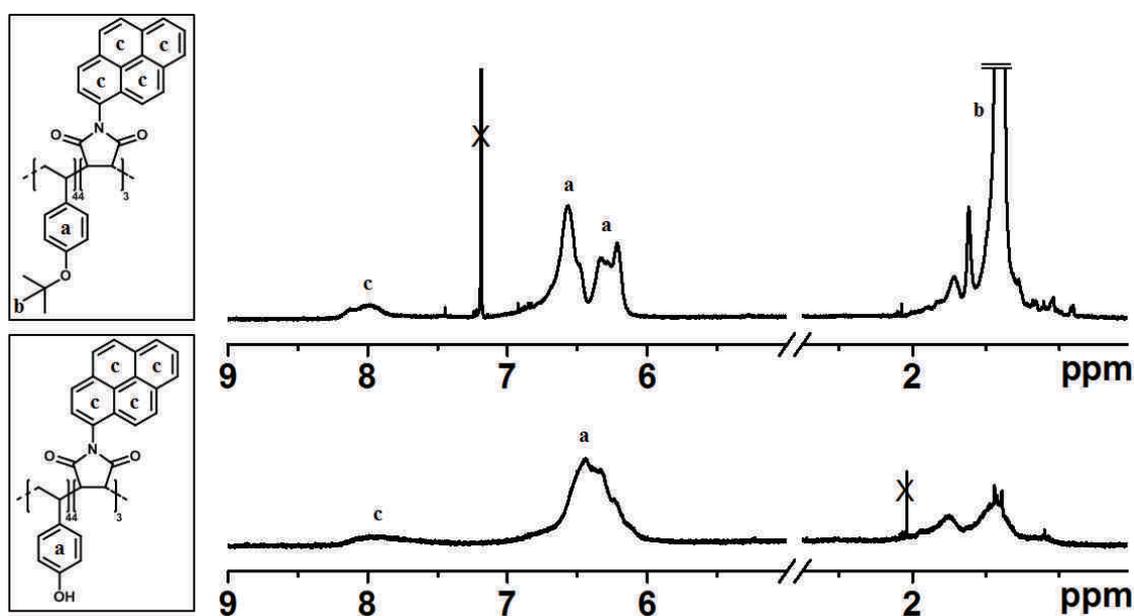
Figure 45. ¹H NMR spectra measured for a well-defined copolymer of **c** with **4** (Entry 11, **Table 4**) before (top) and after (bottom) hydrolytic deprotection in acidic conditions. The top and bottom spectra were recorded in CDCl₃ and CD₃OD, respectively.

In all cases, ^{1}H NMR above confirmed that the sequence-controlled microstructure was preserved after deprotection. For instance, for **1**, typical signals of the MIs units can be observed at 4.3 and 7.1 ppm (**Figure 44**), while for **4**, a broad signal around 8 ppm is distinguishable (**Figure 45**).

In the case of **2**, the acidic treatment also cleaved the Boc protecting group, thus leading to poly(4-hydroxystyrene) containing local primary amine functions (**Figure 46**). The presence of primary amines after deprotection was confirmed by a positive Kaiser test.
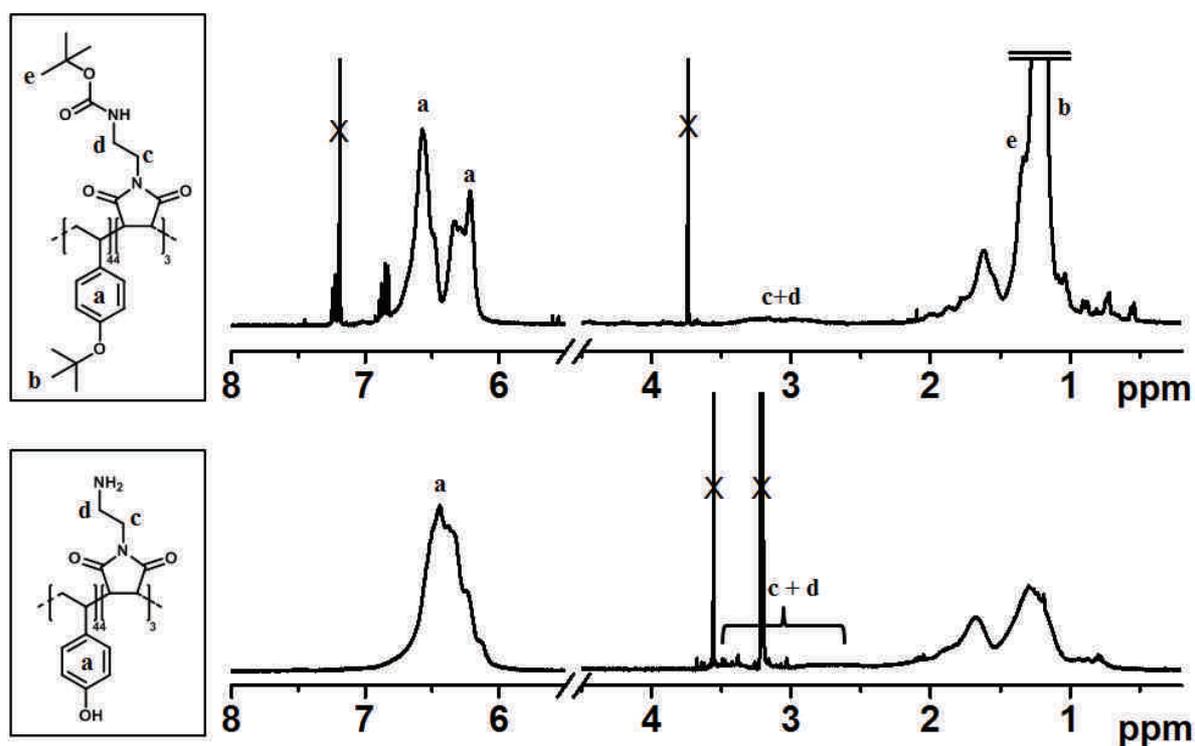
Figure 46. ^{1}H NMR spectra measured for a well-defined copolymer of **c** with **2** (Entry 9, **Table 4**) before (top) and after (bottom) hydrolytic deprotection in acidic conditions. The top and bottom spectra were recorded in CDCl$_3$ and CD$_3$OD, respectively.

II.3 Conclusion

In summary, the present work provides additional evidence on the versatility of sequence-controlled donor-acceptor copolymerizations. Besides the broad alphabet of acceptor monomers described in previous publication [3], a variety of donor monomers can be used in this approach. In particular, the use of strong donor substituents (e.g. *tert*-butoxy) in *para* position of styrenic derivatives leads to particularly precise sequence-controlled copolymerizations. Furthermore, these hydrophobic precursors can be easily transformed into hydrophilic polymers bearing precisely localized functionalities.

References

[1].   Giuseppone, N.; Lutz, J.-F., *Nature,* **2011**, *473*, 40-41.

[2].   Lutz, J.-F., *Nat. Chem.,* **2010**, *2*, 84-85.

[3].   Ouchi, M.; Badi, N.; Lutz, J.-F.; Sawamoto, M., *Nat. Chem.,* **2011**, *3*, 917-924.

[4].   Terashima, T.; Mes, T.; De Greef, T. F. A.; Gillissen, M. A. J.; Besenius, P.; Palmans, A. R. A.; Meijer, E. W., *J. Am. Chem. Soc.,* **2011**, *133*, 4742-4745.

[5].   Thomas, C. M.; Lutz, J.-F., *Angew. Chem., Int. Ed.,* **2011**, *50*, 9244-9246.

[6].   Pfeifer, S.; Zarafshani, Z.; Badi, N.; Lutz, J.-F., *J. Am. Chem. Soc.,* **2009**, *131*, 9195-9197.

[7].   Lutz, J.-F., *Polym. Chem.,* **2010**, *1*, 55-62.

[8].   Pfeifer, S.; Lutz, J.-F., *J. Am. Chem. Soc.,* **2007**, *129*, 9542-9543.

[9].   Ida, S.; Terashima, T.; Ouchi, M.; Sawamoto, M., *J. Am. Chem. Soc.,* **2009**, *131*, 10808-10809.

[10].   Kramer, J. W.; Treitler, D. S.; Dunn, E. W.; Castro, P. M.; Roisnel, T.; Thomas, C. M.; Coates, G. W., *J. Am. Chem. Soc.,* **2009**, *131*, 16042–16044.

[11].   Pfeifer, S.; Zarafshani, Z.; Badi, N.; Lutz, J.-F., *J. Am. Chem. Soc.,* **2009**, *131*, 9195-9197.

[12].   McKee, M. L.; Milnes, P. J.; Bath, J.; Stulz, E.; Turberfield, A. J.; O'Reilly, R. K., *Angew. Chem., Int. Ed.,* **2010**, *49*, 7948-7951.

[13].   Satoh, K.; Matsuda, M.; Nagai, K.; Kamigaito, M., *J. Am. Chem. Soc.,* **2010**, *132*, 10003-10005.

[14].   Satoh, K.; Ozawa, S.; Mizutani, M.; Nagai, K.; Kamigaito, M., *Nat. Commun.,* **2010**, *1*, 1-6.

[15].   Stayshich, R. M.; Meyer, T. Y., *J. Am. Chem. Soc.,* **2010**, *132*, 10920-10934.

[16].   Hibi, Y.; Ouchi, M.; Sawamoto, M., *Angew. Chem., Int. Ed.,* **2011**, *50*, 7434-7437.

[17].   Pfeifer, S.; Lutz, J.-F., *Chem. Eur. J.,* **2008**, *14*, 10949-10957.

[18].   Lutz, J.-F.; Schmidt, B. V. K. J.; Pfeifer, S., *Macromol. Rapid Commun.,* **2011**, *32*, 127-135.

[19].   Berthet, M. A.; Zarafshani, Z.; Pfeifer, S.; Lutz, J.-F., *Macromolecules,* **2010**, *43*, 44-50.

[20].   Lutz, J.-F.; Schmidt, B. V. K. J.; Pfeifer, S., *Macromol. Rapid. Commun.,* **2011**, *32*, 127-135.

[21].   Srichan, S.; Oswald, L.; Zamfir, M.; Lutz, J.-F., *Chem. Commun.,* **2012**, *48*, 1517-1519.

[22].   Kakuchi, R.; Zamfir, M.; Lutz, J.-F.; Theato, P., *Macromol. Rapid Commun.,* **2012**, *33*, 54-60.

[23].   Srichan, S.; Oswald, L.; Zamfir, M.; Lutz, J.-F., *Chem. Commun.,* **2012**, *48*, 1517-1519.

[24].   Qiu, J.; Matyjaszewski, K., *Macromolecules,* **1997**, *30*, 5643-5648.

[25].   Van Herk, A. M., *Macromol. Theory Simul.,* **2000**, *9*, 433-441.

[26].   Conlon, D. A.; Crivello, J. V.; Lee, J. L.; Obrien, M. J., *Macromolecules,* **1989**, *22*, 509-516.

[27].   Higashimura, T.; Kojima, K.; Sawamoto, M., *Makromol. Chem. ,* **1989**, 127-136.

[28].   Gao, B.; Chen, X. Y.; Ivan, B.; Kops, J.; Batsberg, W., *Macromol. Rapid Commun.,* **1997**, *18*, 1095-1100.

[29]. Barclay, G. G.; Hawker, C. J.; Ito, H.; Orellana, A.; Malenfant, P. R. L.; Sinta, R. F., *Macromolecules,* **1998**, *31*, 1024-1031.

[30]. Satoh, K.; Kamigaito, M.; Sawamoto, M., *Macromolecules,* **2000**, *33*, 5830-5835.

[31]. Lee, S. M.; Fréchet, J. M. J., *Macromolecules,* **1994**, *27*, 5160-5166.

[32]. Lee, S. M.; Fréchet, J. M. J.; Willson, C. G., *Macromolecules,* **1994**, *27*, 5154-5159.

Chapter III

On the Synthesis of Sequence-Controlled Poly(Vinyl Benzyl Amine-*co*-N-Substituted Maleimides) Copolymers

Abstract

The sequence-controlled copolymerization of donor and acceptor comonomers was studied for the synthesis of primary amine-containing copolymers with precisely controlled functional microstructures. For this, a large excess of phthalimide-protected vinyl benzyl amine was copolymerized with discrete amounts of *N*-substituted maleimides, namely *N*-benzylmaleimide, *N*-(*n*-propyl)maleimide, 4-(*N*-maleimido)-azobenzene and triisopropylsilyl-protected *N*-propargyl maleimide, in the presence of the commercial alkoxyamine BlocBuilder® MA. The formed copolymers were characterized by ^{1}H NMR and size exclusion chromatography (SEC), and exhibited controlled chain-length, molecular weight distribution and comonomer sequence distribution. After copolymerization, the phthalimide protecting groups were removed by treatment with hydrazine monohydrate to afford vinyl benzyl amine-based copolymers. ^{1}H and ^{13}C NMR characterization of the deprotected samples indicated that the functional *N*-substituted succinimide moieties were preserved in the copolymers after hydrazine monohydrate treatment. Moreover, the obtained sequence-controlled copolymers were readily soluble in acidic water.

Keywords: Sequence-controlled polymers, primary structure, functional polymers, water-soluble polymers, microstructure, orthogonal deprotection.

III.1 Introduction

The synthesis of sequence-controlled copolymers is a topic of increasing importance in recent polymer science [1-4]. Thus, over the last few years, promising concepts have been reported for the preparation of sequence-controlled macromolecules, for example using iterative [5-7], step-growth [8], template [9-12], multiblock [13-15] or kinetic strategies [16,17]. In the latter case, it has been pointed out that well-defined copolymers with complex microstructures can be prepared using comonomers that exhibit very different reactivities [18]. In particular, in a recent series of papers [16,19] our group has described a method based on the controlled radical copolymerization of non-stoichiometric amounts of donor and acceptor comonomers. In this approach, a donor monomer such as styrene is polymerized in excess by atom transfer radical polymerization (ATRP) or nitroxide-mediated polymerization (NMP) and small amounts of acceptor comonomers - that are typically *N*-substituted maleimides (MIs) - are added at controlled times during the course of the reaction [16,20]. In most cases, the acceptor monomers are incorporated into narrow regions of the growing polymer chains immediately after their addition due to a kinetically-favored donor-acceptor cross-propagation [18]. Moreover, the localization of the acceptor comonomer units in the formed polymer backbone can be precisely tuned by using time-controlled MIs additions in conjunction with the controlled/living polymerization mechanism [18]. It was also recently shown that the use of optimized copolymerization feeds significantly minimizes chain-to-chain composition and sequence defects, which are inherent to the radical chain growth mechanism [21]. This simple and original polymerization method was exploited for the synthesis of single-chain functional arrays [22-24], multicyclic topologies [25-27], and dendronized microstructures [28].

In the present work, we investigated a new type of donor comonomer containing a protected primary amine. During the last decades, it was reported that primary amine-containing (co)polymers are interesting structures for applications in aqueous self-assembly, biotechnology and membrane science, in particular due to the fact that they form stable complexes with polyanions [29-34]. These polymers are also reactive and can be easily modified [35]. Different polymerization techniques, including radical, ionic, and ring-opening mechanisms have been employed for the synthesis of amine-containing polymers [36]. However, the direct use of monomers containing free primary amine functions is problematic

in many polymerization methods. For instance, in reversible addition-fragmentation chain transfer (RAFT) process, free primary amines lead to the aminolysis of the thiocarbonylthio chain transfer agents that are used to control the polymerization [36]. Free-amine bearing monomers are also problematic in ATRP due to the fact that the formed polymer chains may displace the ligand of the copper catalyst complex [36,37]. In NMP, Maric and coworkers have shown that small fractions of non-protected amine-containing monomers can be used in copolymerization without altering the apparent control of the reaction [38]. However, above a critical composition, side reactions and a poorer control of the polymerization were observed. Thus, amine-containing polymers are generally prepared using a post-polymerization modification procedure. For instance, poly(vinyl benzyl amine) can be synthesized by radical polymerization of vinyl benzyl chloride followed by a Gabriel [29,31,32] or a Staudinger [39] modification step.

Alternatively, *N*-(*p*-vinylbenzyl)phthalimide (**VBP** in **Scheme 5**) can be used as a protected precursor. This particular monomer has been previously tested in controlled radical polymerizations. For example, Patten and coworkers have studied the ATRP of **VBP** [32]. Block copolymers polystyrene-*b*-polyVBP were first prepared in that work and afterwards deprotected into amphiphilic polystyrene-*b*-poly(vinyl benzyl amine). Fukuda and coworkers have studied the NMP of **VBP** using the TEMPO as a nitroxide [40]. However, mild conversions and relatively broad molecular weight distributions were obtained in this work. More recently, Palmans and coworkers reported optimized NMP conditions for preparing well-defined random copolymers based on styrene and **VBP** [41]. Inspired by these earlier studies, **VBP** was selected in the present work as a donor monomer and tested in sequence-controlled copolymerization with model MIs (**Scheme 5**). These copolymers were synthesized by NMP using the commercially available alkoxyamine BlocBuilder® MA. After copolymerization, the phthalimide protecting groups were removed in order to afford sequence-controlled primary amine-containing copolymers.

Scheme 5. General strategy studied in the present work for the preparation of sequence controlled amine-pendant copolymers. The acronym NMP denotes nitroxide-mediated polymerization. Experimental conditions: I) NMP in toluene solution (solvent/monomer 3:1 v/v), 110 °C. II) Hydrazine monohydrate, EtOH$_{abs.}$, reflux (condition applied specifically for MI **4**).

III.2 Results and Discussion

The sequence-controlled copolymerization of *N*-(*p*-vinyl benzyl)phthalimide and various model *N*-substituted maleimides was studied (**Scheme 5**). NMP was selected as a polymerization method for preparing these copolymers since it allows in general an excellent control of the homopolymerization and copolymerization of styrenic derivatives [42,43].

In particular, the commercially available alkoxyamine BlocBuilder® MA was used as polymerization initiator [44]. All polymerization reactions were conducted in toluene or anisole solution. At first, the homopolymerization of **VBP** was studied (**Table 6**). Polymers with different targeted molecular weight were prepared at 110 °C in anisole (monomer/solvent 1:3 v/v). Moreover, as shown in **Table 6**, the experimental molecular weight of the formed homopolymers depended on the initial monomer/initiator ratio used in

each experiment. All these results suggest that the NMP of **VBP** is well-controlled by BlocBuilder® MA.

Table 6. Experimental conditions and molecular characterization of homopolymers obtained by NMP of **VBP** at 110 °C.[a]

	[VBP]	t_{end}[b]	conv.$_{end}$[c]	M_n[d] [g·mol^{-1}]	$M_{n,th}$[e]	M_w/M_n[d]
P1	20 eq.	360	0.84	7400	4804	1.10
P2	50 eq.	320	0.81	17000	11045	1.09
P3	100 eq.	360	0.80	24700	21440	1.37

[a] All experiments were performed in anisole solution in the presence of 1 eq. of BlocBuilder with VBP/anisole = 1:3 v/v. [b] Final polymerization time. [c] Conversion of **VBP** at the end of the reaction as measured by ^{1}H NMR in CDCl$_3$. [d] Number average molecular weight and molecular weight distribution measured by SEC in THF. [e] $M_{n,th}$ = M$_{VBP}$·conv.$_{VBP}$·[VBP]/[BlocBuilder] + M$_{BlocBuilder}$; where M$_{VBP}$ and M$_{BlocBuilder}$ are the molecular weights of **VBP** and BlocBuilder, respectively.

Figure 47 shows examples of semi-logarithmic plots of monomer conversion versus time and plots of number average molecular weight (M_n) versus monomer conversion obtained in such experimental conditions. The linearity of these two plots indicates that an excellent control of the homopolymerization of **VBP** was obtained in the studied conditions. SEC analysis further confirmed the controlled nature of the polymerization, with unimodal traces and low M_w/M_n being observed up to relatively high conversion with no evidence of high molecular weight species from bimolecular termination (**Figure 47c**).

Encouraged by these promising results, the NMP copolymerization of **VBP** with model *N*-substituted maleimides, such as *N*-benzylmaleimide (**1**), *N*-propyl maleimide (**2**), 4-(*N*-maleimido)azobenzene (**3**), and triisopropylsilyl-protected *N*-propargylmaleimide (**4**) was then investigated as illustrated in **Scheme 5**. Comonomers **1** and **2** were selected as reference monomers due to the fact that their copolymerization kinetics with styrene are well-described in the literature [19,45]. Comonomer **3** was chosen as a model since azobenzene chromophores are interesting moieties that can respond to changes in environmental

conditions, while **4** was selected as an example of a post-functionalizable reactive unit. The sequence-controlled copolymerization of these monomers with **VBP** was monitored by ^{1}H NMR.
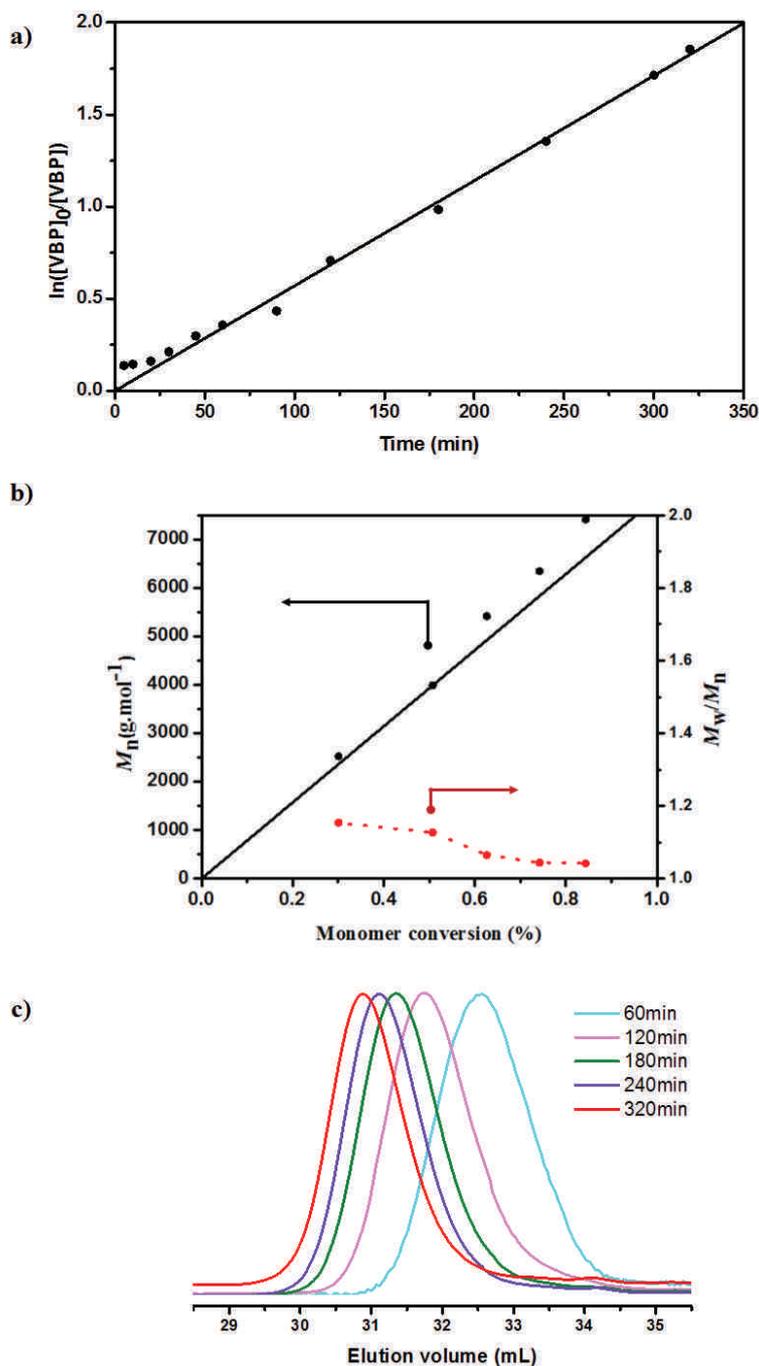
Figure 47. NMP of **VBP** in the presence of BlocBuilder® MA (**P1, Table 6**). a) Semi-logarithmic plots of **VBP** conversion versus time. b) Plot of experimental M_n (black circles), theoretical M_n (black line) and M_w/M_n (red circles) versus monomer conversion. c) SEC chromatograms of aliquots taken during the polymerization of **VBP** after 60 (red line), 120 (green line), 180 (grey line), 240 (blue line) and 320 min (black line).

Figure 48 shows typical copolymerization kinetics recorded for **VBP** with comonomers **3** and **4**. The semi-logarithmic plots of comonomers conversion versus time clearly show that the small amounts of MIs are consumed extremely fast in the presence of a large excess of **VBP**. For example, during the synthesis of copolymer **C3**, quantitative conversion of **3** was observed in 30 minutes, while during the same time interval **VBP** conversion was only about 20 %. Comparable trends were also observed with maleimides **1** and **2** (**Table 7**).
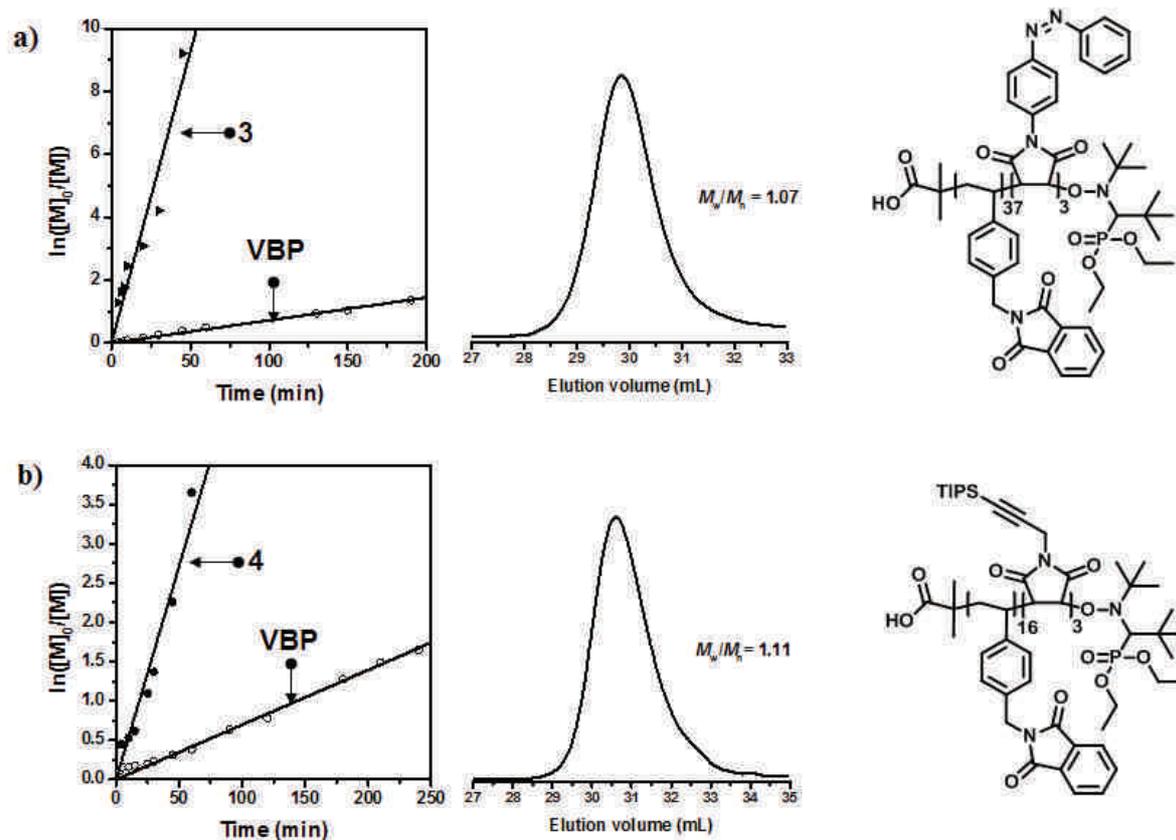

Figure 48. Sequence-controlled NMP of a large excess of **VBP** in the presence of small amounts of *N*-substituted maleimides. a) Maleimide **3**. b) Maleimide **4**. The two displayed examples correspond to copolymers **C3** and **C5** in **Table 7** respectively. Left: semi-logarithmic plot of comonomers conversion versus time. Middle: SEC chromatograms of the final copolymers. Right: corresponding copolymer structures.

Furthermore, the time-controlled incorporation of **4** during the NMP polymerization of **VBP** was studied (**C6**, **Table 7**). In this experiment, **VBP** was first homopolymerized up to 51 % of conversion. Then, **4** was added in the polymerization medium using a degassed syringe. Afterwards, the polymerization was kept for four additional hours until reaching

81 % of **VBP** conversion. As demonstrated in previous publications [16,19,46,47], the MI was copolymerized extremely fast after its addition, and was therefore incorporated in a narrow local region (i.e. approximately in the middle) of the formed copolymer chain. Moreover, all sequence-controlled copolymers synthesized using MIs **1**-**4** exhibited a controlled chain-length and a narrow molecular weight distribution as measured by SEC (**Table 7**).

Table 7. Characterization of copolymers obtained by NMP of **VBP** and MIs.[a]

	VBP [eq.]	MI [eq.]	t_{MIadd}[c] [min]	t_{end}[d] [min]	Conv. VBP·add[e]	Conv. VBP[f]	Conv. VBP·end[g]	M_n[h] [g·mol^{-1}]	$M_{n,th}$[i]	M_w/M_n[h]
C1[b]	50	**1** [3]	0	180	0	0.55	0.95	16500	13449	1.23
C2	50	**2** [5]	0	240	0	0.30	0.88	16100	12662	1.11
C3	50	**3** [3]	0	190	0	0.23	0.74	17800	10955	1.07
C4	50	**4** [3]	0	210	0	0.29	0.84	15000	12314	1.08
C5[j]	20	**4** [3]	0	240	0	0.32	0.81	8100	5521	1.11
C6[j]	20	**4** [3]	205	440	0.51	0.70	0.81	6900	5521	1.08
C7[j]	5	**4** [1]	0	192	0	0.56	0.78	2000	1699	1.05

[a] All experiments were performed in anisole solution **VBP**/anisole = 1:3 v/v at 110 °C. [b] The reaction was conducted at 120 °C. [c] Time at which the MI was added in the polymerization medium. [d] Final polymerization time. [e] Conversion of **VBP** calculated from ^{1}H NMR spectra in CDCl$_3$ when the MI was added. [f] Conversion of **VBP** where 99 % of MI were consumed. [g] Conversion of **VBP** calculated from ^{1}H NMR spectra in CDCl$_3$ at the end of reaction. [h] Values measured by SEC in THF. [i] Theoretical number average molecular weight $M_{n,th}$ = M_{VBP}·conv.$_{VBP}$·[**VBP**]/[BlocBuilder] + M_{MI}·conv.$_{MI}$[MI]/[BlocBuilder] + $M_{BlocBuilder}$; where M_{VBP}, M_{MI} and $M_{BlocBuilder}$ are the molecular weights of **VBP**, **MI** and BlocBuilder respectively. [j] Experiments were performed in toluene solution **VBP**/toluene = 1:3 v/v.

Since, no literature data is available for reactivity ratios between **VBP** and *N*-substituted maleimides using either conventional radical polymerization or controlled one, Jaacks plots were drawn in order to obtain a rough estimation of the copolymerization behavior (**Figure 49**) [48]. For example, a value of 0.04 was measured for the comonomer pair **VBP/3** (**Figure 49a**), thus indicating a strong tendency toward sequence-control [45]. The NMP copolymerization of **VBP** and **4** was studied in toluene (**Figure 49b**). A higher reactivity ratio of 0.13 was calculated in that solvent for the comonomer pair **VBP/4**. This result suggests a slightly less precise MI incorporation in the polyVBP chains. Still, this value shows that this particular comonomer pair is suitable for sequence-controlled copolymerization [18].
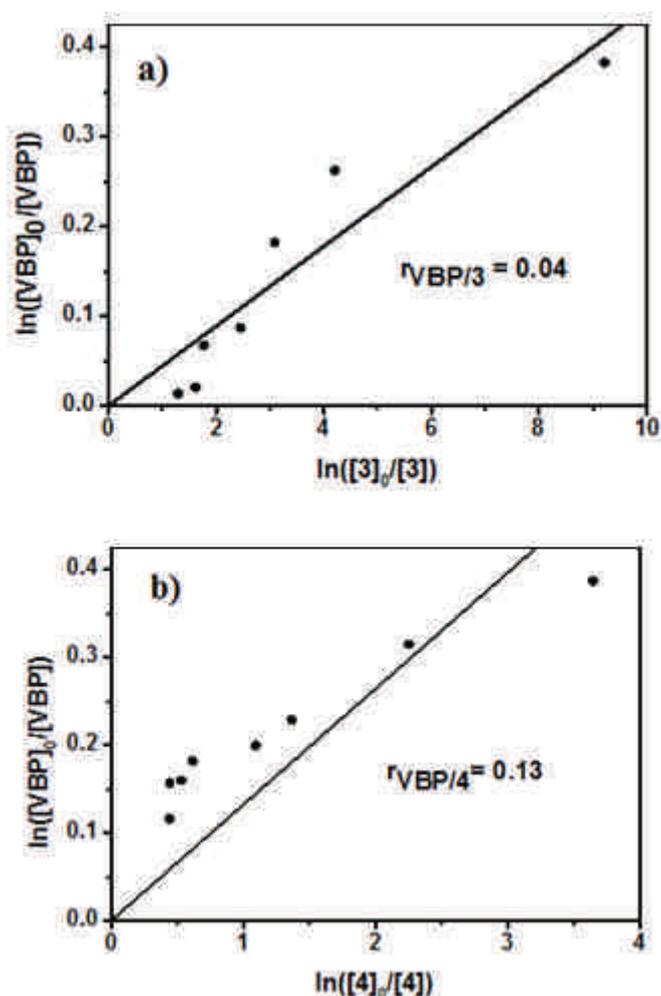

Figure 49. Corresponding Jaacks plots of copolymers. a) **C3** and b) **C5** in **Table 7** respectively.

In order to obtain polymers with free primary amine groups in the side chains, the deprotection of the phthalimide groups of **VBP** was studied. However, this later step is not trivial because it can potentially also lead to ring opening [49] or complete deimidation [50] of the succinimide units in the copolymer as shown in **Scheme 6**. Thus, the deprotection step was carefully studied using ^{1}H and ^{13}C NMR.

This deprotection step is usually performed by hydrazynolysis [32,40,41]. However, in the present case, the synthesized copolymers possess functional succinimide units (i.e. polymerized *N*-substituted maleimides) which can also potentially be cleaved, either partially or fully as shown in reactions in pathway 2 in **Scheme 6**, during the hydrazine monohydrate treatment. Thus, orthogonal deprotection is requested in the present case (pathway 1 in **Scheme 6**). In order to avoid these undesired reactions, a number of preliminary experiments using different concentrations of hydrazine monohydrate have been performed. Hence, the phthalimide groups were easily removed in the copolymers.
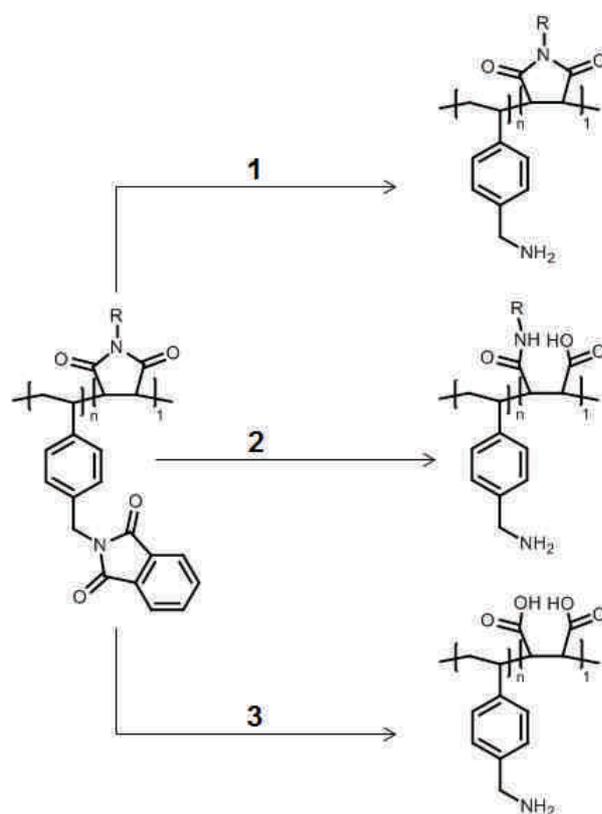
Scheme 6. Cleavage scenarios that may potentially happen during the hydrazine deprotection step and aqueous workup of sequence-controlled copolymers poly(VBP-*co*-N-substituted maleimides). Note that this scheme is simplified for clarity. Depending on the experimental conditions, hydrazide can also be isolated in pathways 2 and 3.

For instance, for copolymer **C4**, quantitative deprotection was obtained in the presence of 57.4 eq. of hydrazine monohydrate; thus affording the corresponding primary amine-containing copolymers **C4´**. As illustrated in **Figure 50** ^{1}H NMR analysis before and after hydrazine treatment clearly confirmed deprotection. The signals due to the phthalimide protecting units at 7.72 and 7.83 ppm fully vanished, whereas the peak at 4.67 ppm corresponding to the methylene protons attached to the phthalimide group were quantitatively shifted to another region of the spectrum.
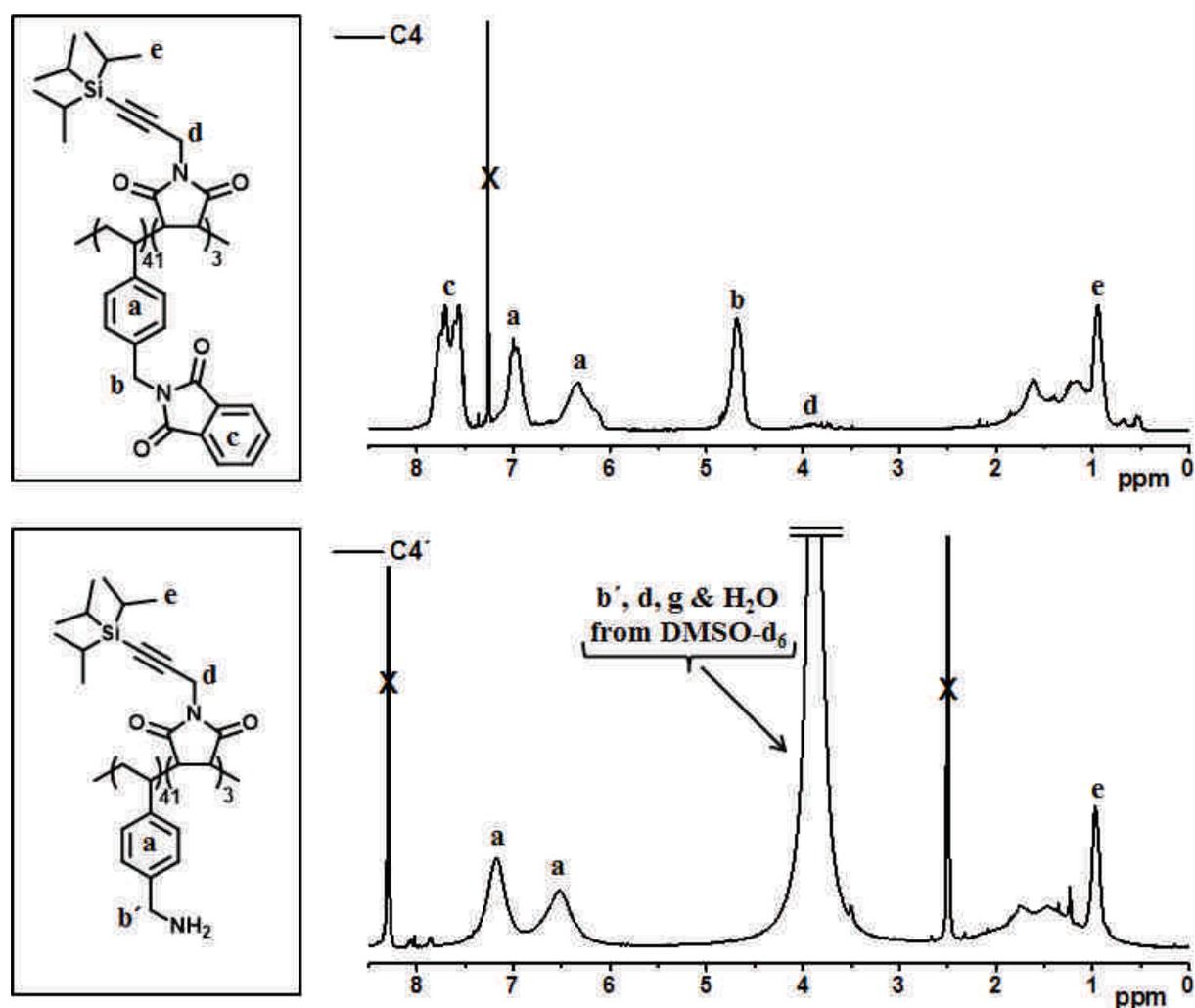

Figure 50. ^{1}H NMR spectra for polymer **C4** (top) and corresponding deprotected polymer **C4´**(bottom). The spectrum for **C4** was recorded in CDCl₃, whereas the one of **C4´** was measured in DMSO-d₆.

It should be however noted that small signals of phthalhydrazide can still be seen at 7.84 and 8.07 ppm in the ^{1}H NMR spectrum of **C4'**, thus indicating that this side product was not

fully removed by dialysis purification. More importantly, the signal of the protons of the TIPS-groups could be still observed at 0.95 ppm in the spectrum of **C4'**. This indicates that the local succinimide units are not fully cleaved during the deprotection step (i.e. pathway 3 in **Scheme 6** can be ruled out). This observation is in accordance with literature data which suggest that harsh hydrazine conditions are necessary to form maleic acid from succinimide units [50].

In order to confirm the orthogonal deprotection of the phthalimide moieties in the copolymers, a model sample with a very short chain-length was prepared (copolymer **C7** in **Table 7**) and deprotected using the aforementioned experimental conditions. **Figure 51** shows a comparison of ^{13}C NMR for polymer **C7** and corresponding deprotected polymer **C7´**.
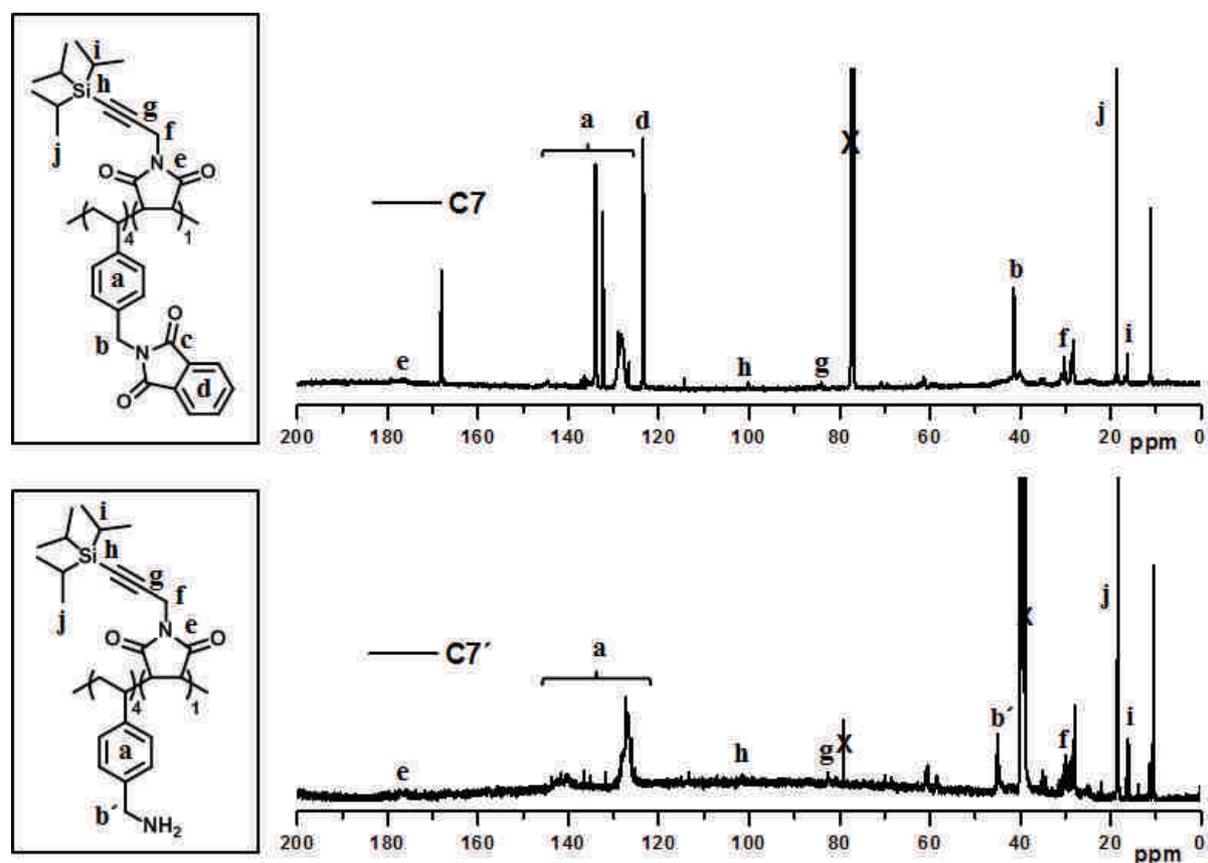

Figure 51. ^{13}C NMR for the model copolymer **C7** and corresponding deprotected polymer **C7´**.

Successful deprotection of the copolymer is confirmed by ^{13}C NMR through the loss of aromatic carbons of the phthalimide rings in the range of 120-140 ppm. If hydrolysis had

also occurred on the TIPS-functionalized succinimide units in the copolymer, one should also observe some signal changes for the succinimide carbons. However, the peaks at 176.36 ppm corresponding to the carbonyl carbons of the succinimide rings remained unchanged before and after deprotection, thus suggesting that pathway 2 in **Scheme 6** is not significantly happening. These results are in agreement with previous observations of Parisi and coworkers who reported that long reaction times are need to ring-open poly(succinimide)s in the presence of hydrazine in ethanolic suspension [49].

FT-IR analysis of copolymer **C7'** also supports that scenario (**Figure 52**). The band at 1567 cm^{-1} indicates that free amine side chains are present in the copolymer. Moreover, the observed band at 1176 cm^{-1} band may be due to the succinimide (C-N-C) stretch, while the band at 1771 and 1710 cm^{-1} are probably due to the symmetric and asymmetric (C=O) stretch in the succinimide moiety. All these results suggest that the sequence-controlled microstructure of the copolymers was preserved after deprotection. Moreover, all the deprotected polymers could be dissolved in water at acidic pH.
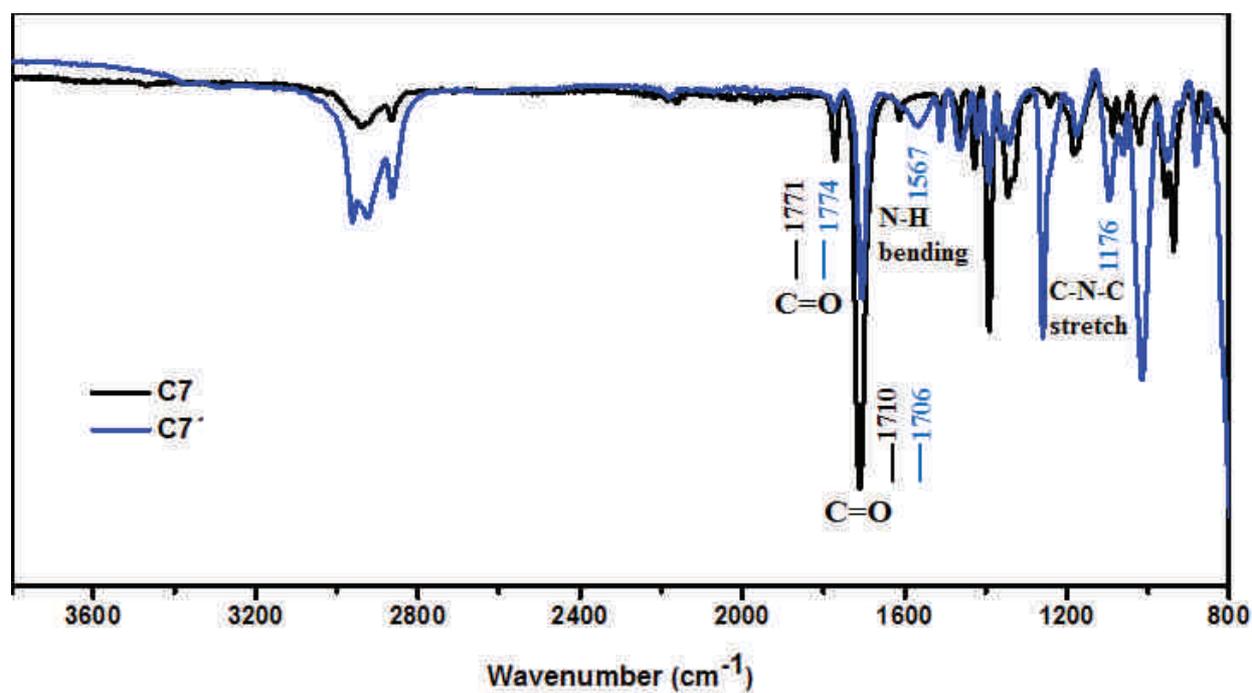

Figure 52. FT-IR spectra for the model copolymer **C7** and corresponding deprotected polymer **C7´**.

III.3 Conclusions

The sequence-controlled copolymerization of *N*-(*p*-vinyl benzyl)phthalimide with various *N*-substituted maleimides was investigated. It was found that the nitroxide-mediated copolymerization of **VBP** and MIs is on the whole well-controlled. Moreover, the reactivity ratios calculated for the different **VBP**/MIs donor-acceptor comonomer pairs indicated that **VBP** is a suitable donor monomer for sequence-controlled copolymerizations. Indeed, it was possible to incorporate small fractions of MIs in local regions of the polyVBP chains, either by adding MIs at the beginning of the reaction or using time-controlled addition protocols. In all cases, the formed copolymers exhibited controlled chain-lengths, molecular weight distributions and primary structures. Moreover, it was possible to transform these well-defined copolymers into water-soluble polyamines using a facile hydrazine deprotection step. ^{1}H NMR, ^{13}C NMR and FT-IR studies indicated that the chosen deprotection conditions cleave quasi-selectively the phthalimide protecting groups of **VBP** but do not influence notably the functional succinimide units in the copolymers. In other words, the deprotected copolymers still exhibit a controlled primary structure. Thus, the present method seems optimal for preparing sequence-controlled polycations and complements our previous findings on sequence-controlled water-soluble copolymers [46,47,51].

References

[1].   Lutz, J.-F.; Ouchi, M.; Liu, D. R.; Sawamoto, M., *Science,* **2013**, *341*, 1238149.

[2].   Badi, N.; Lutz, J. F., *Chem. Soc. Rev.,* **2009**, *38*, 3383-90.

[3].   Lutz, J.-F., *Polym. Chem.,* **2010**, *1*, 55-62.

[4].   Lutz, J.-F., *Nat. Chem.,* **2010**, *2*, 84-85.

[5].   Pfeifer, S.; Zarafshani, Z.; Badi, N.; Lutz, J. F., *J. Am. Chem. Soc.,* **2009**, *131*, 9195-9197.

[6].   Espeel, P.; Carrette, L. L. G.; Bury, K.; Capenberghs, S.; Martins, J. C.; Du Prez, F. E.; Madder, A., *Angew. Chem. Int. Ed.,* **2013**, *52*, 13261-13264.

[7].   Solleder, S. C.; Meier, M. A. R., *Angew. Chem. Int. Ed.,* **2014**, *53*, 711-714.

[8].   Satoh, K.; Ozawa, S.; Mizutani, M.; Nagai, K.; Kamigaito, M., *Nat. Commun.,* **2010**, *1*, 1-6.

[9].   Ida, S.; Terashima, T.; Ouchi, M.; Sawamoto, M., *J. Am. Chem. Soc.,* **2009**, *131*, 10808-10809.

[10].   McKee, M. L.; Milnes, P. J.; Bath, J.; Stulz, E.; Turberfield, A. J.; O'Reilly, R. K., *Angew. Chem. Int. Ed.,* **2010**, *49*, 7948-7951.

[11].   Hibi, Y.; Ouchi, M.; Sawamoto, M., *Angew. Chem. Int. Ed.,* **2011**, *50*, 7434-7437.

[12].   Niu, J.; Hili, R.; Liu, D. R., *Nat. Chem.,* **2013**, *5*, 282-292.

[13].   Zhang, Q.; Collins, J.; Anastasaki, A.; Wallis, R.; Mitchell, D. A.; Becer, C. R.; Haddleton, D. M., *Angew. Chem. Int. Ed.,* **2013**, *52*, 4435-4439.

[14].   Gody, G.; Maschmeyer, T.; Zetterlund, P. B.; Perrier, S., *Nat. Commun.,* **2013**, *4*, 2505. Doi: 10.1038/ncomms3505.

[15].   Anastasaki, A.; Nikolaou, V.; Pappas, G. S.; Zhang, Q.; Wan, C.; Wilson, P.; Davis, T. P.; Whittaker, M. R.; Haddleton, D. M., *Chem. Sci.,* **2014**, *5*, 3536-3542.

[16].   Pfeifer, S.; Lutz, J.-F., *J. Am. Chem. Soc.,* **2007**, *129*, 9542-9543.

[17].   Satoh, K.; Matsuda, M.; Nagai, K.; Kamigaito, M., *J. Am. Chem. Soc.,* **2010**, *132*, 10003-10005.

[18].   Lutz, J.-F., *Acc. Chem. Res.,* **2013**, *46*, 2696-2705.

[19].   Pfeifer, S.; Lutz, J.-F., *Chem. Eur. J.,* **2008**, *14*, 10949-10957.

[20].   Lutz, J.-F.; Schmidt, B. V. K. J.; Pfeifer, S., *Macromol. Rapid Commun.,* **2011**, *32*, 127-135.

[21].   Zamfir, M.; Lutz, J.-F., *Nat. Commun.,* **2012**, *3*, 1138.

[22].   Berthet, M.-A.; Zarafshani, Z.; Pfeifer, S.; Lutz, J.-F., *Macromolecules,* **2009**, *43*, 44-50.

[23].   Chan-Seng, D.; Zamfir, M.; Lutz, J.-F., *Angew. Chem. Int. Ed.,* **2012**, *51*, 12254-12257.

[24].   Baradel, N.; Fort, S.; Halila, S.; Badi, N.; Lutz, J.-F., *Angew. Chem. Int. Ed.,* **2013**, *52*, 2335-2339.

[25].   Schmidt, B. V. K. J.; Fechler, N.; Falkenhagen, J.; Lutz, J.-F., *Nat. Chem.,* **2011**, *3*, 234-238.

[26].   Zamfir, M.; Theato, P.; Lutz, J.-F., *Polym. Chem.,* **2012**, *3*, 1796-1802.

[27]. Shishkan, O.; Zamfir, M.; Gauthier, M. A.; Börner, H. G.; Lutz, J.-F., *Chem. Commun.,* **2014**, *50*, 1570-1572.

[28]. Baradel, N.; Fort, S.; Halila, S.; Badi, N.; Lutz, J.-F., *Angew. Chem. Int. Ed.,* **2013**, *52*, 2335-2339.

[29]. Mitchell, A. R.; Kent, S. B. H.; Erickson, B. W.; Merrifield, R. B., *Tetrahedron Lett.,* **1976**, *17*, 3795-3798.

[30]. Charreyre, M.-T.; Razafindrakoto, V.; Veron, L.; Delair, T.; Pichot, C., *Macromol. Chem. Phys.,* **1994**, *195*, 2141-2152.

[31]. Adams, J. H.; Cook, R. M.; Hudson, D.; Jammalamadaka, V.; Lyttle, M. H.; Songster, M. F., *J. Org. Chem.,* **1998**, *63*, 3706-3716.

[32]. Gravano, S. M.; Borden, M.; von Werne, T.; Doerffler, E. M.; Salazar, G.; Chen, A.; Kisak, E.; Zasadzinski, J. A.; Patten, T. E.; Longo, M. L., *Langmuir,* **2002**, *18*, 1938-1941.

[33]. Jaeger, W.; Bohrisch, J.; Laschewsky, A., *Prog. Polym.Sci.,* **2010**, *35*, 511-577.

[34]. Laschewsky, A., *Curr. Opin. Colloid Interface Sci.,* **2012**, *17*, 56-63.

[35]. Bohrisch, J.; Eisenbach, C.; Jaeger, W.; Mori, H.; Müller, A. E.; Rehahn, M.; Schaller, C.; Traser, S.; Wittmeyer, P., New Polyelectrolyte Architectures. In *Polyelectrolytes with Defined Molecular Architecture I*, Schmidt, M., Ed. Springer Berlin Heidelberg: **2004**; Vol. 165, pp 1-42.

[36]. Janoschka, T.; Teichler, A.; Krieg, A.; Hager, M. D.; Schubert, U. S., *J. Polym. Sci. Part A: Polym. Chem.,* **2012**, *50*, 1394-1407.

[37]. Summers, G. J.; Ndawuni, M. P.; Summers, C. A., *Polym. Int.,* **2003**, *52*, 158-163.

[38]. Marić, M.; Lessard, B. H.; Consolante, V.; Ling, E. J. Y., *React. Funct. Polym.,* **2011**, *71*, 1137-1147.

[39]. Ting, W.-H.; Dai, S. A.; Shih, Y.-F.; Yang, I. K.; Su, W.-C.; Jeng, R.-J., *Polymer,* **2008**, *49*, 1497-1505.

[40]. Ohno, K.; Izu, Y.; Tsujii, Y.; Fukuda, T.; Kitano, H., *Eur. Polym. J.,* **2004**, *40*, 81-88.

[41]. Stals, P. J. M.; Phan, T. N. T.; Gigmes, D.; Paffen, T. F. E.; Meijer, E. W.; Palmans, A. R. A., *J. Polym. Sci. Part A: Polym. Chem.,* **2012**, *50*, 780-791.

[42]. Lacroix-Desmazes, P.; Lutz, J.-F.; Boutevin, B., *Macromol. Chem. Phys.,* **2000**, *201*, 662-669.

[43]. Lutz, J.-F.; Lacroix-Desmazes, P.; Boutevin, B., *Macromol. Rapid Commun.,* **2001**, *22*, 189-193.

[44]. Nicolas, J.; Guillaneuf, Y.; Lefay, C.; Bertin, D.; Gigmes, D.; Charleux, B., *Prog Polym Sci,* **2013**, *38*, 63-235.

[45]. Lutz, J.-F.; Schmidt, B. V. K. J.; Pfeifer, S., *Macromol Rapid Commun,* **2011**, *32*, 127-135.

[46]. Srichan, S.; Oswald, L.; Zamfir, M.; Lutz, J.-F., *Chem. Commun.,* **2012**, *48*, 1517-1519.

[47]. Srichan, S.; Mutlu, H.; Badi, N.; Lutz, J.-F., *Angew. Chem. Int. Ed.,* **2014**, *53*, 9231-9235.

[48]. Jaacks, V., *Makromol. Chem.,* **1972**, *161*, 161-172.

[49]. Meirim MG, N. E., Parisi F., *Angew. Makromol. Chem.,* **1990**, *175*, 141-156.

[50]. Go, D.; Jeon, H.; Kim, T.; Kim, G.; Choi, J.; Lee, J.; Kim, J.; Yoo, H.-O.; Bae, Y., *Macromol. Res.,* **2008**, *16*, 659-662.

[51]. Srichan, S.; Chan-Seng, D.; Lutz, J.-F., *ACS Macro Lett.,* **2012**, *1*, 589-592.

Chapter IV

Precision PEGylated Polymers Obtained by Sequence-Controlled Copolymerization and Post-Polymerization Modification

Abstract

Copolymers containing water-soluble poly(ethylene glycol) (PEG) side-chains and precisely-controlled functional microstructures were synthesized by sequence-controlled copolymerization of donor and acceptor comonomers, that is, styrenic derivatives and *N*-substituted maleimides. Two routes were compared for the preparation of these structures: (a) the direct use of a PEG-styrene macromonomer as donor comonomer, and (b) the use of an alkyne-functionalized styrenic comonomer, which was PEGylated by copper-catalyzed alkyne-azide cycloaddition after polymerization. The latter method was found to be the most versatile and enabled the synthesis of high-precision copolymers. For example, PEGylated copolymers containing precisely positioned fluorescent (e.g. pyrene), switchable (e.g. azobenzene) and reactive functionalities (e.g. an activated ester) were prepared.

Keywords: Alkyne-azide cycloaddition, donor-acceptor copolymerization, post-polymerization modification, sequence-controlled polymer, water-soluble polymer.

IV.1. Introduction

The development of synthetic polymers with controlled sequences of monomers is a topic that has received increasing attention in recent fundamental polymer science [1-3]. Indeed, as shown in many recent studies [4-12], monomer sequence regulation opens up previously unexplored avenues for controlling the structure, properties and functions of synthetic macromolecules. Consequently, a number of methods have been described for the preparation of sequence-controlled polymers. Many of them aim at making perfectly monodisperse sequenced-defined polymers. Such structures can be obtained using iterative syntheses [13-17], templates [18,19] or complex molecular machines [20]. An alternative strategy consists of regulating monomer feeds and reactivity in conventional polymerization methods such as chain-growth or step-growth polymerizations [21-25]. Such approaches are usually not perfect but allow some degree of control over comonomer sequence distribution.

The earliest example of such a strategy was reported by our group [26]. It is a one-pot kinetic process that allows precise incorporation of *N*-substituted maleimides (MIs) in specific regions of styrene-based polymer backbones [27-29]. In this approach, the polymers are prepared using a controlled/living radical polymerization (CRP) method such as atom transfer radical polymerization (ATRP) and nitroxide-mediated polymerization (NMP), in which all chains are initiated in the early stages of the reaction and grow simultaneously at the same rate [30-32]. When different comonomers are used in such a controlled/living mechanism, their incorporation in the growing chains depends on their chemical reactivity. For example, acceptor comonomers (e.g. MIs) and donor comonomers (e.g. styrene) have usually a very strong tendency to copolymerize (i.e. cross-propagation is kinetically favored compared to homopolymerization). Thus, in CRP conditions, MIs are usually incorporated in the chains directly after their addition to the reaction mixture, even if the donor comonomer is used in large (e.g. 20-100 folds) excess [33]. Hence, by the time-controlled additions of MIs, it is possible to create polymers with complex microstructures in a one-pot process [26,34]. The macromolecules synthesized by this process are donor homopolymers containing positionable functional MI "patches". Of course, these copolymers are not perfectly sequence-defined. Owing to the statistical nature of chain-growth copolymerizations, chain-to-chain sequence inhomogeneity is still present in these polymers [33]. Thus, these copolymers are generally referred to as "sequence-controlled" rather than "sequence-defined" [35].

Nevertheless, the method is simple and versatile, and therefore enables the synthesis of macromolecular structures of unprecedented complexity [36-40].

Although most of the polymers prepared by this approach were based on hydrophobic polystyrene backbones, the method can also be extended to the preparation of sequence-controlled water-soluble polymers. For example, we recently reported the synthesis of sequence-controlled copolymers based on poly(vinyl benzoic acid) (PVBA) [41], poly(4-hydroxystyrene) (PHS) [42] and poly(vinyl benzyl amine) (PVBAm) [43] backbones. However, although interesting, these examples were not fully satisfying. Indeed, a limited control over comonomer sequence distribution was possible in the case of PVBA and PHS-based copolymers and PVBAm could only be dissolved in water under high alkaline or acidic conditions respectively. Thus, to date, there is no example of non-ionic sequence-controlled copolymers that can be dissolved in water at a neutral pH value. Such polymers could be of high fundamental importance. For example, it is known that graft polymers with oligo(ethylene glycol) (OEG) side-chains are very useful alternatives to traditional linear poly(ethylene glycol) (PEG) for applications in biology and medicine [44-47]. Moreover, these polymers often exhibit interesting stimuli-responsive properties in aqueous media [48,49]. Thus, the placement of functional groups (e.g. hydrophobic moieties, fluorescent markers or reactive groups) at specific locations on such polymers could enable fine-tuning of their properties in water.

IV.2. Results and discussion

In this context, we describe herein a facile method for preparing sequence-controlled PEGylated polymers. These macromolecules were prepared by sequence-controlled copolymerization of styrenic derivatives and *N*-substituted maleimides. We compared two different strategies for the synthesis of these polymers (**Scheme 7**). The most obvious approach is the direct use of a PEG-functionalized styrenic macromonomer (**Scheme 7**, approach a) [50,51]. Thus, the nitroxide-mediated polymerization (NMP) of vinyl benzyl ethers of OEG (**1**) was first investigated. Different macromonomers with 7, 9 and 10 OEG units were tested. These experiments were performed using the commercial alkoxyamine BlocBuilder® MA in anisole solution. Although a broad range of experimental conditions was screened, the radical homopolymerization of **1** could not be well-controlled. Polymers

with a broad molecular weight distribution were obtained in all cases as shown in **Table 8**. These results are not suitable for the sequence-controlled copolymerization of styrenes and *N*-substituted maleimides. Indeed, as mentioned previously [33], our strategy requires that the polymerization of the styrenic monomer, which is used in large excess (20-100 molar equivalents as compared to initiator), is perfectly controlled to minimize chain-to-chain structural inhomogeneity.

Scheme 7. Strategies investigated in the present work for the preparation of sequence-controlled PEGylated copolymers. a) Direct copolymerization of a PEG-styrene macromonomer with *N*-substituted maleimides. b) Post-polymerization modification approach, in which azido-PEGs were grafted on alkyne-functional sequence-controlled precursors. The acronym NMP denotes nitroxide-mediated polymerization. Experimental conditions: (I) [Styrenic monomer]/[*N*-substituted maleimide]/[BlocBuilder® MA] = 20/1/1, anisole, 115 °C; (II) TBAF, THF, room temperature, overnight (this procedure was only applied to copolymers based on monomer **3** and MIs **4-7**; (III) CuBr/dNBipy, THF, room temperature. dNBipy = 4,4′-dinonyl-2-2,2′-bipyridine, TIPS = triisopropylsilyl, TMS = trimethylsilyl.

Alternatively, post-polymerization modification strategy was studied for the preparation of sequence-controlled PEGylated polymers (**Scheme 7**, approach b). This concept relies on the use of alkyne-functionalized styrenic monomers that were first copolymerized with *N*-substituted maleimides and afterwards PEGylated by copper-catalyzed azide-alkyne cycloaddition (CuAAC) [52]. The first crucial point in this strategy was the choice of the appropriate alkyne-containing monomer. The most tempting option was to use a styrenic derivative bearing an unprotected terminal-alkyne substituent on the *para* position of its aromatic ring, for example, 4-propargyloxystyrene (**2**) [53]. However, the NMP of this monomer is in general poorly-controlled. Although the experimental kinetics fulfilled the criteria of a controlled/living mechanism, the formed polymers exhibited a broad molecular weight distribution. This behavior is most probably due to radical additions on the unprotected acetylene groups [54].

Table 8. Selected results of nitroxide-mediated polymerization studies of monomers **1**, **2** and **3** represented in **Scheme 7**.[a]

	M [b] [eq.]	M/S [b]	T [c] [°C]	t_{end} [d] [min]	conv.$_M$ [e]	M_n [f] [g·mol^{-1}]	$M_{n,th}$ [g] [g·mol^{-1}]	M_w/M_n [f]
1	**1** (50)	1/1	120	360	0.92	19500	25400	1.92
2	**2** (50)	-	100	480	0.39	10500	6600	1.63
3	**2** (100)	1/0.5	115	180	0.35	7100	7600	1.82
4	**3** (100)	1/0.5	115	420	0.68	17400	16000	1.84
5	**3** (50)	1/1.0	115	380	0.72	11800	8700	1.18
6	**3** (50)	1/1.5	115	480	0.75	12200	9000	1.20
7	**3** (50)	1/2.0	115	340	0.50	9400	6140	1.14

[a] All homopolymerizations were performed in the presence of 1 equivalent of BlocBuilder® MA. [b] **M** and **S** represent monomer and solvent, respectively. [c] Temperature of the polymerization. [d] t_{end} denotes the final polymerization time. [e] Conversion of **1**, **2** and **3** at the end of the reaction as estimated from ^{1}H NMR spectra in CDCl$_3$. [f] Average molecular weight and molecular weight distribution determined by SEC in THF. [g] Theoretical $M_{n,th} = M_M \cdot \text{Conv.}_M \cdot [M]/[\text{BlocBuilder}] + M_{\text{BlocBuilder}}$ where M_M and $M_{\text{BlocBuilder}}$ are molecular weights of the corresponding monomers and BlocBuilder, respectively.

Confronted with these limitations, we selected TMS-protected propargyloxystyrene (**3**) as a donor monomer [53,55]. The NMP homopolymerization of **3** was studied at different concentration in anisole solution (**Table 8**). In all cases, the polymerization proceeded well according to first-order kinetics with reasonable conversions. However, it was found that the control of the homopolymerization was significantly influenced by the initial monomer concentration of monomer **3**. Under semi-dilute conditions (monomer/solvent = 1:0.5 v/v), the formed homopolymers exhibited broad bimodal molecular weight distributions ($M_w/M_n \approx$ 1.8). Better control was obtained at higher monomer dilution (with an initial monomer/solvent ratio of 1:1 v/v). The best results were obtained at a monomer/solvent ratio of 1:2 v/v. Under these optimized conditions, well-defined polymers with controlled molecular weights and narrow molecular (e.g. $M_w/M_n \approx 1.14$) weight distributions were obtained as shown in **Table 9.** Moreover, the homopolymerization of **3** was later performed with different chain-length using this condition. In all cases, the obtained polymers were well-defined and exhibited a control over molecular weight and molecular weight distribution (**Table 9** and **Figure 53**).

Table 9. Properties of homopolymers of **3** prepared by nitroxide-mediated polymerization under optimized reaction conditions.[a]

	3 [eq.]	**t_{end}[b] [min]**	**conv.$_3$[c]**	**M_n[d] [g·mol^{-1}]**	**$M_{n.th}$[e] [g·mol^{-1}]**	**M_w/M_n[d]**
1	100 eq.	360	0.49	11700	12700	1.29
2	50 eq.	340	0.50	9400	6140	1.14
3	20 eq.	312	0.76	5000	3900	1.14

[a] All homopolymerizations were performed in the presence of 1 equivalent of BlocBuilder in anisole at 115 °C, **3**/anisole = 1:2 v/v. [b] Final polymerization time. [c] Conversion of **3** at the end of the reaction as estimated from ^{1}H NMR spectra in CDCl$_3$. [d] Determined by SEC in THF. [e] Theoretical $M_{n,th}$ = M$_3$·Conv.$_3$·[**3**]/[BlocBuilder] + M$_{BlocBuilder}$ where M$_3$ and M$_{BlocBuilder}$ are molecular weights of **3** and BlocBuilder, respectively.
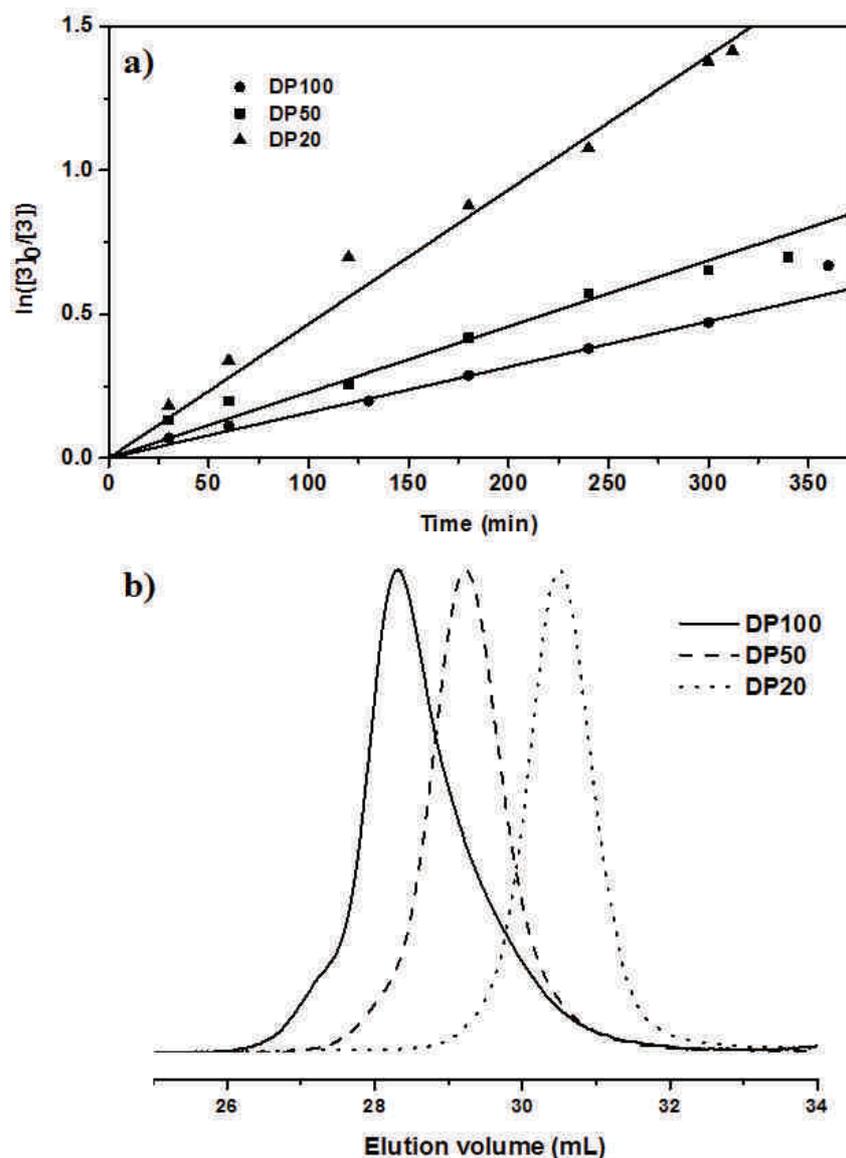
**Figure 53.** Characterization of homopolymers of **3** represented in **Table 9**. a) Semi-logarithmic plot of monomer conversion versus time for NMP of **3** with DP100 (circles), DP50 (squares) and DP20 (triangles), respectively. b) SEC trace of the homopolymers DP100 (solid line), DP50 (dashed line) and DP20 (dotted line), respectively.

These optimal experimental conditions were selected for the sequence-controlled copolymerization of **3** with *N*-substituted maleimides (**Table 10**). In particular, five acceptor comonomers were tested in this study (**Scheme 7**): *N*-(1-pyrenyl) maleimide (**4**), 4-(*N*-maleimido) azobenzene (**5**), *N*-(1-pyrenemethyl) maleimide (**6**), pentafluorophenyl 4-maleimidobenzoate (**7**) and TIPS-protected *N*-propargyl maleimide (**8**). Monomers **4** and **6** were chosen since they enable the precise incorporation of a pyrene group in the polymer

chain. It is known that such fluorescent and hydrophobic moieties are particularly interesting for the characterization of water-soluble polymers [56]. Monomer **5** bears a photo-switchable azobenzene group, which is also of interest for tuning the hydrophilic-hydrophobic balance of PEG-based polymers [57]. Monomers **7** and **8** contain reactive functionalities that can be used after polymerization for local chain modification [52,58]. The NMP copolymerization of a large excess of **3** (20 molar equivalents as compared to the initiator) with discrete amounts of *N*-substituted maleimides (an equimolar amount with respect to the initiator) enabled sequence-control. As demonstrated in previous publications [27-29], by time-controlled additions, the MIs can be positioned at any desired location in the polymer chains (i.e. the red bar in **Scheme 7** can be virtually placed anywhere). Thus, various copolymers with different microstructures were prepared (**Table 10**). In all cases, kinetic monitoring of the copolymerization by ^{1}H NMR spectroscopy evidenced a sequence-controlled copolymerization behavior. For example, **Figure 54** shows the copolymerization kinetics recorded for the copolymerization of **3** and **7**.

Table 10. Copolymers of **3** with *N*-substituted maleimides.[a]

	MI	t_{add}[b] [min]	t_{end}[c] [min]	conv.[d]	M_n[e] [g·mol^{-1}]	$M_{n,th}$[f] [g·mol^{-1}]	M_w/M_n[e]
C1	**4**	120	315	0.72	4000	4000	1.14
C2	**5**	0	300	0.75	3900	3800	1.20
C3	**6**	120	240	0.71	4800	3600	1.14
C4	**7**	180	340	0.81	5000	4500	1.13
C5	**8**	120	240	0.78	4700	4200	1.18

[a] Experimental conditions: 115 °C, [**3**]/[**MI**]/[BlocBuilder] = 20/1/1, anisole in solution (**3**/anisole = 1:2 v/v, except for the synthesis of **C2** in which case a 1/1 was used). [b] Time at which the **MI** was added in the polymerization medium. [c] Final polymerization time. [d] Conversion of **3** at the end of the reaction. [e] The number average molecular weight (M_n) and the molecular weight distribution (M_w/M_n) were determined by SEC in THF. [f] $M_{n,th}$ = M$_3$·Conv.$_3$·[**3**]/[BlocBuilder] + M$_{MI}$·Conv.$_{MI}$[**MI**] /[BlocBuilder] + M$_{BlocBuilder}$ where M$_3$, M$_{MI}$ and M$_{BlocBuilder}$ are molecular weights of **3**, **MI** and BlocBuilder, respectively.
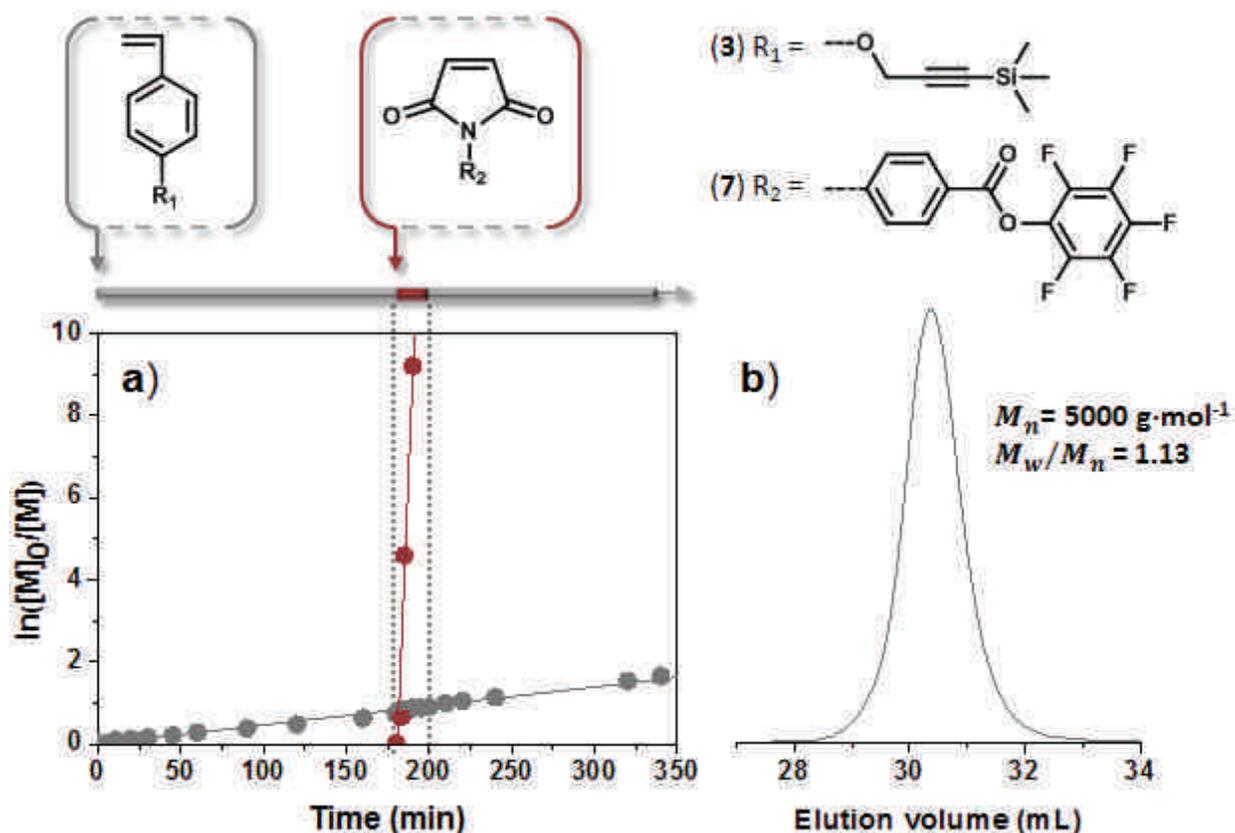
Figure 54. Example of sequence-controlled copolymerization: NMP of donor comonomer **3** and acceptor comonomer **7** using BlocBuilder® MA in anisole solution. a) Semi-logarithmic plots of comonomers conversion versus time. b) SEC chromatogram of the final copolymer after isolation. This example corresponds to copolymer **C4** in **Table 10**.

In this example, **7** was introduced into the reaction medium after the homopolymerization of **3** for 3 h (i.e. at a conversion of 52 %). Directly after its addition, **7** was quantitatively polymerized within 10 min, whereas the conversion of **3** increased by only 5 %. Afterwards the homopolymerization of **3** was pursued for an additional 2 h. These kinetic results show that **7** can be incorporated at very precise positions along the polymer backbone. Comparable kinetic trends were observed for all other copolymers (the results were shown in Experimental part of this thesis). Moreover, all the formed copolymers exhibited a controlled molecular weight and a narrow molecular weight distribution (**Table 10**). In general, polymers prepared by the sequence-controlled copolymerization of donor and acceptor comonomers exhibit a narrow composition distribution [33].

Afterwards, PEGylation of the sequence-controlled copolymers was investigated. Emrick and coworkers reported a few years ago that CuAAC is an efficient reaction for preparing graft copolymers with PEG side-chains [59]. Indeed, it enables a high-yield "grafting-onto" process. Thus, we tested this method for grafting PEG side-chains on the sequence-controlled backbones. The TMS groups of the pendant alkynes of the homopolymers and copolymers were cleaved with TBAF (**Figure 55**). In all cases, ^{1}H NMR showed quantitative TMS deprotection and the formation of terminal alkyne units.
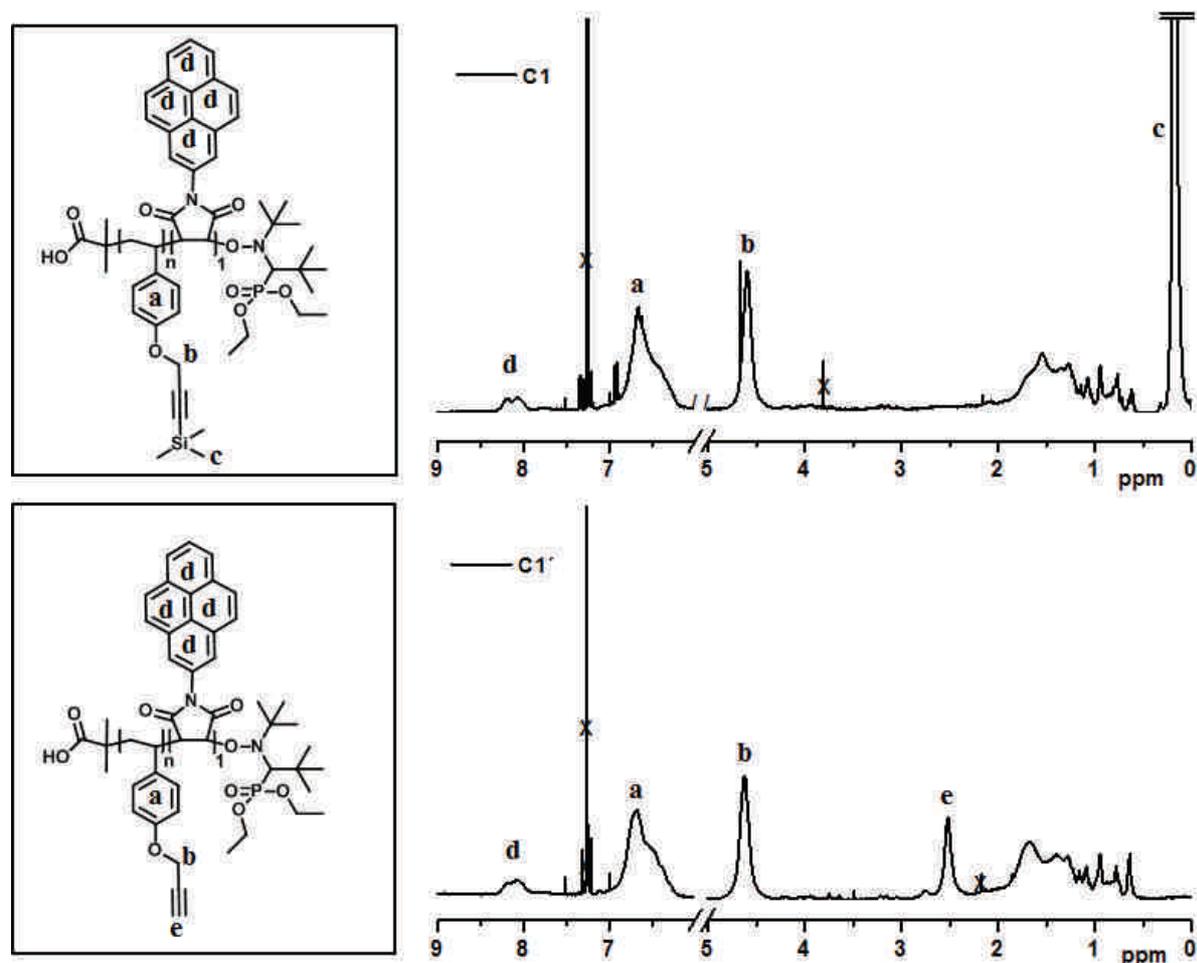
Figure 55. Example of ^{1}H NMR spectra (in CDCl$_3$) of copolymer **C1** before (top) and after removal of TMS protecting group **C1'** (bottom).

The result was also confirmed by size-exclusion chromatography (SEC) analysis. The deprotected copolymers appeared at higher elution volume than their protected precursors. In most cases, the apparent weight loss after deprotection was about 25 %, which suggests

complete removal of the TMS groups. Moreover, all copolymers remained well-defined after deprotection (**Table 11**).

Table 11. Characterization of copolymers **C1**, **C2**, **C3**, **C4** and **C5**, respectively, after removal of TMS[a] and consequent Cu(I)-catalyzed alkyne-azide Huisgen's 1,3 dipolar cycloaddition (CuAAC)[b] with α-methoxy-ω-azido-PEG.

Parent polymer	After deprotection[a]			After CuAAC[b]	
	M_n[c] (g·mol^{-1})	$M_{n,th}$[d] (g·mol^{-1})	M_w/M_n[c]	M_n[e] (g·mol^{-1})	M_w/M_n[e]
C1	3000	2900	1.16	21000	1.04
C2	2400	3000	1.32	18000	1.13
C3	4200	3000	1.10	12200	1.12
C4[f]	3700	3300	1.16	19200	1.15
C5[g]	3500	3200	1.18	15300	1.15

[a] Experimental conditions: TBAF, THF, RT, overnight. [b] Experimental conditions: CuBr/dNBipy, THF, RT, 24 h. [c] Determined by SEC in THF. [d] Theoretical $M_{n,th}$ after deprotection = M_2·Conv.$_2$·[**2**]/[BlocBuilder] + M_{MI}·Conv.$_{MI}$·[MI] /[BlocBuilder] + $M_{BlocBuilder}$ where M_2, M_{MI} and $M_{BlocBuilder}$ are molecular weights of **2**, MI and BlocBuilder, respectively. [e] Determined by SEC in THF before dialysis is performed to the polymers. [f] Prior the CuAAC reaction, the pentaflurophenyl activated ester group was locally modified by reaction with hexylamine as shown in **Figure 58b**. [g] Experimental conditions: DBU, MeCN:H$_2$O (19:1), 60 °C, 5 min.

The alkyne-functionalized copolymers were afterwards PEGylated by CuAAC with α-methoxy-ω-azido-PEG ($M_n \approx$ 2000 g·mol^{-1}). ^{1}H NMR spectroscopy analysis indicated a nearly quantitative modification step. Indeed, the signal of the terminal alkyne hydrogen atoms of the polymer fully disappeared after CuAAC, and characteristic signals due to the formation of a triazole ring appeared at 7.8 ppm (**Figure 56**).
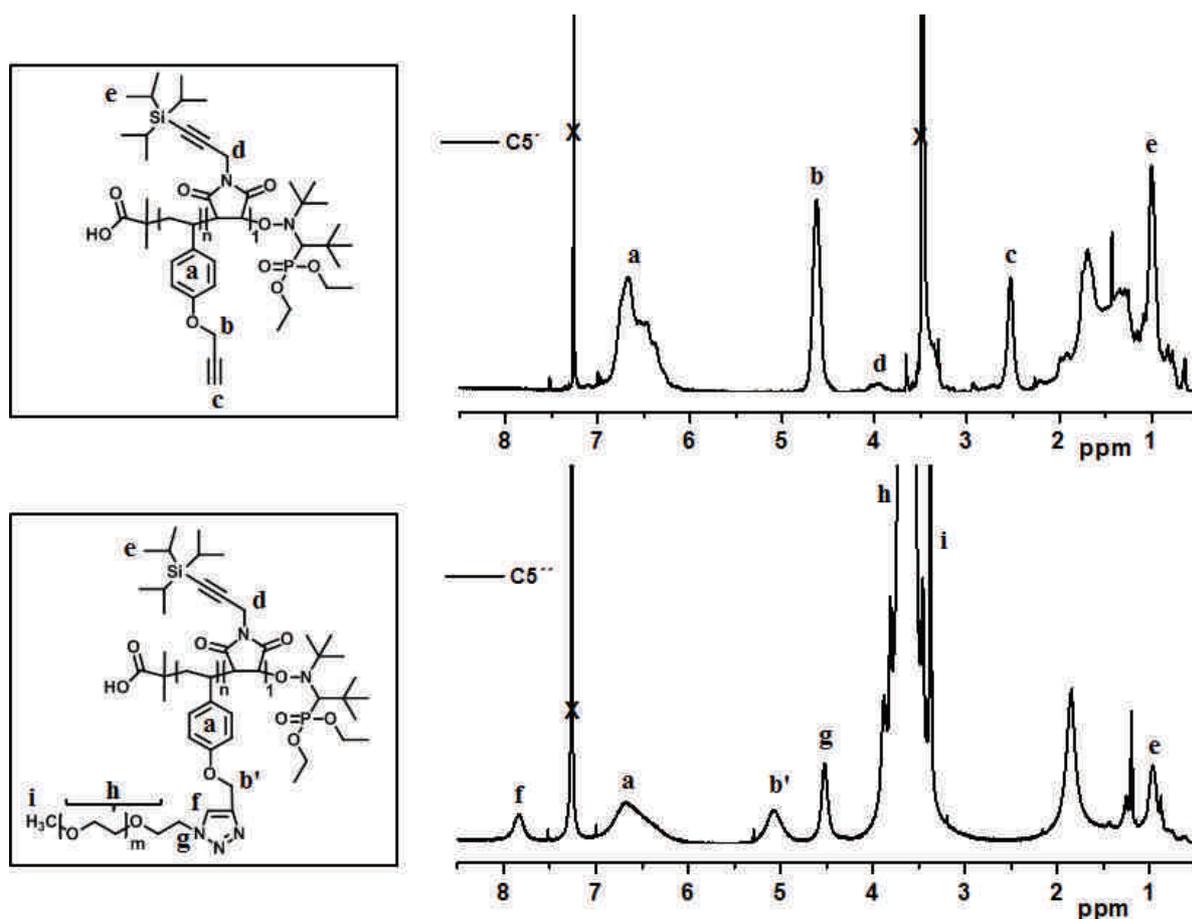
Figure 56. Example of ^{1}H NMR spectra (in CDCl$_3$) of deprotected copolymer **C5'** (top) and PEGylated copolymer by CuAAC **C5''** (bottom).

SEC also indicated the formation of well-defined PEGylated graft copolymers as shown in **Figure 57** and **Table 11**. Indeed, a significant molecular weight increase was observed in all cases. This apparent gain in molecular weight (ΔM) was, however, lower than expected in most cases (e.g. for **C1**, a gain of 18000 g·mol^{-1} was measured instead of 30000 g·mol^{-1}). This underestimation is most probably due to the grafted topology of the formed copolymers. It is well-known that the hydrodynamic volume of PEG-grafted copolymers is smaller than that of linear SEC standards of similar molecular weight [60]. This assumption is also supported by an apparent decrease in the molecular weight distribution after PEGylation (**Table 11**). In all cases, the formed copolymers were found to be readily soluble in neutral water. Furthermore, ^{1}H NMR spectroscopy indicated that the sequence-controlled microstructure of the copolymers remained intact after PEGylation.
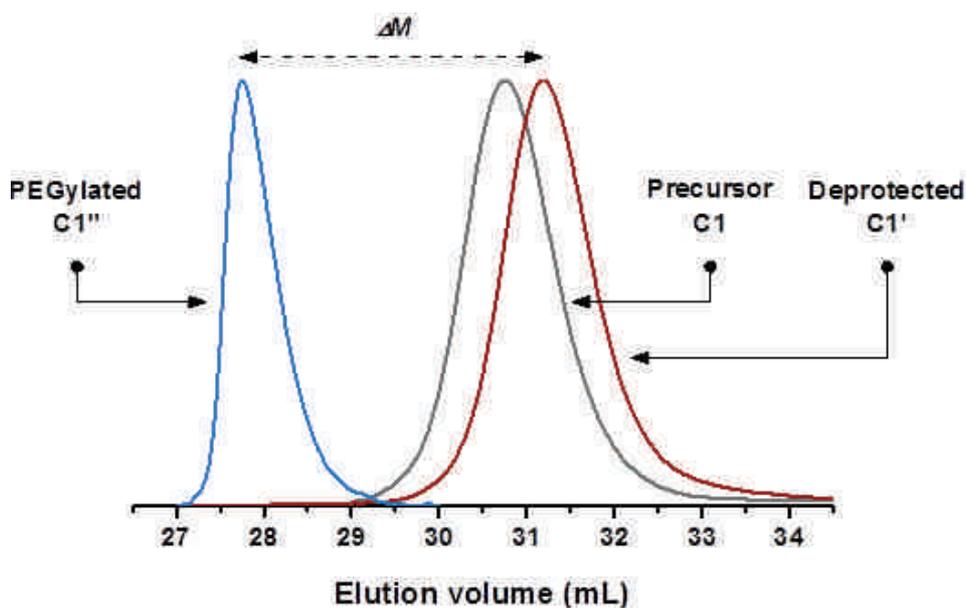
Figure 57. SEC chromatograms recorded in THF for the sequence-controlled copolymer **C1** before modification (grey), after removal of TMS protecting group (**C1'**, red) and after CuAAC PEGylation (**C1"**, blue). For clarity, the signal of the remaining PEG-N$_3$ chains eluting at 30.7 mL was removed from the blue chromatogram. The raw chromatograms of the PEGylated copolymer before and after dialysis can be seen in Experimental part.

The results described in the previous paragraph show that approach b (**Scheme 7**) is simple and efficient for the preparation of sequence-controlled PEGylated copolymers. Moreover, this approach is compatible with additional post-modification steps. The functional microstructure of the copolymers can be tuned using double-modification protocols [61]. For example, the sequence-controlled copolymer **C4**, which contains a pentafluorophenyl-activated ester group, was first locally modified by treatment with hexylamine (**Figure 58b**) [58]. Afterwards, the TMS protecting group of the backbone was removed (**Figure 58c**), and the polymer was PEGylated (**Figure 58d**). Site-selective CuAAC can also be performed on these copolymers [39]. For example, copolymer **C5** contains a TMS-protected propargyloxystyrene backbone and a TIPS-protected local succinimide site. Owing to the larger excess of TMS groups in the copolymer, selective deprotection was only possible by using a 1,8-diazabicyclo[5.4.0]undec-7-ene DBU-based protocol instead of the conventional K$_2$CO$_3$ [62]. Subsequently, the polymer was selectively PEGylated by CuAAC. After PEGylation, the TIPS protecting groups were removed with TBAF, thus making the alkyne site accessible for further modifications.
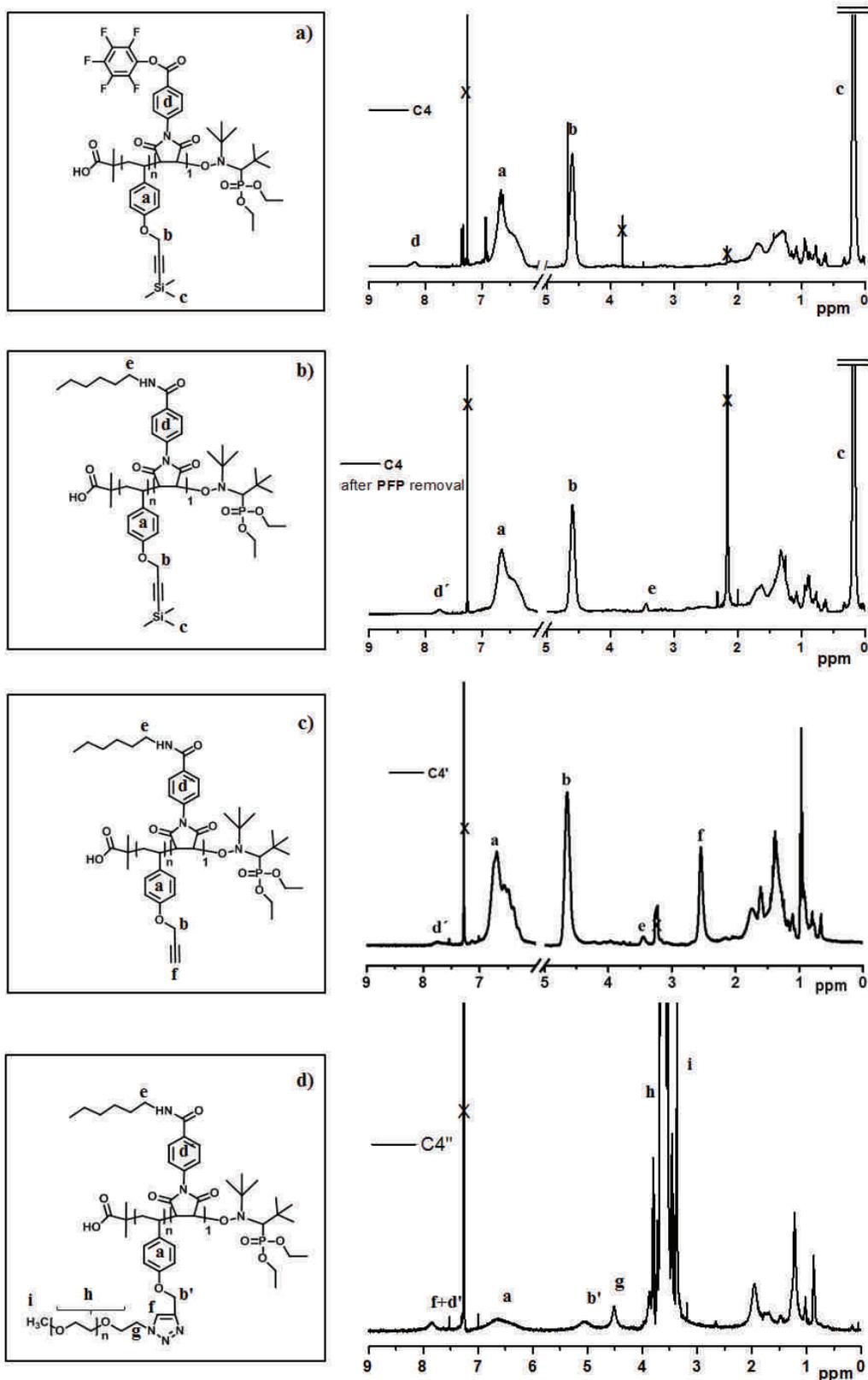
Figure 58. Example of ^{1}H NMR spectra of a) Copolymer **C4** before modification. b) After post-modification of activated ester PFP-group with hexylamine. c) Removal of TMS protecting group (**C4'**) and d) PEGylated copolymer by CuAAC (**C4''**).

IV.3. Conclusion

In summary, the sequence-controlled copolymerization of donor and acceptor comonomers enables the preparation of PEGylated polymers with precisely controlled functional microstructures. However, the use of vinyl benzyl ethers of OEG as donor monomer is not recommended. A finer control of the primary structure was possible with a CuAAC post-polymerization modification strategy. This method enables the synthesis of a wide range of tailored functional PEGylated copolymers. This new class of macromolecules opens interesting avenues in the field of water-soluble polymers. Indeed, as elegantly shown by Terashima, Sawamoto and co-workers [63], precise microstructure variations (e.g. inclusion of discrete hydrophobic sites) in hydrophilic copolymers allow fine-tuning of their properties in water. It is also clear that the present strategy is not restricted to PEGylation. Indeed, as shown in numerous publications, CuAAC post-modification can be used to prepare a wide variety of functional backbones (e.g. glycopolymers, polyelectrolytes, and polymers with high glass transition temperatures) [52,64]. Thus, the present method is probably the most versatile approach reported to date for the preparation of functional sequence-controlled copolymers.

References

[1].   Lutz, J.-F.; Ouchi, M.; Liu, D. R.; Sawamoto, M., *Science,* **2013**, *341*, 1238149.

[2].   Badi, N.; Lutz, J. F., *Chem. Soc. Rev.,* **2009**, *38*, 3383-3390.

[3].   Lutz, J. F., *Polym. Chem.,* **2010**, *1*, 55-62.

[4].   Rojas, G.; Inci, B.; Wei, Y.; Wagener, K. B., *J. Am. Chem. Soc.,* **2009**, *131*, 17376-17386.

[5].   Seitz, M. E.; Chan, C. D.; Opper, K. L.; Baughman, T. W.; Wagener, K. B.; Winey, K. I., *J. Am. Chem. Soc.,* **2010**, *132*, 8165-8174.

[6].   Li, J.; Stayshich, R. M.; Meyer, T. Y., *J. Am. Chem. Soc.,* **2011**, *133*, 6910-6913.

[7].   Terashima, T.; Mes, T.; De Greef, T. F. A.; Gillissen, M. A. J.; Besenius, P.; Palmans, A. R. A.; Meijer, E. W., *J. Am. Chem. Soc.,* **2011**, *133*, 4742-4745.

[8].   Giuseppone, N.; Lutz, J.-F., *Nature,* **2011**, *473*, 40-41.

[9].   Thomas, C. M.; Lutz, J.-F., *Angew. Chem., Int. Ed.,* **2011**, *50*, 9244-9246.

[10].   Li, J.; Rothstein, S. N.; Little, S. R.; Edenborn, H. M.; Meyer, T. Y., *J. Am. Chem. Soc.,* **2012**, *134*, 16352-16359.

[11].   Sun, J.; Teran, A. A.; Liao, X.; Balsara, N. P.; Zuckermann, R. N., *J. Am. Chem. Soc.,* **2013**, *135*, 14119-14124.

[12].   Sun, J.; Teran, A. A.; Liao, X.; Balsara, N. P.; Zuckermann, R. N., *J. Am. Chem. Soc.,* **2014**, *136*, 2070-2077.

[13].   Minoda, M.; Sawamoto, M.; Higashimura, T., *Macromolecules,* **1990**, *23*, 4889-4895.

[14].   Zuckermann, R. N.; Kerr, J. M.; Kent, S. B. H.; Moos, W. H., *J. Am. Chem. Soc.,* **1992**, *114*, 10646-10647.

[15].   Pfeifer, S.; Zarafshani, Z.; Badi, N.; Lutz, J.-F., *J. Am. Chem. Soc.,* **2009**, *131*, 9195-9197.

[16].   Espeel, P.; Carrette, L. L. G.; Bury, K.; Capenberghs, S.; Martins, J. C.; Du Prez, F. E.; Madder, A., *Angew. Chem., Int. Ed.,* **2013**, *52*, 13261-13264.

[17].   Solleder, S. C.; Meier, M. A. R., *Angew. Chem., Int. Ed.,* **2014**, *53*, 711-714.

[18].   McKee, M. L.; Milnes, P. J.; Bath, J.; Stulz, E.; Turberfield, A. J.; O'Reilly, R. K., *Angew. Chem. Int. Ed.,* **2010**, *49*, 7948-7951.

[19].   Niu, J.; Hili, R.; Liu, D. R., *Nat. Chem.,* **2013**, *5*, 282-292.

[20].   Lewandowski, B.; De Bo, G.; Ward, J. W.; Papmeyer, M.; Kuschel, S.; Aldegunde, M. J.; Gramlich, P. M. E.; Heckmann, D.; Goldup, S. M.; D'Souza, D. M.; Fernandes, A. E.; Leigh, D. A., *Science,* **2013**, *339*, 189-193.

[21].   Ida, S.; Terashima, T.; Ouchi, M.; Sawamoto, M., *J. Am. Chem. Soc.,* **2009**, *131*, 10808-10809.

[22].   Satoh, K.; Matsuda, M.; Nagai, K.; Kamigaito, M., *J. Am. Chem. Soc.,* **2010**, *132*, 10003-10005.

[23]. Satoh, K.; Ozawa, S.; Mizutani, M.; Nagai, K.; Kamigaito, M., *Nat. Commun.,* **2010**, *1*, 6.

[24]. Hibi, Y.; Ouchi, M.; Sawamoto, M., *Angew. Chem., Int. Ed.,* **2011**, *50*, 7434-7437.

[25]. Nakatani, K.; Ogura, Y.; Koda, Y.; Terashima, T.; Sawamoto, M., *J. Am. Chem. Soc.,* **2012**, *134*, 4373-4383.

[26]. Pfeifer, S.; Lutz, J.-F., *J. Am. Chem. Soc.,* **2007**, *129*, 9542-9543.

[27]. Pfeifer, S.; Lutz, J. F., *Chem. Eur. J.,* **2008**, *14*, 10949-10957.

[28]. Lutz, J.-F.; Schmidt, B. V. K. J.; Pfeifer, S., *Macromol. Rapid Commun.,* **2011**, *32*, 127-135.

[29]. Zamfir, M.; Lutz, J.-F., *Nat. Commun.,* **2012**, 1138.

[30]. Ouchi, M.; Terashima, T.; Sawamoto, M., *Chem. rev.,,* **2009**, *109*, 4963-5050.

[31]. Tebben, L.; Studer, A., *Angew. Chem. Int. Ed.,* **2011**, *50*, 5034-5068.

[32]. Matyjaszewski, K.; Tsarevsky, N. V., *J. Am. Chem. Soc.,* **2014**, *136*, 6513-6533.

[33]. Lutz, J.-F., *Acc. Chem. Res.,* **2013**, *46*, 2696-2705.

[34]. Chan-Seng, D.; Zamfir, M.; Lutz, J.-F., *Angew. Chem. Int. Ed.,* **2012**, *51*, 12254-12257.

[35]. Zamfir, M.; Lutz, J.-F., Controlling Polymer Primary Structure Using CRP: Synthesis of Sequence-Controlled and Sequence-Defined Polymers. In *Progress in Controlled Radical Polymerization: Materials and Applications*, American Chemical Society: **2012**; Vol. 1101, pp 1-12.

[36]. Berthet, M. A.; Zarafshani, Z.; Pfeifer, S.; Lutz, J.-F., *Macromolecules,* **2010**, *43*, 44-50.

[37]. Schmidt, B. V. K. J.; Fechler, N.; Falkenhagen, J.; Lutz, J.-F., *Nat. Chem.,* **2011**, *3*, 234-238.

[38]. Zamfir, M.; Theato, P.; Lutz, J.-F., *Polym. Chem.,* **2012**, *3*, 1796-1802.

[39]. Baradel, N.; Fort, S.; Halila, S.; Badi, N.; Lutz, J.-F., *Angew. Chem. Int. Ed.,* **2013**, *52*, 2335-2339.

[40]. Shishkan, O.; Zamfir, M.; Gauthier, M. A.; Börner, H. G.; Lutz, J.-F., *Chem. Commun.,* **2014**, *50*, 1570-1572.

[41]. Srichan, S.; Oswald, L.; Zamfir, M.; Lutz, J.-F., *Chem. Commun.,* **2012**, *48*, 1517-1519.

[42]. Srichan, S.; Chan-Seng, D.; Lutz, J.-F., *ACS Macro Lett.,* **2012**, *1*, 589-592.

[43]. Srichan, S.; Mutlu, H.; Lutz, J.-F., *Eur. Polym. J,,* available online DOI: 10.1016/j.eurpolymj.2014.09.002.

[44]. Tao, L.; Mantovani, G.; Lecolley, F.; Haddleton, D. M., *J. Am. Chem. Soc.,* **2004**, *126*, 13220-13221.

[45]. Lutz, J.-F., *J. Polym. Sci. Part A, Polym. Chem.,* **2008**, *46*, 3459-3470.

[46]. Chang, C.-W.; Bays, E.; Tao, L.; Alconcel, S. N. S.; Maynard, H. D., *Chem. Commun.,* **2009**, 3580-3582.

[47]. Joralemon, M. J.; McRae, S.; Emrick, T., *Chem. Commun.,* **2010**, *46*, 1377-1393.

[48]. Lutz, J.-F.; Akdemir, O.; Hoth, A., *J. Am. Chem. Soc.,* **2006**, *128*, 13046-13047.

[49]. Magnusson, J. P.; Khan, A.; Pasparakis, G.; Saeed, A. O.; Wang, W.; Alexander, C., *J. Am. Chem. Soc.,* **2008**, *130*, 10852-10853.

[50]. Zhao, B.; Li, D.; Hua, F.; Green, D. R., *Macromolecules,* **2005**, *38*, 9509-9517.

[51]. Weiss, J.; Li, A.; Wischerhoff, E.; Laschewsky, A., *Polym. Chem.,* **2012**, *3*, 352-361.

[52]. Lutz, J.-F., *Angew. Chem., Int. Ed.,* **2007**, *46*, 1018-1025.

[53]. Fleischmann, S.; Komber, H.; Voit, B., *Macromolecules,* **2008**, *41*, 5255-5264.

[54]. Ciftci, M.; Kahveci, M. U.; Yagci, Y.; Allonas, X.; Ley, C.; Tar, H., *Chem. Commun.,* **2012**, *48*, 10252-10254.

[55]. Lang, A. S.; Thelakkat, M., *Polym. Chem.,* **2011**, *2*, 2213-2221.

[56]. Branham, K. D.; Shafer, G. S.; Hoyle, C. E.; McCormick, C. L., *Macromolecules,* **1995**, *28*, 6175-6182.

[57]. Dirani, A.; Laloyaux, X.; Fernandes, A. E.; Mathy, B.; Schicke, O.; Riant, O.; Nysten, B.; Jonas, A. M., *Macromolecules,* **2012**, *45*, 9400-9408.

[58]. Kakuchi, R.; Zamfir, M.; Lutz, J.-F.; Theato, P., *Macromol. Rapid Commun.,* **2012**, *33*, 54-60.

[59]. Parrish, B.; Breitenkamp, R. B.; Emrick, T., *J. Am. Chem. Soc.,* **2005**, *127*, 7404-7410.

[60]. Lutz, J.-F.; Hoth, A., *Macromolecules,* **2006**, *39*, 893-896.

[61]. Günay, K. A.; Theato, P.; Klok, H.-A., *J. Polym. Sci. Part A, Polym. Chem.,* **2013**, *51*, 1-28.

[62]. Yeom, C.-E. K., M. J.; Choi, W.; Kim, B. M., *Synlett,* **2008**, 565-568.

[63]. Terashima, T.; Sugita, T.; Fukae, K.; Sawamoto, M., *Macromolecules,* **2014**, *47*, 589-600.

[64]. Mandal, J.; Krishna Prasad, S.; Rao, D. S. S.; Ramakrishnan, S., *J. Am. Chem. Soc.,* **2014**, *136*, 2538-2545.

Chapter V

Synthesis and Characterization of Sequence-Controlled Semi-Crystalline Comb Copolymers: Influence of Primary Structure on Materials Properties

Abstract

Sequence-controlled semi-crystalline copolymers were prepared by nitroxide-mediated copolymerization of a large excess of octadecylstyrene with small amounts of functional *N*-substituted maleimides (i.e. *N*-propyl maleimide, *N*-benzyl maleimide, pentafluorophenyl 4-maleimidobenzoate, 4-(*N*-maleimido)azobenzene, *N*-(1-pyrenyl)maleimide and *N*-(2-(amino-Boc)ethylene)maleimide. These copolymers were prepared in bulk at 110 °C using the commercial alkoxyamine BlocBuilder® MA as initiator and control agent. Time-controlled additions protocols were used to place the *N*-substituted maleimides at precise chain location along the poly(octadecylstyrene) backbones. Size exclusion chromatography (SEC) and ^{1}H NMR studies indicated that well-defined copolymers with controlled monomer sequences, composition, chain-length and molecular weight distribution were formed in all cases. Although possessing an atactic backbone, these polymers exhibit a semi-crystalline behavior. The electron diffraction method indicated that the octadecyl side-chains form lamellar phases. Moreover differential scanning calorimetry studies evidenced a melting temperature in the range 40-45 °C and a crystallization temperature around 30-35 °C. It was observed that melting is influenced by the composition and sequence-distribution of the copolymers. Thus, small microstructural variations allow a precise control over order-disorder transitions.

Keywords: Sequence-controlled semi-crystalline copolymer, lamellar phases, crystallization behaviour.

V.1 Introduction

The synthesis of sequence-controlled polymers is an important emerging trend in recent polymer science [1]. Indeed, the precise positioning of monomer units along a polymer chain allows a new level of control over molecular [2-5], supramolecular [6-10] and macroscopic [11-16] properties of synthetic macromolecules. As summarized in recent reviews [1,17-19], many sequence-controlled polymerization methods are available or under development. In particular, significant efforts have been recently made to control monomer sequences in radical chain-growth polymerizations. Achieving this aim is difficult because radical polymerizations typically involve highly-reactive short-lived species. However, interesting concepts have been proposed to control monomer sequences in such processes [20-27]. For instance, comonomers with opposite double bond polarities (i.e. donor and acceptor comonomers) offer interesting prospects for controlling monomer sequence distribution in chain-growth radical processes. Such monomers have been used for several decades to prepare AB, AAB or ABC alternating copolymers [28-35]. In recent years, our group has shown that donor-acceptor copolymerizations can be regulated even more precisely and thus can be used to 'write' molecular information on synthetic polymer chains [32]. Our concept utilizes time-controlled feeds of very small amounts of acceptor comonomers (e.g. *N*-substituted maleimides) during the controlled/living homopolymerization of a large excess of a donor monomer (e.g. styrene) [20,21]. The discrete additions of acceptor monomers allow formation of very small information patches (typically 1 or 2 monomer units) at controlled positions along the donor polymer backbone. In other words, *N*-substituted maleimides are used as a molecular "ink" to encrypt well-defined polymer chains. This approach is, of course, not perfectly sequence-regulated [36]. As pointed out in earlier publications [20,31,32], our strategy relies on a radical chain-growth mechanism, and therefore sequence-distributions still exist in the formed materials, even though they can be significantly minimized [37]. Nevertheless, the approach is easy and versatile. For instance, it was recently shown that it allows synthesis of complex polymer structures such as single-chain functional arrays [38-40], multicyclic topologies [41,42], and dendronized microstructures [43]. Moreover, this approach is not limited to styrene but can be extended to other donor monomers [32]. For instance, we have recently reported the synthesis of sequence-controlled water-soluble polymers using *para*-substituted styrenic derivatives as donor monomers [44,45].

Copolymers prepared to date using our sequence-controlled copolymerization strategy were all amorphous materials. Indeed, the copolymerization of *N*-substituted maleimides and styrenic derivatives is a free radical process that does not allow control over main-chain tacticity [46]. It should be however noted that atactic polymers are not always amorphous [47]. For instance, atactic graft copolymers with long paraffin side-chains (e.g. C_{12} and higher) do form ordered crystalline phases [48-50]. Overberger and coworkers have described during the 1950s the synthesis and radical polymerization of *para*-substituted styrenic derivatives with long alkyl substituents (e.g. C_8-C_{18} and higher) [51]. However, this class of polymers has been much less studied than their methacrylate analogues over the past years. In a recent study, López-Carrasquero and coworkers have reported that styrenic derivatives with alkyl side-chains in the range C_{16}-C_{22} lead to semi-crystalline polymers with melting temperature above room temperature [52]. For instance, polymers of *p*-octadecylstyrene (**1**) melt at about 40 °C. However, the structure of the formed crystalline materials was not described in details. It was therefore interesting to study **1** (**Figure 59**) as a donor monomer in our sequence-controlled polymerization approach.
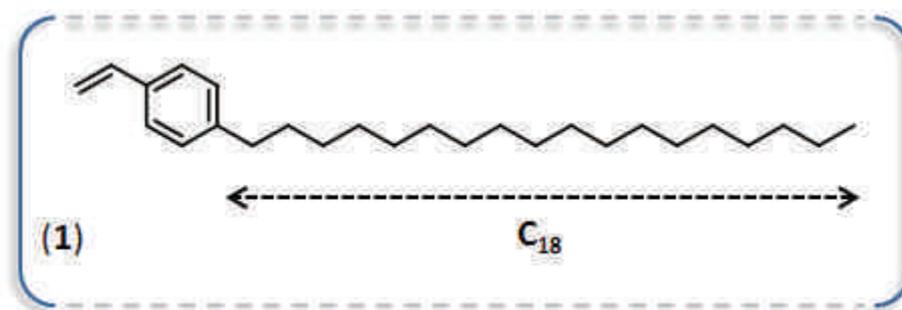
Figure 59. Molecular structure of *p*-octadecylstyrene (donor monomer studied in the present chapter).

In particular, the main objective of this work was to synthesize sequence-controlled semi-crystalline copolymers and to estimate the influence of copolymer microstructure on materials properties. Very few such studies have been reported so far. The influence of block or random comonomer sequences on the melting behavior of semi-crystalline polymers has been extensively studied [53,54]. In comparison, only a few studies have explored the relationship between precise molecular features and materials properties [55-59]. However, as mentioned earlier, the control of primary structure may significantly influence macroscopic behaviors [11,14]. In this context, we report, in the present work, the

synthesis by nitroxide-mediated polymerization (NMP) of well-defined homopolymers and copolymers of **1**. Using the sequence-controlled polymerization strategy described above, **1** was copolymerized with various *N*-substituted maleimides models (**2**-**7**, **Figure 60**). In order to study the influence of chain microstructure on melting behavior, small amounts of the acceptor comonomers (i.e. 3 or 6 equivalents as compared to initiator) were incorporated at different locations along the poly(octadecylstyrene) backbones. The molecular structure of the formed copolymers was examined using size-exclusion chromatography (SEC) and ^{1}H NMR. The semi-crystalline materials were studied by differential scanning calorimetry and by electron diffraction.
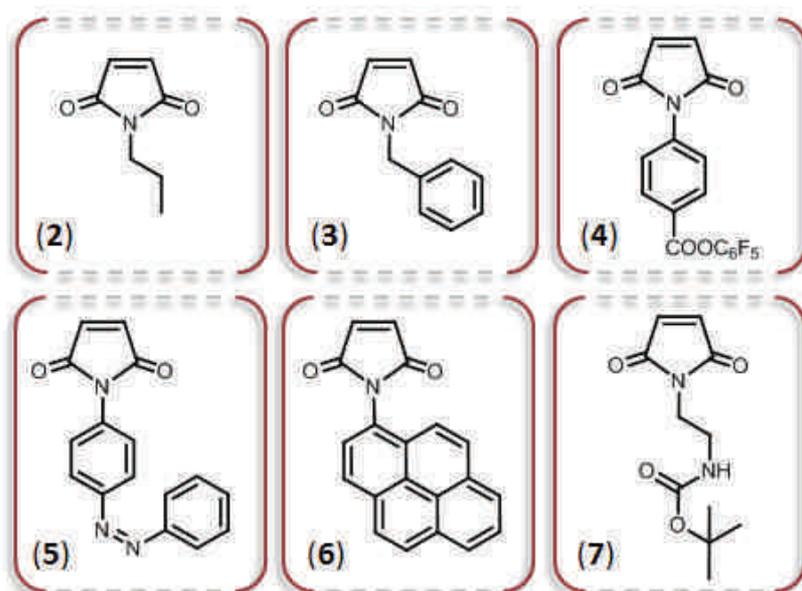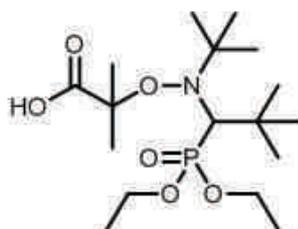
Figure 60. Molecular structure of a) Acceptor comonomers studied in the present work and b) Commercial alkoxyamine BlocBuilder® MA used as initiator in NMP polymerization.

V.2. Results and discussion

The polymers prepared in this work were synthesized by nitroxide-mediated polymerization using the commercial alkoxyamine BlockBuilder® MA. To the best of our knowledge, the controlled radical polymerization of **1** was never described in the literature. Therefore, a series of homopolymerizations was first carried out in order to identify optimal experimental conditions for the synthesis of well-defined poly(octadecylstyrene). Indeed, our sequence-controlled copolymerization concept requires a high degree of control over chain-length and molecular weight distribution [32]. **Table 12** shows the characterization of three homopolymers of **1** with different targeted chain-lengths. These experiments were performed in bulk at 110 °C. In all cases, a controlled/living homopolymerization was observed.

Table 12. Properties of homopolymers of **1** prepared by NMP.[a]

	1 [eq.]	BlocBuilder® MA	t_{end}[b] [min]	Conv.$_1$[c]	M_n[d] [g·mol^{-1}]	$M_{n,th}$[e]	M_w/M_n[d]
H1	20	1 eq.	360	0.89	7300	6700	1.09
H2	50	1 eq.	360	0.87	13400	15900	1.12
H3	100	1 eq.	360	0.57	17800	20700	1.16

[a] All homopolymerizations were performed in bulk at 110 °C. [b] Final polymerization time. [c] Conversion of **1** at the end of the reaction as estimated from ^{1}H NMR spectra in CDCl$_3$. [d] Average molecular weight and molecular weight distribution determined by SEC in THF. [e] Theoretical molecular weight, $M_{n,th}$ = M$_1$·Conv.$_1$·[**1**]/[BlocBuilder] + M$_{BlocBuilder}$ where M$_1$ and M$_{BlocBuilder}$ are molecular weights of **1** and BlocBuilder respectively.

As shown in **Figure 61**, the semi-logarithmic plots of monomer conversion versus time are linear. In addition, SEC measurements indicate the formation of well-defined polymers with narrow molecular weight distributions. Moreover, the measured molecular weights shown in **Table 12** are in good agreement with calculated molecular weight values, thus indicating that (i) the polymerization is well-controlled and (ii) the polystyrene SEC calibration is reliable to characterize poly(octadecylstyrene) samples.
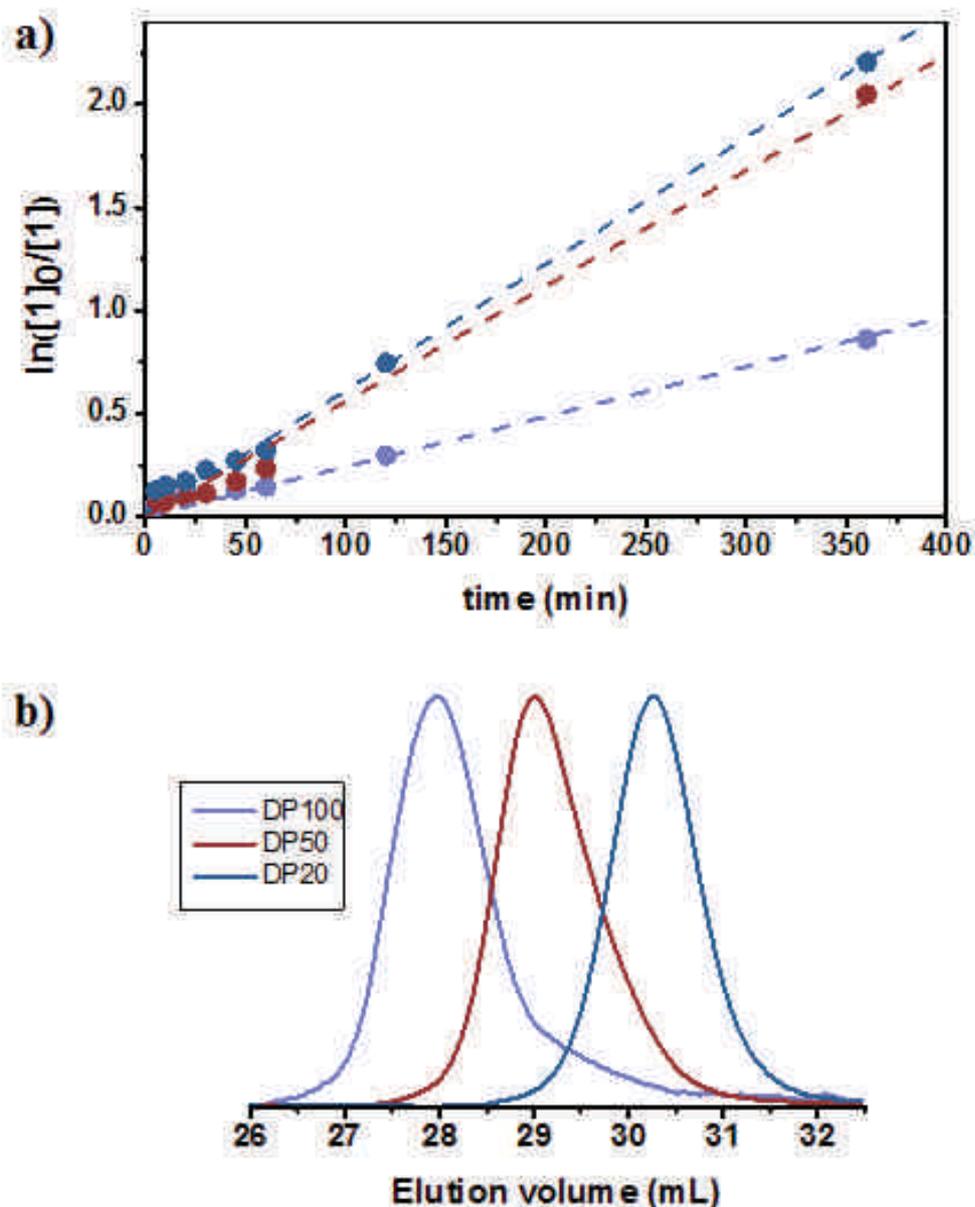
Figure 61. a) Corresponding semi-logarithmic plots of monomer conversion versus time recorded for the nitroxide-mediated homopolymerization of **1** DP20 (blue), DP50 (red) and DP100 (purple). b) SEC chromatograms recorded in THF for homopolymers.

The materials properties of the formed homopolymers **H1**-**H3** were characterized by DSC and electron diffraction. As described in the literature, these polymers do form semi-crystalline phases at ambient temperature. DSC analyses indicate that the melting temperatures T_m and crystallization temperatures T_c depend on molecular weight (i.e. sample **H3** has T_m and T_c values about 1°C higher than sample **H1**). **Figure 62** shows the DSC curves obtained for sample **H3**. The first temperature cycle indicates a melting temperature T_{m1} of

48.8 °C and a T_c of 34 °C. However, T_m is significantly lower (T_{m2} = 43.5 °C) during a second temperature cycle. This behavior is due to a slow reorganization of the crystalline phase. Indeed, a long tail on the lower side of the melting peak indicates that the crystalline material produced during the cooling stage at 10 °C/min is only poorly organized. Similar tailing was also observed when a DSC heating rate of 5 °C/min was used. The tail corresponds to approximately 35 % of the whole melting peak surface area. By contrast, it is only of about 5 % during the first heating cycle that was performed on a sample "aged" at room temperature.
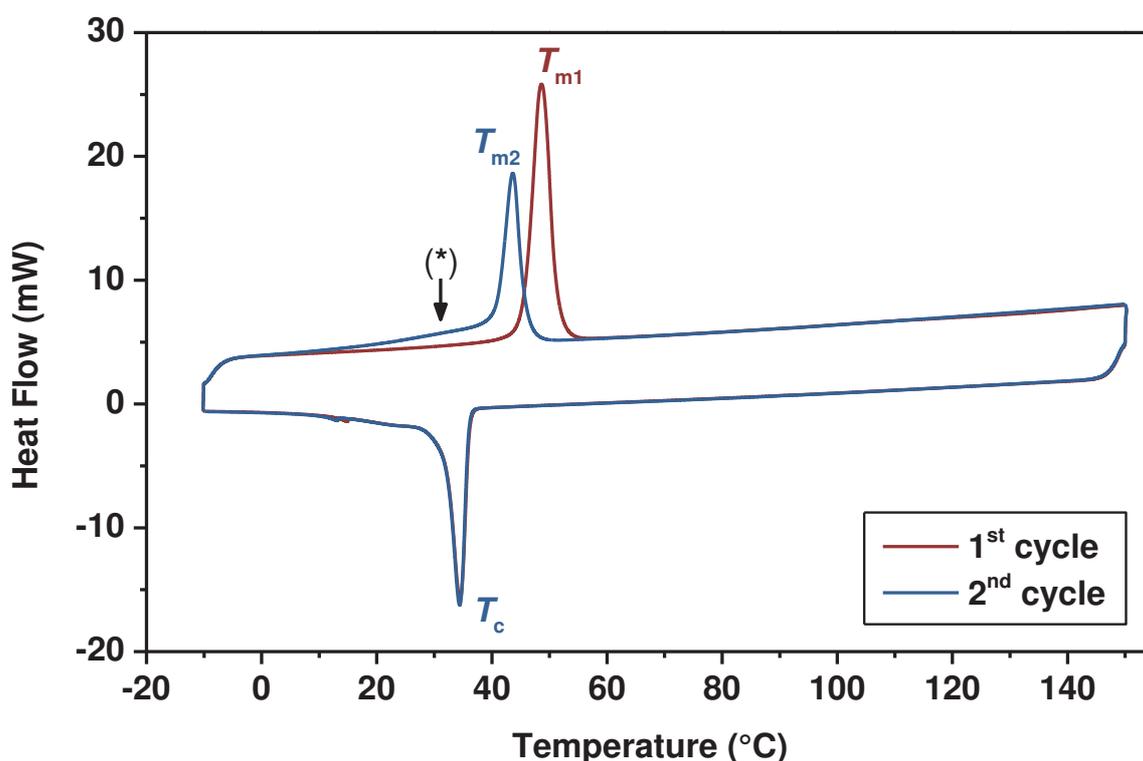
Figure 62. DSC curves measured for a homopolymer of 1 (sample **H3** in **Table 122**). First and second temperature cycles are drawn in red and blue, respectively. (*) The black arrow indicates the tailing that is observed during the second temperature cycle.

The slow reorganization of the material was confirmed by a series of DSC experiments. Stainless steel capsules containing **H3** were analyzed by DSC (i.e. 3 temperature cycles) and let rest at room temperature for several days before being reanalyzed. After two days, the crystalline phase is only partially reorganized (i.e. the tail corresponds to approximately 13 % of the whole melting peak). A complete reorganization (sharper melting

peak) was only observed after standing of the semi-crystalline material for two weeks at room temperature in the DSC capsule. The structure of the material was established on thin films epitaxially deposited on benzoic acid. **Figure 63** shows the corresponding electron diffraction patterns obtained with sample **H3**. Part (a) corresponds to a pseudo-fiber pattern analogous to that of a disordered polyethylene (PE) phase, indicating that the alkyl chains interact with the substrate when they become ordered. The pattern has been indexed accordingly, using a hexagonal unit-cell of parameters a = b = 4.7 Å, c = 2.5 Å. Since in these epitaxially crystallized films, the lamellar structure is seen edge-on, the low angle part of the pattern (enlarged in part (b)) displays reflections – here the second (at 16.4 Å) and third (at 10.8 Å) order – of the lamellar periodicity (i.e. the sum of the amorphous layer and crystalline part thicknesses). This lamellar periodicity L is thus about 32.6 Å. Part (c) represents a diffraction pattern from parts of the film that crystallized in the absence of benzoic acid. The thin film now crystallizes with the lamellae oriented parallel to the substrate. The diffraction pattern has pure hexagonal symmetry and indicates again a so-called rotator phase of the alkyl chains, with a cross-section of 19.9 Å^2 [60,61]. Further, the pattern indicates that the chain axis is parallel to the electron beam, thus normal to the lamellar surface. The alkyl segment length is on the order of 25 Å. In addition, weight fractions of the PSt and alkyl side-chains parts are about 30 and 70 %, respectively. Since the densities are comparable, the amorphous part should be around 10 Å thick and the crystalline layer around 23 Å thick. This value corresponds roughly to the total length of the alkyl chain, which excludes the existence of double layers and suggests that alkyl chains attached to two successive amorphous layers interdigitate to a significant extent in the crystalline part of the lamellar structure (**Figure 63, left**).
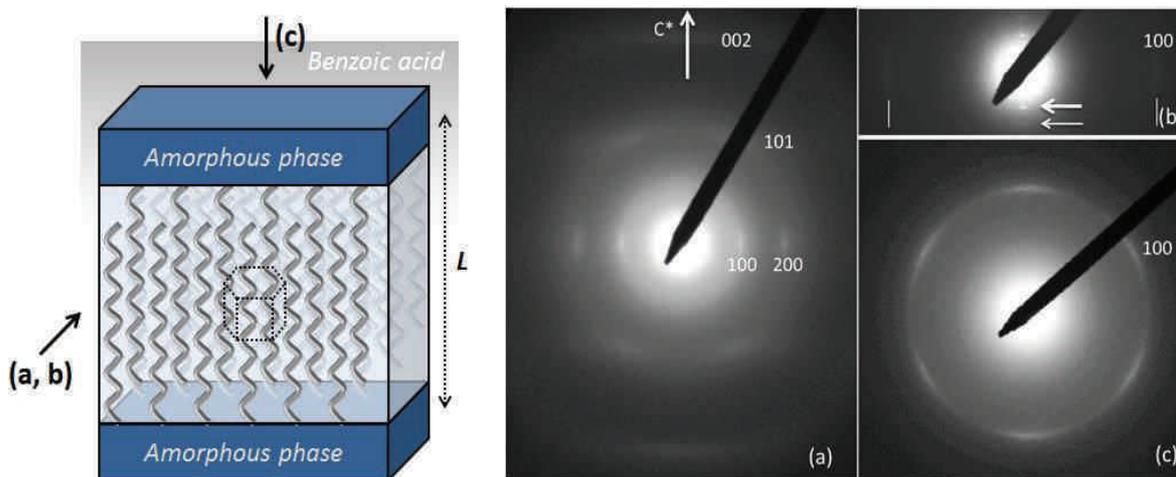
Figure 63. Characterization by electron diffraction of the semi-crystalline morphology of poly(octadecylstyrene). The orientation of the electron beam relative to the lamella in parts a, b, and c is indicated in the sketch. The dotted hexagonal structure in the sketch represents the unit cell of the alkyl chains packing. Right: a) Diffraction pattern of a thin layer of sample **H3** epitaxially crystalized on benzoic acid, with indexing of the reflections. The alkyl chain axis is vertical. b) The center part of part (a) taken with a longer camera length in order to record the low angle diffraction pattern of the stacked, edge-on multilamellar structure. Only the second (bold arrow) and third (thinner arrow) orders of the lamellar periodicity L (see sketch) are visible. The first order reflection is masked by the primary beam. c) Electron diffraction taken from a thin layer of sample **H3**. The alkyl chain axis is normal to the layer surface.

The sequence-controlled copolymerization of **1** with various *N*-substituted maleimides (structures **2-7** in **Figure 60**) was then studied. The optimized experimental conditions used in homopolymerizations experiments were also selected to perform the copolymerizations. In most experiments, 3 molar equivalents of *N*-substituted maleimides were used as compared to BlocBuilder® MA. As described in previous publications [20,31,32], this ratio allows formation of local chain patches containing 3 *N*-substituted succinimide units on average. Time-controlled comonomer feeds were used to control precisely the chain-localization of these patches. In all cases, a well-controlled copolymerization process occurred. As shown in **Table 13**, all the formed copolymers exhibit a controlled molecular weight and a narrow molecular weight distribution.

Table 13. Properties of copolymers obtained by sequence-controlled copolymerization of **1** and *N*-substituted maleimides.[a]

		MI	t_{add}[b] [min]	t_{end}[c] [min]	Conv. t_{add}[d]	Conv. t_{end}[d]	M_n[e] [g·mol⁻¹]	$M_{n,th}$[f]	M_w/M_n[e]
C1		2	0	248	0	0.81	12600	15200	1.27
C2		2	60	300	0.25	0.81	12900	15200	1.15
C3		2	180	300	0.52	0.76	12400	14400	1.13
C4		2	230	300	0.74	0.87	15400	16400	1.16
C5		2	180	280	0.61	0.81	29500	15700	1.40
C6		3	171	300	0.38	0.70	13000	13400	1.17
C7		4	0	345	0	0.90	14000	17000	1.34
C8		4	70	320	0.29	0.85	10100	16750	1.29
C9		4	120	280	0.33	0.68	11200	13700	1.17
C10		4	240	310	0.52	0.65	10400	13200	1.22
C11		4	426	460	0.69	0.77	13800	15300	1.22
C12		4	115	225	0.41	0.75	10100	16000	1.31
C13		5	65	360	0.37	0.84	10400	16200	1.32
C14		5	150	300	0.47	0.84	14200	16200	1.14
C15		5	241	360	0.66	0.83	10800	16000	1.31
C16		6	70	395	0.39	0.82	10100	15000	1.33
C17		7	122	380	0.39	0.78	10600	15000	1.17

[a] Experimental conditions: bulk, 110 °C, $[\mathbf{1}]_0/[\mathbf{MI}]_{tadd}/[\text{BlocBuilder}]_0 = 50:3:1$ in all cases except for entries **C5** and **C12** where $[\mathbf{1}]_0/[\mathbf{MI}]_{tadd}/[\text{BlocBuilder}]_0 = 50:6:1$. Experiment **C11** was performed in anisole solution, **1**/anisole = 1:1 v/v. [b] Time at which the MI was added in polymerization medium. [c] Final polymerization time. [d] Conversion of **1** calculated from ¹H NMR spectra in CDCl₃. [e] Average molecular weight and molecular weight distribution determined by SEC in THF. [f] $M_{n,th} = M_{\mathbf{1}} \cdot \text{Conv.}_{\mathbf{1}} \cdot [\mathbf{1}]/[\text{BlocBuilder}] + M_{\mathbf{MI}} \cdot \text{conv.}_{\mathbf{MI}} \cdot [\mathbf{MI}]/[\text{BlocBuilder}] + M_{\text{BlocBuilder}}$.

Moreover, all studied *N*-substituted maleimides exhibit a strong cross-propagation tendency with **1** and were therefore incorporated extremely precisely in the formed poly(octadecylstyrene) chains. For example, **Figure 64** shows the semi-logarithmic plot of monomer conversion versus time of the copolymerization of **1** and **2** (**2** was added after 52 % of monomer conversion of **1**). In fact, the electron-donating character of the C_{18} alkyl chain in **1** has probably a beneficial influence on the donor-acceptor sequence-controlled copolymerization process [45].
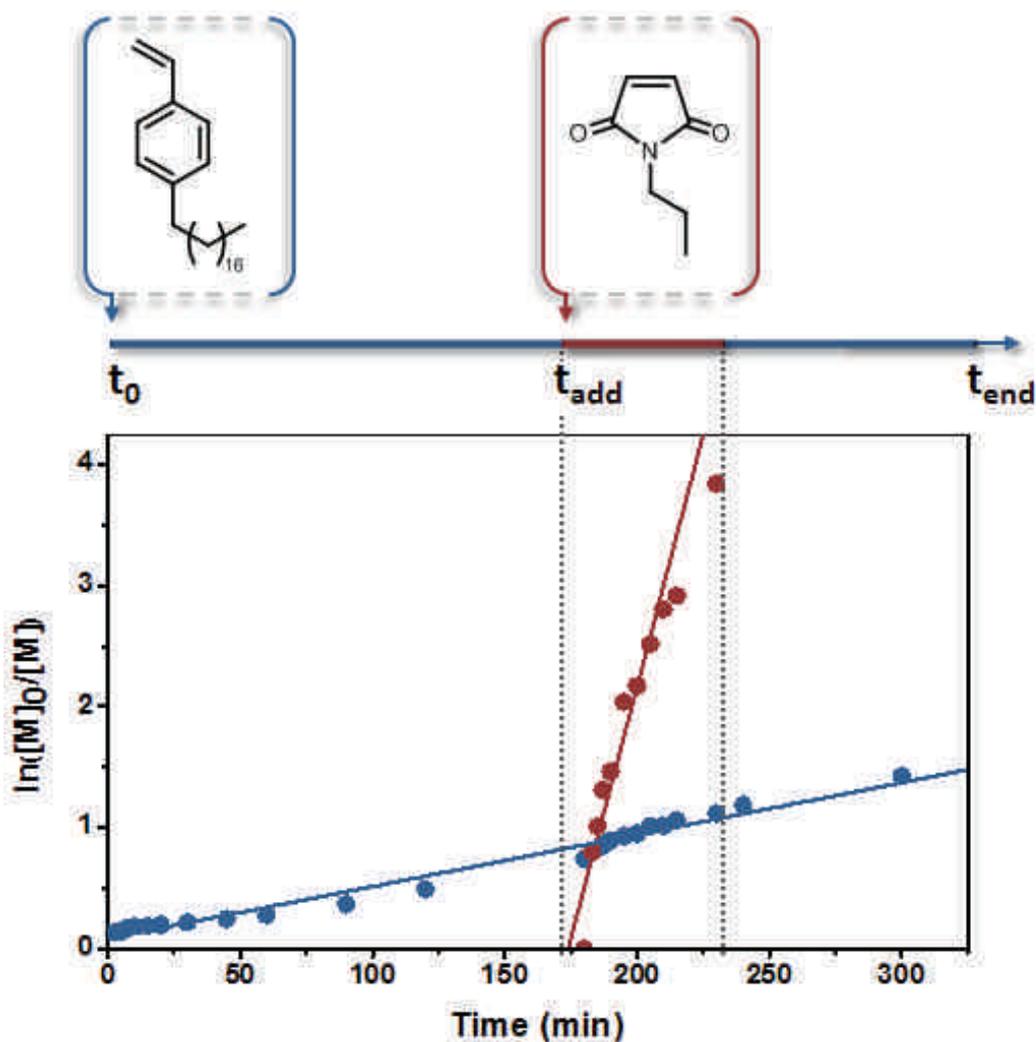
Figure 64. Semi-logarithmic plot of monomer conversion versus time recorded for the sequence-controlled copolymerization of **1** and **2**. This experiment corresponds to copolymer **C3** in **Table 13**.

The influence of microstructure on the melting and crystallization behavior of the copolymers was studied. Their crystalline structure was examined by electron diffraction on thin films epitaxially deposited on benzoic acid. In general, the electron diffraction patterns of the copolymers are very similar to those described for the homopolymer. This result is not surprising because the morphological/diffraction analysis "sees" only the crystalline part of the material. The periodicity determined from the low angle diffraction is however larger than for the homopolymer. This would suggest a crystalline part made of a double-layer rather than interdigitated aliphatic segments. However, this difference may be related to vagaries of the crystallization conditions in the benzoic acid procedure. This is clearly an aspect that needs further analysis. The copolymers were also studied by DSC.

Figure 65 shows the evolution of melting temperature T_m and crystallization temperature T_c as a function of the incorporated *N*-substituted maleimide. All the samples analyzed in this figure are fully comparable and have the same degree of polymerization (i.e. DP ~ 35-40) and the same primary structure (i.e. in each case the *N*-substituted maleimide patch was placed approximately at 1/3 of the formed copolymer chain as sketched in **Table 13**). Because of the slow reorganization of these materials after melting, the T_m and T_c values displayed in **Figure 65** were measured during the first temperature cycle of the DSC analysis. It should be reminded that the first temperature cycle is usually discarded in DSC studies in order to remove the thermal history of the sample. In the present case, however, the first cycle probably gives the most accurate description of the fully organized semi-crystalline polymer. Indeed, as shown above, DSC thermograms measured during the first cycle are comparable to those obtained after annealing and extended reorganization of the materials in the DSC capsule. **Figure 65** indicates a noticeable influence of copolymer composition on the semi-crystalline behavior. For instance, copolymers **C2**, **C6**, **C9**, **C13**, **C16** and **C17** exhibit T_m values that are about 4-5 °C lower that the corresponding homopolymer **H2**. T_c is also influenced by the presence of *N*-substituted succinimide units in the chain but to a lower degree than T_m. Typically, the measured crystallization temperatures for the copolymers are about 1-3 °C lower than for the homopolymer. These results show that very small quantities of functional *N*-substituted succinimide units in the chains influences melting and crystallization.
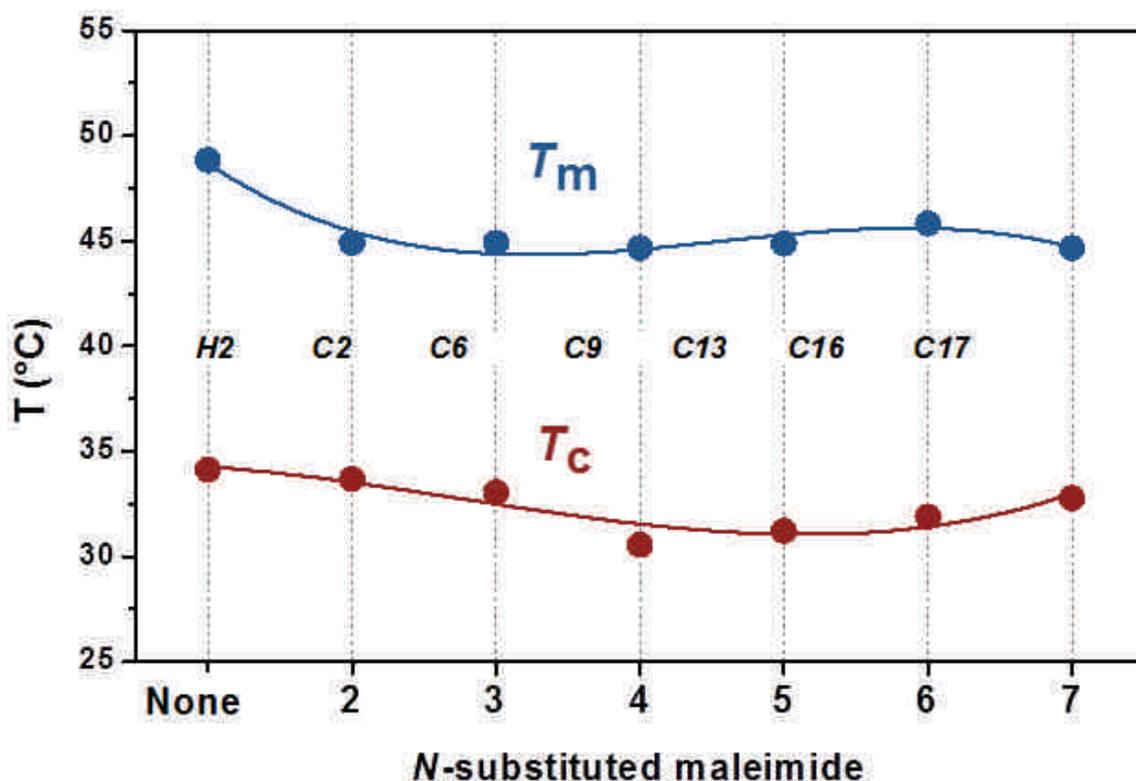
Figure 65. Melting temperatures T_m (blue) and crystallization temperatures T_c (red) recorded by DSC for a homopolymer and copolymers of **1** with various *N*-substituted maleimides. All samples have approximately the same molecular weight. In all copolymers, the *N*-substituted maleimides were placed approximately at 1/3 of the chain. The T_m and T_c were recorded during the first temperature cycle.

Besides this obvious composition effect, it was observed that primary structure (i.e. monomer sequence distribution) also influences melting and crystallization. Samples with a similar chain-length and composition but with different primary structure (i.e. series **C7**-**C11**) were analyzed by DSC. A clear difference was observed when the maleimide were incorporated at the very beginning of the chain or inside the chain. For instance, sample **C7** exhibited a T_m of 45.4 °C, whereas sample **C10** exhibited a T_m value of 44.6 °C. This behavior is probably due to the fact that functional succinimide units located close to the chain-end disturb less polymer organization than those that are included inside the chain. However, it was not possible to measure the influence of more subtle microstructure variations on the crystallization behavior. For instance, samples **C8**-**C11** have all very similar T_m and T_c values. Some minor differences were observed (i.e. deviations of about 0.2-0.3 °C)

but they are within the range of error of the DSC measurements and can therefore not be taken into account.

Some of the copolymers in **Table 13** were also modified after copolymerization. For instance, copolymers containing pentafluorophenyl-activated ester units (i.e. series **C7**-**C12**) can be reacted with compounds containing primary amine groups [62,63]. As a proof of principle, some of these copolymers were reacted with *n*-propylamine. ^{1}H NMR **(Figure 66)** and FT-IR analysis **(Figure 67)** indicated the quantitative modification of the activated esters sites.
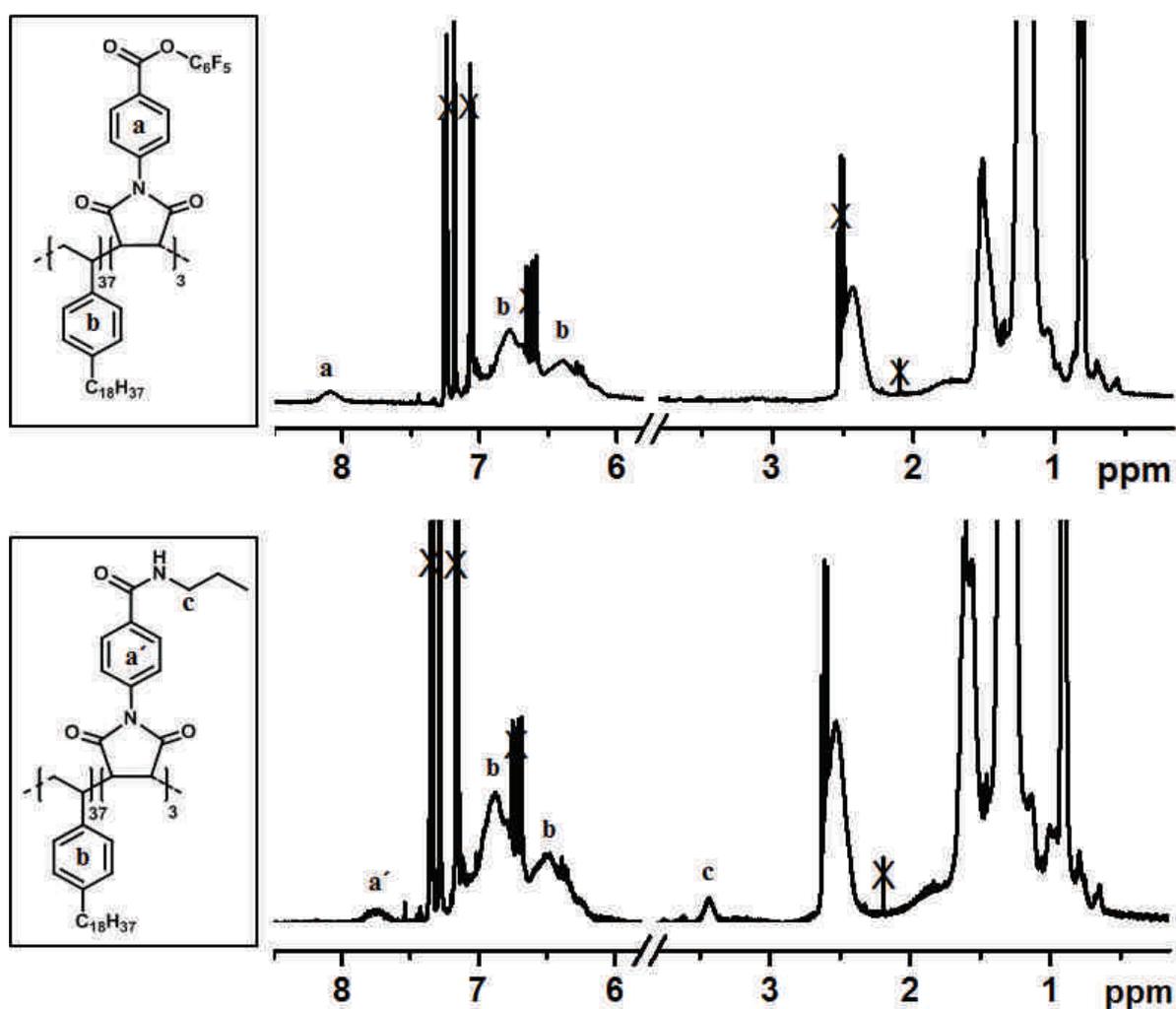
Figure 66. ^{1}H NMR spectra of a copolymer of **1** and **4** before (top) and after modification with *n*-propylamine (bottom). The microstructure of this sample is similar to the one of copolymer **C9** in **Table 13**.
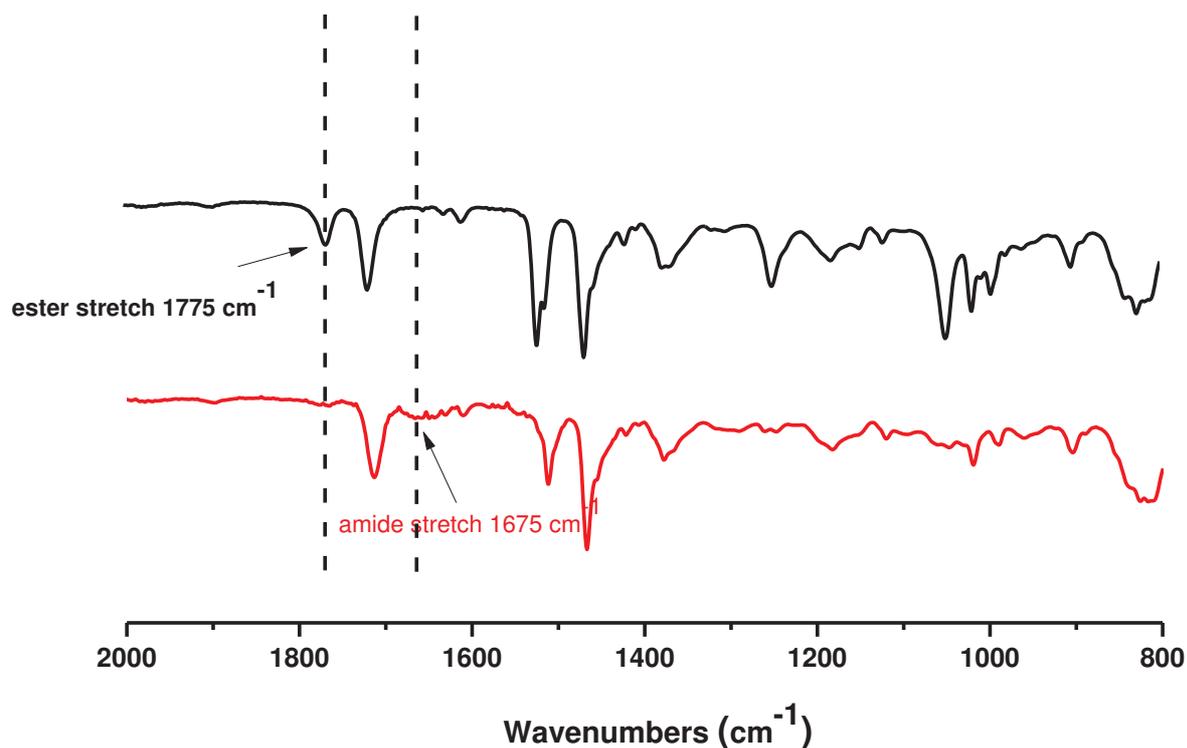
Figure 67. FT-IR spectra of a copolymer of **1** and **4** before (top) and after modification with *n*-propylamine (bottom). The microstructure of this sample is similar to the one of copolymer **C9** in **Table 13**.

Similarly, copolymers containing Boc-protected amines (i.e. **C17**) can be easily deprotected after copolymerization. It was found that these post-polymerization modifications influence the semi-crystalline behavior of the copolymers. For example, the melting temperature of sample **C17** increases by approximately 2 °C after deprotection of the amine sites (**Figure 68**). An opposite trend was observed for the copolymers containing pentafluorophenyl sites. Typically, the melting temperature of the copolymers decreased of about 2 °C after reaction with *n*-propylamine. These experimental results should be interpreted with great caution since the observed differences are within the error range of DSC analysis and could also be due to sample preparation. Nevertheless, these results suggest that the materials properties of sequence-controlled poly(octadecylstyrene) derivatives can be further tuned using post-polymerization modifications.
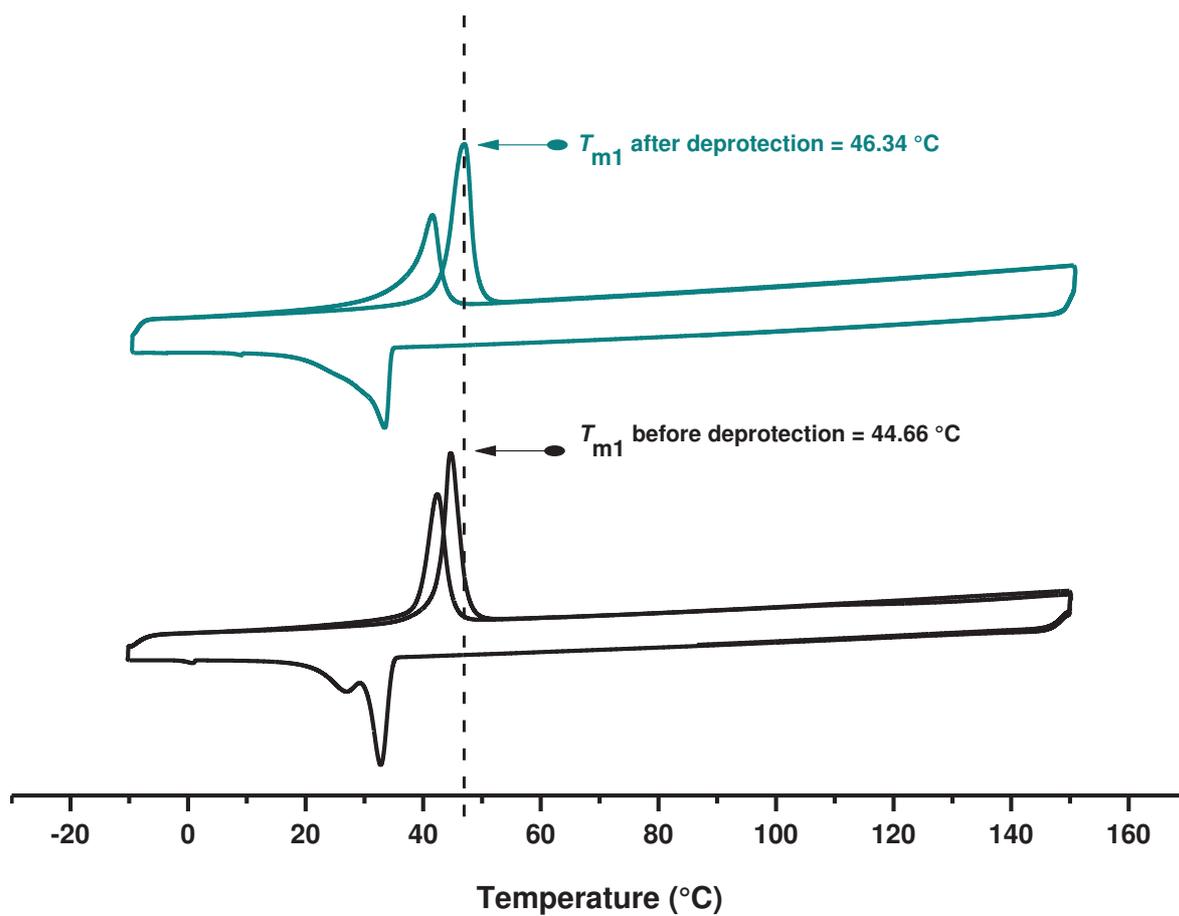
Figure 68. DSC curves measured for a coopolymer **C17** before (top) and after (bottom) removal of Boc protecting group.

V.3. Conclusion

Well-defined poly(octadecylstyrene) homopolymers and copolymers poly(octadecylstyrene-*co-N*-substituted maleimides) were prepared by nitroxide-mediated copolymerization. For the copolymers, time-controlled addition protocols were used to place the *N*-substituted maleimides at chosen locations along the poly(octadecylstyrene) backbones. ^{1}H NMR kinetic studies indicated that a precise sequence-regulation was obtained in all cases, thus confirming that octadecylstyrene is a suitable donor monomer for donor-acceptor sequence-controlled copolymerizations. Therefore, a full library of copolymers with controlled chain-lengths, molecular weight distributions, compositions and monomer sequences was prepared. Both homopolymers and copolymers exhibited a semi-crystalline behavior. DSC measurements indicated that all sample display a melting temperature around 40-45 °C and a crystallization temperature around 30 °C. The semi-crystalline structure of these comb polymers was examined using the electron diffraction method. It was found that their alkyl side-chains form interdigitated lamellar crystalline phases. Furthermore, it was observed that the microstructure (i.e. composition and sequence distribution) of the copolymers impact significantly the materials properties. Indeed, very small amounts of acceptor comonomers (i.e. about 3 units per chain) influence markedly melting and crystallization temperatures. These results indicate that the properties of semi-crystalline copolymers can be finely tuned using controlled copolymerization protocols.

References

[1].   Lutz, J.-F.; Ouchi, M.; Liu, D. R.; Sawamoto, M., *Science,* **2013**, *341*.

[2].   Hartmann, L.; Börner, H. G., *Adv. Mater.,* **2009**, *21*, 3425-3431.

[3].   Ouchi, M.; Badi, N.; Lutz, J.-F.; Sawamoto, M., *Nat. Chem.,* **2011**, *3*, 917-924.

[4].   Trinh, T. T.; Oswald, L.; Chan-Seng, D.; Lutz, J.-F., *Macromol. Rapid Commun.,* **2014**, *35*, 141-145.

[5].   Niu, J.; Hili, R.; Liu, D. R., *Nat Chem,* **2013**, *5*, 282-292.

[6].   Börner, H. G., *Prog. Polym. Sci.,* **2009**, *34*, 811-851.

[7].   Kudirka, R.; Tran, H.; Sanii, B.; Nam, K. T.; Choi, P. H.; Venkateswaran, N.; Chen, R.; Whitelam, S.; Zuckermann, R. N., *Biopolymers,* **2011**, *96*, 586-595.

[8].   Terashima, T.; Mes, T.; De Greef, T. F. A.; Gillissen, M. A. J.; Besenius, P.; Palmans, A. R. A.; Meijer, E. W., *J. Am. Chem. Soc.,* **2011**, *133*, 4742-4745.

[9].   Giuseppone, N.; Lutz, J.-F., *Nature,* **2011**, *473*, 40-41.

[10].   Rosales, A. M.; McCulloch, B. L.; Zuckermann, R. N.; Segalman, R. A., *Macromolecules,* **2012**, *45*, 6027-6035.

[11].   Stayshich, R. M.; Meyer, T. Y., *J. Am. Chem. Soc.,* **2010**, *132*, 10920-10934.

[12].   Thomas, C. M.; Lutz, J.-F., *Angew. Chem., Int. Ed.,* **2011**, *50*, 9244-9246.

[13].   van Zoelen, W.; Zuckermann, R. N.; Segalman, R. A., *Macromolecules,* **2012**, *45*, 7072-7082.

[14].   Norris, B. N.; Zhang, S.; Campbell, C. M.; Auletta, J. T.; Calvo-Marzal, P.; Hutchison, G. R.; Meyer, T. Y., *Macromolecules,* **2013**, *46*, 1384-1392.

[15].   Palermo, E. F.; McNeil, A. J., *Macromolecules,* **2012**, *45*, 5948-5955.

[16].   Natalello, A.; Werre, M.; Alkan, A.; Frey, H., *Macromolecules,* **2013**, *46*, 8467-8471.

[17].   Badi, N.; Lutz, J.-F., *Chem. Soc. Rev.,* **2009**, *38*, 3383-3390.

[18].   Lutz, J.-F., *Polym. Chem.,* **2010**, *1*, 55-62.

[19].   Lutz, J.-F., *Nat. Chem.,* **2010**, *2*, 84-85.

[20].   Pfeifer, S.; Lutz, J.-F., *J. Am. Chem. Soc.,* **2007**, *129*, 9542-9543.

[21].   Pfeifer, S.; Lutz, J.-F., *Chem. Eur. J.,* **2008**, *14*, 10949-10957.

[22].   Ida, S.; Terashima, T.; Ouchi, M.; Sawamoto, M., *J. Am. Chem. Soc.,* **2009**, *131*, 10808-10809.

[23].   Satoh, K.; Matsuda, M.; Nagai, K.; Kamigaito, M., *J. Am. Chem. Soc.,* **2010**, *132*, 10003-10005.

[24].   Hibi, Y.; Ouchi, M.; Sawamoto, M., *Angew. Chem., Int. Ed.,* **2011**, *50*, 7434-7437.

[25].   Tong, X.; Guo, B.-h.; Huang, Y., *Chem. Commun.,* **2011**, *47*, 1455-1457.

[26].   Houshyar, S.; Keddie, D. J.; Moad, G.; Mulder, R. J.; Saubern, S.; Tsanaktsidis, J., *Polym. Chem.,* **2012**, *3*, 1879-1889.

[27]. Vandenbergh, J.; Reekmans, G.; Adriaensens, P.; Junkers, T., *Chem. Commun.,* **2013**, *49*, 10358-10360.

[28]. Cowie, J. M. G., *Alternating Copolymers*. Plenum Press: New York, **1985**.

[29]. Kirci, B.; Lutz, J.-F.; Matyjaszewski, K., *Macromolecules,* **2002**, *35*, 2448-2451.

[30]. Klumperman, B., *Polym. Chem.,* **2010**, *1*, 558-562.

[31]. Lutz, J.-F.; Schmidt, B. V. K. J.; Pfeifer, S., *Macromol. Rapid Commun.,* **2011**, *32*, 127-135.

[32]. Lutz, J.-F., *Acc. Chem. Res.,* **2013**, *46*, 2696-2705.

[33]. Hisano, M.; Takeda, K.; Takashima, T.; Jin, Z.; Shiibashi, A.; Matsumoto, A., *Macromolecules,* **2013**, *46*, 7733-7744.

[34]. Hisano, M.; Takeda, K.; Takashima, T.; Jin, Z.; Shiibashi, A.; Matsumoto, A., *Macromolecules,* **2013**, *46*, 3314-3323.

[35]. Matsuda, M.; Satoh, K.; Kamigaito, M., *Macromolecules,* **2013**, *46*, 5473-5482.

[36]. Zamfir, M.; Lutz, J.-F., Controlling Polymer Primary Structure Using CRP: Synthesis of Sequence-Controlled and Sequence-Defined Polymers. In *Progress in Controlled Radical Polymerization: Materials and Applications*, Matyjaszewski, K.; Sumerlin, B. S.; Tsarevsky, N. V., Eds. **2012**; Vol. 1101, pp 1-12.

[37]. Zamfir, M.; Lutz, J.-F., *Nat. Commun.,* **2012**, *3*, 1138.

[38]. Berthet, M. A.; Zarafshani, Z.; Pfeifer, S.; Lutz, J.-F., *Macromolecules,* **2010**, *43*, 44-50.

[39]. Chan-Seng, D.; Zamfir, M.; Lutz, J.-F., *Angew. Chem., Int. Ed.,* **2012**, *51*, 12254-12257.

[40]. Baradel, N.; Fort, S.; Halila, S.; Badi, N.; Lutz, J.-F., *Angew. Chem., Int. Ed.,* **2013**, *52*, 2335-2339.

[41]. Schmidt, B. V. K. J.; Fechler, N.; Falkenhagen, J.; Lutz, J.-F., *Nat. Chem.,* **2011**, *3*, 234-238.

[42]. Zamfir, M.; Theato, P.; Lutz, J.-F., *Polym. Chem.,* **2012**, *3*, 1796-1802.

[43]. Baradel, N.; Gok, O.; Zamfir, M.; Sanyal, A.; Lutz, J.-F., *Chem. Commun.,* **2013**, *49*, 7280-7282.

[44]. Srichan, S.; Oswald, L.; Zamfir, M.; Lutz, J.-F., *Chem. Commun.,* **2012**, *48*, 1517-1519.

[45]. Srichan, S.; Chan-Seng, D.; Lutz, J.-F., *ACS Macro Lett.,* **2012**, *1*, 589-592.

[46]. Badi, N.; Chan-Seng, D.; Lutz, J.-F., *Macromol. Chem. Phys.,* **2013**, *214*, 135-142.

[47]. Du, V. A.; Manners, I., *Macromolecules,* **2013**, *46*, 4742-4753.

[48]. Platé, N. A.; Shibaev, V. P.; Petrukhin, B. S.; Zubov, Y. A.; Kargin, V. A., *J. Polym. Sci. Part A-1, Polym. Chem.,* **1971**, *9*, 2291-2298.

[49]. Hsieh, H. W. S.; Post, B.; Morawetz, H., *J. Polym. Sci., Polym. Phys. Ed.,* **1976**, *14*, 1241-1255.

[50]. Qin, S.; Matyjaszewski, K.; Xu, H.; Sheiko, S. S., *Macromolecules,* **2003**, *36*, 605-612.

[51]. Overberger, C. G.; Frazier, C.; Mandelman, J.; Smith, H. F., *J. Am. Chem. Soc.,* **1953**, *75*, 3326-3330.

[52]. López-Carrasquero, F.; Giammanco, G.; Díaz, A.; Dávila, J.; Torres, C.; Laredo, E., *Polym. Bull.,* **2009**, *63*, 69-78.

[53]. Kunisada, H.; Yuki, Y.; Kondo, S.; Wada, K., *Polym. J.,* **1991**, *23*, 1365-1370.

[54]. Hung, J.; Cole, A. P.; Waymouth, R. A., *Macromolecules,* **2003**, *36*, 2454-2463.

[55]. Watson, M. D.; Wagener, K. B., *Macromolecules,* **2000**, *33*, 8963-8970.

[56]. Hopkins, T. E.; Wagener, K. B., *Macromolecules,* **2003**, *36*, 2206-2214.

[57]. Alamo, R. G.; Jeon, K.; Smith, R. L.; Boz, E.; Wagener, K. B.; Bockstaller, M. R., *Macromolecules,* **2008**, *41*, 7141-7151.

[58]. Berda, E. B.; Wagener, K. B., *Macromolecules,* **2008**, *41*, 5116-5122.

[59]. Matsui, K.; Seno, S.; Nozue, Y.; Shinohara, Y.; Amemiya, Y.; Berda, E. B.; Rojas, G.; Wagener, K. B., *Macromolecules,* **2013**, *46*, 4438-4446.

[60]. Scaringe, R. P., *Trans. Am. Crystall. Assoc.,* **1992**, *28*, 11-23.

[61]. Dorset, D. D., *Crystallography of the Polymethylene Chain. An Inquiry into the Structure of Waxes*. Oxford University Press: **2005**.

[62]. Kakuchi, R.; Zamfir, M.; Lutz, J.-F.; Theato, P., *Macromol. Rapid Commun.,* **2012**, *33*, 54-60.

[63]. Theato, P., *J. Polym. Sci. Part A, Polym. Chem.,* **2008**, *46*, 6677-6687.

General Discussion and Conclusion

GENERAL DISCUSSION AND CONCLUSION

Copolymers with controlled comonomer sequences, molecular weights and narrow molecular weight distributions were successfully prepared by non-stoichiometric NMP of styrenic derivatives and *N*-substituted maleimides. The copolymerization of a donor (electron rich monomer such as styrene) with an acceptor monomer (electron poor monomer such as maleimide) enables the formation of macromolecules with controlled microstructure. Since the acceptor monomer was introduced in a small amount compared to the donor monomer, it was possible to incorporate it locally in the chains.
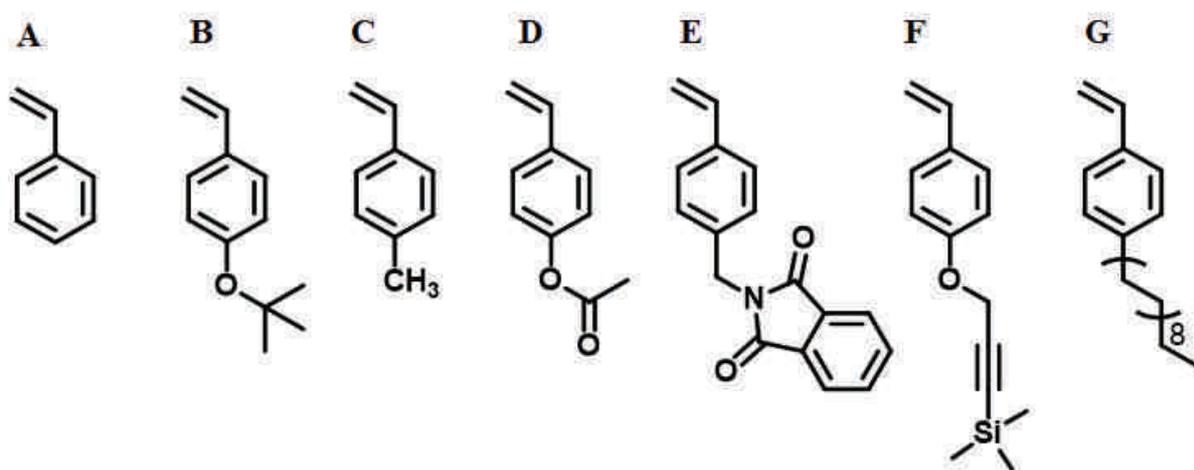
Figure 69. Styrenic derivatives used as donor monomers in this thesis to prepare sequence-controlled polymers by NMP copolymerization with a discrete amount of *N*-substituted maleimides.

This PhD work clearly show that styrene is not the only donor monomer that can be used to copolymerize with *N*-substituted maleimides in the precise positioning concept to form copolymers. The study was extended to other monomers such as 4-*tert*-butoxystyrene (**B**), 4-methylstyrene (**C**), 4-acetoxystyrene (**D**), *N*-(*p*-vinyl benzyl)phthalimide (**E**), TMS-propargyloxystyrene (**F**) and 4-octadecylstyrene (**G**) (**Figure 69**). In the second chapter of this thesis, the research was devoted to the study of the influence of the substituent located at *para* position of styrenic derivatives. Three donor monomers were selected: **B**, **C** and **D**. The insertion of small quantities of maleimides in these polymer backbones was done in a precise manner in all cases. However, the precise incorporation of maleimides in each donor monomer chain was slightly different. It was found that the degree of precision depends on

the substituents present on the styrenic derivatives. For example, the reactivity ratio of **B** when copolymerized with *N*-benzylmaleimide (BzMI) has been reported as a very low value (0.028) as compared to monomer (**A)** (0.041), **C (**0.045**)** and **D (**0.059**)** [1]. This result indicates the high degree of alternation which is due to the electron donating properties of the *tert*-butoxy substituent. The electron properties of a substituent at *para* position can be indicated also by looking at the chemical shift of the vinyl peak of the monomers measured by NMR [2]. In this case, the vinyl signals of monomer **C** and **D** are shifted downfield compared to the signals of styrene. Whilst, the vinyl signals of monomer **B** are shifted upfield indicating that monomers **C** and **D** are less electron-rich while the monomer **C** is more electron-rich than styrene. Thus a high cross-propagation was observed in the case of the use of monomer **B**. The reactivity ratio (r) of donor monomers when copolymerized with maleimides was simply determined throughout this dissertation by using Jaacks method [3]. Since the donor monomer was used in a large excess compared to maleimide, the calculation of reactivity ratio was simplified by considering only one propagating chain in the reaction. Therefore, two possibilities of propagating reactions were occurring instead of four (see **I.3.2 copolymer in radical polymerization**). The integration of a general equation derived by Mayo and Lewis [4] facilitated the calculation of the reactivity ratio of monomer by considering the rate of monomer consumption. It meant that the reactivity ratio can be determined by plotting the semi-logarithmic of monomer conversion versus time. Indeed, the slop of the obtained line is equal to the reactivity ratio. In this study, it was evidenced that the use of strong donor substituents at *para* position of styrenic derivatives led to particularly precise sequence-controlled copolymerizations. Furthermore, the obtained copolymers were easily transformed into hydrophilic 4-polyhydroxystyrene using a simple hydrolytic step.

In the following chapter of the thesis the donor monomers possessing strong donor substituents such as **E**, **F** and **G** were chosen. Monomer **E** was used in **chapter III** to synthesize sequence-controlled poly(vinyl benzyl amine)s classified as a cationic polyelectrolyte [5]. However, in this chapter the synthesis was more complicated since the donor monomer was displaying a succinimide functional group that was also present on the *N*-substituted maleimide. Therefore, the orthogonal deprotection was challenging. However, the sequence-controlled polymers obtained in chapter II and chapter III were soluble in aqueous solution only under alkaline or acidic conditions. Hence, the aim of chapter IV was to

synthesize sequence-controlled polymers that can be soluble in aqueous solution at a neutral pH.

TMS-POS monomer (**F**) was selected and studied in **chapter IV** [6] because it offered the opportunity to be post-modified using copper-catalyzed alkyne-azide cycloaddition (CuAAC) reaction. After several polymerizations were attempted, it was found that the polymerizations of **F** were well-controlled under semi-dilute conditions. The volume of solvent should respect the ratio 2:1 v/v to the monomer in order to avoid termination reactions. This latter reaction was evidenced by the broad molecular weight distribution obtained when monomer **G** was polymerized at high concentration. TMS protecting group was generally labile and can be easily removed from the polymers using a common source of fluoride such as TBAF. The grafting of α-methoxy-ω-azido-PEG on the free alkyne units of sequence-controlled copolymers afforded a biocompatible water-soluble copolymer. The post-polymerization modification using click chemistry can be easily conducted with efficiency in a common organic solvent such as THF at ambient temperature. It is important to note that in this case, we need two equivalents of PEG as compared to one alkyne unit because the PEGylation can be prevented by two neighbors grafted PEG. Hence, the excess of PEG units helps to promote their accessibilities. However, the unreacted PEGs can be removed almost quantitatively from the polymers by using a dialysis technique. Moreover, the double PEGylation can be also performed in the case where the polymer contains another available alkyne site for example, TMS-POS copolymerized with TIPS propargylmaleimide.

Chapter V, the last section of the thesis focused on the preparation of sequence-controlled semi-crystalline copolymers [7]. In general, the polymers obtained in the present sequence-controlled copolymerization strategy possess a random orientation of styrenic units since the tacticity of the prepared polymers were uncontrolled. Monomers exhibiting a long alkyl side chain can be a way to enable the preparation of crystalline polymers because the crystalline network can be also formed due to a long paraffin side chain as reported in the literature [8]. Thus, monomer **G** having C-18 alkyl side chains was selected. Sequence-controlled semi-crystalline comb copolymers were successfully prepared by copolymerization of this donor monomer with a small amount of several models of *N*-substituted maleimides. The latter was added at different places along the polymer backbone in order to investigate the influence of the microstructure on the crystallization behavior of polymers. As indicated by

differential scanning calorimetry (DSC) analyses, the copolymers with different microstructures (composition and sequence distribution) possessed clearly different melting and crystallization temperatures. It was observed that melting temperature of the homopolymers was higher than the one measured for the copolymers. Furthermore, the examination of the copolymer structures was made in collaboration with Dr. Bernard Lotz by using transmission electronic microscopy (TEM) technique. The results showed that our copolymers formed interdigitated lamellar crystalline phase due to their alkyl side chains and they crystallized in hexagonal geometry. This structure was in accordance with that reported in the literature; hexagonal pattern was obtained in most case for the polymers bearing *n*-alkyl side-chain [9,10].

In conclusion, it was shown during these three years of doctoral researches that other donor monomers in particular *para*-substituted styrene derivatives (**Figure 69**, monomer **B-G**) can be used instead of styrene to copolymerize with MIs in a sequence-controlled fashion. This research is in fact advanced in preparation of new sequence-controlled materials that exhibit interesting properties such as sequence-controlled polyelectrolytes, sequence-controlled biocompatible water soluble polymers, and sequence-controlled semi-crystalline polymers by using a facile and versatile method. This fundamental research can certainly offer a broader scope of properties, since other functional sequence-controlled polymers backbone such as glycopolymers, recognition polymer chains, or polymers with high glass transition temperatures, could still be envisaged.

References

[1].   Srichan, S.; Chan-Seng, D.; Lutz, J.-F., *ACS Macro Lett.,* **2012**, *1*, 589-592.

[2].   Ten Brummelhuis, N.; Weck, M., *ACS Macro Lett.,* **2012**, *1*, 1216-1218.

[3].   Jaacks, V., *Makromol. Chem.,* **1972**, *161*, 161-172.

[4].   Mayo, F. R.; Lewis, F. M., *J. Am. Chem. Soc.,* **1944**, *66*, 1594-1601.

[5].   Srichan, S.; Mutlu, H.; Lutz, J.-F., *Eur. Polym. J.,* **2014**, *available online*, DOI: 10.1016/j.eurpolymj.2014.09.002.

[6].   Srichan, S.; Mutlu, H.; Badi, N.; Lutz, J.-F., *Angew. Chem., Int. Ed.,* **2014**, *53*, 9231-9235.

[7].   Srichan, S.; Kayunkid, N.; Oswald, L.; Lotz, B.; Lutz, J.-F., *Macromolecules,* **2014**, *47*, 1570-1577.

[8].   López-Carrasquero, F.; Giammanco, G.; Díaz, A.; Dávila, J.; Torres, C.; Laredo, E., *Polym. Bull.,* **2009**, *63*, 69-78.

[9].   Platé, N. A.; Shibaev, V. P., *J. Polym. Sci., Part D: Macromol. Rev.,* **1974**, *8*, 117-253.

[10].   Jordan, E. F.; Feldeisen, D. W.; Wrigley, A. N., *J. Polym. Sci., Part A-1: Polym. Chem.,* **1971**, *9*, 1835-1851.

Experimental section

1. **Chemicals:**

Compounds and solvents placed on the lists below were used as received.

Compounds	Suppliers	Purity (%)
Acetoxystyrene	Aldrich	96 %
Anisole	Sigma-Aldrich	99 %
Alkoxyamine BlocBuilder® MA	Arkema	97 %
N-benzylmaleimide	Alfa Aesar	99 %
4-*tert*-butoxystyrene	Aldrich	96 %
Tetra-*n*-butylammonium fluoride (TBAF)	Alfa Aesar	1 M solution in THF
1,8-diazabicyclo[5.4.0]undec-7-ene (DBU)	Sigma Aldrich	98 %
4,4'-dinonyl-2,2'-bipyridine (dNBipy)	Alfa Aesar	97 %
Hexylamine	Alfa Aesar	99 %
Hydrazine monohydrate ($NH_2.NH_2xH_2O$)	Alfa Aesar	99 %+
Hydrochloric acid (HCl)	Sigma-Aldrich	37% in aqueous solution
4-(*N*-maleimido)-azobenzene	Alfa Aesar	95 %
N-(*n*-propyl)maleimide	Alfa Aesar	94 %
N-(1-pyrenyl)maleimide	Sigma Aldrich	-
Methoxypolyethylene glycol azide (PEG) (CH_3O-PEG-N_3) M_n = 2.000 g·mol^{-1}	Rapp polymer	>99 %
4-Methylstyrene	Fluka	>99 %
Potassium phthalimide	Alfa Aesar	98 %
Sodium hydroxide NaOH	Analar normapur	99 %
Sulfuric acid (H_2SO_4)	Fluka	95-97 %
4-vinylbenzylchloride	Aldrich	≥90 %
Solvents	**Suppliers**	**Purity (%)**
Dimethylformamide (DMF)	Sigma-Aldrich	≥99 %
Dioxane	Fluka	99.5 %
Ethanol, absolute (EtOH$_{abs}$)	Prolabo	99.9 %
Methanol (MeOH)	Carlo Erba	99.9 %
Tetrahydrofuran (THF)	Carlo Erba	-
Toluene	Sigma-Aldrich	≥99.7 %

N-(2-(amino-Boc)ethylene)maleimide [1], pentafluorophenyl 4-maleimidobenzoate [2], *N*-(1-pyrenemethyl)maleimide [3,4], and 1-(3-(triisopropylsilyl)prop-2-ynyl)-1H-pyrrole-2,5-dione [5] were prepared following literature protocols. THF (99 %, Aldrich, stabilized with BHT) was dried and distilled over sodium-benzophenone. Copper (I) bromide (Sigma-Aldrich, 98 %) was stirred in glacial acetic acid in order to remove any soluble oxidized species, filtered, washed with ethanol, and dried under vacuum. Styrene (Sigma-Aldrich, 99 %) was distilled over calcium hydride under vacuum and stored under argon at -25 °C before use. All solvent were degassed prior to use for the polymerization.

2. Characterization methods:

✓ Nuclear Magnetic Resonance (NMR) spectroscopy

^{1}H NMR (400 MHz) and ^{13}C NMR (100 MHz) spectra were recorded in CDCl$_3$, CD$_3$OD or DMSO-d_6 on a Bruker Advance spectrometer equipped with Ultrashield magnets. The conversions of styrenic derivative monomers were calculated by comparing the integration of the double bond protons of monomers at 5.75 ppm to the integration of the aromatic protons and formed polymer present at 6.28-7.50 ppm. The conversion of the *N*-substituted maleimides was determined by comparing the integration of characteristic peaks of each *N*-substituted maleimide as monomer and formed polymer when incorporated on the polymer chain. The chemical shifts are reported in ppm (δ). All NMR data were reported as following: chemical shift, multiplicity (s = singlet, d = doublet, t = triplet, q =quartet, b= broad, bs = broad singlet, bm = broad multiplet). ^{19}F NMR (400 MHz) was used in the case of post-modification of pentafluorophenyl 4-maleimidobenzoate.

✓ Size Exclusion Chromatography (SEC)

Molecular weights (M_n) and molecular weight distribution (M_w/M_n) were determined by using a SEC coupled online to a multi-angle laser light scattering (MALLS), refractive index (Shimatzu SPD M20A RI) and ultra violet (UV) detectors, and equipped with two different column systems: five PLgel 10 µm Mixed-B columns or four PLgel 5 µm Mixed-C columns. The measurements were performed at 30 °C in THF with a flow rate of 1 mL·min^{-1} using a Shimadzu LC20AD pump. Toluene was used as internal reference. The molecular weight

calibration was based on sixteen narrow molecular weight linear polystyrene standards from polymer laboratories. A fixed d_n/d_c value of 0.186 was used for all polymers, exceptionally, the SEC results of poly(vinyl benzyl phthalimide) (**Chapter III**) were obtained using a fixed d_n/d_c value of 0.171 and the M_n and M_w/M_n values displayed for this chapter were measured with the light scattering detector. The refractive index increment d_n/d_c was determined on a Optilab rEX. Solutions of poly(VBP) in THF with known concentrations (10, 8, 6, 4.1, and 2.1 g·L^{-1}) were prepared. 3 ml of each solution was injected. After the injections were completed, the slope of the plot of RI signal against concentration allowed calculation of a refractive index increment.

✓ Differential Scanning Calorimetry (DSC)

The thermograms were recorded on a Perkin Elmer Diamond DSC using stainless steel capsules under a nitrogen atmosphere. 10 °C/min or 5 °C/min heating and cooling rates were used over the temperature ranging from -40 °C to +150 °C. The melting temperature (T_m) was recorded at the peak maximum of the endotherm.

✓ Fourier transform infrared spectroscopy (ATR-FTIR)

The experiment was conducted on a Bruker Vertex 70 spectrophotometer in ATR mode in a range of 800 – 4000 cm^{-1}. Samples were measured in solid form at room temperature.

✓ Transmission Electronic Microscopy (TEM)

The structure of polymers was characterized by electron diffraction with a Philips CM12 microscope equipped with a digital camera (Megaview III, Soft Imaging Systems). The material was oriented by epitaxial growth on benzoic acid following a standard co-melting procedure: a thin film of the polymer is covered with crystals of benzoic acid, the sample is heated above the melting point of benzoic acid (~127 °C) and cooled to room temperature. Benzoic acid crystallizes first, and crystallization of the polymer takes place on the freshly formed crystals of benzoic acid. After dissolution of the benzoic acid substrate in hot ethanol, the polymer film is coated with a carbon film, floated on water and deposited on a TEM grid before analysis.

✓ **Kaiser test**

The Kaiser test was used to detect the presence of primary amine groups in the copolymer after removal of Boc protecting groups. Three solutions, 0.25 g ninhydrin in 5 mL ethanol, 80 % phenol in EtOH (w/v) and 2 mL 0.001M KCN in 98 mL pyridine were prepared. A few mg of polymers were placed in a small vial and 3-4 drops of each solution were added. The vial was heated with a heat-gun for few minutes. The violet color of polymers grains and solution indicated a positive Kaiser test.

3. Experimental protocols:

📖 The synthesis for Chapter II: Influence of strong electron-donor monomers in sequence-controlled polymerization

II.1. General procedure for nitroxide-mediated homopolymerization of a-d
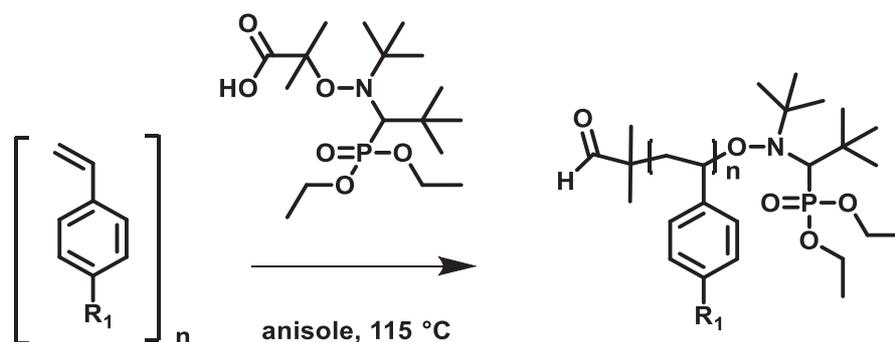
Homopolymers of donor monomer were synthesized by nitroxide-mediated homopolymerization in anisole solution. Similar procedures were used for all homopolymerization. The typical procedure is illustrated here for the polymerization corresponding to Entry 3 of **Table 3**. A mixture of donor monomer **c** (1.5 mL, 7.96 mmol, 100 eq.), BlocBuilder® MA (0.03 g, 0.0796 mmol, 1 eq.) and anisole (1.5 mL, 1:1 volume ratio with respect to monomer) were placed in a 10 mL flask equipped with a stirring bar and the solution was purged under argon. The tube was then immersed in an oil bath thermostated at 105 °C for 5 h. Samples were withdrawn periodically during the course of the homopolymerization and were analyzed by ^{1}H NMR spectroscopy. The resulting homopolymer was precipitated from THF into cold methanol. The precipitate was collected

by filtration, washed with methanol and dried overnight in a vacuum oven at room temperature. The purified polymer was characterized by ^{1}H NMR and SEC. (The kinetics of homopolymerization and SEC chromatograms were shown in **Figure 39**).

Entry 1 (polystyrene, **a**): White solid, 0.4 g (43 %). ^{1}H NMR (400 MHz, CDCl$_3$, δ in ppm): 0.61-2.29 (bm, -CH- and -CH_2- units of styrenic backbone + units of BlocBuilder® MA), 6.27-7.24 (bm, -Ar-H of a). SEC (THF): M_n = 7900 g·mol^{-1}, M_w/M_n = 1.11.

Entry 2 (polymethylstyrene, **b**): White solid, 0.42 g (60 %). ^{1}H NMR (400 MHz, CDCl$_3$, δ in ppm): 0.60-2.07 (bm, -CH- and -CH_2- units of styrenic backbone + units of BlocBuilder® MA), 2.27 (bs, -Ar-CH_3), 6.13-7.12 (bm, -Ar-H of **b**). SEC (THF): M_n = 7900 g·mol^{-1}, M_w/M_n = 1.15.

Entry 3 (poly(*tert*-butoxystyrene), **c**): White solid, 0.38 (51 %). ^{1}H NMR (400 MHz, CDCl$_3$, δ in ppm): 0.56-2.10 (bm, -CH- and -CH_2- units of styrenic backbone + units of BlocBuilder® MA), 1.28 (bs, -O-C(CH_3)$_3$), 6.14-6.88 (bm, -Ar-H of **c**). SEC (THF): M_n = 12500 g·mol^{-1}, M_w/M_n = 1.14.

Entry 4 (polyacetoxystyrene, **d**): White solid, 0.56 g (74 %). ^{1}H NMR (400 MHz, CDCl$_3$, δ in ppm): 0.59-2.05 (bm, -CH- and -CH_2- units of styrenic backbone + units of BlocBuilder® MA), 2.25 (bs, -O-CO-CH_3), 6.21-7.00 (broad, -Ar-H of **d**). SEC (THF): M_n = 11300 g·mol^{-1}, M_w/M_n = 1.16.

II.2. General procedure for nitroxide mediated copolymerization of donor monomer (a-d) with *N*-substituted maleimides
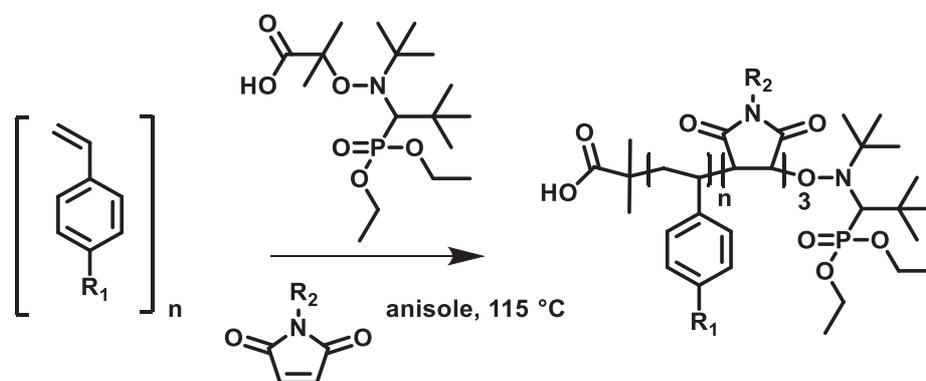
Copolymers of **a**, **b**, **c** and **d** with *N*-substituted maleimides were synthesized by nitroxide-mediated copolymerization in anisole solution. A following example corresponds to Entry 3 in **Table 4**. In a small flask, 3 mL (15.9 mmol, 50 eq.) of **c**, 180 mg (0.95 mmol, 3 eq.) of **1**, BlocBuilder® MA (0.125 g, 0.318 mmol, 1 eq.) and anisole (3 mL, 1:1 volume ratio with respect to monomer) were added. The tube was capped by a rubber septum, purged with argon for a few minutes and then immersed in an oil bath thermostated at 115 °C for 5 h. Samples were withdrawn at regular intervals for ^{1}H NMR analysis in order to monitor the incorporation of the maleimide on the growing copolymer chains. The viscous solution was diluted with THF and the polymer was recovered by precipitation in methanol and dried overnight at room temperature. The purified polymer was characterized by ^{1}H NMR and the number molecular weight (M_n) and molecular weight distribution (M_w/M_n) of the copolymer were determined by SEC. (The kinetic of Entries 1-4 in **Table 4** were shown in **Figure 40**).

Entry 1: White solid, 1.43 g (78 %). ^{1}H NMR (400 MHz, CDCl$_3$, δ in ppm): 0.52-2.32 (bm, -C*H*- and -C*H$_2$*- units of styrenic backbone + -C*H*- units of maleimide backbone + units of BlocBuilder® MA), 4.13-4.57 (bs, -C*H$_2$*-Ar- of **1**), 6.04-7.37 (bm, -Ar-*H* of **a** + -Ar-*H*- of **1**). SEC (THF): M_n = 6000 g·mol^{-1}, M_w/M_n = 1.20.

Entry 2: White solid, 1.72 g (55 %). ^{1}H NMR (400 MHz, CDCl$_3$, δ in ppm): 0.57-2.06 (bm, -C*H*- and -C*H$_2$*- units of styrenic backbone + -C*H*- units of maleimide backbone + units of BlocBuilder® MA), 2.27 (bs, -Ar-C*H$_3$*), 4.14-4.59 (bs, -C*H$_2$*-Ar- of **1**), 6.13-7.07 (bm, -Ar-*H* of **b**), 7.11-7.34 (bs, -CH$_2$-Ar-*H* of **1**). SEC (THF): M_n = 6600 g·mol^{-1}, M_w/M_n = 1.24.

Entry 3: White solid, 1.62 g (62 %). ^{1}H NMR (400 MHz, CDCl$_3$, δ in ppm): 0.56-2.17 (bm, -C*H*- and -C*H$_2$*- units of styrenic backbone + -C*H*- units of maleimide backbone + units of BlocBuilder® MA), 1.25 (bs, -O-C(C*H$_3$*)$_3$), 4.13-4.56 (bs, -C*H$_2$*-Ar- of **1**), 6.05-7.01 (bm, -Ar-*H* of **c**), 7.05-7.35 (bm, -CH$_2$-Ar-*H* of **1**). SEC (THF): M_n = 10300 g·mol^{-1}, M_w/M_n = 1.15.

Entry 4: White solid, 0.59 g (30 %). ^{1}H NMR (400 MHz, CDCl$_3$, δ in ppm): 0.57-2.03 (bm, -C*H*- and -C*H$_2$*- units of styrenic backbone + -C*H*- units of maleimide backbone + units of BlocBuilder® MA), 2.25 (bs, -O-CO-C*H$_3$*), 4.21-4.63 (bs, -C*H$_2$*-Ar- of **1**), 6.19-7.15 (bm, -Ar-*H* of **d**), 7.15-7.32 (bs, -CH$_2$-Ar-*H* of **1**). SEC (THF): M_n = 8700 g·mol^{-1}, M_w/M_n = 1.32.
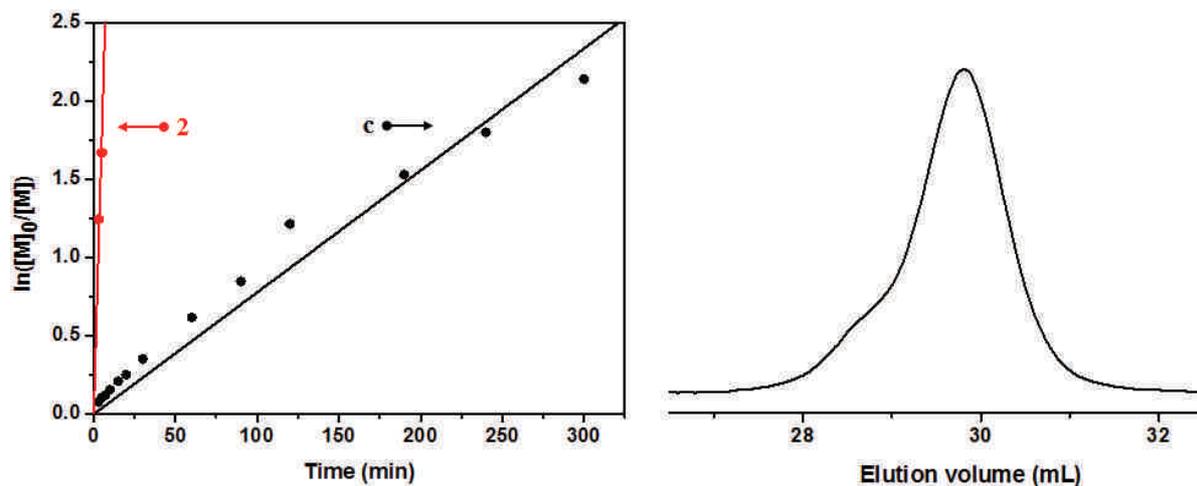
Entry 9: White solid, 0.160 g (10 %). ^{1}H NMR (400 MHz, CDCl$_3$, δ in ppm): 0.51-2.11 (bm, -C*H*- and -C*H*$_2$- units of styrenic backbone + -C*H*- units of maleimide backbone + units of BlocBuilder® MA), 1.25 (bs, -O-C(C*H*$_3$)$_3$ + -NH-CO-O-(C*H*$_3$)$_3$ of **2**), 2.66-3.58 (bs, -C*H*$_2$-C*H*$_2$-NH- of **2**), 4.13-4.56 (bs, -C*H*$_2$-Ar- of **c**), 6.04-7.14 (bm, -Ar-*H* of **c**). SEC (THF): M_n = 10200 g·mol^{-1}, M_w/M_n = 1.15.
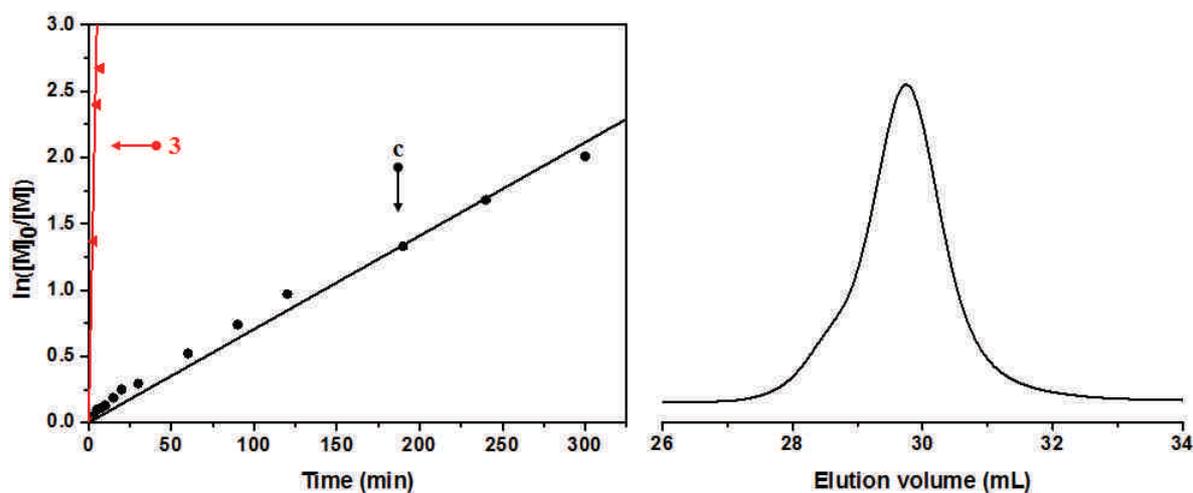
Entry 10: White solid, 1 g (58 %). ^{1}H NMR (400 MHz, CDCl$_3$, δ in ppm): 0.52-1.99 (bm, -C*H*- and -C*H*$_2$- units of styrenic backbone + -C*H*- units of maleimide backbone + units of BlocBuilder® MA), 1.25 (bs, -O-C(C*H*$_3$)$_3$), 6.14-6.98 (bm, -Ar-*H* of **c**), 7.50 and 7.91 (bs, -Ar-*H* of **3**). SEC (THF): M_n = 9400 g·mol^{-1}, M_w/M_n = 1.25.
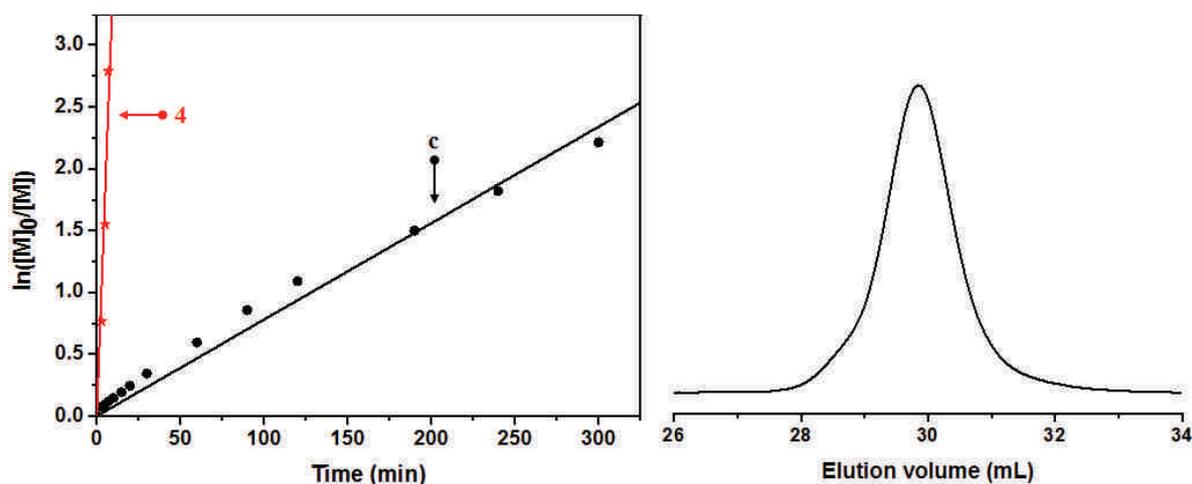
Entry 11: Pale yellow solid, 1 g (55 %). ^{1}H NMR (400 MHz, CDCl$_3$, δ in ppm): 0.48-2.06 (bm, -CH- and -CH_2- units of styrenic backbone + -CH- units of maleimide backbone + units of BlocBuilder® MA), 1.25 (bs, -O-C(CH_3)$_3$), 6.08-7.06 (broad, -Ar-H of **c**), 7.82-8.32 (bm, -Ar-H of **4**). SEC (THF): M_n = 8900 g·mol^{-1}, M_w/M_n = 1.19.

II.3. Example of NMP of donor monomers (a-d) with a kinetically-controlled addition of *N*-substituted maleimides
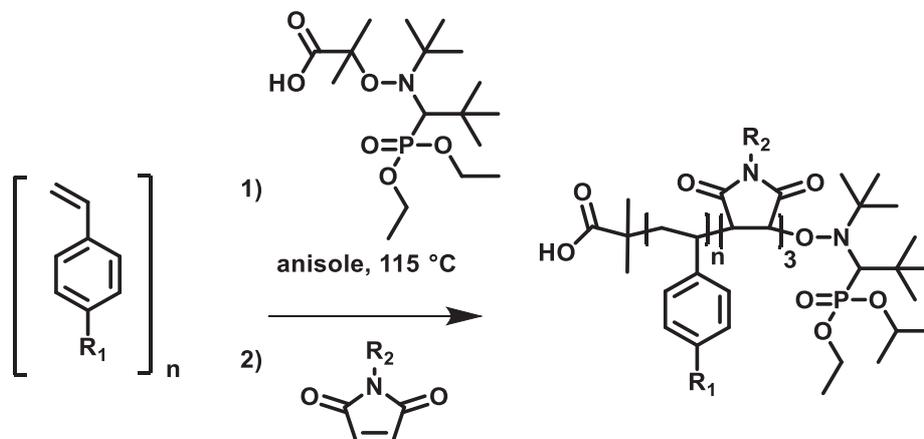
The present example corresponds to Entry 7 in **Table 4**. 3 mL of monomer **c** (15.9 mmol, 50 eq.), 125 mg of BlocBuilder® MA (0.318 mmol, 1 eq.), and 2.8 mL of anisole were added in a small flask equipped with a stirring bar. The flask was then sealed with a rubber septum, purged with dry argon and then immersed in an oil bath thermostated at 115 °C. After 100 min of reaction, a degassed solution of maleimide **1** (0.180 g, 0.95 mmol, 3 eq.) in 0.2 mL of anisole was added with a degassed syringe in the reaction mixture. Samples were withdrawn periodically for ^{1}H NMR analysis in order to monitor the incorporation of maleimide in the growing copolymer chains. After 5 h, the reaction mixture was diluted in THF and the

Page | 172

resulting solution was slowly poured into an excess of methanol under stirring in order to precipitate the polymer. The precipitate was collected by filtration, washed with methanol and dried overnight in a vacuum oven at room temperature. The purified polymer was characterized by ^{1}H NMR and SEC. (The kinetic of Entries 5-8 in **Table 4** were shown in **Figure 40**).

Entry 5: White solid, 1.32 g (72.5 %). ^{1}H NMR (400 MHz, CDCl₃, δ in ppm): 0.56-2.33 (bm, -C*H*- and -C*H*₂- units of styrenic backbone + -C*H*- units of maleimide backbone + units of BlocBuilder® MA), 4.14-4.55 (bs, -C*H*₂-Ar- of **1**), 6.17-7.39 (bm, -Ar-*H* of **a** + -Ar-*H*- of **1**). SEC (THF): M_n = 6900 g·mol⁻¹, M_w/M_n = 1.17.

Entry 6: White solid, 1.15 g (66 %). ^{1}H NMR (400 MHz, CDCl₃, δ in ppm): 0.59-2.04 (bm, -C*H*- and -C*H*₂- units of styrenic backbone + -C*H*- units of maleimide backbone + units of BlocBuilder® MA), 2.27 (bs, -Ar-C*H*₃), 4.15-4.57 (bs, -C*H*₂-Ar- of **1**), 6.10-7.09 (bm, -Ar-*H* of **b**), 7.10-7.34 (bm, -CH₂-Ar-*H* of **1**). SEC (THF): M_n = 6500 g·mol⁻¹, M_w/M_n =1.20.

Entry 7: White solid, 1.15 g (43 %). ^{1}H NMR (400 MHz, CDCl₃, δ in ppm): 0.56-2.20 (bm, -C*H*- and -C*H*₂- units of styrenic backbone + -C*H*- units of maleimide backbone + units of BlocBuilder® MA), 1.26 (bs, -O-C(C*H*₃)₃), 4.14-4.60 (bs, -C*H*₂-Ar- of **1**), 6.04-6.88 (bm, -Ar-*H* of **c**), 7.03-7.34 (bm, -CH₂-Ar-*H* of **1**). SEC (THF): M_n = 10000 g·mol⁻¹, M_w/M_n = 1.13.

Entry 8: White solid, 1.78 g (79 %). ^{1}H NMR (400 MHz, CDCl₃, δ in ppm): 0.56-2.05 (bm, -C*H*- and -C*H*₂- units of styrenic backbone + -C*H*- units of maleimide backbone + units of BlocBuilder® MA), 2.26 (bs, -O-CO-C*H*₃), 4.18-4.63 (bs, -C*H*₂-Ar- of **1**), 6.11-7.07 (bm, -Ar-*H* of **d**), 7.09-7.36 (bm, -CH₂-Ar-*H* of **1**). SEC (THF): M_n = 11200 g·mol⁻¹, M_w/M_n = 1.27.

II.4. Example of hydrolytic deprotection of *tert*-butyl group [6,7]
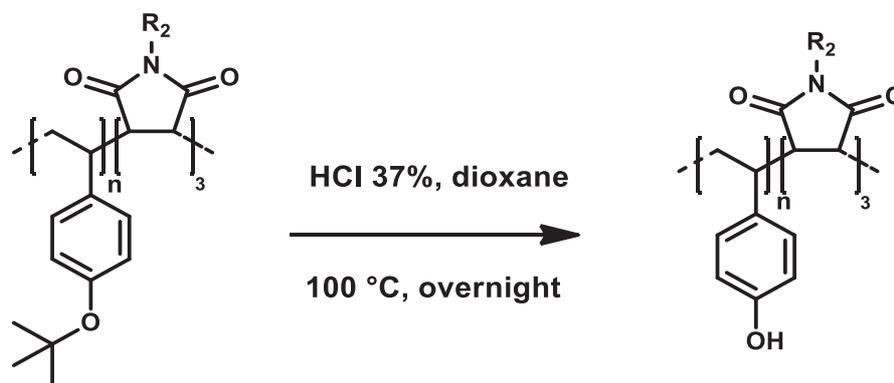
Homo- and copolymers based on **c** were deprotected under the same condition. This example corresponds to homopolymer Entry 3 in **Table 4**. 0.2 g of the homopolymer **c** (M_n = 12500 g·mol^{-1}) were dissolved in 2 mL of dioxane in a 10 mL round bottom flask. Then, 0.32 mL of HCl (37%) was added and the flask was capped with a condenser. The hydrolysis was completed overnight at 100°C under argon atmosphere and subsequently cooled to room temperature. The product was precipitated in cold water, collected by filtration, washed with water and dried overnight in a vacuum oven at room temperature. The purified deprotected polymer was characterized by ^{1}H NMR in CD$_3$OD.

H3': Brown powder, 0.04 g (20 %). ^{1}H NMR (400 MHz, CD$_3$OD, δ in ppm): 0.73-2.12 (bm, -C*H*- and -C*H$_2$*- units of styrenic backbone + units of BlocBuilder® MA), 6.10-6.94 (bm, -Ar-*H* of **c**).

Entry 3': Brown powder, 0.20 g (40 %). ^{1}H NMR (400 MHz, CD$_3$OD, δ in ppm): 0.69-2.38 (bm, -C*H*- and -C*H$_2$*- units of styrenic backbone + -C*H*- units of maleimide backbone + units of BlocBuilder® MA), 4.16-4.66 (bs, -C*H$_2$*-Ar- of **1**), 6.03-6.91 (bm, -Ar-*H* of **c**), 7.04-7.34 (bm, -Ar-*H* of **1**).

Entry 9': Brown powder, 0.23 g 46 %). ^{1}H NMR (400 MHz, CD$_3$OD, δ in ppm): 0.74-2.34 (bm, -C*H*- and -C*H$_2$*- units of styrenic backbone + -C*H*- units of maleimide backbone + units of BlocBuilder® MA), 2.56-3.75 (bs, -C*H$_2$*-C*H$_2$*-NH- of **2**), 6.07-7.01 (broad, -Ar-*H* of **c**).

Entry 10': Brown powder, 0.31 g (62 %). ^{1}H NMR (400 MHz, CD$_3$OD, δ in ppm): 0.70-2.19 (bm, -C*H*- and -C*H$_2$*- units of styrenic backbone + -C*H*- units of maleimide

backbone + units of BlocBuilder® MA), 6.03-7.03 (bm, -Ar-*H* of **c**), 7.51 and 7.90 (bs, -Ar-*H* of **3**).

Entry 11': Brown powder, 0.27 g (54 %). ^{1}H NMR (400 MHz, CD$_3$OD, δ in ppm): 0.73-2.06 (bm, -C*H*- and -C*H*$_2$- units of styrenic backbone + -C*H*- units of maleimide backbone + units of BlocBuilder® MA), 6.04-7.02 (bm, -Ar-*H* of **c**), 7.64-8.37 (bm, -Ar-*H* of **4**).

II.5. Example of hydrolytic deprotection of acetoxy group [8]
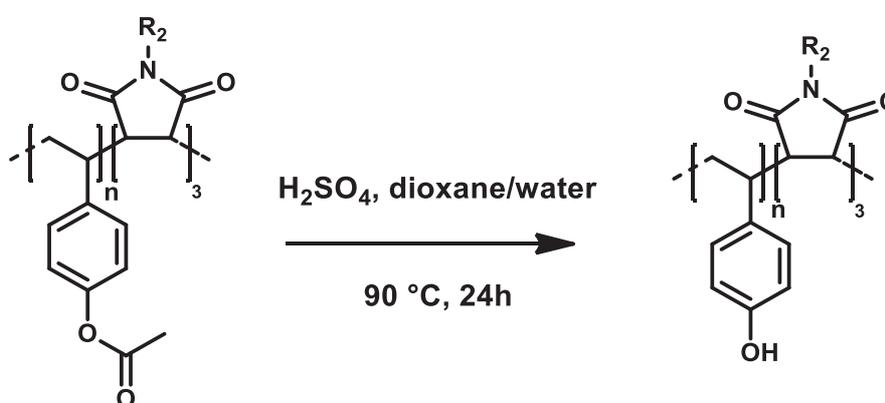
The same procedure was used for all homo- and copolymers based on **d**. This example corresponds to homopolymer Entry 4 in **Table 4**. 0.5 g of the homopolymer based on **d** (M_n = 11300 g·mol^{-1}), dioxane (3.5 mL), water (3 mL) and sulfuric acid (5 drops) were placed in a 25 mL round bottom flask, which was then placed in an oil bath at 90 °C. After 24 h, the reaction was cooled to room temperature. The polymers were recovered by precipitation in cold water, washed with water and dried overnight in a vacuum oven at room temperature. The purified deprotected polymer was characterized by ^{1}H NMR in CD$_3$OD.

H4': Brown powder, 0.23 g (46 %). ^{1}H NMR (400 MHz, CD$_3$OD, δ in ppm): 0.72-2.26 (bm, -C*H*- and -C*H*$_2$- units of styrenic backbone + units of BlocBuilder® MA), 6.11-6.88 (bm, -Ar-*H* of **d**).

Entry 4': Brown powder, 0.20 g (40 %). ^{1}H NMR (400 MHz, CD$_3$OD, δ in ppm): 0.73-2.29 (bm, -C*H*- and -C*H*$_2$- units of styrenic backbone + -C*H*- units of maleimide backbone + units of BlocBuilder® MA), 4.14-4.55 (bs, -C*H*$_2$-Ar- of **1**), 6.09-6.90 (bm, -Ar-*H* of **d**), 7.01-7.29 (bm, -Ar-*H* of **1**).

II.5. Solubility test

	aqueous NaOH solution			water	MeOH	THF
	pH 13	pH 12	pH 11	pH 5-6	pH 6	pH 6
Homopolymer based on c	√	√ overnight	X	X	√	√
Copolymers based on c	√	X	X	X	√	√
Homopolymer based on d	√	√ overnight	X	X	√	√
Copolymer based on d	√	X	X	X	√	√

(3-4 mg/ 2 mL)

📖 The synthesis for Chapter III: On the synthesis of sequence-controlled poly(vinyl benzyl amine-*co*-N-substituted maleimides) copolymers

III.1. The synthesis of *N*-(*p*-vinyl benzyl)phthalimide monomer (VBP) [9,10]
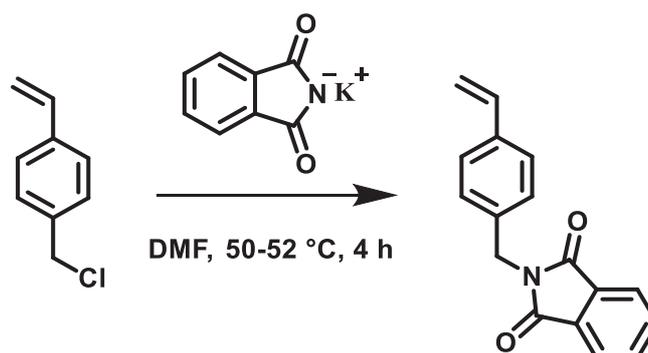
13.41 g (71 mmol, 1 eq.) of potassium phthalimide was dissolved in 40 mL DMF, 10 mL (10.83 g, 71 mmol, 1 eq.) of vinylbenzyl chloride was then added, the reaction mixture was stirred at 50 °C for 4 h. The reaction was cooled down to room temperature and diluted with CHCl₃ (150 mL). The mixture was extracted with 0.2N NaOH aqueous solutions (2X150 mL) and with distilled water (2X150 mL). The combining organic layers were dried over Na₂SO₄. The solvent was evaporated under reduce pressure yielding a white solid, which was recrystallized from MeOH to give a pure product in 86 % of yield.

^{1}H NMR (400 MHz, CDCl₃, δ in ppm): 4.83 (s, 2H, -Ar-C*H*₂-N-), 5.22 (d, 1H, -CH=C*H*₂), 5.73 (d, 1H, -CH=C*H*₂), 6.68 (dd, 1H, -C*H*=CH₂), 7.34-7.41 (m, 4H, phenyl protons of benzyl

unit), 7.71 (d, 2H, phenyl protons of phthalimide unit), 7.85 (d, 2H, phenyl protons of phthalimide unit).
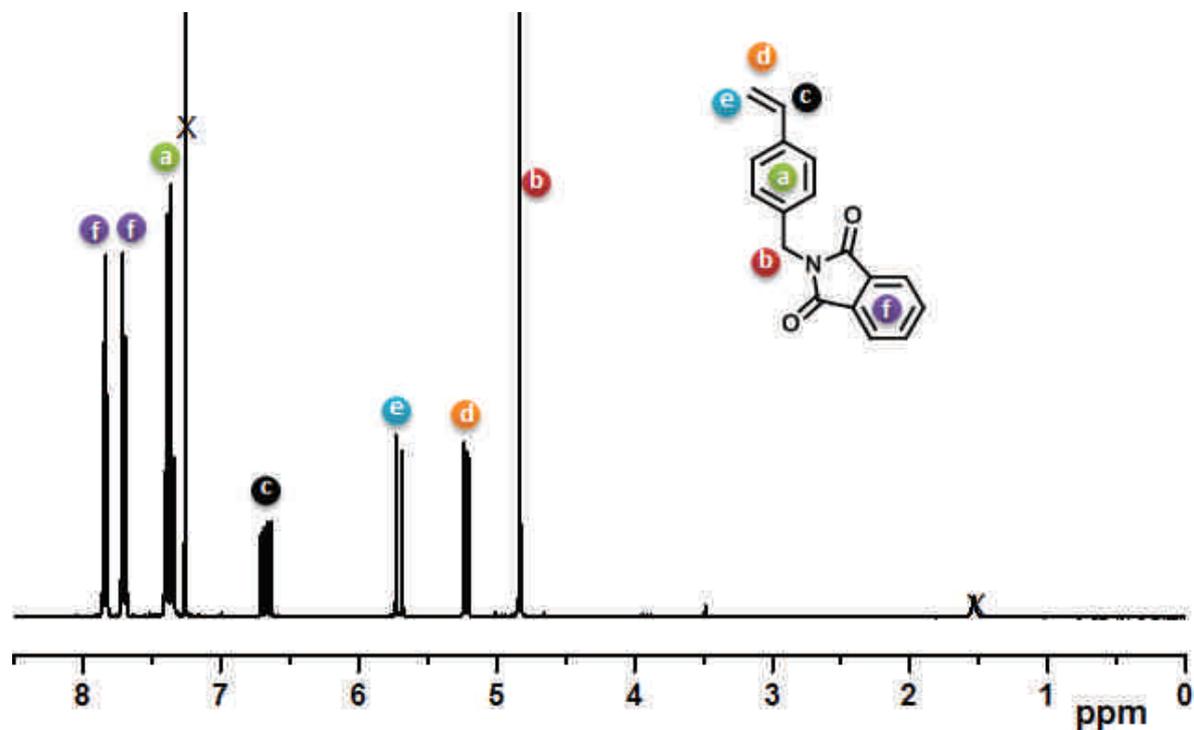
III.2. Example of nitroxide-mediated homopolymerization of VBP monomer
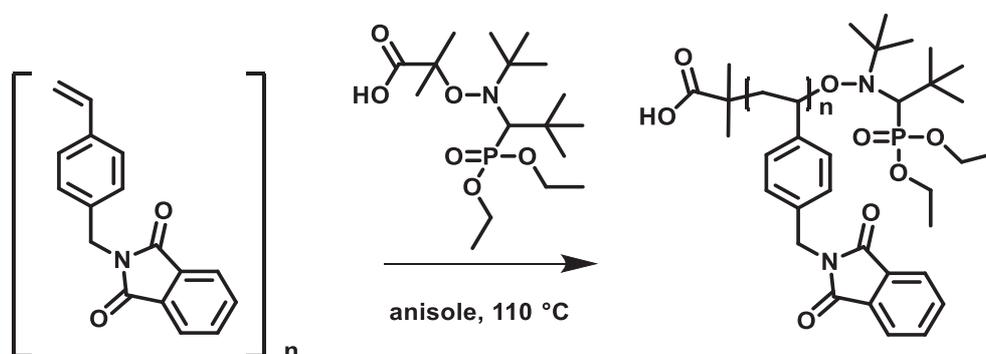
Homopolymers of *N*-(*p*-vinyl benzyl)phthalimide were synthesized by NMP. A typical procedure is described below. This example corresponds to polymer **P1** in **Table 6**. *N*-(*p*-vinyl benzyl)phthalimide (1 g, 3.80 mmol, 20 eq.) and BlocBuilder® MA (75 mg, 0.19 mmol, 1 eq.) were placed in a 10 mL flask containing a stir bar. The flask was then capped with a septum and degassed with dry argon. Degassed anisole (3 mL, 3:1 volume ratio with respect to monomer) was then added using a degassed syringe. The flask was heated in an oil bath preheated at 110 °C. Samples were periodically taken for NMR analysis in order to

determine the monomer conversion. After 320 min of reaction, the reaction mixture was concentrated and dissolved in small a quantity of THF. The polymer was obtained by precipitation into an excess of cold methanol. The precipitate was collected by filtration and dried under vacuum overnight at room temperature. The purified polymer was characterized by ^{1}H NMR and SEC.
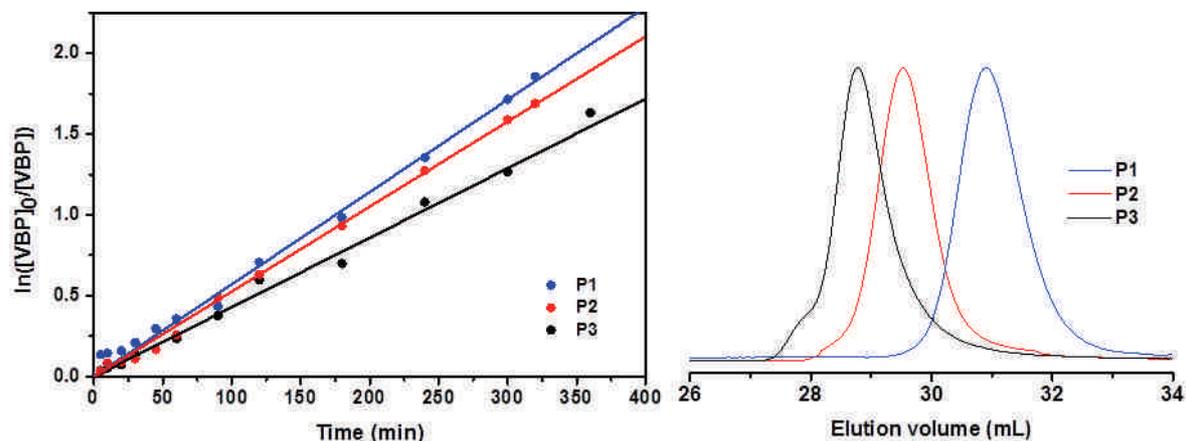
P1: White solid, 0.426 g (55 %). ^{1}H NMR (400 MHz, CDCl$_3$, δ in ppm): 0.39-1.91 (bm, -C*H*- and -C*H$_2$*- units of styrenic backbone + units of BlocBuilder® MA), 4.71 (bs, -Ar-C*H$_2$*-N-CO- of **VBP**), 6.06-7.24 (bm, -Ar-*H* of phenyl), 7.44-7.89 (bm, -N-CO-Ar-*H* of phthalimide). SEC (THF): M_n = 7400 g·mol^{-1}, M_w /M_n = 1.10.

P2: White solid, 0.600 g (74 %). ^{1}H NMR (400 MHz, CDCl$_3$, δ in ppm): 0.40-1.95 (bm, -C*H*- and -C*H$_2$*- units of styrenic backbone + units of BlocBuilder® MA), 4.72 (bs, -Ar-C*H$_2$*-N-CO- of **VBP**), 6.05-7.21 (bm, -Ar-*H* of phenyl), 7.42-7.86 (bm, -N-CO-Ar-*H* of phthalimide). SEC (THF): M_n = 17200 g·mol^{-1}, M_w /M_n = 1.09.

P3: White solid, 0.315 g (40 %). ^{1}H NMR (400 MHz, CDCl$_3$, δ in ppm): 0.38-1.91 (bm, -C*H*- and -C*H$_2$*- units of styrenic backbone + units of BlocBuilder® MA), 4.70 (bs, -Ar-C*H$_2$*-N-CO- of **VBP**), 6.10-7.30 (bm, -Ar-*H* of phenyl), 7.46-7.91 (bm, -N-CO-Ar-*H* of phthalimide). SEC (THF): M_n = 24700 g·mol^{-1}, M_w /M_n = 1.37.

III.3. Example of sequence-controlled copolymerization of VBP with *N*-substituted maleimide
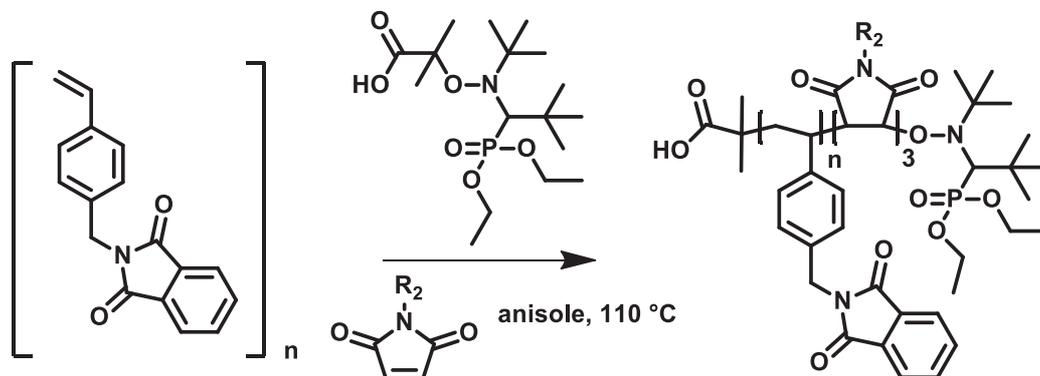
This particular example corresponds to copolymer **C5** in **Table 7**. Copolymer of *N*-(*p*-vinylbenzyl)phthalimide with TIPS-MI was synthesized by NMP in anisole or toluene. In a 10 mL round bottom flask, 1.2 g of *N*-(*p*-vinyl benzyl)phthalimide (4.55 mmol, 20 eq), 199 mg of TIPS-MI (0.69 mmol, 3 eq), 90 mg of BlocBuilder® MA (0.23 mmol, 1 eq) and 3.6 mL of a degassed toluene were added (monomer/solvent = 1:3 v/v). The flask was purged with argon for few minutes and then placed into an oil bath preheated at 110 °C for 4 h. Samples were withdrawn for NMR analysis in order to monitor the incorporation of TIPS-MI in the growing copolymer chains. The mixture was then diluted with small amount of THF which was slowly poured into an excess of cold methanol. The white precipitate was collected by filtration and dried overnight at room temperature. The precipitation was repeated in order to further purify the polymer. The purified polymer was then characterized by ^{1}H NMR and SEC.
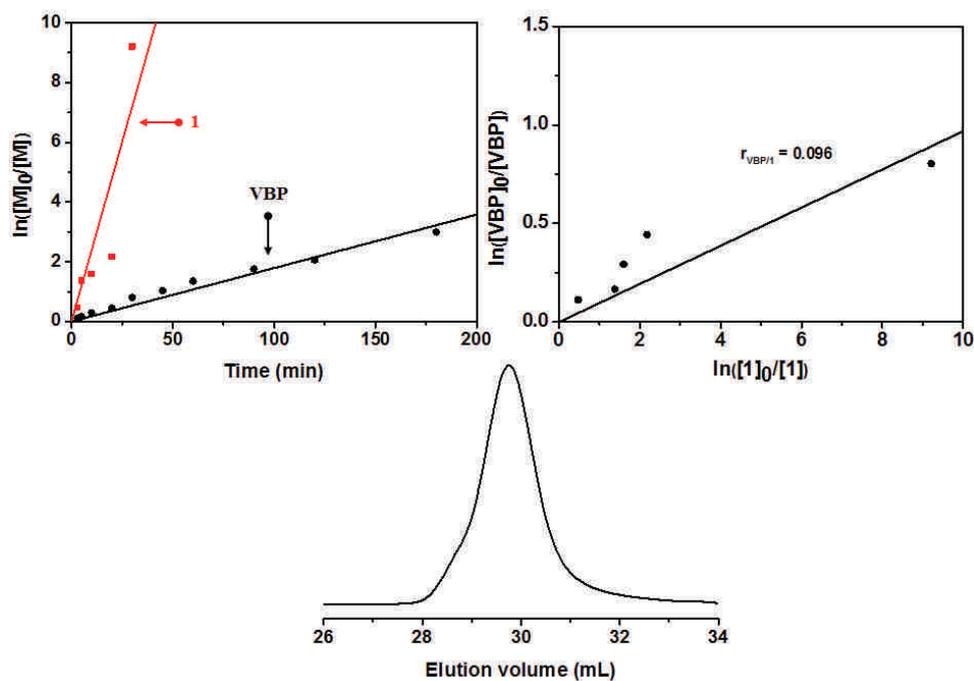
C1: White solid, 0.75 g (79 %). ^{1}H NMR (400 MHz, CDCl$_3$, δ in ppm): 0.38-2.08 (bm, -C*H*- and -C*H$_2$*- units of styrenic backbone + -C*H*- units of maleimide backbone + units of BlocBuilder® MA), 3.99-4.38 (bs, -C*H$_2$*-Ar of **1**), 4.69 (bs, -Ar-C*H$_2$*-N-CO- of **VBP**), 6.00-7.17 (bm, -Ar-*H* of phenyl), 7.21-7.36 (bm, -Ar-*H* of **1**), 7.45-7.97 (bm, -N-CO-Ar-*H* of phthalimide). SEC (THF): M_n = 16500 g·mol^{-1}, M_w/M_n = 1.23.
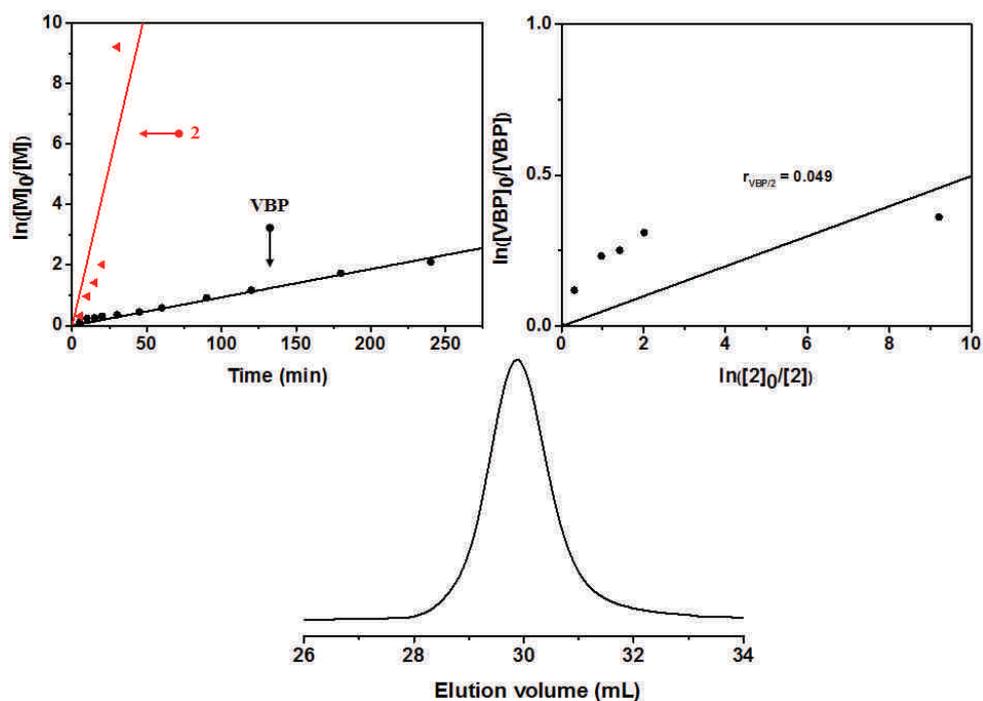
C2: White solid, 1.32 g (75 %). ^{1}H NMR (400 MHz, CDCl$_3$, δ in ppm): 0.21-1.89 (bm, -C*H*- and -C*H$_2$*- units of styrenic backbone + -C*H*- units of maleimide backbone + units of BlocBuilder® MA), 2.73-3.31 (bs, -C*H$_2$*-CH$_2$-CH$_3$ of **2**), 4.68 (bs, -Ar-C*H$_2$*-N-CO- of **VBP**), 5.98-7.22 (bm, -Ar-*H* of phenyl), 7.44-8.00 (bm, -N-CO-Ar-*H* of phthalimide). SEC (THF): M_n = 16100 g·mol^{-1}, M_w /M_n = 1.11.

C3: White solid, 0.88 g (75 %). ^{1}H NMR (400 MHz, CDCl$_3$, δ in ppm): 0.39-1.97 (bm, -C*H*- and -C*H$_2$*- units of styrenic backbone + -C*H*- units of maleimide backbone + units of BlocBuilder® MA), 4.68 (bs, -Ar-C*H$_2$*-N-CO- of **VBP**), 6.04-7.23 (bm, Ar-*H* of phenyl), 7.41-8.08 (bm, -N-C=O-Ar-*H* of phthalimide + -Ar-*H* of **3**). SEC (THF): M_n = 17800 g·mol^{-1}, M_w /M_n = 1.07. (The kinetic and SEC chromatogram were shown in **Figure 48**).
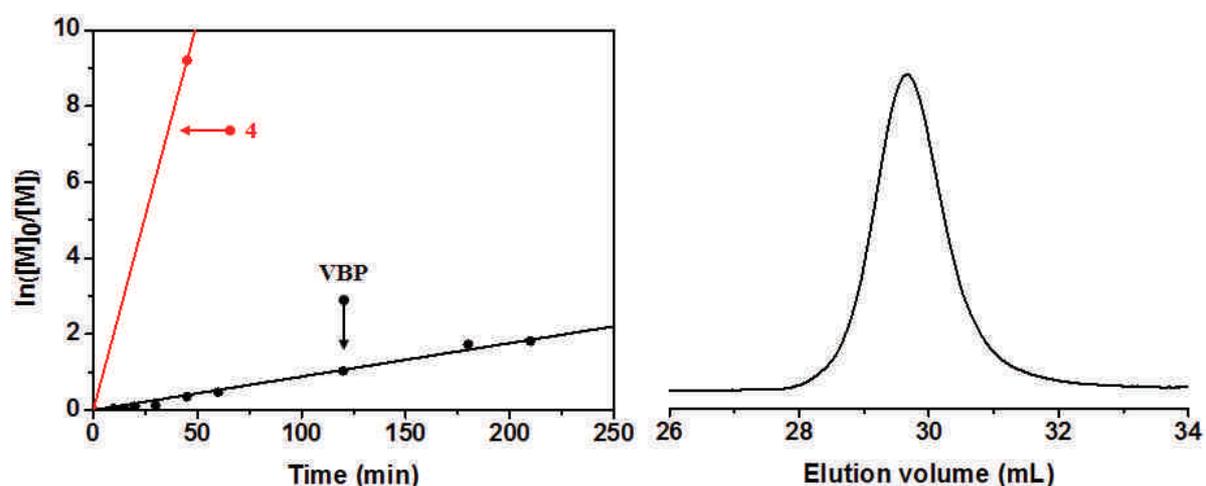
C4: White solid, 0.87 g (71 %). ^{1}H NMR (400 MHz, CDCl$_3$, δ in ppm): 0.25-2.05 (bm, -C*H*- and -C*H$_2$*- units of styrenic backbone + -C*H*- units of maleimide backbone + units of BlocBuilder® MA), 0.93 (bs, -Si-(*iPr)$_3$* of **4**), 3.73-4.10 (bs, -C*H$_2$*-C≡C-Si-(*iPr)$_3$* of **4**), 4.69 (bs, -Ar-C*H$_2$*-N-CO- of **VBP**), 5.98-7.20 (bm, -Ar-*H* of phenyl), 7.42-7.88 (bm, -N-CO-Ar-*H* of phthalimide). SEC (THF): M_n = 15000 g·mol^{-1}, M_w /M_n = 1.08.

C5: White solid, 0.836 g (86 %). ^{1}H NMR (400 MHz, CDCl$_3$, δ in ppm): 0.21-2.14 (bm, -C*H*- and -C*H$_2$*- units of styrenic backbone + -C*H*- units of maleimide backbone + units of BlocBuilder® MA), 0.94 (bs, -Si-(*iPr)$_3$* of **4**), 3.76-4.19 (bs, -C*H$_2$*-C≡C-Si-(*iPr)$_3$* of **4**), 4.71 (bs, -Ar-C*H$_2$*-N-CO- of **VBP**), 6.01-7.25 (bm, -Ar-*H* of phenyl), 7.46-8.10 (bm, -N-CO-Ar-*H* of phthalimide). SEC (THF): M_n = 8100 g·mol^{-1}, M_w /M_n = 1.11. (The kinetic and SEC chromatogram were shown in **Figure 48**).
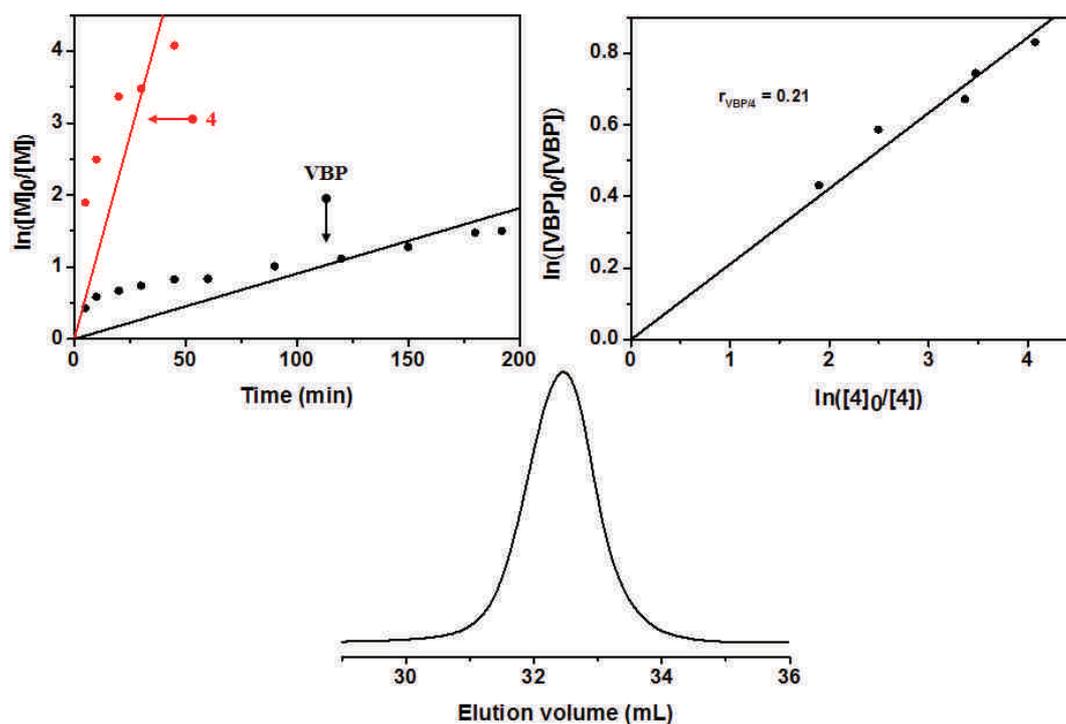
C7: White solid, 0.3 g (33 %). ^{1}H NMR (400 MHz, CDCl$_3$, δ in ppm): 0.39-1.96 (bm, -C*H*- and -C*H*$_2$- units of styrenic backbone + -C*H*- units of maleimide backbone + units of BlocBuilder® MA), 0.96 (bs, -Si-(*iPr*)$_3$ of **4**), 3.66-4.26 (bs, -C*H*$_2$-C≡C-Si-(*iPr*)$_3$ of **4**), 4.76 (bs, -Ar-C*H*$_2$-N-CO- of **VBP**), 6.04-7.44 (bm, Ar-*H* of phenyl), 7.51-8.12 (bm, -N-CO-Ar-*H* of phthalimide). SEC (THF): M_n = 2000 g·mol^{-1}, M_w/M_n = 1.05.

III.4. Example of sequence-controlled copolymerization of VBP with a time-controlled addition of a *N*-substituted maleimide.
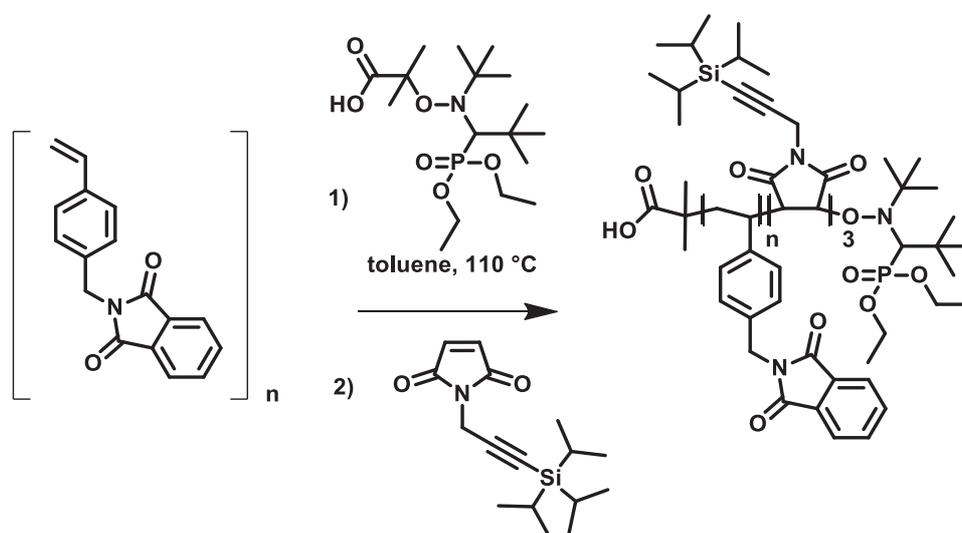
This particular example corresponds to copolymer **C6** in **Table 7**. 1.2 g of *N*-(*p*-vinyl benzyl)phthalimide (4.55 mmol, 20 eq.) and 90 mg of BlocBuilder® MA (0.23 mmol, 1 eq.) were dissolved in 3.4 mL of degassed toluene. The mixture was purged with argon for 5-10 minutes and then immediately immersed in an oil bath preheated at 110 °C. The monomer conversion was followed by ^{1}H NMR. After 205 min of reaction, a degassed solution of TIPS-MI (200 mg, 0.69 mmol, 3 eq.) in 0.2 mL of toluene was added through a degassed syringe (51 % conversion of *N*-(*p*-vinyl benzyl)phthalamide at this stage). Samples were withdrawn for NMR analysis in order to monitor the incorporation of TIPS-MI in the growing copolymer chains. After 440 min, the reaction mixture was dissolved in small amount of THF and precipitated into an excess of cold methanol. The precipitate was collected by filtration, washed with methanol and dried at room temperature overnight. The purified polymer was then characterized by ^{1}H NMR and SEC.
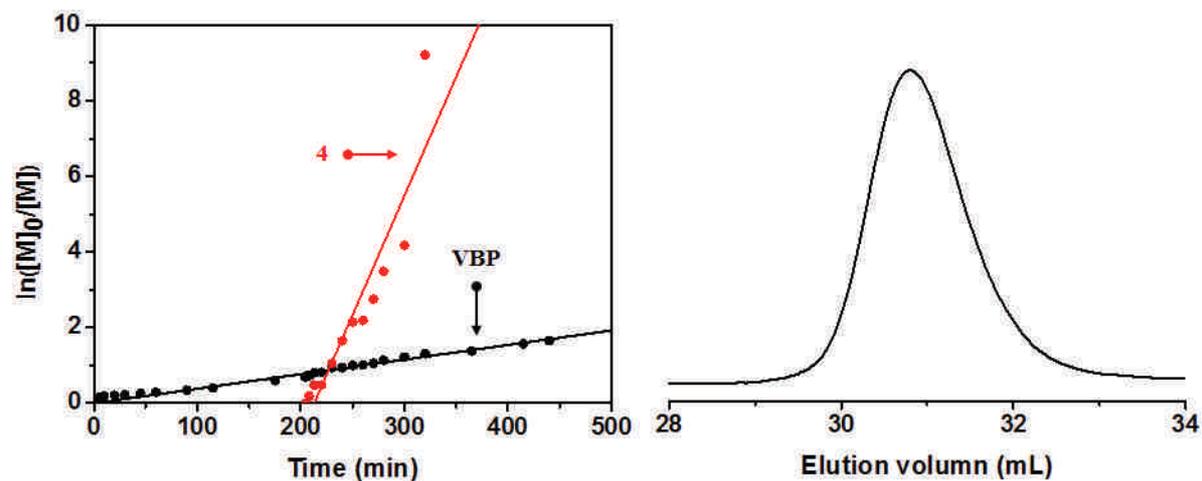
C6: White solid, 0.56 g (60 %). ^{1}H NMR (400 MHz, CDCl$_3$, δ in ppm): 0.40-1.98 (bm, -C*H*- and -C*H$_2$*- units of styrenic backbone + -C*H*- units of maleimide backbone + units of BlocBuilder® MA), 0.94 (bs, -Si-(*iPr*)$_3$ of **4**), 3.78-4.16 (bs, -C*H$_2$*-C≡C-Si-(*iPr*)$_3$ of **4**), 4.72 (bs, -Ar-C*H$_2$*-N-CO- of **VBP**), 6.03-7.23 (bm, Ar-*H* of phenyl), 7.47-7.96 (bm, -N-CO-Ar-*H* of phthalimide). SEC (THF): M_n = 6900 g·mol^{-1}, M_w/M_n = 1.08.

III.5. General procedure for the selective deprotection of the polymers C4.
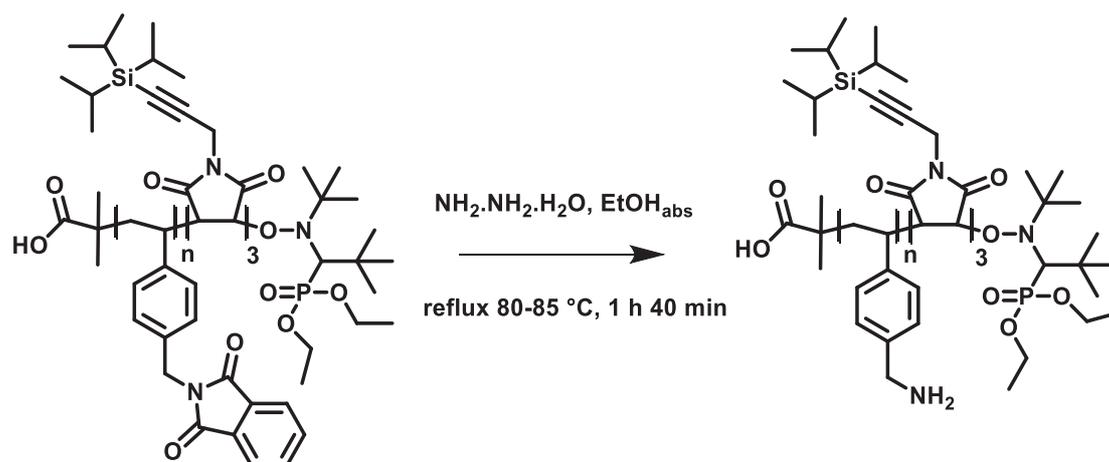
Phthalimide protecting groups in (co)polymers were removed using a procedure adapted from the literature [11]. In a flask, 300 mg of copolymer **C4** in **Table 7** (0.02 mmol, 1 eq.) was dissolved in 1.5 mL of absolute ethanol and treated under dry argon and heated under reflux. A solution of hydrazine monohydrate (63 mg, 1.25 mmol, 57.4 eq.) in 0.12 mL of absolute ethanol was added. After stirring up for 1 h 40 min, a white precipitate was formed in the flask. The mixture was cooled down to room temperature and ethanol was removed under reduced pressure. The solid residue was solubilized in 20 mL of chloroform and 20 mL of 20% aqueous NaOH was added. The aqueous phase was separated and extracted with chloroform (3X15 mL). The organic phases were combined and dried over Na_2SO_4. The chloroform was removed affording a product. The polymer was purified by dialysis against a DMSO/H_2O (2:8) solution using Spectra/Por® Dialysis membrane with a molecular weight cut-off of 6-8000 g·mol^{-1}, dried under vacuum and characterized by ^{1}H NMR. (The NMR spectra before and after deprotection were illustrated in **Figure 50**).

Shiny brown solid, 0.122 g (41 %). ^{1}H NMR (400 MHz, DMSO-d_6, δ in ppm): 0.46-1.89 (bm, -C*H*- and -C*H$_2$*- units of styrenic backbone + -CH- units of maleimide backbone + units of BlocBuilder® MA), 0.97 (bs, -Si-(*iPr*)$_3$ of **4**), 3.89 (broad, -C*H$_2$*-NH$_2$- + -C*H$_2$*-C≡C-Si-(*iPr*)$_3$ of **4** + H_2O from DMSO-d_6), 6.13-7.36 (bm, Ar-*H* of phenyl), 7.84 and 8.07 (dd, phthalhydrazide).The ^{1}H NMR below corresponds to the deprotected polymer before and after dialysis.
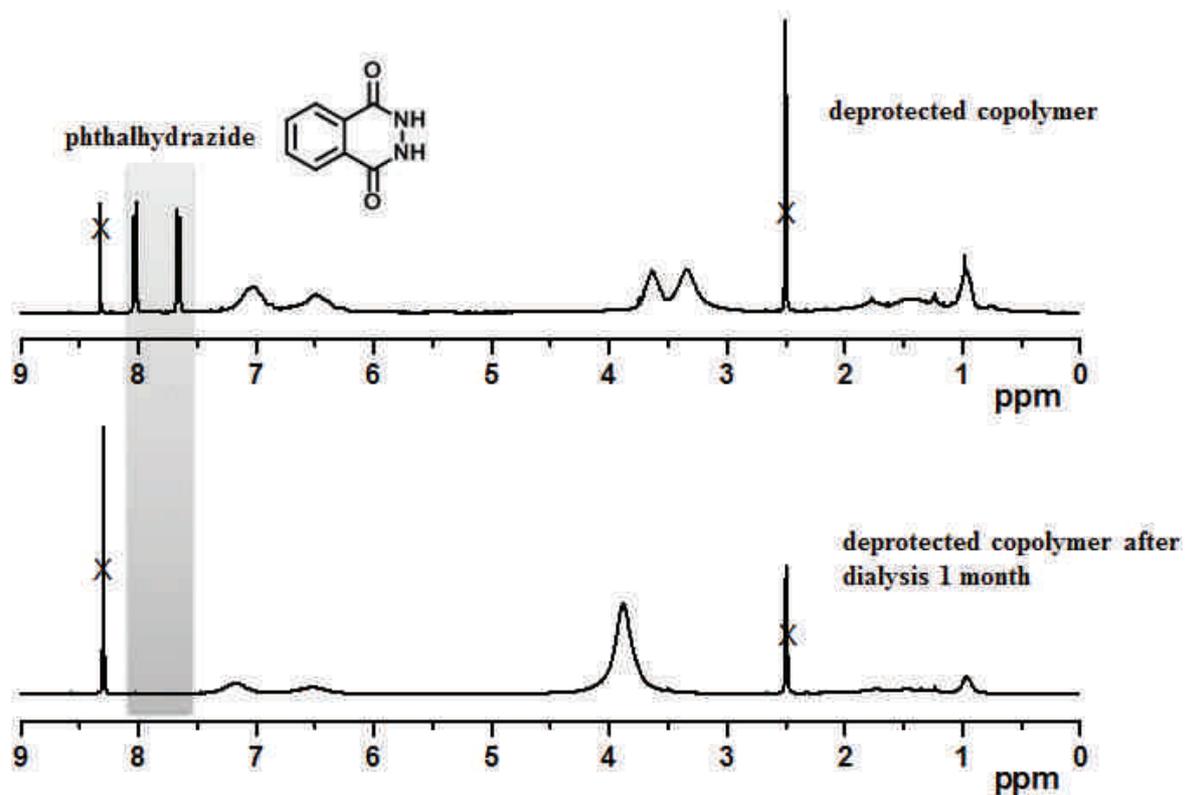
III.6. Solubility test
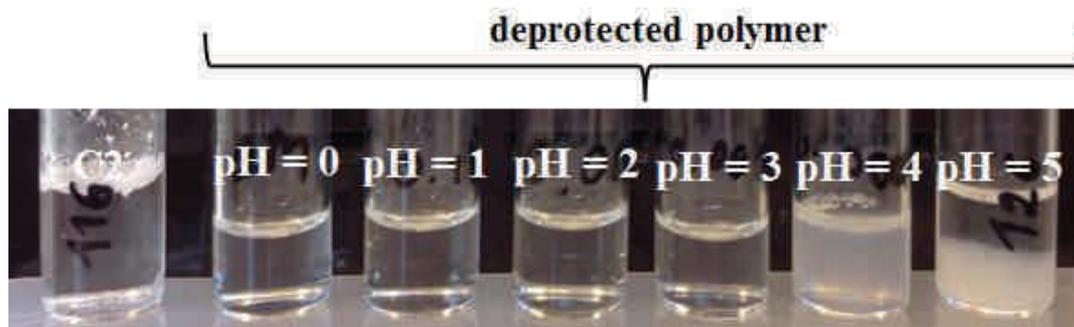
2.2 mg of copolymer **C2** before and after removal of phthalimide protecting group was dissolved in 0.5 mL of aqueous solution at different pH.

⚏ The synthesis for Chapter IV: Precision PEGylated polymers obtained by sequence-controlled copolymerization and post-polymerization modification

IV.1. Monomer synthesis

PEG-styrene macromonomer (**1**) is available in our laboratory and was prepared following literature protocol [12]. The synthesis of monomers (**2**) and (**3**) is described below.

☞ Synthesis of 4-propargyloxystyrene monomer (2)[13]
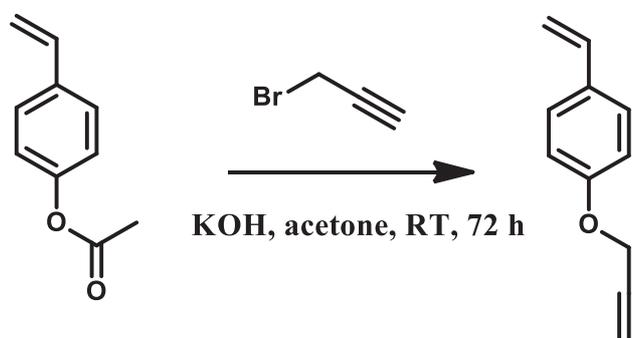
KOH (16.49 g, 0.294 mol, 3 eq.) was added to a solution of acetoxystyrene (15.9 g, 0.098 mol, 1 eq.) in 100 mL deionized water. The mixture was stirred for 2 h at room temperature. The solution of 5.15 mL (21.86 g, 0.147 mol, 1.5 eq.) of propargyl bromide (80 % in toluene) in 60 mL acetone was then added dropwise to the orange solution. The reaction mixture was stirred at room temperature for 72 h, after which the acetone was removed under reduced pressure and the remaining aqueous solution was extracted three times with chloroform. The organic layer was dried over Na_2SO_4. The solvent was removed under reduced pressure. The crude product was purified by alumina basic column chromatography using 100:1 hexane/ethyl acetate as the eluent, giving a clear liquid in 80 % of yield. The product was dried under vacuum overnight and characterized by ^{1}H NMR.

^{1}H NMR (400 MHz, CDCl₃, δ in ppm): 2.55 (s, 1H, -C≡C*H*), 4.72 (s, 2H, -O-C*H*₂-C≡CH), 5.15 (d, 1H, -CH=C*H*₂), 5.68 (d, 1H, -CH=C*H*₂), 6.69 (dd, 1H, -C*H*=CH₂), 6.98 (d, 2H, -Ar-*H*), 7.38 (d, 2H, -Ar-*H*).
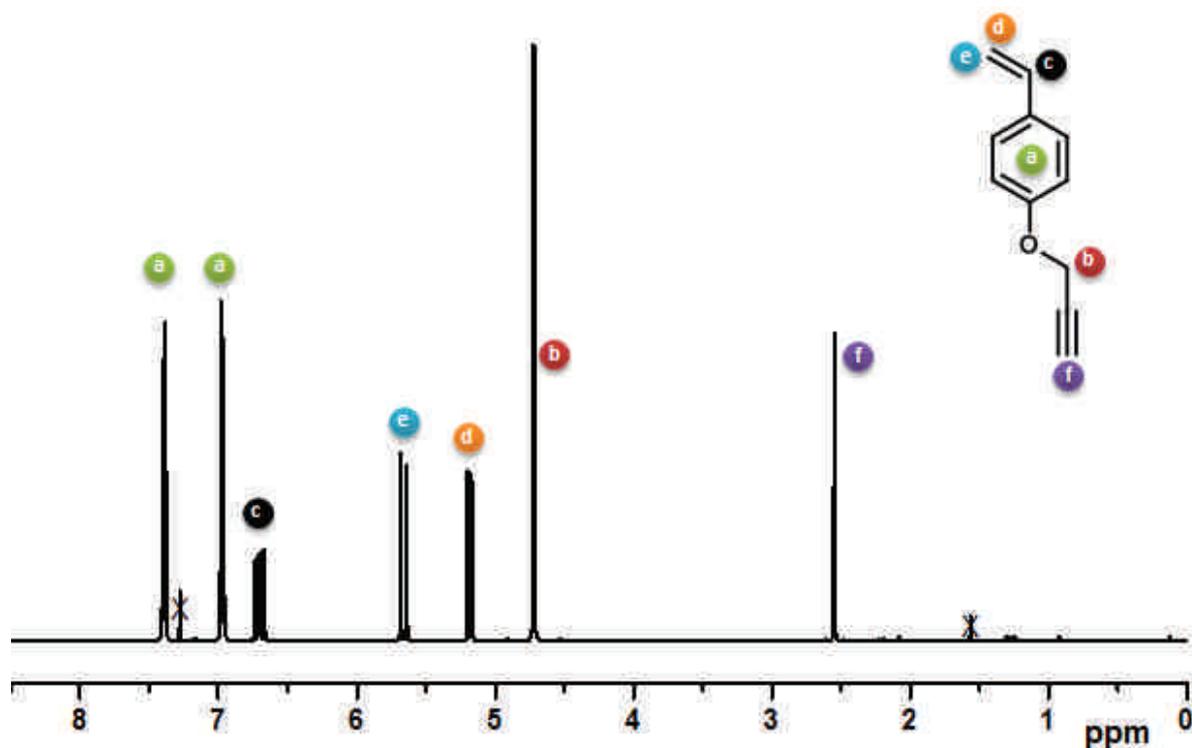
☞ Synthesis of TMS-protected propargyloxystyrene monomer (3)[14,15]

In a 100 mL two-neck round-bottom flask, equipped with a condenser, 1.26 g (8.7 mmol, 0.1 eq.) of silver chloride and 14 g (90.7 mmol, 1.04 eq.) of DBU were dispersed in 86 mL of dry dichloromethane and 13.8 g (87.2 mmol, 1 eq.) of 4-(propargyloxy)styrene was added under an argon atmosphere. The suspension was heated under reflux and 13.53 g (122 mmol, 1.4 eq.) of trimethylsilyl chloride were dropped slowly. After 24 h, the reaction mixture was cooled to room temperature. The crude product was washed with 1M HCl (100 mL), NaHCO₃ and deionized water. The combined organic layers were dried over Na₂SO₄, the organic layer was evaporated. The pure product was isolated by column

chromatography on silica gel using a gradient from pure n-hexane at the beginning and hexane/ethyl acetate (95/5) as eluent resulting in 11 g (55 %) of a colorless oil. The product was dried under vacuum overnight and characterized by ^{1}H NMR.

^{1}H NMR (400 MHz, CDCl$_3$, δ in ppm): 0.20 (s, -Si-(CH_3)$_3$), 4.68 (s, 2H, -O-CH_2-C≡CH), 5.17 (d, 1H, -CH=CH_2), 5.66 (d, 1H, -CH=CH_2), 6.69 (dd, 1H, -CH=CH$_2$), 6.96 (d, 2H, -Ar-H), 7.37 (d, 2H, -Ar-H).
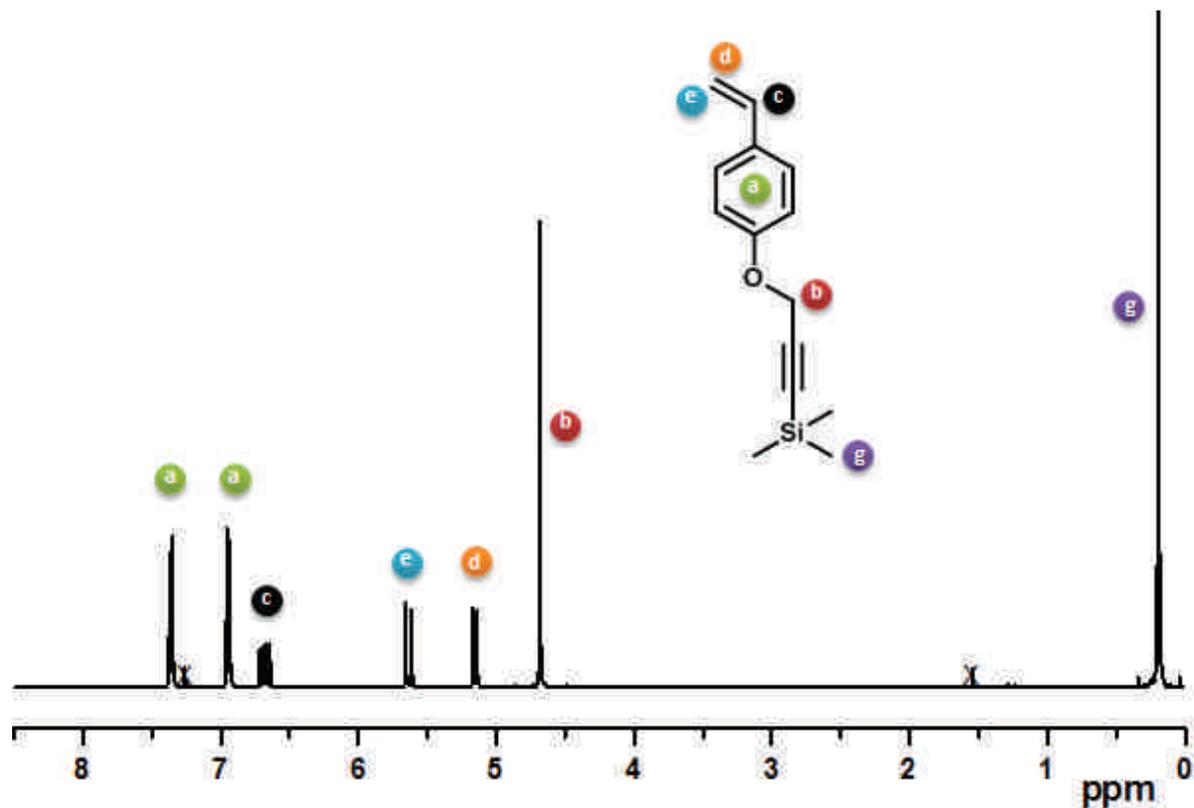
IV.2. Example of nitroxide-mediated homopolymerization of 1

anisole, 120 °C
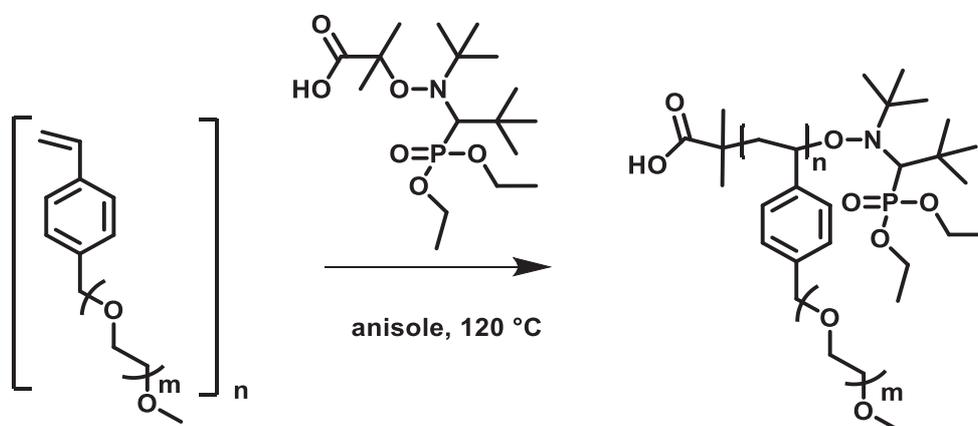
The procedure illustrated here corresponds to the Entry 1 in **Table 8**. BlocBuilder® MA (0.0278 g, 7.3x10^{-5} mol, 1 eq.) was added into a 25 mL flask equipped with a stirring bar. The flask was sealed with a rubber septum, degassed to remove oxygen, and subsequently 2.0 mL of degassed anisole was added into the flask through a degassed syringe. To the stirring solution 4-vinylbenzyl methoxynona(ethylene glycol)ether **1** (1.9862 g, 3.6x10^{-3} mol, 50 eq.) was added, and the solution was purged for 10 min to remove any residual oxygen. The flask was placed into an oil bath preheated at 120 °C. The kinetics of reaction was monitored at regular intervals by ^{1}H NMR using an argon-exchanged syringe for withdrawing samples from the reaction media. After polymerization proceeded for 360 min, the flask was removed from the oil bath and the mixture was allowed to cool naturally to room temperature. The anisole was removed by rotary evaporation and the remaining polymer was purified by dialysis against water using Spectra/Por® Dialysis membrane with a molecular weight cut-off of 6-8000 g·mol^{-1}. The final monomer conversion of **1** was 0.92 as determined by ^{1}H NMR. The purified polymer was characterized by SEC (THF): M_n = 19500 g·mol^{-1}, M_w/M_n = 1.92 (high molecular weight shoulder peak was observed).

IV.3. Example of nitroxide-mediated homopolymerization of 2
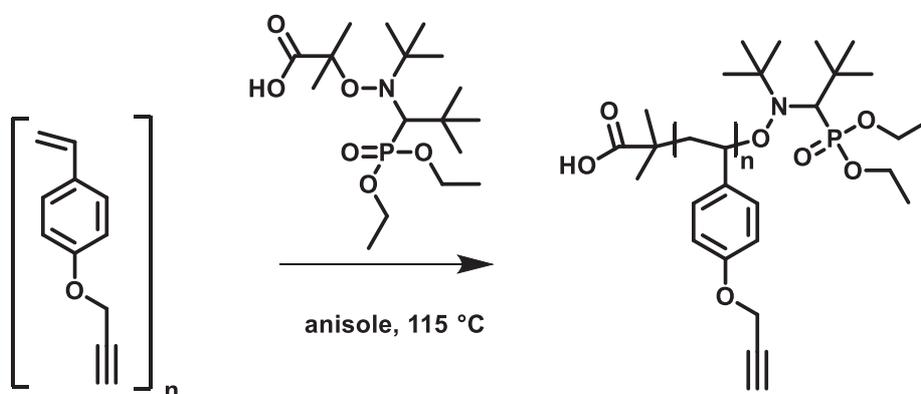
Homopolymers of 4-propargyloxystyrene (**2**) were synthesized by NMP either in bulk or using anisole as a solvent. The procedure illustrated here corresponds to Entry 3 in **Table 8**. BlocBuilder® MA (0.0248 g, 6.32x10^{-5} mol, 1 eq.) was added into a 10 mL flask equipped with a stirring bar. The flask was sealed with a rubber septum, degassed to remove oxygen, and subsequently 0.5 mL of a degassed anisole was added into the flask through a degassed syringe. **2** (1.0 g, 6.32x10^{-3} mol, 100 eq.) was then added and the reaction mixture was purged with dry argon for additional 10 min to remove any residual oxygen. The flask was placed into an oil bath preheated at 115 °C. The kinetics of reaction was monitored by

^{1}H NMR. After the polymerization proceeded for 180 min, the flask was removed from the oil bath and the mixture was allowed to cool naturally to room temperature. The remaining anisole was removed by rotary evaporation and the remaining polymer was purified by precipitation in cold methanol. The final polymer was washed with MeOH and dried under vacuum at room temperature. The purified polymer was characterized by ^{1}H NMR and SEC.

White solid, 0.2 g (46 %). ^{1}H NMR (400 MHz, CDCl$_3$, δ in ppm): 0.57-2.27 (bm, -CH- and -CH_2- units of styrenic backbone + units of BlocBuilder® MA), 2.52 (t, -C-C≡CH), 4.62 (bs, -O-CH_2-), 6.15-7.03 (bm, -Ar-H of **2**). SEC (THF): M_n = 7100 g·mol^{-1}, M_w /M_n = 1.82.

➢ Semi-logarithmic of monomer conversion versus time and SEC chromatogram of NMP homopolymerization of **2** performed at different conditions, a) in bulk and b) in anisole for Entry 2 and Entry 3 of **Table 8** respectively.
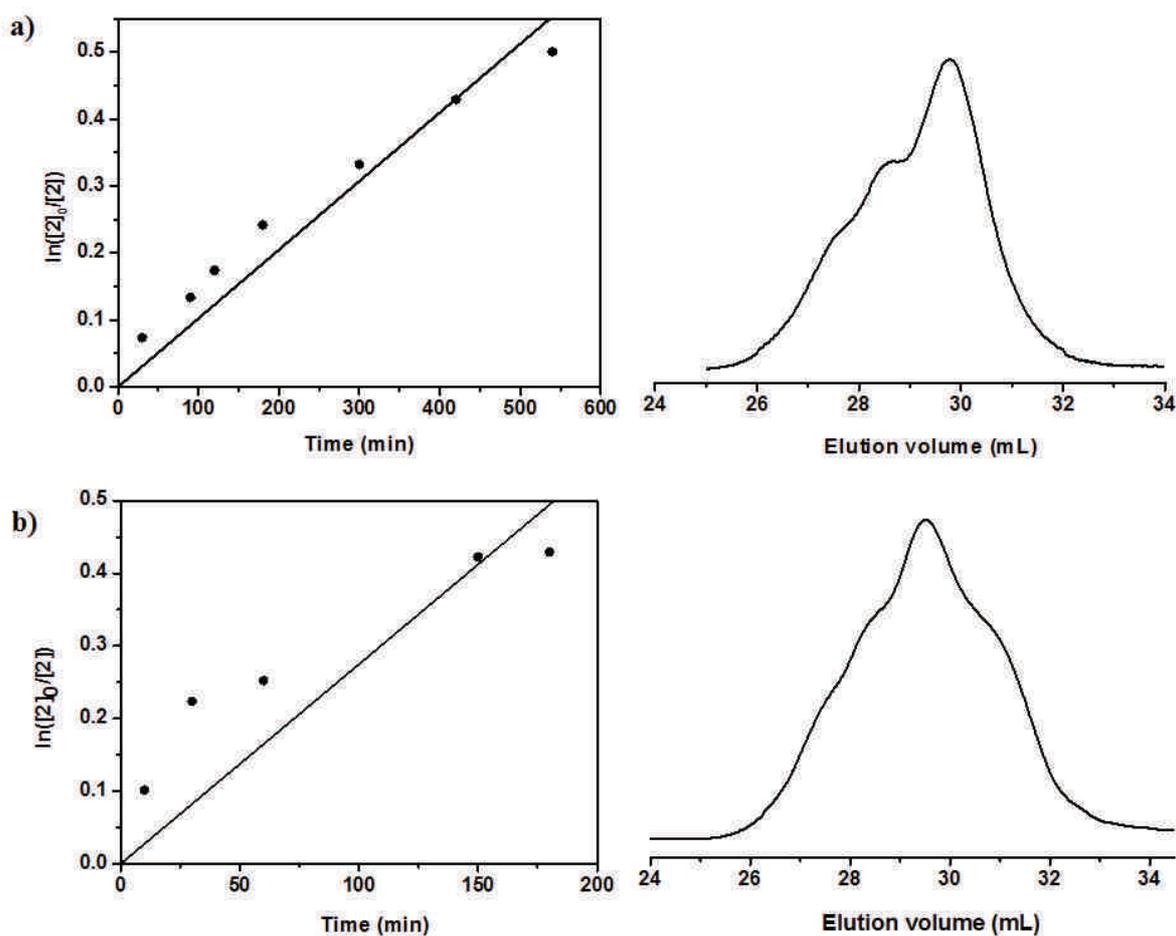
IV.4. Example of nitroxide-mediated homopolymerization of 3
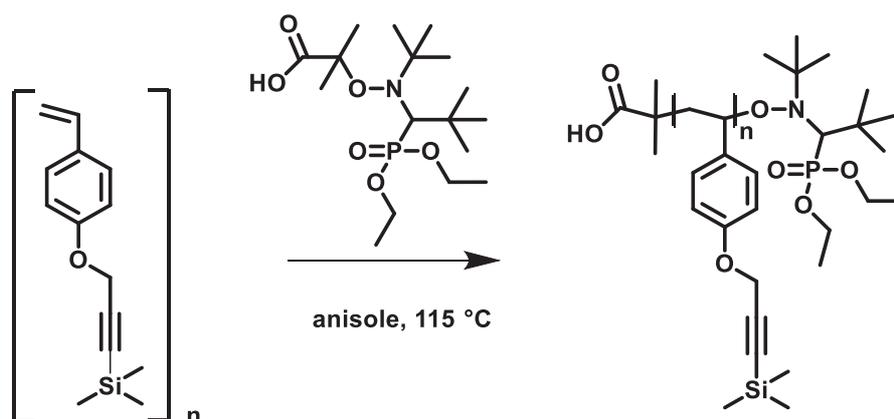
Homopolymers of 4-(trimethylsilyl)propargyloxystyrene (**3**) were synthesized by NMP. A typical procedure is described below. This particular example corresponds to Entry 3 in **Table 9**. BlocBuilder® MA (0.049 g, 0.125 mmol, 1 eq.) was added into a 10 mL flask equipped with a stirring bar. The flask was sealed with a rubber septum and subsequently degassed to remove oxygen. 1.2 mL of degassed anisole was added into the flask through a degassed syringe. Approximately 0.6 mL of **3** (0.58 g, 2.52 mmol, 20 eq.) was then added to this solution and purged with argon for 10 min to remove residual oxygen. The flask was placed into an oil bath which was preheated at 115 °C. During the polymerization, samples were taken via a degassed syringe at regular intervals for ^{1}H NMR spectroscopy and SEC analysis. After 312 min of reaction, the remaining anisole was removed by rotary evaporation and the obtained polymer was dissolved in THF, and consequently precipitated in cold methanol. The precipitate was collected by filtration, washed with MeOH and dried under vacuum at room temperature. The purified polymer was characterized by ^{1}H NMR and SEC.
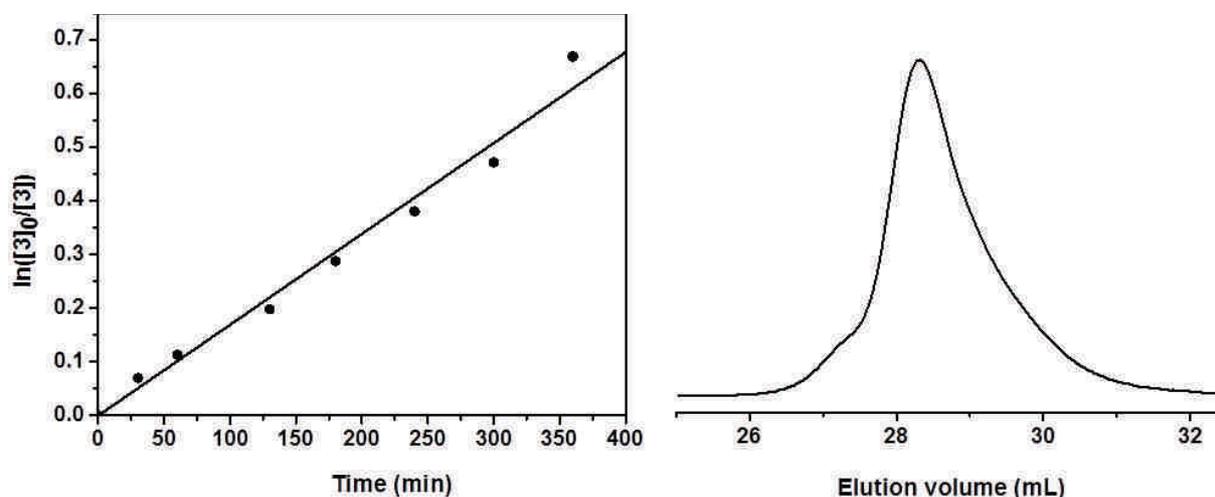
H1: White powder, 0.320 g (76 %). ^{1}H NMR (400 MHz, CDCl$_3$, δ in ppm): 0.21 (bs, -Si-(CH_3)$_3$), 0.61-2.09 (bm, -CH- and -CH_2- units of styrenic backbone + units of BlocBuilder® MA), 4.62 (bs, -O-CH_2-), 6.21-7.09 (bm, -Ar-H of **3**). SEC (THF): M_n = 11700 g·mol^{-1}, M_w/M_n = 1.29.
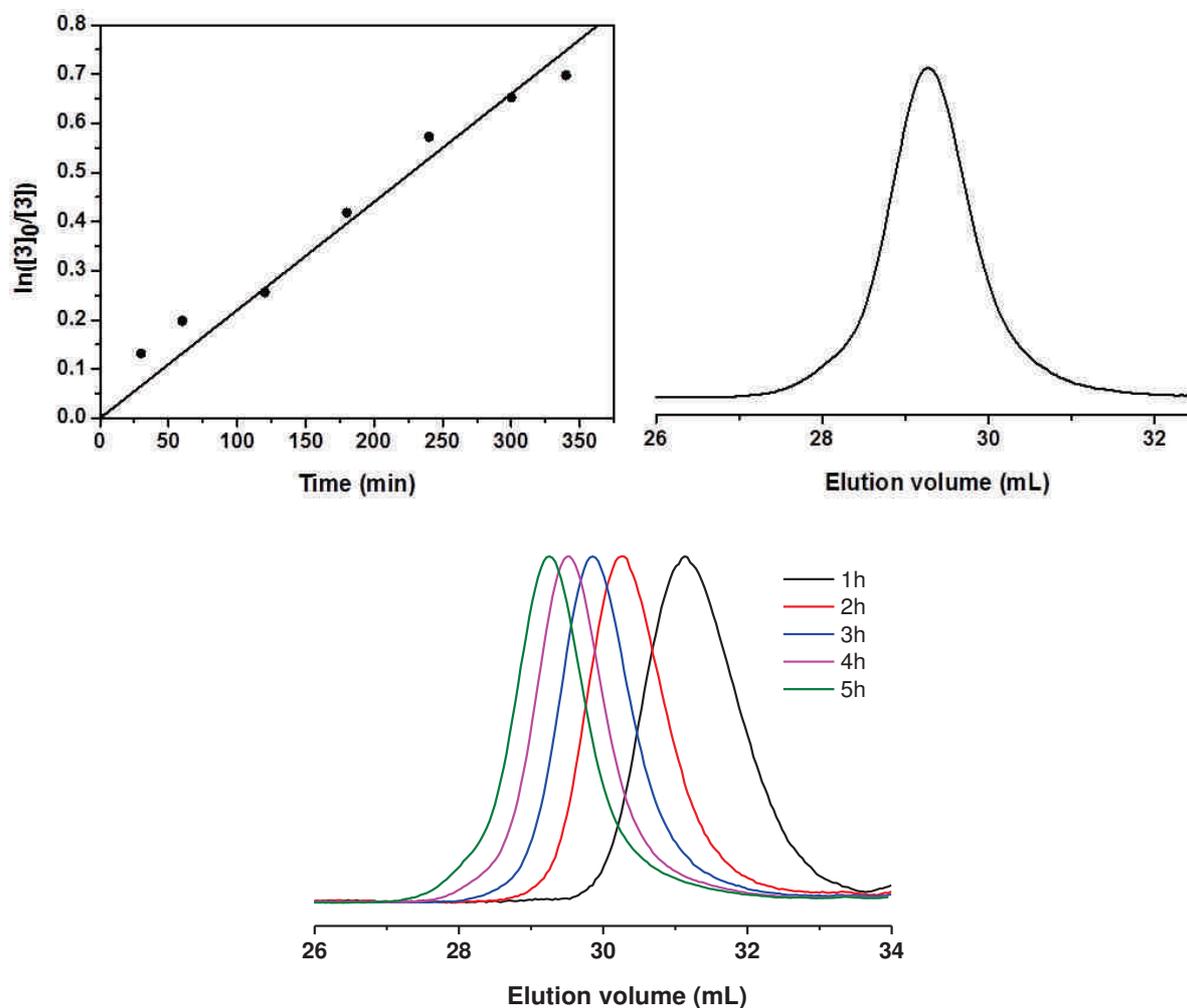
H2: White powder, 0.270 g (90 %). ^{1}H NMR (400 MHz, CDCl$_3$, δ in ppm): 0.18 (bs, -Si-(CH_3)$_3$), 0.56-2.20 (bm, -CH- and -CH_2- units of styrenic backbone + units of BlocBuilder® MA), 4.59 (bs, -O-CH_2-), 6.11-6.88 (bm, -Ar-H of **3**). SEC (THF): M_n = 9400 g·mol^{-1}, M_w/M_n = 1.14.
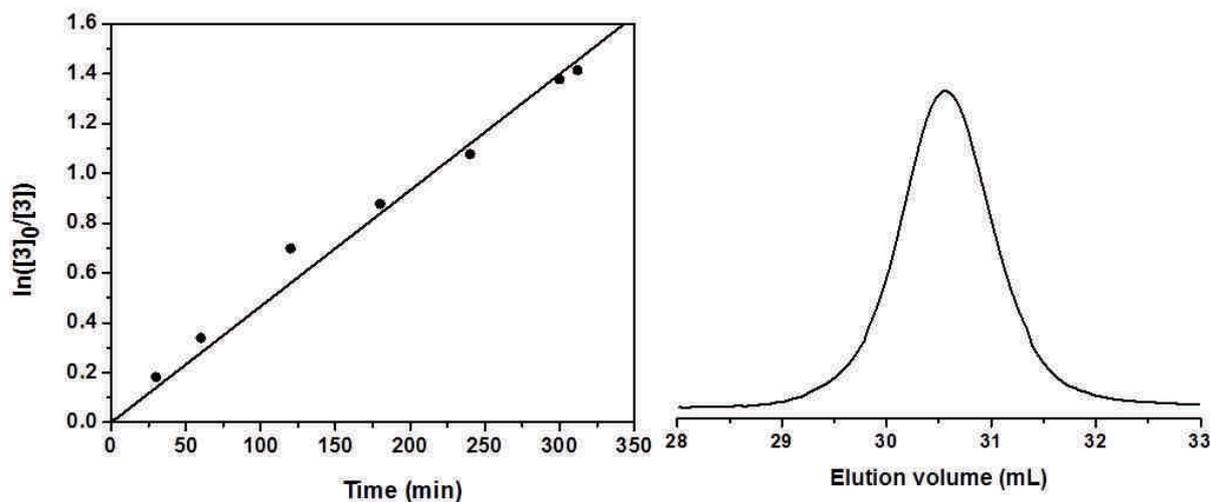
H3: White powder, 0.140 g (32 %). ^{1}H NMR (400 MHz, CDCl$_3$, δ in ppm): 0.19 (bs, -Si-(CH$_3$)$_3$), 0.54-1.98 (bm, -CH- and -CH_2- units of styrenic backbone + units of BlocBuilder® MA), 4.59 (bs, -O-CH_2-), 6.20-6.87 (bm, -Ar-H of **3**). SEC (THF): M_n = 5000 g·mol^{-1}, M_w/M_n = 1.14.

IV.5. Example of sequence-controlled NMP of 3 and different *N*-substituted maleimides
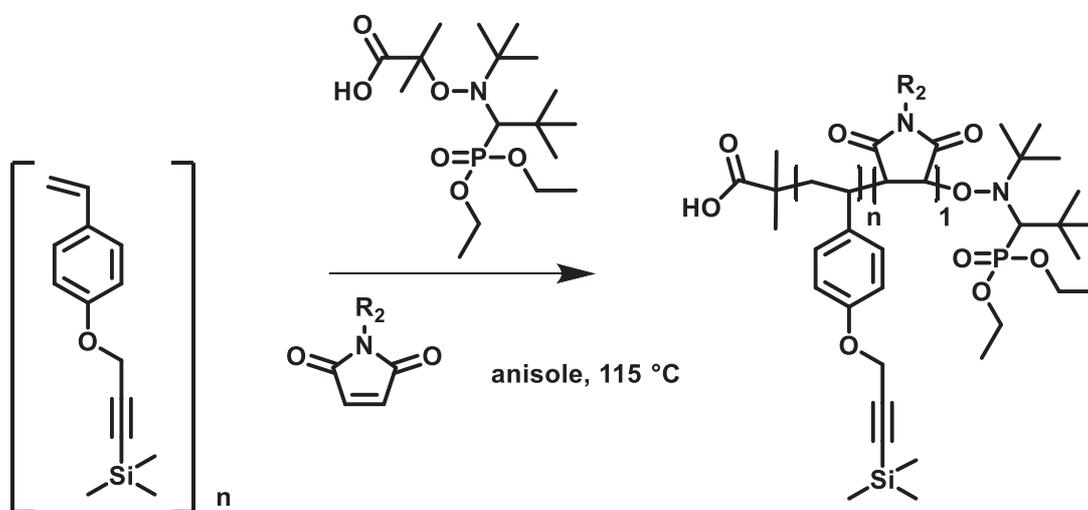
Copolymers of **3** with functional *N*-substituted maleimides **4**, **5**, **6**, **7** and **8** were synthesized by NMP in anisole. A typical procedure is described below. This particular example corresponds to Entry 1 in **Table 10**. BlocBuilder® MA (0.213 g, 0.542 mmol, 1 eq.) was added into a 10 mL flask equipped with a stirring bar. The flask was capped by a rubber septum, purged with dry argon for 10 min and consequently 4.8 mL of degassed anisole was added using a degassed syringe. Then 2.5 mL of **3** (2.5 g, 10.8 mmol, 20 eq.) was added to the reaction flask under argon atmosphere. The mixture was immersed in an oil bath thermostated

at 115 °C. After 120 min of reaction a degassed solution of **4** (0.161 g, 0.542 mmol, 1 eq.) in 0.2 mL of anisole was added into the reaction through a degassed syringe (44% conversion of **3** at this stage). Samples were taken periodically via a degassed syringe for NMR and SEC analysis in order to monitor the incorporation of **4** in the growing copolymer chains. After 315 min, the reaction was stopped and cooled down. The remaining anisole was removed by rotary evaporation and the obtained polymer was dissolved in THF, and consequently precipitated in ice-cold methanol. The precipitate was collected by filtration and dried under vacuum at room temperature overnight. The dried polymer was characterized by ^{1}H NMR and SEC. Similar copolymerization procedures were performed for maleimides **6** and **8** with **3**. On the other hand, the incorporation of **5** and **7** in the growing polymer chain of **3** was at the beginning for maleimide **5**, and after 180 min of reaction (52 % conversion of **3** at this stage) for maleimide **7**, respectively. The final copolymers **C2**, **C3**, **C4** and **C5** in **Table 10** were characterized by ^{1}H NMR and SEC.
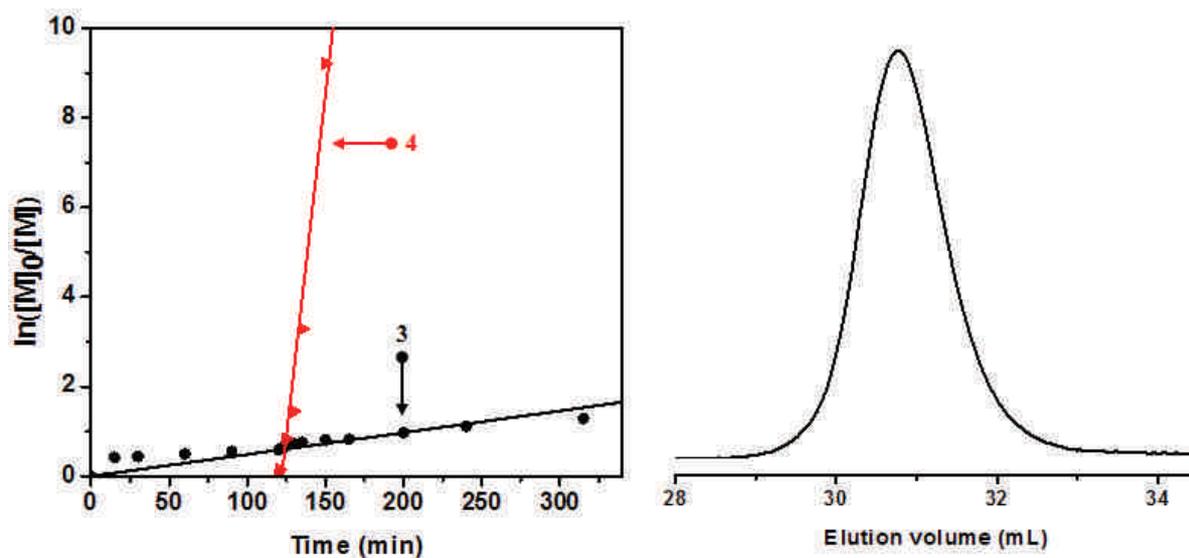
C1: White yellow powder, 0.9 g (41 %). ^{1}H NMR (400 MHz, CDCl$_3$, δ in ppm): 0.18 (bs, -Si-(CH$_3$)$_3$), 0.55-2.24 (bm, -C*H*- and -C*H*$_2$- units of styrenic backbone + -C*H*- units of maleimide backbone + units of BlocBuilder® MA), 4.61 (bs, -O-C*H*$_2$-), 5.99-7.11 (bm, -Ar-*H* of **3**), 7.62-8.36 (bm, -Ar-*H* of **4**). SEC (THF): M_n = 4000 g·mol^{-1}, M_w / M_n = 1.14.
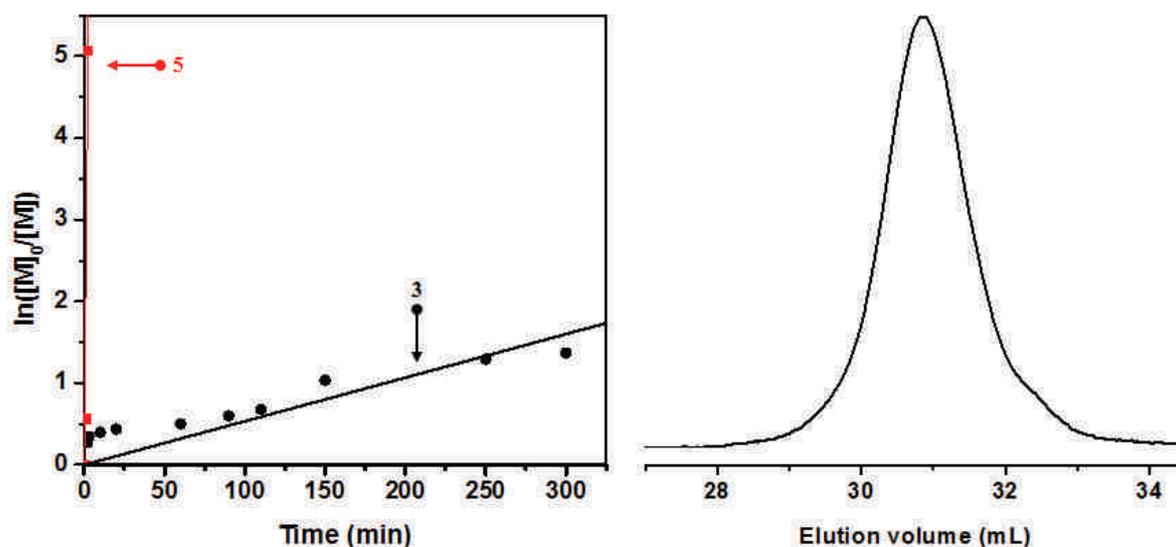
C2: White powder, 1.0 g (47 %). ^{1}H NMR (400 MHz, CDCl$_3$, δ in ppm): 0.19 (bs, -Si-(CH$_3$)$_3$), 0.52-1.89 (bm, -C*H*- and -C*H*$_2$- units of styrenic backbone + -C*H*- units of maleimide backbone + units of BlocBuilder® MA), 4.60 (bs, -OC*H*$_2$-), 6.14-7.02 (bm, -Ar-*H* of **3**), 7.38-7.56 (bm, -Ar-*H* of **5**) 7.74-8.06 (bm, -Ar-*H* of **5**). SEC (THF): M_n = 3900 g·mol^{-1}, M_w/M_n = 1.20.
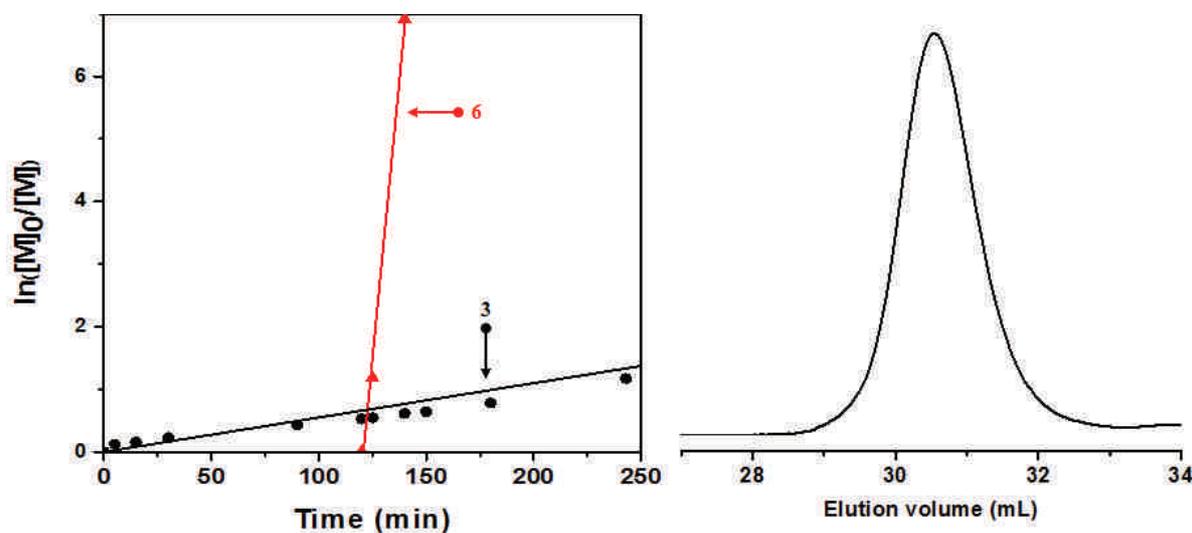
C3: White yellow powder, 1.26 g (48 %). ^{1}H NMR (400 MHz, CDCl$_3$, δ in ppm): 0.21 (bs, -Si-(CH$_3$)$_3$), 0.53-2.29 (bm, -C*H*- and -C*H*$_2$- units of styrenic backbone + -C*H*- units of maleimide backbone + units of BlocBuilder® MA), 4.59 (bs, -O-C*H*$_2$-), 4.89-5.30 (bm, -C*H*$_2$- of **6**) 6.09-6.95 (bm, -Ar-*H* of **3**), 7.78-8.24 (bm, -Ar-*H* of **6**). SEC (THF): M_n = 4800 g·mol^{-1}, M_w/M_n = 1.14.

C4: White powder, 1.0 g (37 %). ^{1}H NMR (400 MHz, CDCl$_3$, δ in ppm): 0.18 (bs, -Si-(CH_3)$_3$), 0.55-2.39 (bm, -CH- and -CH_2- units of styrenic backbone + -CH- units of maleimide backbone + units of BlocBuilder® MA), 4.60 (bs, -O-CH_2-), 6.12-7.00 (bm, -Ar-H of **3**), 8.05-8.36 (bm, -Ar-H of **7**). ^{19}F NMR (400 MHz, CDCl$_3$ δ in ppm): -152.42, -157.85, -162.13. SEC (THF): M_n = 5000 g·mol^{-1}, M_w/M_n = 1.13. (The kinetic was shown in **Figure 54**)
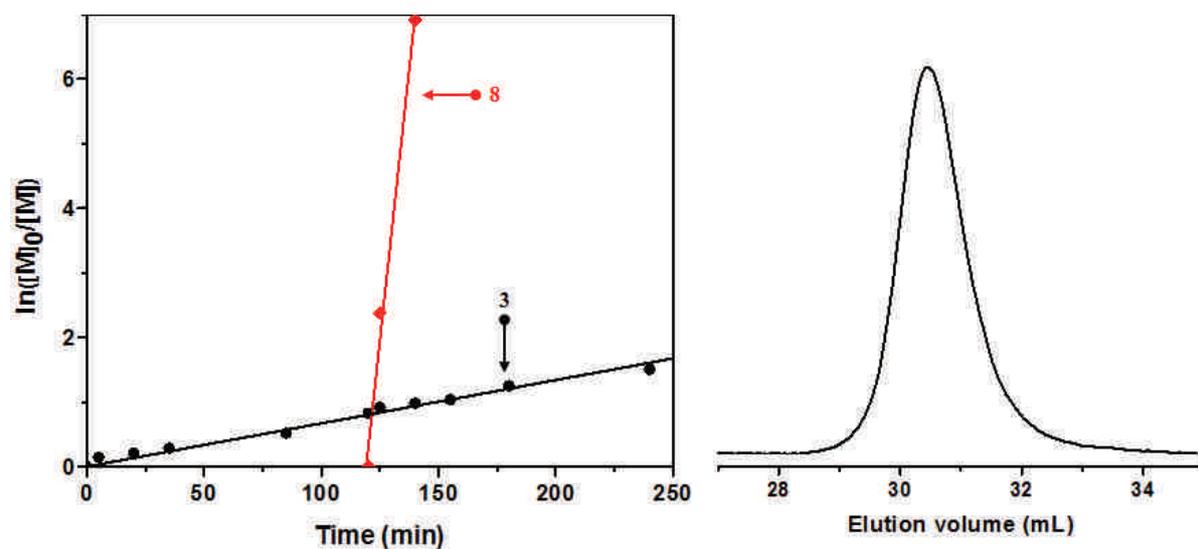
C5: White powder, 0.9 g (35 %). ^{1}H NMR (400 MHz, CDCl$_3$, δ in ppm): 0.17 (bs, -Si-(CH_3)$_3$), 0.99 (bs, -CH_2-C≡C-Si-(iPr)$_3$), 0.55-2.39 (bm, -CH- and -CH_2- units of styrenic backbone + -CH- units of maleimide backbone + units of BlocBuilder® MA), 3.94 (bs, -CH_2-C≡C-Si-(iPr)$_3$), 4.60 (bs, -O-CH_2-), 6.05-6.99 (bm, -Ar-H of **3**). SEC (THF): M_n = 4700 g·mol^{-1}, M_w/M_n = 1.18.

IV.6. Post-polymerization modification of activated ester with PFP- group in polymer C4
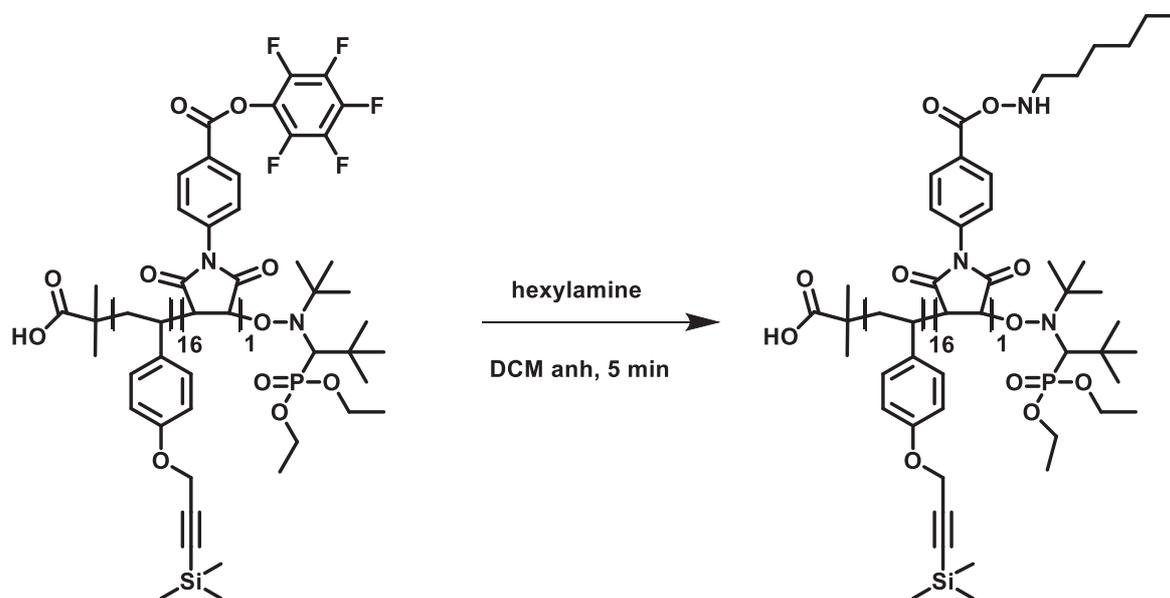
This modification corresponds to copolymer containing PFP moiety (Entry 4, in **Table 10**). 0.9 g (0.18 mmol, 1 eq.) of **C4** was dissolved in 6 mL of anhydrous dichloromethane, and the solution was purged for 10 min with dry argon. Then 0.264 mL (1.8 mmol, 10 eq. per 1 unit of PFP functionality) of hexylamine was added. The mixture was stirred under an argon atmosphere at room temperature for an additional 5 min. Afterwards, dichloromethane was removed under vacuum. The residual reaction mixture was then dissolved in small quantities of THF and precipitated in cold methanol. The dried copolymer was collected and characterized by ^{1}H NMR, ^{19}F NMR and SEC.
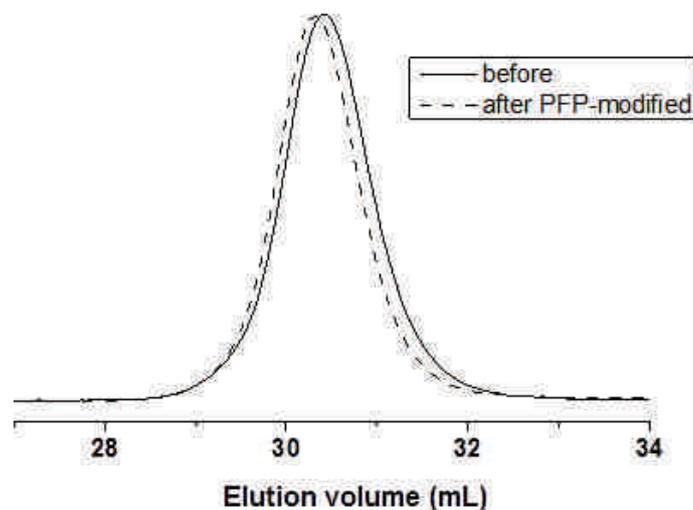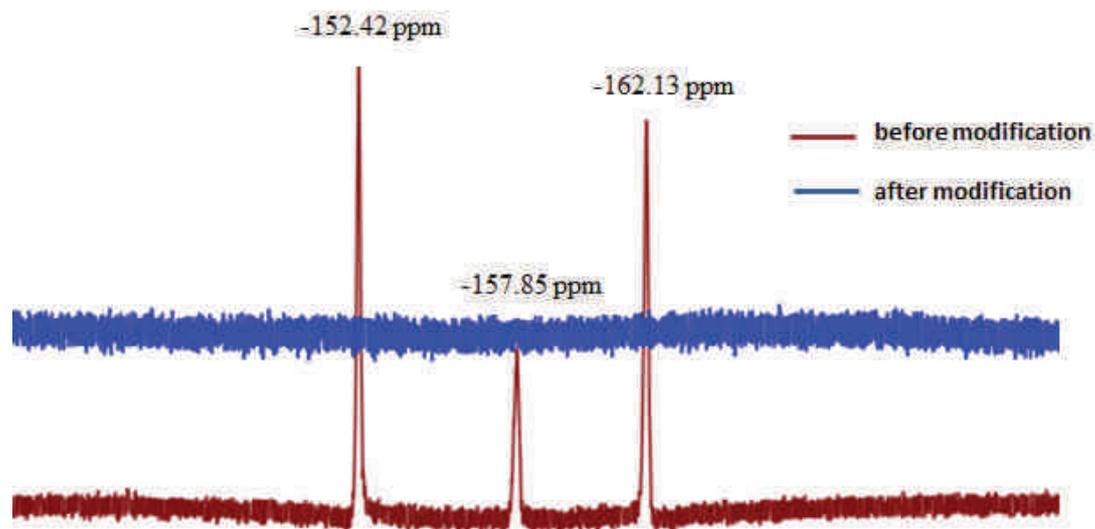
C4 PFP-modified: White powder, 0.520 g (62 %). ^{1}H NMR (400 MHz, CDCl$_3$, δ in ppm): 0.18 (bs, -Si-(CH_3)$_3$), 0.40-2.25 (bm, -CH- and -CH_2- units of styrenic backbone + -CH- units of maleimide backbone + units of BlocBuilder® MA + - CO-NH-(CH_2)$_5$-CH_3 of **phenylhexylamide**), 3.44 (t, -CO-NH-CH_2- of phenylhexylamide), 4.61 (bs, -O-CH_2-), 5.97-7.16 (bm, -Ar-H of **3**), 7.58-7.94 (bm, Ar-H of **phenylhexylamide**). No peak observed in ^{19}F NMR spectrum. SEC (THF): M_n = 4700 g·mol^{-1}, M_w/M_n = 1.2.

IV.7. General procedure for deprotection of TMS in copolymers
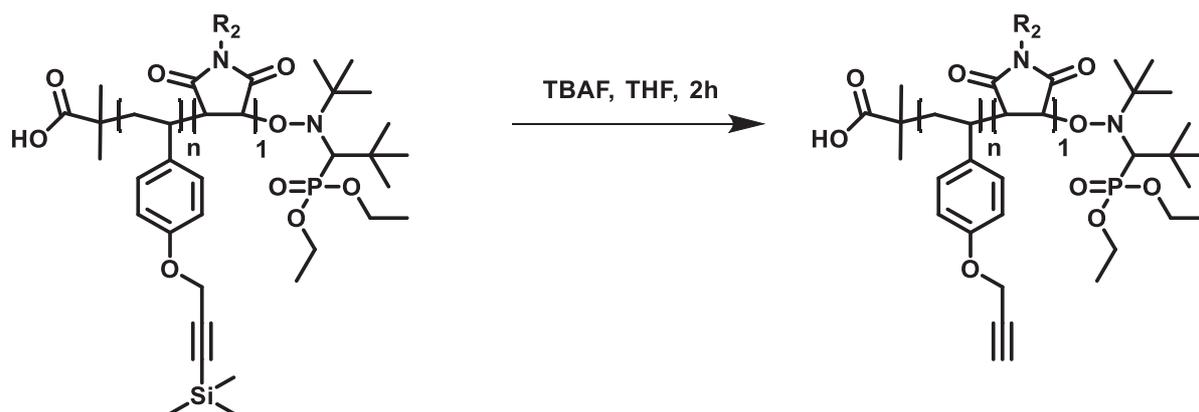
TMS protecting group in polymers **C1**, **C2**, **C3** and **C4** were removed by employing the representative procedure below. Polymer **C1** (0.350 g, M_n = 4050 g·mol^{-1}, 8.64x10^{-5} mol, Entry 1 in **Table 10**) was dissolved in 5 mL of THF in a 10 mL round bottom flask. Then, 2.47 mL (8.536x10^{-3} mol, 100 eq. polymer) of TBAF (1M in THF) was added dropwise. The

reaction was stirred for 2 h under argon at room temperature. Once the reaction was finished, the excess of THF (3/4 of the initial volume) was evaporated under reduced pressure, and consequently the polymer was then precipitated into an excess of cold methanol. Polymer was collected as a powder and dried under vacuum at room temperature. Dry polymers were characterized by ^{1}H NMR and SEC.
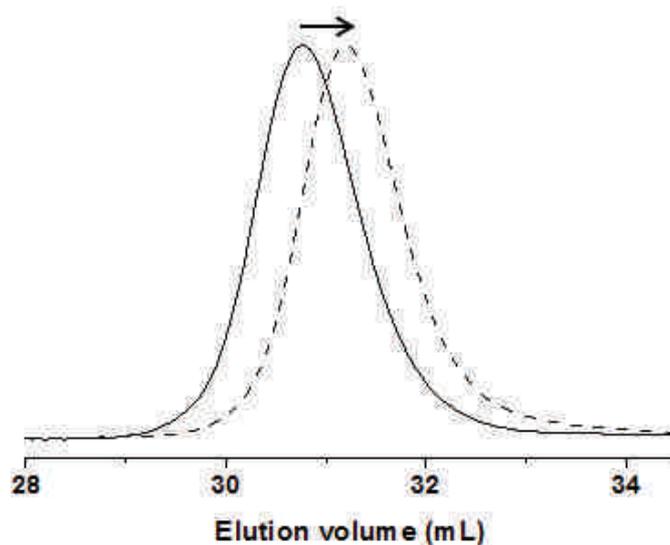
C1′: White powder, 0.100 g (30 %). ^{1}H NMR (400 MHz, CDCl$_3$, δ in ppm): 0.42-2.24 (bm, -CH- and -CH_2- units of styrenic backbone + -CH- units of maleimide backbone + units of BlocBuilder® MA), 2.52 (bs, - C≡CH), 4.61 (bs, -O-CH_2-), 6.09-7.21 (bm, -Ar-H of **3**), 7.82-8.33 (bm, -Ar-H of **4**). SEC (THF): M_n = 3000 g·mol^{-1}, M_w/M_n = 1.16.
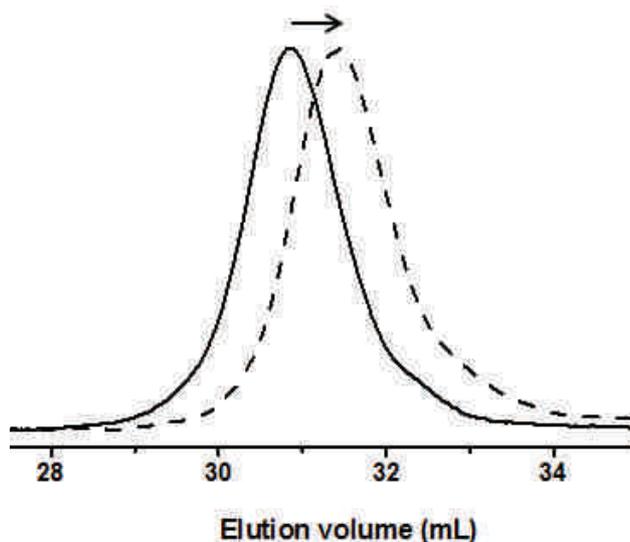
C2′: Pale yellow powder, 0.050 g (40 %). ^{1}H NMR (400 MHz, CDCl$_3$, δ in ppm): 0.47-2.30 (bm, -CH- and -CH_2- units of styrenic backbone + -CH- units of maleimide backbone + units

of BlocBuilder® MA), 2.52 (t, - C≡CH), 4.64 (bs, -O-CH_2-), 6.16-7.16 (bm, -Ar-H of **3**), 7.49 and 7.89 (bs, -Ar-H of **5**). SEC (THF): M_n = 2400 g·mol^{-1}, M_w/M_n = 1.32.
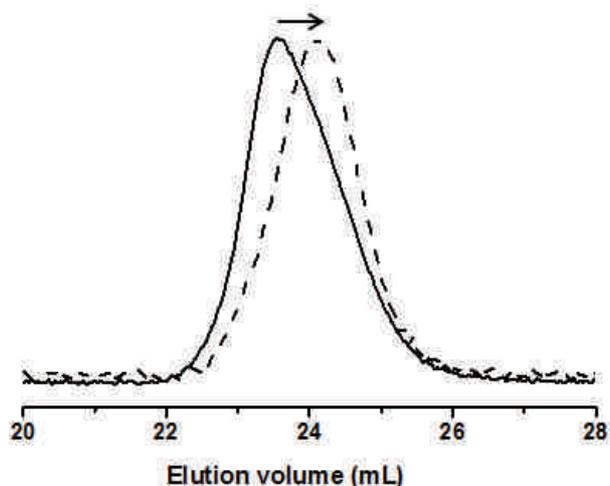
C3′: White powder, 0.095 g (39 %). ^{1}H NMR (400 MHz, CDCl$_3$, δ in ppm): 0.53-2.25 (bm, -CH- and -CH_2- units of styrenic backbone + -CH- units of maleimide backbone + units of BlocBuilder® MA), 2.52 (t, - C≡CH), 4.63 (bs, -O-CH_2-), 4.89-5.27 (bs, -CH_2- of **6**) 5.84-7.09 (bm, -Ar-H of **3**), 7.81-8.29 (bs, -Ar-H of **6**). SEC (THF): M_n = 4200 g·mol^{-1}, M_w/M_n = 1.10.
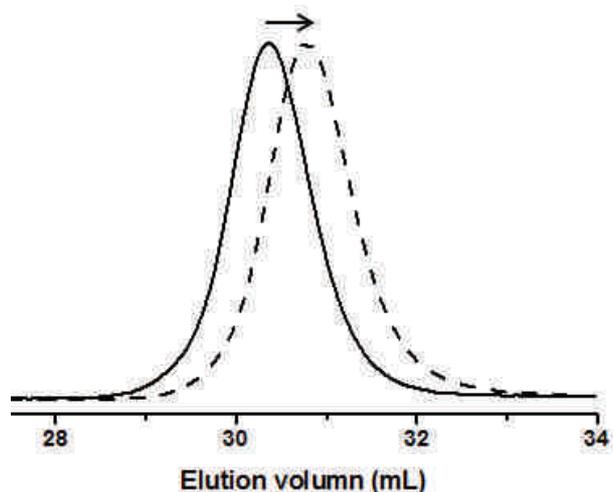
C4′: White powder, 0.160 g (40 %). ^{1}H NMR (400 MHz, CDCl$_3$, δ in ppm): 0.30-2.29 (bm, -CH- and -CH_2- units of styrenic backbone + -CH- units of maleimide backbone + units of BlocBuilder® MA + -CO-NH-(CH_2)$_5$-CH_3 of **phenylhexylamide**), 2.53 (t, - C≡CH), 3.42 (t, -CO-NH-CH_2- of **phenylhexylamide**), 4.62 (bs, -O-CH_2-), 5.76-7.21 (bm, -Ar-H of **3**), 7.43-7.94 (bm, -Ar-H of **phenylhexylamide**). SEC (THF): M_n = 3700 g·mol^{-1}, M_w/M_n = 1.16.

IV.8. Selective deprotection procedure for copolymer C5 [16]
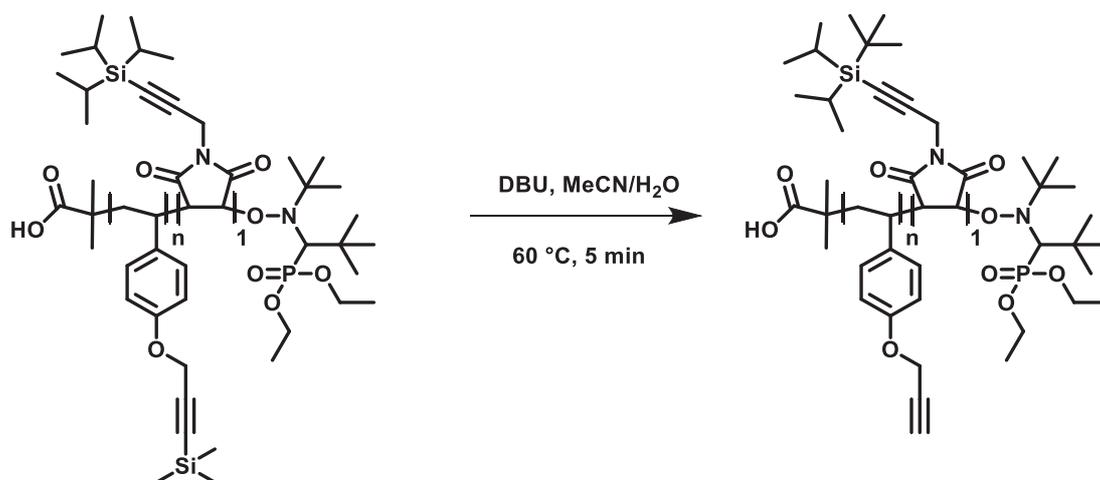
To a magnetically stirred solution of polymer **C5** (0.125 g, $M_n = 4700$ g·mol^{-1}, 0.0267 mmol, Entry 5 in **Table 10**) in 1.9 mL MeCN and 0.1 mL H$_2$O mL at 60 °C was added DBU (0.2 mL, 1.34 mmol, 50 eq.). The stirring was continued for an additional 5 min. After completion of the reaction (confirmed by ^{1}H NMR analysis), the resulting reaction mixture was concentrated under reduced pressure and purified by precipitatation in cold water. Polymer was collected as a white powder and dried under vacuum at room temperature.
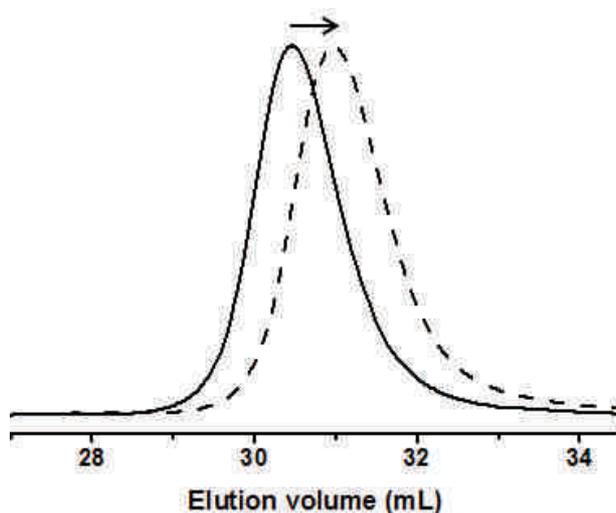
C5′: White powder, 0.080 g (82 %). ^{1}H NMR (400 MHz, CDCl$_3$, δ in ppm): 0.99 (bs, -CH_2-C≡C-Si-(*i*Pr)$_3$), 0.37-2.29 (bm, -CH- and -CH_2- units of styrenic backbone + -CH- units of maleimide backbone + units of BlocBuilder® MA), 2.52 (t, - C≡CH), 3.95 (bs, -CH_2-C≡C-Si-(*i*Pr)$_3$), 4.63 (bs, -O-CH_2-), 6.01-7.15 (bm, -Ar-H of **3**). SEC (THF): $M_n = 3500$ g·mol^{-1}, $M_w/M_n = 1.18$.

IV.9. General procedure for CuAAC PEGylation [17]
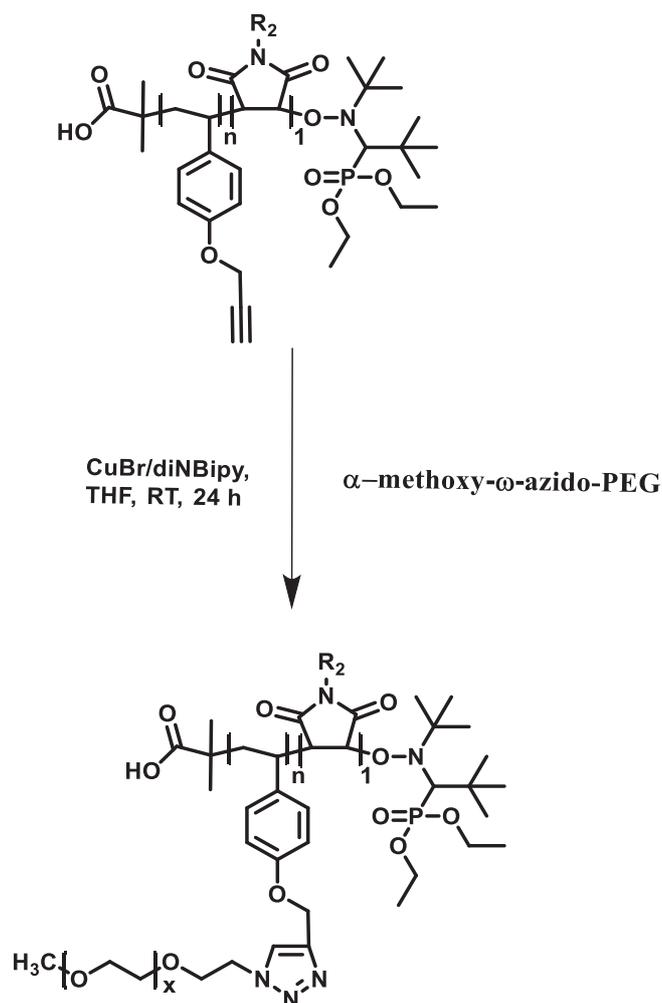
Azide end-functionalized PEG was grafted onto deprotected polymers using Cu(I)-catalyzed alkyne-azide Huisgen's 1,3 dipolar cycloaddition (CuAAC) with α-methoxy-ω-azido-PEG. The general procedure was described below. Deprotected polymer **C1′**, **Table 11** (0.0172 g, M_n = 3000 g·mol^{-1}, 5.733x10^{-6} mol, 1 eq.) and α-methoxy-ω-azido-PEG (0.372 g, M_n = 2000 g·mol^{-1}, 1.58x10^{-4} mol, 2 eq. per alkyne functionality) were added in a 10 mL round bottom flask and were degassed for 30 min with argon. A solution of CuBr (0.001 g, 6.15x10^{-6} mol, 1 eq.) and 4,4'-dinonyl-2,2'-bipyridine (dNBipy) (0.0052 g, 12.3x10^{-6} mol, 2 eq.) in 2 mL THF was added. The reaction was allowed to proceed for 24 h at room temperature. After evaporating the solvents, the polymer was dissolved in small quantities of THF and precipitated in cold diethyl ether. The excess of unreacted PEG was removed from the polymer by dialysis against water using Spectra/Por® Dialysis membrane with a molecular weight cut-off of 6-8000 g.mol^{-1}. The purified polymer was then characterized by ^{1}H NMR and SEC.
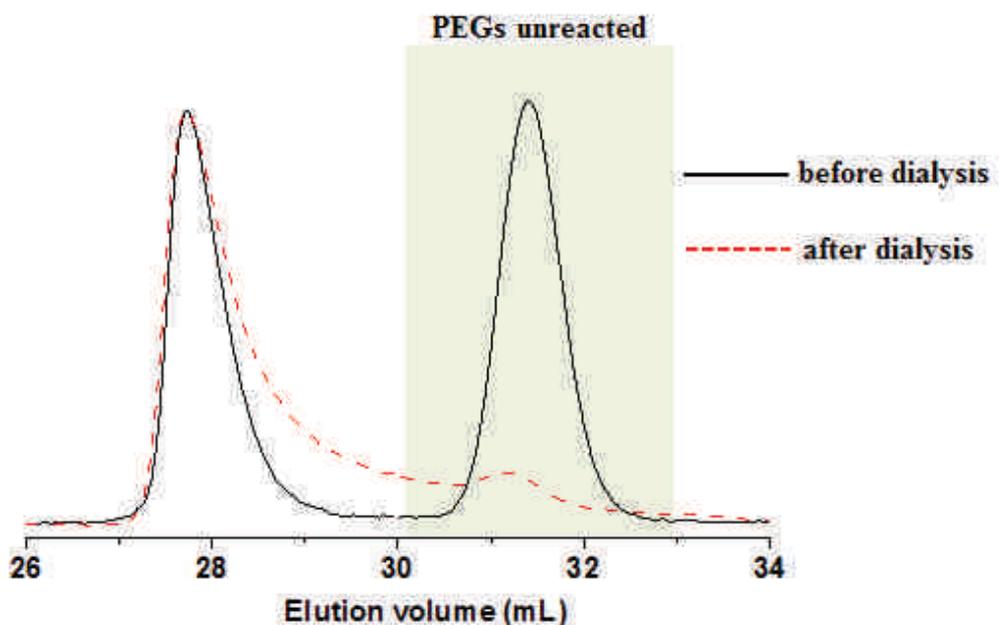
C1'': White powder, 0.260 g. ^{1}H NMR (400 MHz, CDCl$_3$, δ in ppm): 0.49-1.95 (bm, -CH- and -CH_2- units of styrenic backbone + -CH- units of maleimide backbone + units of BlocBuilder® MA), 3.66 (b, PEG backbone), 4.52 (bs, -CH_2-PEG), 5.09 (bs, -O-CH_2-), 6.14-6.96 (bm, -Ar-H of **3**), 7.81 (bs, triazole), 7.91-8.32 (bm, -Ar-H of **4**). Before dialysis: SEC (THF): M_n = 21000 g·mol^{-1}, M_w/M_n = 1.04. (12.2 % residual unreacted α-methoxy-ω-azido-PEG remained after 2 weeks of dialysis).
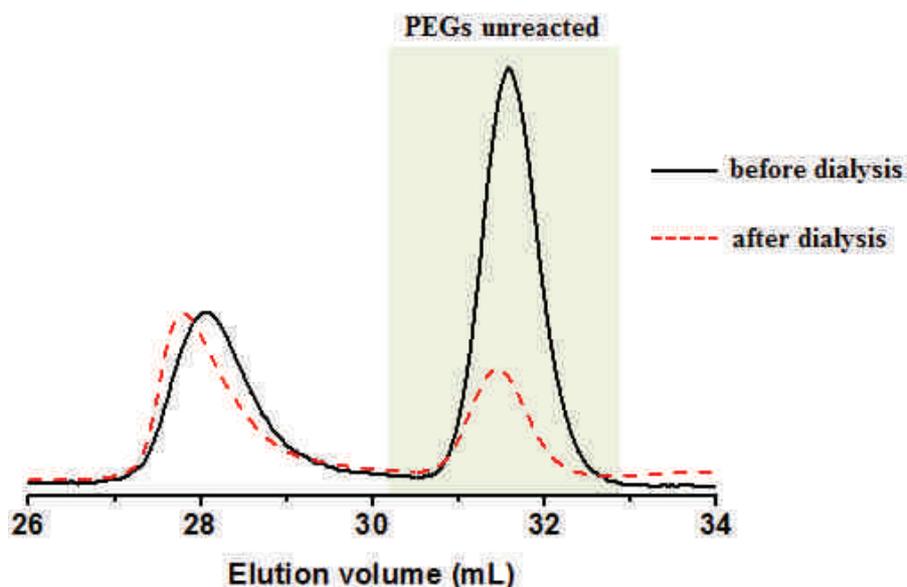
C2'': Brown powder, 0.230 g. ^{1}H NMR (400 MHz, CDCl$_3$, δ in ppm): 0.53-1.97 (bm, -CH- and -CH_2- units of styrenic backbone + -CH- units of maleimide backbone + units of BlocBuilder® MA), 3.64 (b, PEG backbone), 4.52 (bs, -CH_2-PEG), 5.06 (bs, -O-CH_2-), 6.15-

6.93 (bm, -Ar-*H* of **3**), 7.84 (bs, triazole), 7.51 and 7.72 (bs, -Ar-*H* of **5**). Before dialysis: SEC (THF): $M_n =$ 18000 g·mol^{-1}, $M_w/M_n =$ 1.13. (27 % residual unreacted α-methoxy-ω-azido-PEG remained after 5 days of dialysis).
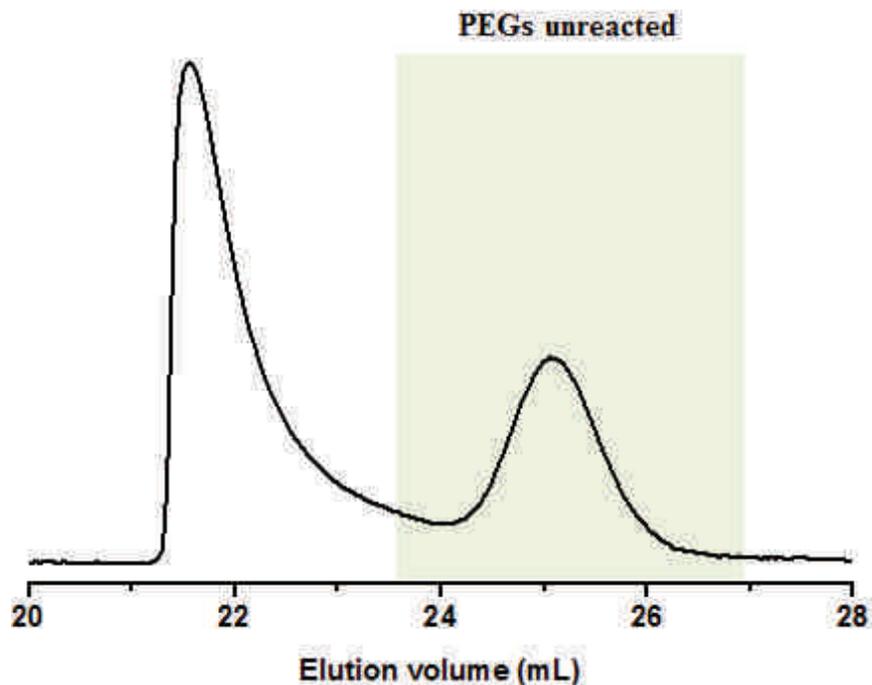
C3'': Brown powder, 0.255 g. ^{1}H NMR (400 MHz, CDCl$_3$, δ in ppm): 0.47-2.26 (bm, -C*H*- and -C*H*$_2$- units of styrenic backbone + -C*H*- units of maleimide backbone + units of BlocBuilder® MA), 3.63 (b, PEG backbone), 4.50 (bs, -C*H*$_2$-PEG), 5.05 (bs, -O-C*H*$_2$-), 6.02-6.97 (bm, -Ar-*H* of **3**), 7.82 (bs, triazole), 7.64 -8.24 (bm, -Ar-*H* of **6**). Before dialysis: SEC (THF): $M_n =$ 12200 g·mol^1, $M_w/M_n =$ 1.12.
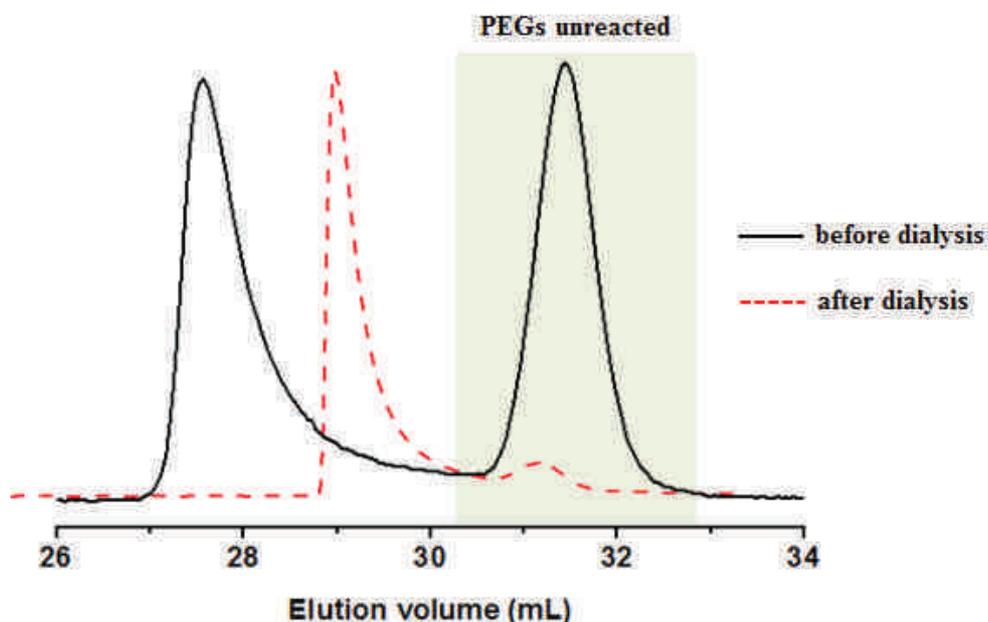
C4'': Brown powder, 0.230 g. ^{1}H NMR (400 MHz, CDCl$_3$, δ in ppm): 0.43-2.16 (bm, -C*H*- and -C*H*$_2$- units of styrenic backbone + -C*H*- units of maleimide backbone + units of BlocBuilder® MA), 3.63 (b, PEG backbone + -CO-NH-C*H*$_2$- of **phenylhexylamide**), 4.51 (b, -C*H*$_2$-PEG), 5.05 (bs, -O-C*H*$_2$-), 5.97-7.10 (bm, -Ar-*H* of **3**), 8.01 (bs, triazole), 7.68–8.16 (bm, -Ar-*H* of **phenylhexylamide**). Before dialysis: SEC (THF): M_n = 19200 g·mol^{-1}, M_w/M_n = 1.15. (8 % residual unreacted α-methoxy-ω-azido-PEG remained after 1 month of dialysis).
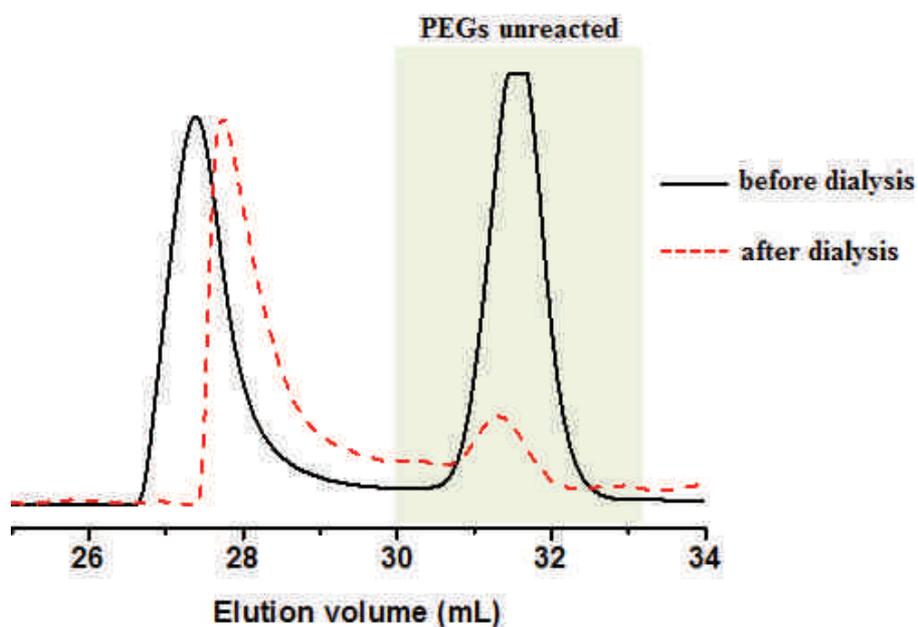
C5": Brown powder, 0.037 g. ^{1}H NMR (400 MHz, CDCl$_3$, δ in ppm): 0.97 (bs, -CH$_2$-C≡C-Si-(*iPr*)$_3$), 0.47-2.32 (bm, -C*H*- and -C*H*$_2$- units of styrenic backbone + -C*H*- units of maleimide backbone + units of BlocBuilder® MA), 3.64 (b, PEG backbone + -C*H*$_2$-C≡C-Si-(*i*Pr)$_3$), 4.52 (bs, -C*H*$_2$-PEG), 5.03 (bs, -O-C*H*$_2$-), 5.94-7.03 (bm, -Ar-*H* of **3**), 7.82 (bs, triazole). Before dialysis: SEC (THF): M_n = 15300 g·mol^{-1}, M_w/M_n = 1.15. (21 % residual unreacted α-methoxy-ω-azido-PEG remained after 10 days of dialysis).

IV.10. Solubility test

C4: copolymer
C": PEGylated copolymer
* copolymer after dialysis
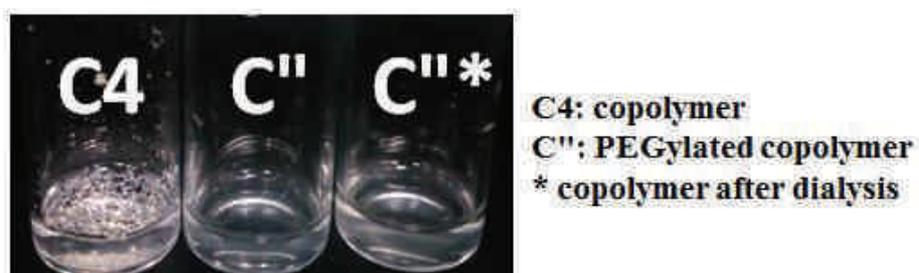
4 mg of copolymer **C4**, before and after CuAAC reaction, was dissolved in 1 mL of aqueous solution at pH 5-6.

The synthesis for Chapter V: Synthesis and characterization of sequence-controlled semi-crystalline comb copolymers: Influence of primary structure on materials properties

V.1. Synthesis of octadecylstyrene monomer (1)

The *p*-octadecylstyrene monomer was synthesized in three steps [18,19] according to the scheme below.
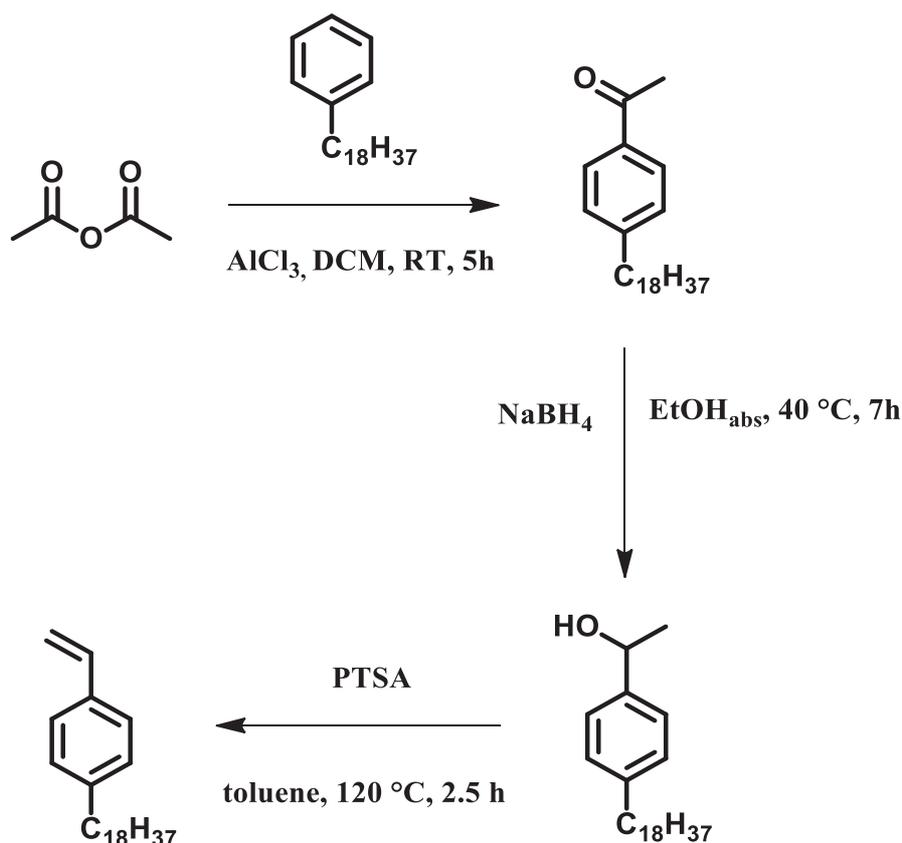
Acetic anhydride (5.435 g, 53.24 mmol, 2.2 eq.) in 6 mL of anhydrous CH_2Cl_2 was added to a stirred mixture of $AlCl_3$ (14.2 g, 106.5 mmol, 4.4 eq.) in 50 mL of CH_2Cl_2 at 0 °C over 7 min. After stirring for 30 min at 0 °C, a solution of octadecylbenzene (8 g, 24.2 mol, 1 eq.) in 8 mL of CH_2Cl_2 was added dropwise and the reaction mixture was stirred for 5 h at room temperature. Then, the reaction mixture was poured onto crushed ice (100 mL). The separated organic layer was washed sequentially with 10% aqueous HCl solution (2X80 mL), saturated aqueous Na_2CO_3 (2X80 mL), and brine (2X80 mL), dried over anhydrous Na_2SO_4, and all solvent were evaporated under reduce pressure. The crude product was purified by recrystallization from MeOH affording ***p*-octadecylacetophenone.**

White solid, 8 g (88.7 %).^{1}H NMR (400 MHz, CDCl$_3$, δ in ppm): 0.89 (t, 3H, - CH$_2$-CH_3-), 1.26 (broad band, 32H, -Ar-CH$_2$-(CH_2)$_{16}$-CH$_3$), 2.59 (s, 3H, -C=O-CH_3), 2.67 (t, 2H, -Ar-CH_2-(CH$_2$)$_{16}$-CH$_3$), 7.27 (d, 2H, -Ar-H), 7.88 (d, 2H, -Ar-H).

To a stirred mixture of 4 g (10.7 mmol, 1 eq.) of p-octadecylacetophenone in 120 mL of EtOH$_{abs}$, 0.121 g (3.21 mmol, 0.3 eq.) of NaBH$_4$ was added at 0 °C (10 aliquots). The mixture was heated at 40 °C for 3 h and the reaction was monitored by ^{1}H NMR. The solution of NaBH$_4$ (0.3 eq.) in 10 mL EtOH$_{abs}$ was added in order to complete the reaction. The mixture was stirred for an additionally 4 h. EtOH$_{abs}$ was removed using a rotary evaporator, the crude product was dissolved in 130 mL of *n*-hexane and washed sequentially with 10% aqueous HCl solution (2X60 mL). The organic layer was washed with saturated NaCl (2X60 mL), dried over anhydrous Na$_2$SO$_4$, filtered, concentrated, and crystallized in hexane. The **p-(octadecylphenyl)methylcarbinol** was filtered and dried under vacuum.

White solid, 3.2 g (80 %). ^{1}H NMR (400 MHz, CDCl$_3$, δ in ppm): 0.88 (t, 3H, -CH$_2$-CH_3-), 1.26 (broad brand, 30H, -CH$_2$-(CH_2)$_{15}$-CH$_3$), 1.49 (d, 3H, -OH-CH-CH_3), 1.60 (q, 2H, -Ar-CH$_2$-(CH_2)-(CH$_2$)$_{15}$-CH3), 2.59 (t, 2H, -Ar-CH_2-(CH$_2$)$_{16}$-CH$_3$), 4.89 (q, 1H, -OH-CH-CH$_3$), 7.17 (d, 2H, -Ar-H), 7.30 (d, 2H, -Ar-H).

To a solution of 2.7 g (7.2 mmol, 1 eq.) of (*p*-octadecylphenyl)methylcarbinol in 250 mL of toluene in a flask equipped with a Dean-Stark trap was added 0.0556 g (0.3 mmol, 4 % mol) of *p*-toluenesulfonic acid monohydrate (PTSA). The solution was heated under reflux (∼120 °C) for 2.5 h, the reaction mixture was then cooled to room temperature, washed with distilled H$_2$O (150 mL), and dried over anhydrous Na$_2$SO$_4$. Toluene was removed under reduced pressure affording **p-octadecylstyrene**. The resulting product was purified by column chromatography using silica gel as stationary phase and n-pentane/DCM: 8/2 and 7/3 as eluent subsequently.

White solid, 2 g (78 %). ^{1}H NMR (400 MHz, CDCl$_3$, δ in ppm): 0.88 (t, 3H, -CH$_2$-CH_3-), 1.26 (broad band, 30H, -CH$_2$-(CH_2)$_{15}$-CH$_3$), 1.60 (q, 2H, -Ar-CH$_2$-(CH_2)-(CH$_2$)$_{15}$-CH$_3$), 2.59 (t, 2H, -Ar-CH_2-(CH$_2$)$_{16}$-CH$_3$), 5.19 (d, 2H, -Ar-H), 5.72 (d, 2H, -Ar-H), 6.19 (dd, 1H, CH$_2$-CH-Ar-), 7.14 (d, 2H, -Ar-H), 7.33 (d, 2H, -Ar-H).
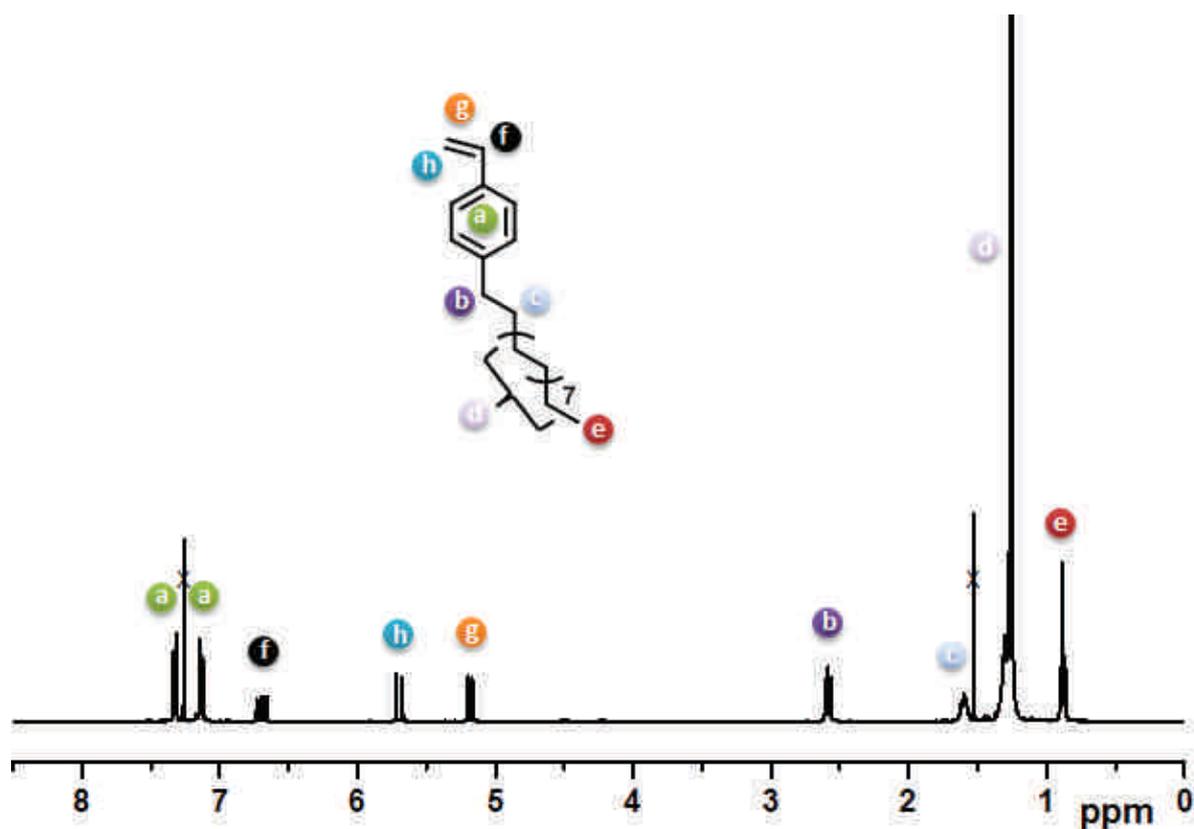
V.2. General procedure for nitroxide-mediated homopolymerization of 1
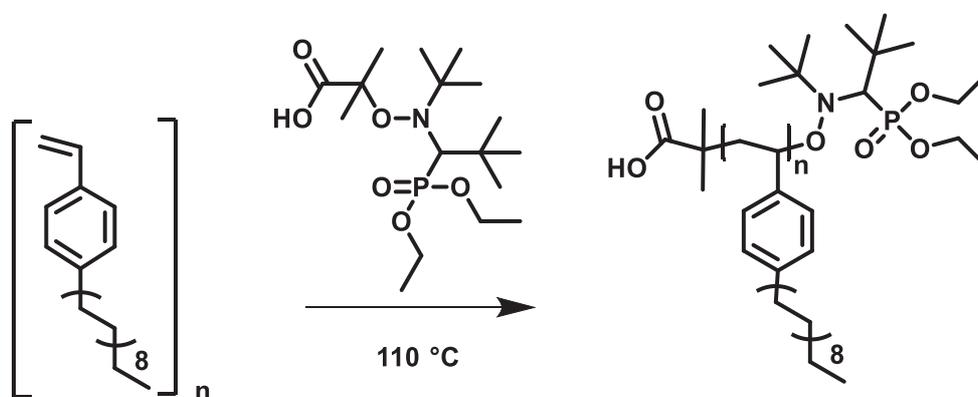
The described example corresponds to Entry **H2** in **Table 12**. Octadecylstyrene (**1**) (1 g, 2.80 mmol, 50 eq.) and BlocBuilder® MA (0.022 g, 0.056 mmol, 1 eq.) were added into a 10 mL flask equipped with a stirring bar. The flask was sealed with a rubber septum and subsequently degassed for 10 min with argon to remove oxygen. The reactor was placed into an oil bath preheated to 110 °C. Aliquots were taken in order to follow the kinetics of the reaction. After 6 h, the obtained polymer was purified by dissolution in THF (or chloroform) and repeated precipitations in cold methanol. The precipitate was collected by filtration,

washed and dried under vacuum at room temperature. The purified polymer was characterized by ^{1}H NMR, DSC and SEC. (* T_m and T_c values displayed were measured during the first temperature cycle of the DSC analysis).

H1: White powder, 150 mg (20 %). ^{1}H NMR (400 MHz, CDCl$_3$, δ in ppm): 0.88 (t, -CH$_2$-CH_3), 0.58-2.07 (bm, -CH- and -CH_2-, units of styrenic backbone + units of BlocBuilder® MA), 1.27 (bs, -Ar-CH$_2$-CH$_2$-(CH_2)$_{15}$-CH$_3$), 1.56 (bs, -Ar-CH$_2$-CH_2-(CH$_2$)$_{15}$-CH$_3$), 2.51 (bs, -Ar-CH_2-(CH$_2$)$_{16}$-CH$_3$), 6.14-7.06 (bm, -Ar-H of **1**). DSC: T_m = 47.50 °C, T_c = 32.18 °C. SEC (THF): M_n = 7300 g·mol^{-1}, M_w /M_n = 1.09.

H2: White powder, 236 mg (30 %). ^{1}H NMR (400 MHz, CDCl$_3$, δ in ppm): 0.88 (t, -CH$_2$-CH_3), 0.55-2.18 (bm, -CH- and -CH_2-, units of styrenic backbone + units of BlocBuilder® MA), 1.26 (bs, -Ar-CH$_2$-CH$_2$-(CH_2)$_{15}$-CH$_3$), 1.51 (bs, -Ar-CH$_2$-CH_2-(CH$_2$)$_{15}$-CH$_3$), 2.47 (bs, -Ar-CH_2-(CH$_2$)$_{16}$-CH$_3$), 6.09-6.97 (bm, -Ar-H of **1**). DSC: T_m = 48.84 °C, T_c = 34.12 °C. SEC (THF): M_n = 13400 g·mol^{-1}, M_w /M_n = 1.12.

H3: White powder, 500 mg (52 %). ^{1}H NMR (400 MHz, CDCl$_3$, δ in ppm): 0.88 (t, -CH$_2$-CH_3), 0.59-2.08 (bm, -CH- and -CH_2-, units of styrenic backbone + units of BlocBuilder® MA), 1.27 (bs, -Ar-CH$_2$-CH$_2$-(CH_2)$_{15}$-CH$_3$), 1.53 (bs, -Ar-CH$_2$-CH_2-(CH$_2$)$_{15}$-CH$_3$), 2.48 (bs, -Ar-CH_2-(CH$_2$)$_{16}$-CH$_3$), 6.08-6.95 (bm, -Ar-H of **1**). DSC: T_m = 48.80 °C, T_c = 34.00 °C. SEC (THF): M_n = 17800 g·mol^{-1}, M_w /M_n = 1.16.

V.3. General procedure for nitroxide-mediated copolymerization of 1 with *N*-substituted maleimide
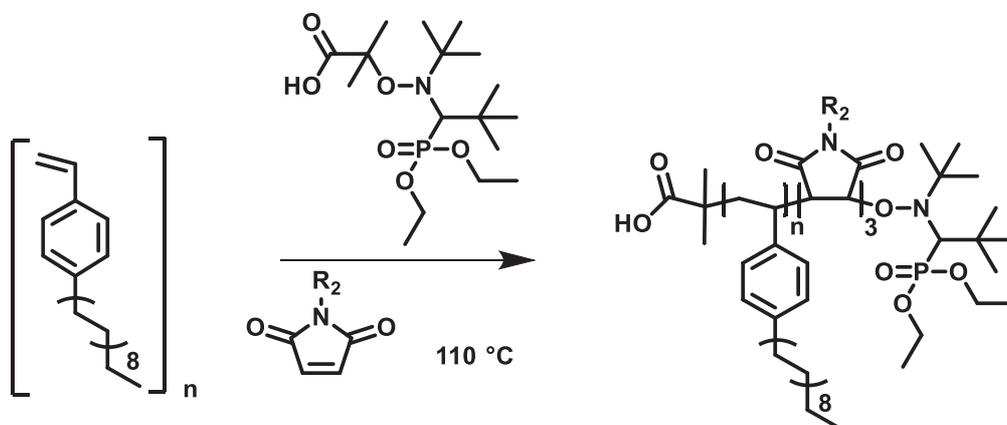
Copolymers of **1** with functional *N*-substituted maleimides were synthesized by nitroxide-mediated copolymerization in bulk. The example below corresponds to Entry 7 in **Table 13**. In a 10 mL flask, 1 g (2.8 mmol, 50 eq.) of **1**, 64 mg (0.168 mmol, 3 eq.) of **4** and 22 mg (5.6×10^{-5} mol, 1 eq.) of BlocBuilder® MA were added. The flask was capped by a rubber septum, purged with dry argon for 10 min and then immersed in a thermostated oil bath at 110 °C. During the copolymerization, aliquots were withdrawn for ^{1}H NMR analysis in order to monitor the incorporation of maleimide in the growing copolymer chains. After the monomer conversion was reached around 90 %, the reaction was stopped, and the flask was cooled to room temperature. The polymer was solubilized in a small volume of THF (or chloroform) and precipitated in an excess of cold methanol. The filtered precipitate was dried under vacuum at room temperature overnight and was characterized by DSC*, ^{1}H NMR, and SEC. (* T_m and T_c values displayed were measured during the first temperature cycle of the DSC analysis).
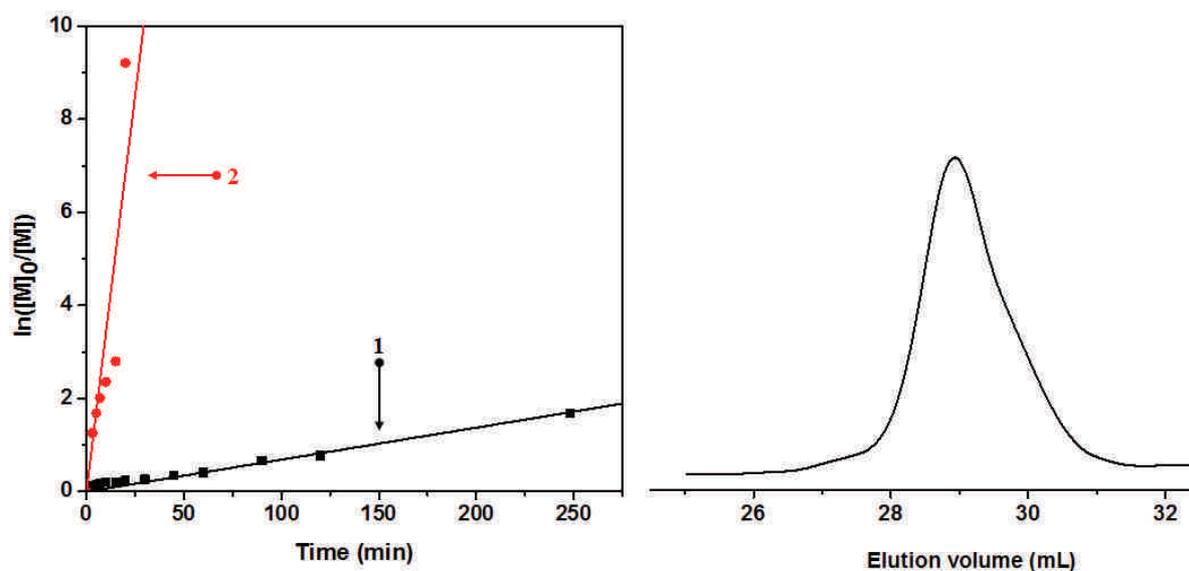
C1: White powder, 237 mg (30 %, precipitated five times). ^{1}H NMR (400 MHz, CDCl$_3$, δ in ppm): 0.88 (t, -CH$_2$- C*H*$_3$), 0.31-2.19 (bm, -C*H*- and -C*H*$_2$- units of styrenic backbone + -C*H*- units of maleimide backbone + units of BlocBuilder® MA), 1.27 (bs, -Ar-CH$_2$-CH$_2$-(C*H*$_2$)$_{15}$-CH$_3$), 1.53 (bs, -Ar-CH$_2$-C*H*$_2$-(CH$_2$)$_{15}$-CH$_3$), 2.49 (bs, -Ar-C*H*$_2$-(CH$_2$)$_{16}$-CH$_3$), 2.89-3.42 (bs, -N-C*H*$_2$-CH$_2$-CH$_3$), 6.03-7.20 (bm, -Ar-*H* of **1**). DSC: T_m = 45.90 °C, T_c = 33.87 °C. SEC (THF): M_n = 12600 g·mol^{-1}, M_w /M_n = 1.27.
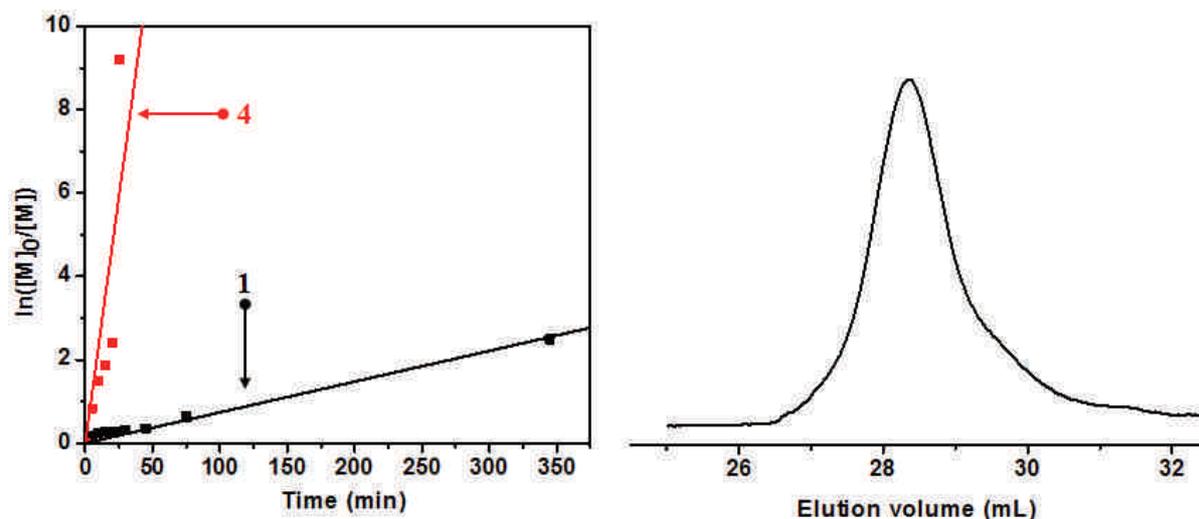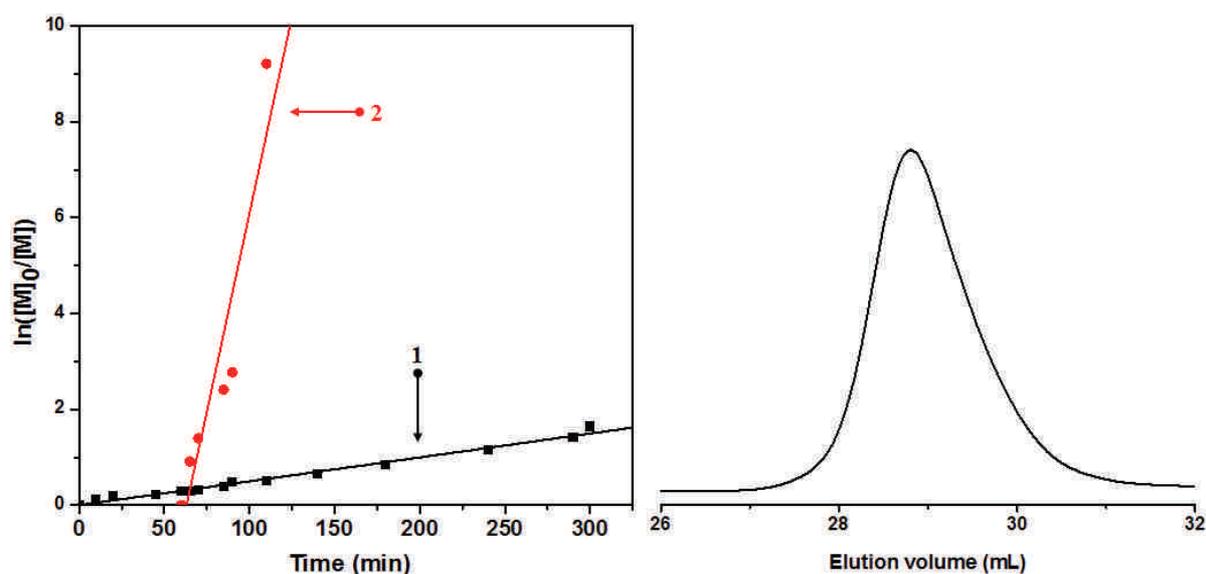
C7: white powder, 400 mg (44 %). ^{1}H NMR (400 MHz, CDCl$_3$, δ in ppm): 0.89 (t, -CH$_2$-CH$_3$), 0.56-2.03 (bm, -CH- and -CH$_2$- units of styrenic backbone + -CH- units of maleimide backbone + units of BlocBuilder® MA), 1.26 (bs, -Ar-CH$_2$-CH$_2$-(CH$_2$)15-CH$_3$), 1.56 (bs, -Ar-CH$_2$-CH$_2$-(CH$_2$)$_{15}$-CH$_3$), 2.47 (bs, -Ar-CH$_2$-(CH$_2$)$_{16}$-CH$_3$), 6.09-7.20 (bm, -Ar-H of **1**), 8.03-8.32 (bm, Ar-H, of **4**). DSC: T_m = 45.36 °C, T_c = 29.85 °C. SEC (THF): M_n= 14000 g·mol^{-1}, M_w /M_n = 1.34.

V.4. General procedure for nitroxide-mediated copolymerization of 1 with a time-controlled addition of *N*-substituted maleimide
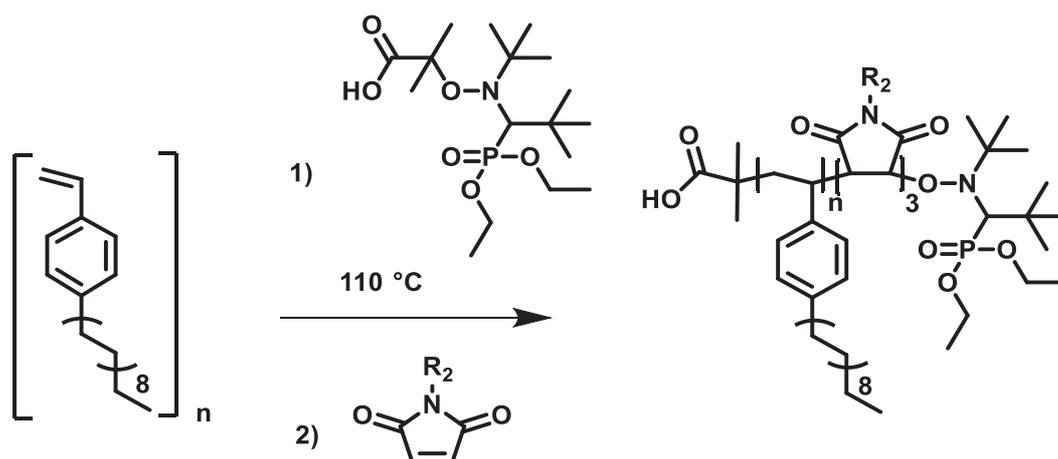
This present example corresponds to Entry **C11** in **Table 13**. 1 g of **1** (2.80 mmol, 50 eq.) and 22 mg of BlocBuilder® MA (0.056 mmol, 1 eq.) were added to a small flask equipped with a stirring bar. The flask was then sealed with a septum and purged with dry argon for 10 min. 0.8 mL of a degassed anisole was added using a degassed syringe. The reaction was

conducted in an oil bath at 110 °C. After 426 min of homopolymerization (i.e. about 70% conversion of **1**), a degassed solution of **4** (64 mg, 0.168 mmol, 3 eq.) in 0.2 mL of anisole was added into the reaction through a degassed syringe. Aliquots were taken periodically with a degassed syringe for NMR analysis in order to monitor the incorporation of **4** in the growing copolymer chains. After 460 min, the reaction was stopped. The polymer was dissolved in THF or chloroform and precipitated in cold methanol. The precipitate was collected by filtration and dried under vacuum at room temperature. The polymer was characterized by ^{1}H NMR, DSC and SEC.

C2: White powder, 200 mg (30 %). ^{1}H NMR (400 MHz, CDCl$_3$, δ in ppm): 0.89 (t, -CH$_2$-C*H*$_3$), 0.40-2.13 (bm, -C*H*- and -C*H*$_2$- units of styrenic backbone + -C*H*- units of maleimide backbone + units of BlocBuilder® MA), 1.27 (bs, -Ar-CH$_2$-CH$_2$-(C*H*$_2$)$_{15}$-CH$_3$), 1.54 (bs, -Ar-CH$_2$-C*H*$_2$-(CH$_2$)$_{15}$-CH$_3$), 2.48 (bs, -Ar-C*H*$_2$-(CH$_2$)$_{16}$-CH$_3$), 2.92-3.34 (bs, -N-C*H*$_2$-CH$_2$-CH$_3$), 6.10-7.18 (bm, -Ar-*H* of **1**). DSC: T_m = 44.91 °C, T_c = 33.88 °C. SEC (THF): M_n = 12900 g·mol^{-1}, M_w / M_n = 1.15.
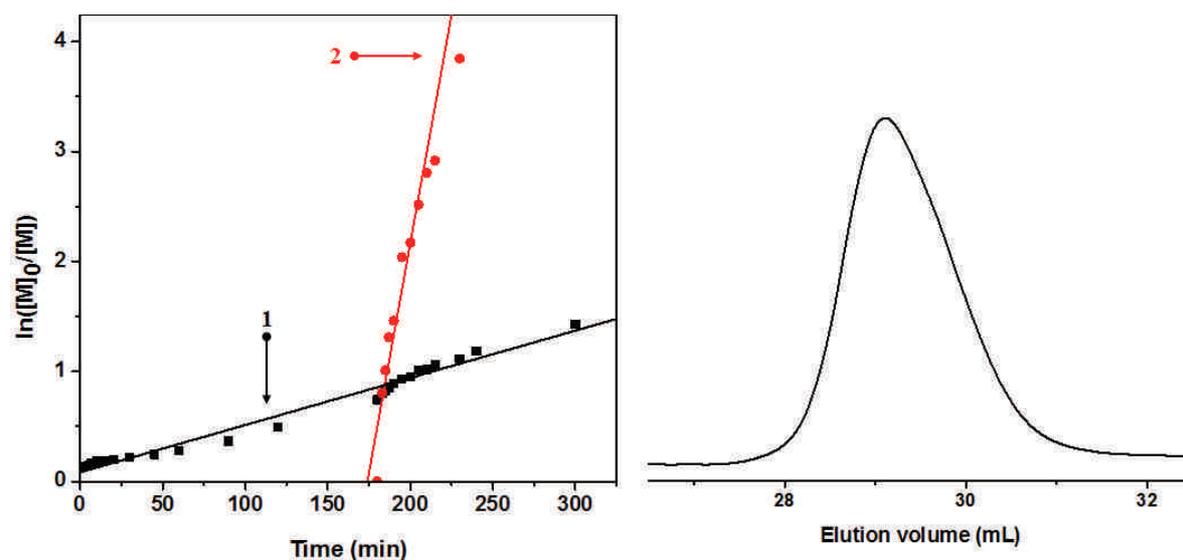
C3: White powder, 200 mg (26 %, precipitated three times). ^{1}H NMR (400 MHz, CDCl$_3$, δ in ppm): 0.88 (t, -CH$_2$- C*H*$_3$), 0.31-2.15 (bm, -C*H*- and -C*H*$_2$- units of styrenic backbone + -C*H*- units of maleimide backbone + units of BlocBuilder® MA), 1.27 (bs, -Ar-CH$_2$-CH$_2$-(C*H*$_2$)$_{15}$-CH$_3$), 1.54 (bs, -Ar-CH$_2$-C*H*$_2$-(CH$_2$)$_{15}$-CH$_3$), 2.50 (bs, -Ar-C*H*$_2$-(CH$_2$)$_{16}$-CH$_3$), 2.93-3.39 (broad, -N-C*H*$_2$-CH$_2$-CH$_3$), 6.07-7.19 (broad, -Ar-*H*). DSC: T_m = 46.53 °C, T_c = 34.61 °C. SEC (THF): M_n = 12400 g·mol^{-1}, M_w /M_n = 1.13.
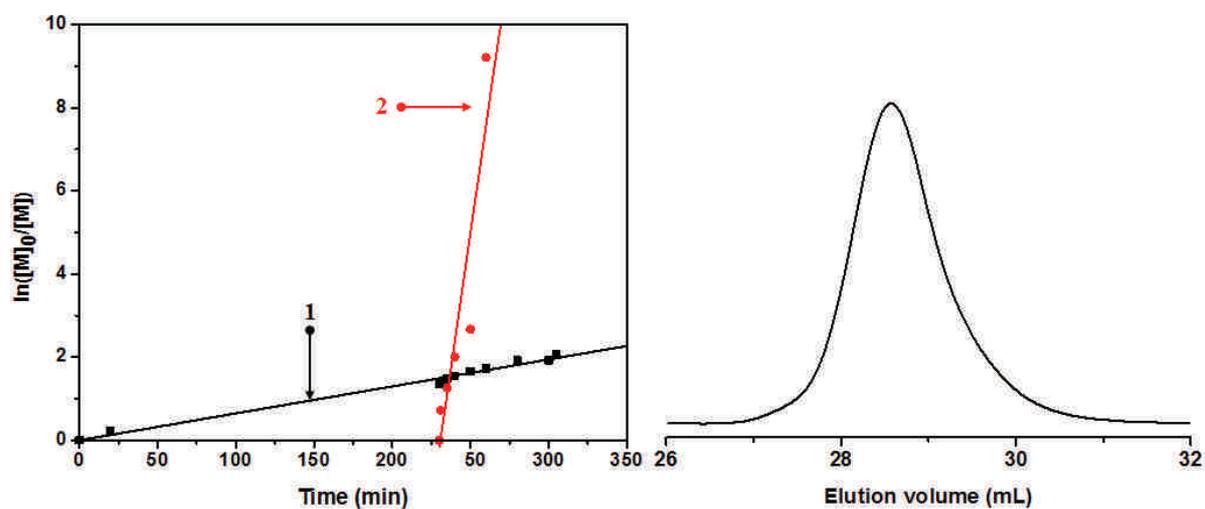
C4: White powder, 400 mg (51 %). ^{1}H NMR (400 MHz, CDCl$_3$, δ in ppm): 0.89 (t, -CH$_2$-C*H*$_3$), 0.40-2.13 (bm, -C*H*- and -C*H*$_2$- units of styrenic backbone + -C*H*- units of maleimide backbone + units of BlocBuilder® MA), 1.27 (bs, -Ar-CH$_2$-CH$_2$-(C*H*$_2$)$_{15}$-CH$_3$), 1.55 (bs, -Ar-CH$_2$-C*H*$_2$-(CH$_2$)$_{15}$-CH$_3$), 2.48 (bs, -Ar-C*H*$_2$-(CH$_2$)$_{16}$-CH$_3$), 2.94-3.36 (bs, -N-C*H*$_2$-CH$_2$-CH$_3$), 6.05-7.29 (bm, -Ar-*H* of **1**). DSC: T_m = 45.31 °C, T_c = 33.84 °C. SEC (THF): M_n = 15400 g·mol^{-1}, M_w /M_n = 1.16.
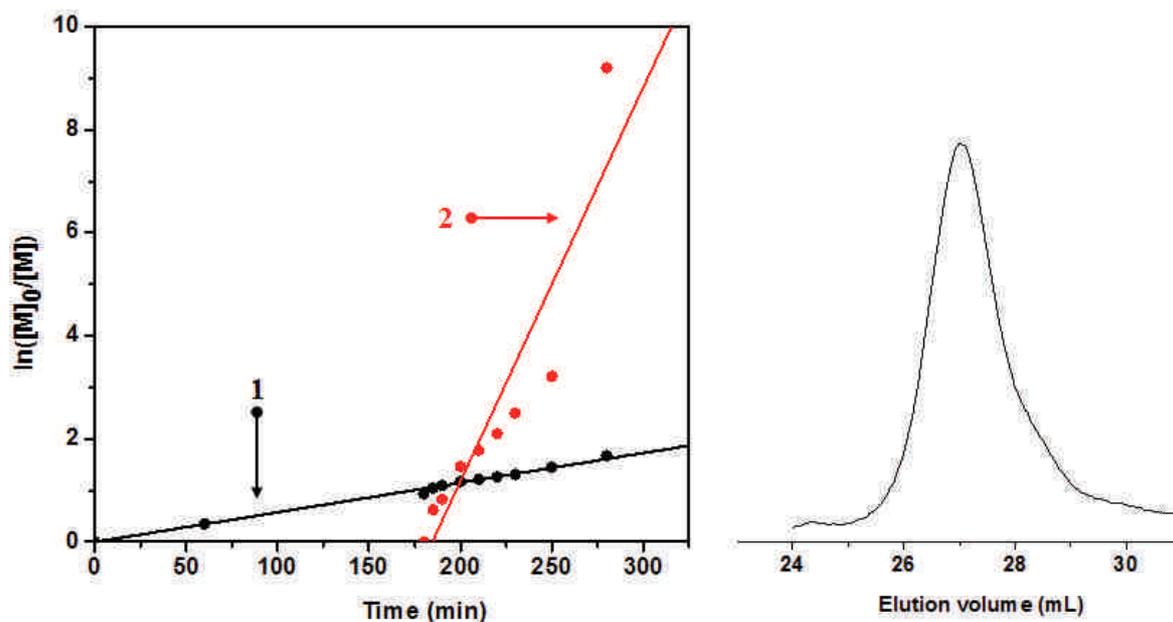
C5: White powder, 387 mg (60 %). ^{1}H NMR (400 MHz, CDCl$_3$, δ in ppm): 0.89 (t, -CH$_2$-CH_3), 0.32-2.02 (bm, -CH- and -CH_2-, units of styrenic backbone + -CH- units of maleimide backbone + units of BlocBuilder® MA), 1.27 (bs, -Ar-CH$_2$-CH$_2$-(CH_2)$_{15}$-CH$_3$), 1.56 (bs, -Ar-CH$_2$-CH_2-(CH$_2$)$_{15}$-CH$_3$), 2.47 (bs, -Ar-CH_2-(CH$_2$)$_{16}$-CH$_3$), 2.91-3.41 (bs, -N-CH_2-CH$_2$-CH$_3$), 6.12-7.25 (bm, -Ar-H of **1**). DSC: T_m = 45.28 °C, T_c = 32.47 °C. SEC (THF): M_n = 29500 g·mol^{-1}, M_w /M_n = 1.40.
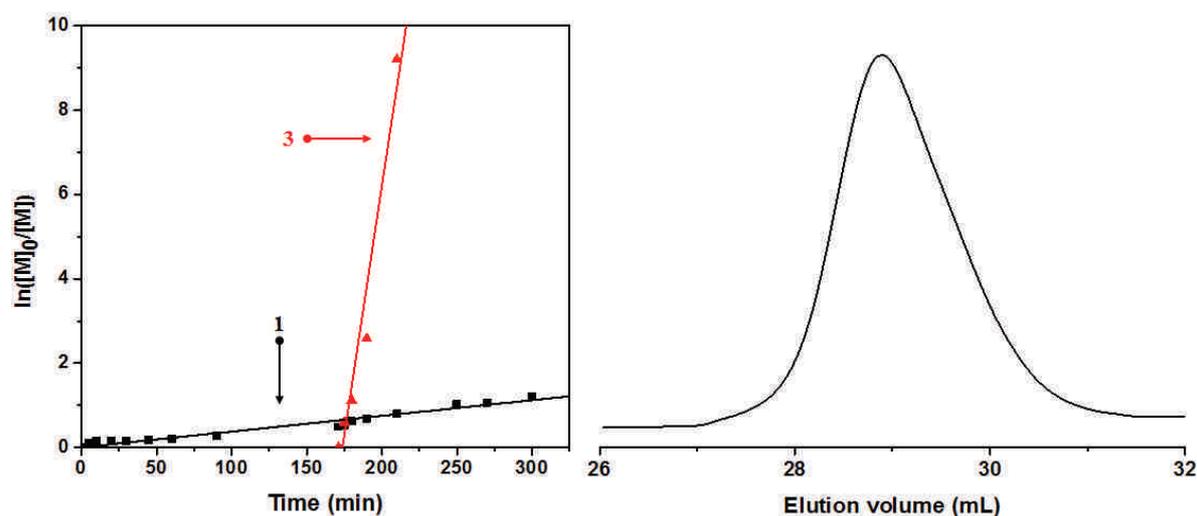
C6: White powder, 130 mg (19 %). ^{1}H NMR (400 MHz, CDCl$_3$, δ in ppm): 0.88 (t, -CH$_2$-CH_3), 0.59-2.08 (bm, -CH- and -CH_2- units of styrenic backbone + -CH- units of maleimide backbone + units of BlocBuilder® MA), 1.27 (bs, -Ar-CH$_2$-CH$_2$-(CH_2)$_{15}$-CH$_3$), 1.53 (bs, -Ar-CH$_2$-CH_2-(CH$_2$)$_{15}$-CH$_3$), 2.48 (bs, -Ar-CH_2-(CH$_2$)$_{16}$-CH$_3$), 4.36 (bs, -N-CH_2- of **3**),

6.08-7.01 (bm, -Ar-H of **1**), 7.03-7.26 (bm, -Ar-H of **3**). DSC: T_m = 44.92 °C, T_c = 33.05 °C. SEC (THF): M_n = 13000 g·mol^{-1}, M_w/M_n = 1.17.
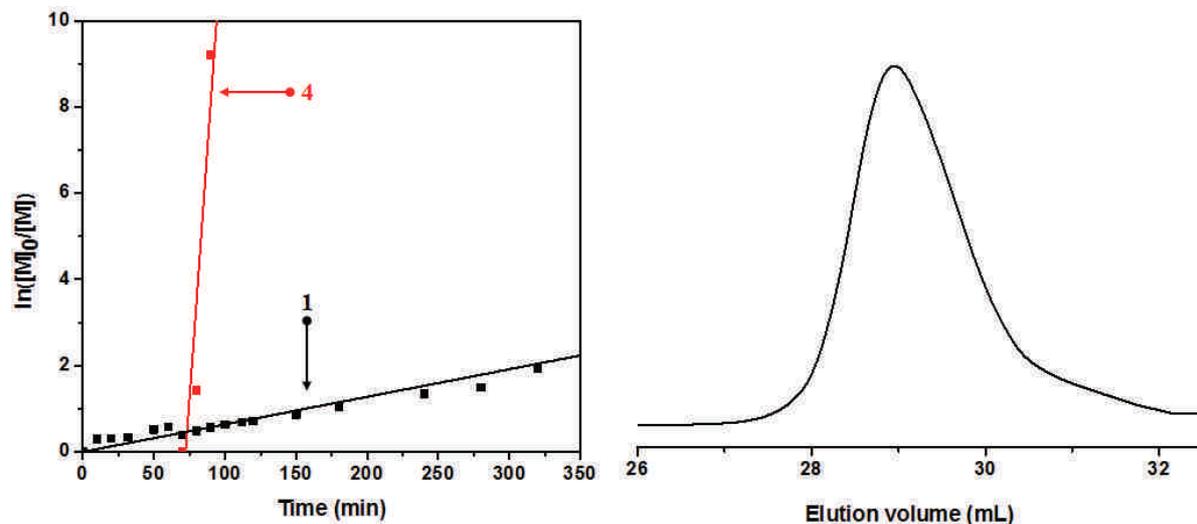
C8: white powder, 320 mg (47 %). ^{1}H NMR (400 MHz, CDCl$_3$, δ in ppm): 0.88 (t, -CH$_2$-CH_3), 0.58-2.04 (bm, -CH- and -CH_2- units of styrenic backbone + -CH- units of maleimide backbone + units of BlocBuilder® MA), 1.26 (bs, -Ar-CH$_2$-CH$_2$-(CH_2)$_{15}$-CH$_3$), 1.55 (bs, -Ar-CH$_2$-CH_2-(CH$_2$)$_{15}$-CH$_3$), 2.49 (bs, Ar-CH_2-(CH$_2$)$_{16}$-CH$_3$), 6.08-7.30 (bm, -Ar-H of **1**), 8.03-8.34 (bm, -Ar-H of **4**). ^{19}F NMR (400 MHz, CDCl3 δ in ppm): -152.38, -157.61, -162.16. DSC: T_m = 44.67 °C, T_c = 30.55 °C. SEC (THF): M_n = 10100 g·mol^{-1}, M_w/M_n = 1.29.
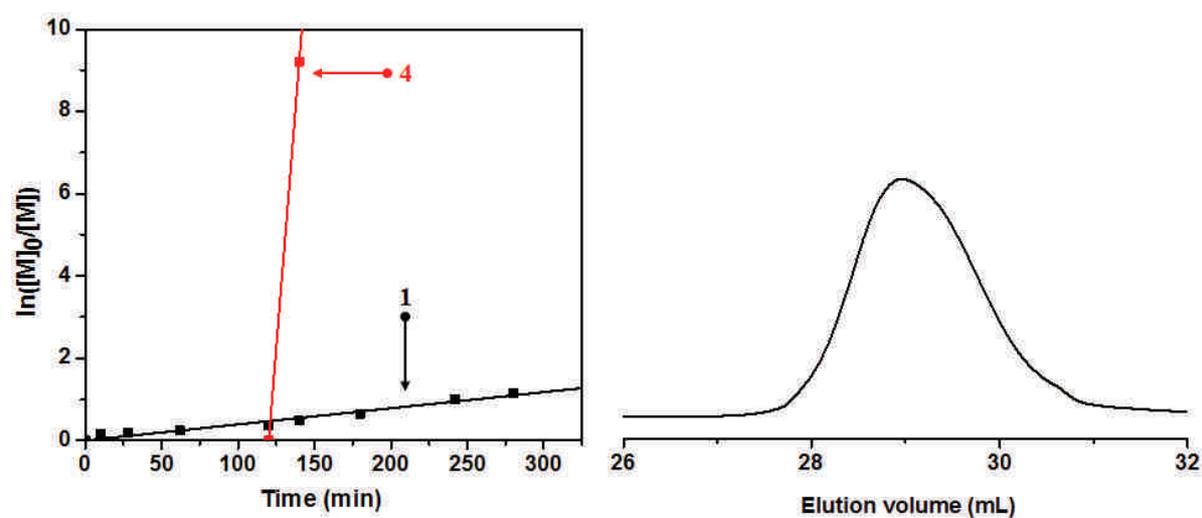
C9: white powder, 1.2 g (88 %). ^{1}H NMR (400 MHz, CDCl$_3$, δ in ppm): 0.88 (t, -CH$_2$- CH_3), 0.56-2.03 (bm, -CH- and -CH_2- units of styrenic backbone + -CH- units of maleimide backbone + units of BlocBuilder® MA), 1.26 (bs, -Ar-CH$_2$-CH$_2$-(CH_2)$_{15}$-CH$_3$), 1.58 (bs,

-Ar-CH$_2$-CH_2-(CH$_2$)$_{15}$-CH$_3$), 2.49 (bs, -Ar-CH_2-(CH$_2$)$_{16}$-CH$_3$), 6.11-7.23 (bm, -Ar-H of **1**), 8.02-8.28 (bm, Ar-H of **4**). DSC: T_m = 44.62 °C, T_c = 30.73 °C. SEC (THF): M_n = 11200 g·mol^{-1}, M_w /M_n = 1.17.
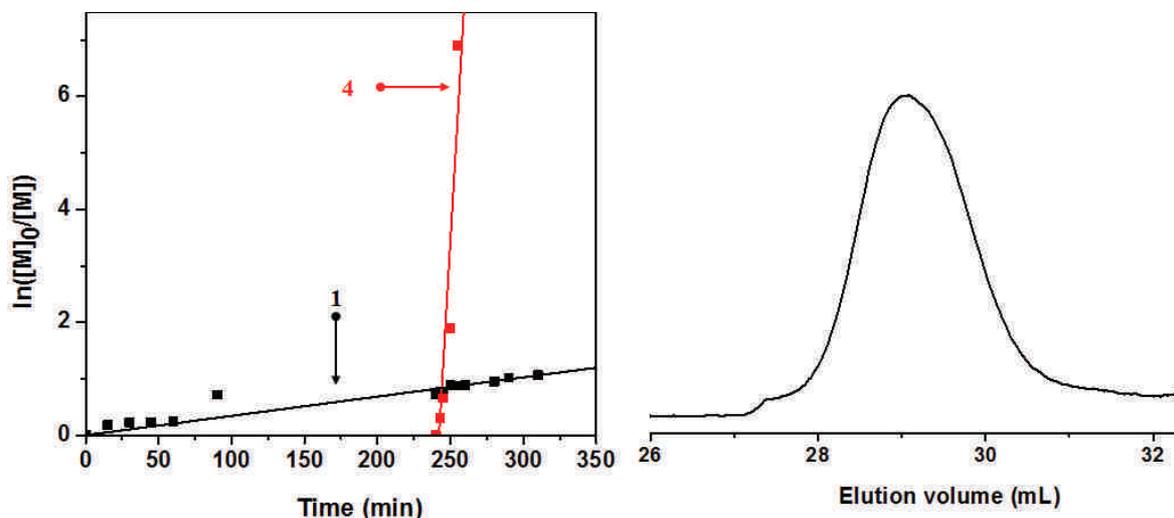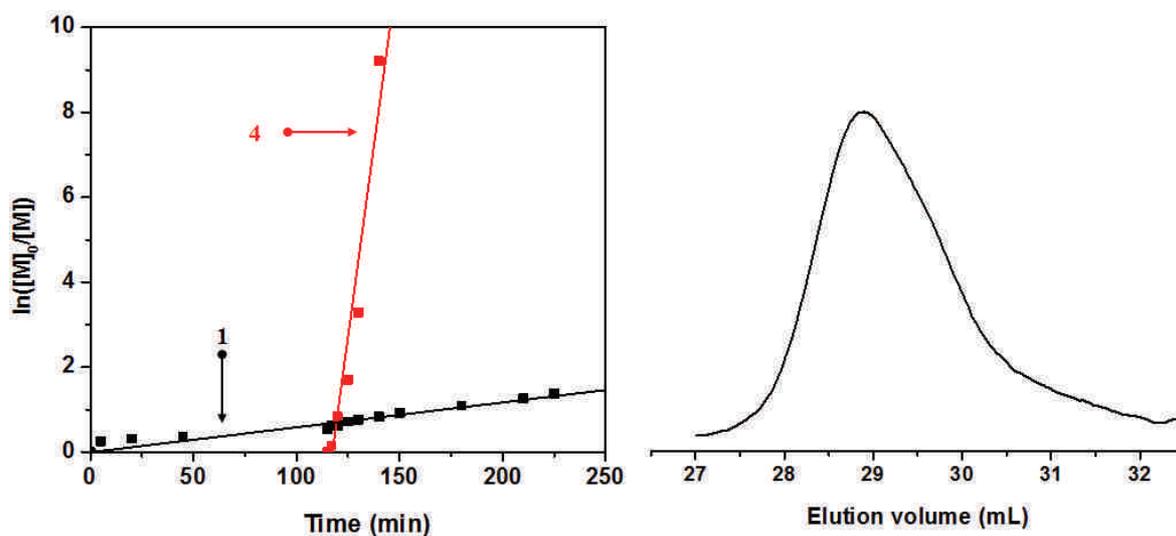

C10: white powder, 620 mg (63 %). ^{1}H NMR (400 MHz, CDCl$_3$, δ in ppm): 0.90 (t, -CH$_2$-CH_3), 0.55-2.10 (bm, -CH- and -CH_2- units of styrenic backbone + -CH- units of maleimide backbone + units of BlocBuilder® MA), 1.27 (bs, -Ar-CH$_2$-CH$_2$-(CH_2)$_{15}$-CH$_3$), 1.59 (bs, -Ar-CH$_2$-CH_2-(CH$_2$)$_{15}$-CH$_3$), 2.50 (bs, -Ar-CH_2-(CH$_2$)$_{16}$-CH$_3$), 6.10-7.29 (bm, -Ar-H), 8.02-8.33 (bm, -Ar-H of **4**). DSC: T_m = 44.67 °C, T_c = 30.66 °C. SEC (THF): M_n = 10400 g·mol^{-1}, M_w /M_n = 1.22.
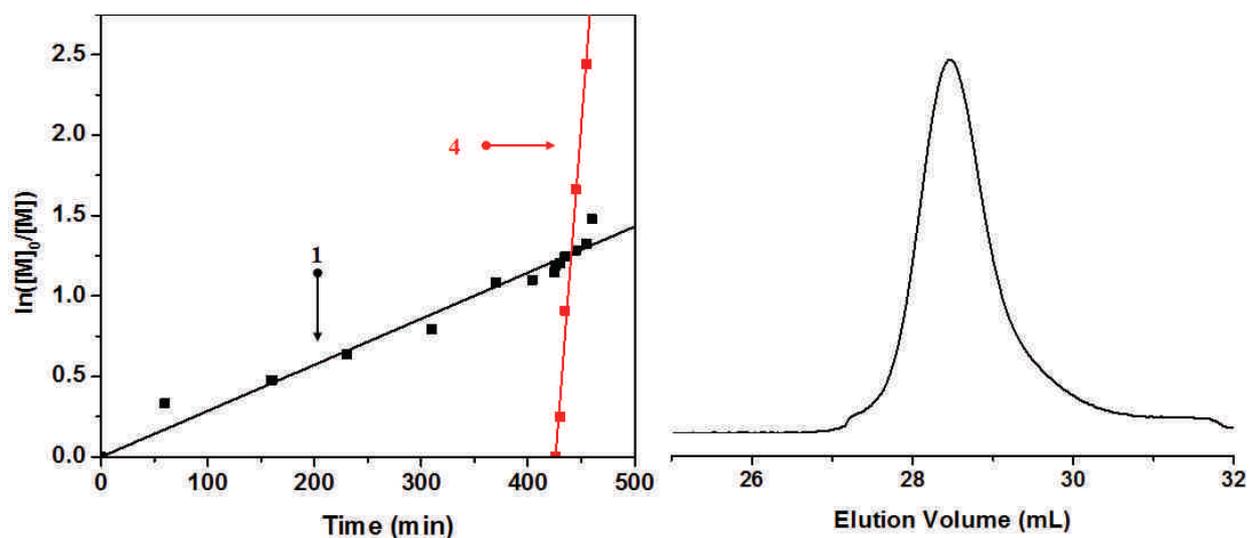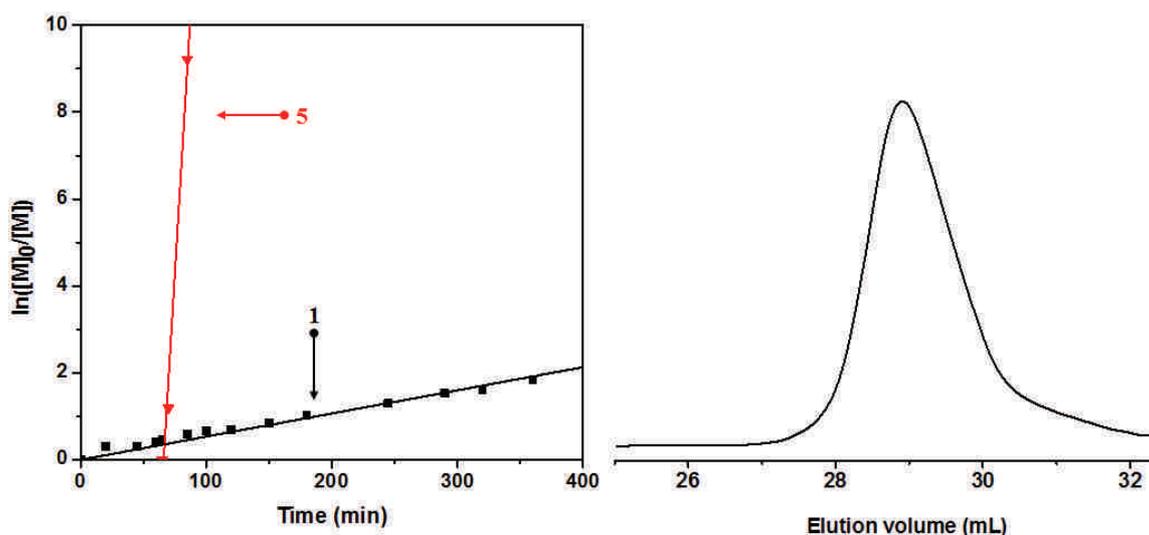

C11: white powder, 500 mg (65 %). ^{1}H NMR (400 MHz, CDCl$_3$, δ in ppm): 0.88 (t, -CH$_2$-CH_3), 0.56-2.03 (bm, -CH- and -CH_2- units of styrenic backbone + -CH- units of maleimide backbone + units of BlocBuilder® MA), 1.27 (bs, -Ar-CH$_2$-CH$_2$-(CH_2)$_{15}$-CH$_3$), 1.57 (bs,

-Ar-CH$_2$-CH_2-(CH$_2$)$_{15}$-CH$_3$), 2.49 (bs, -Ar-CH_2-(CH$_2$)$_{16}$-CH$_3$), 6.10-7.16 (bm, -Ar-H), 8.03-8.31 (bm, -Ar-H of **4**). DSC: T_m = 43.95 °C, T_c = 31.08 °C. SEC (THF): M_n = 13800 g·mol^{-1}, M_w /M_n = 1.22.
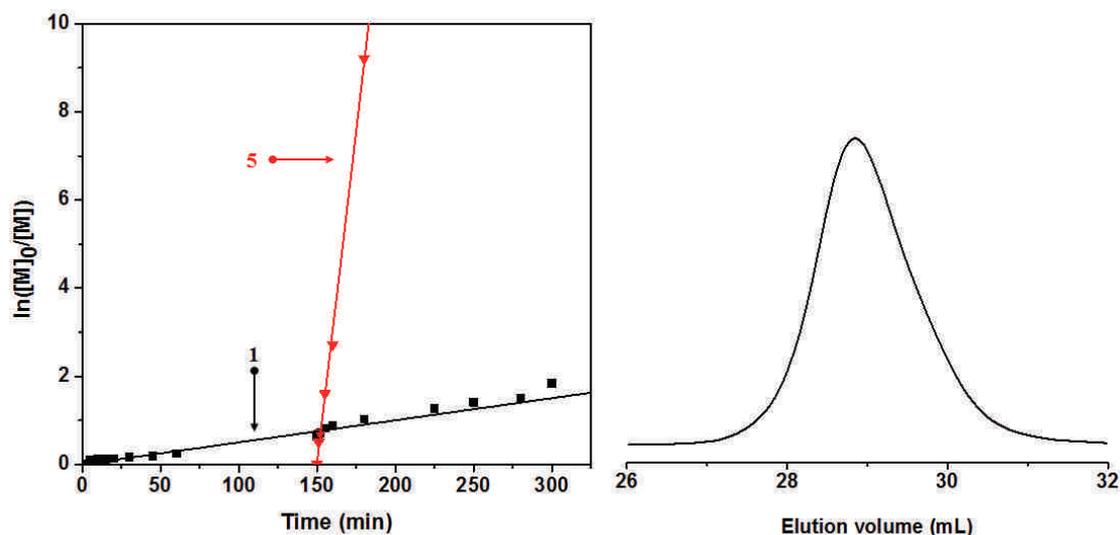

C12: white powder, 530 mg (71 %). ^{1}H NMR (400 MHz, CDCl$_3$, δ in ppm): 0.88 (t, -CH$_2$-CH_3), 0.56-2.03 (bm, -CH- and -CH_2- units of styrenic backbone + -CH- units of maleimide backbone + units of BlocBuilder® MA), 1.26 (bs, -Ar-CH$_2$-CH$_2$-(CH_2)$_{15}$-CH$_3$), 1.58 (bs, -Ar-CH$_2$-CH_2-(CH$_2$)$_{15}$-CH$_3$), 2.49 (bs, -Ar-CH_2-(CH$_2$)$_{16}$-CH$_3$), 6.07-7.26 (bm, -Ar-H), 8.02-8.29 (bm, -Ar-H of **4**). DSC: T_m = 44.37 °C, T_c = 27.87 °C. SEC (THF): M_n = 10100 g·mol^{-1}, M_w /M_n = 1.31.
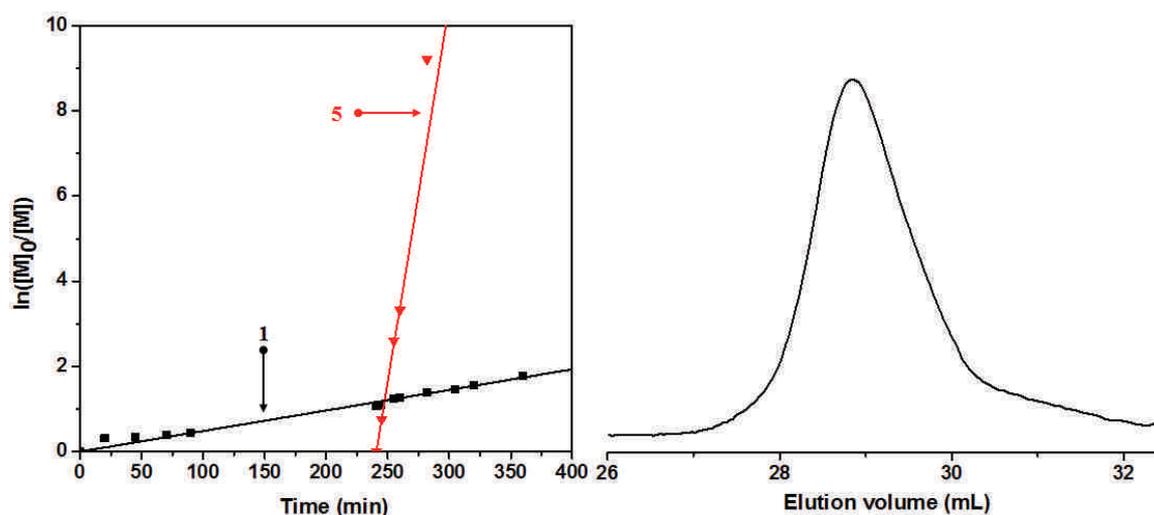

C13: White powder, 213 mg (32 %, precipitated twice). ^{1}H NMR (400 MHz, CDCl$_3$, δ in ppm): 0.88 (t, -CH$_2$- CH_3), 0.58-2.07 (bm, -CH- and -CH_2- units of styrenic backbone + -

C*H*- units of maleimide backbone + units of BlocBuilder® MA), 1.27 (bs, -Ar-CH$_2$-CH$_2$-(CH$_2$)$_{15}$-CH$_3$), 1.53 (bs, -Ar-CH$_2$-C*H*$_2$-(CH$_2$)$_{15}$-CH$_3$), 2.48 (bs, -Ar-C*H*$_2$-(CH$_2$)$_{16}$-CH$_3$), 6.11-7.21 (bm, -Ar-*H* of **1**), 7.47 and 7.89 (bs, Ar-*H* of **5**). DSC: T_m = 44.87 °C, T_c = 31.22 °C. SEC (THF): M_n = 10400 g·mol^{-1}, M_w /M_n = 1.32.
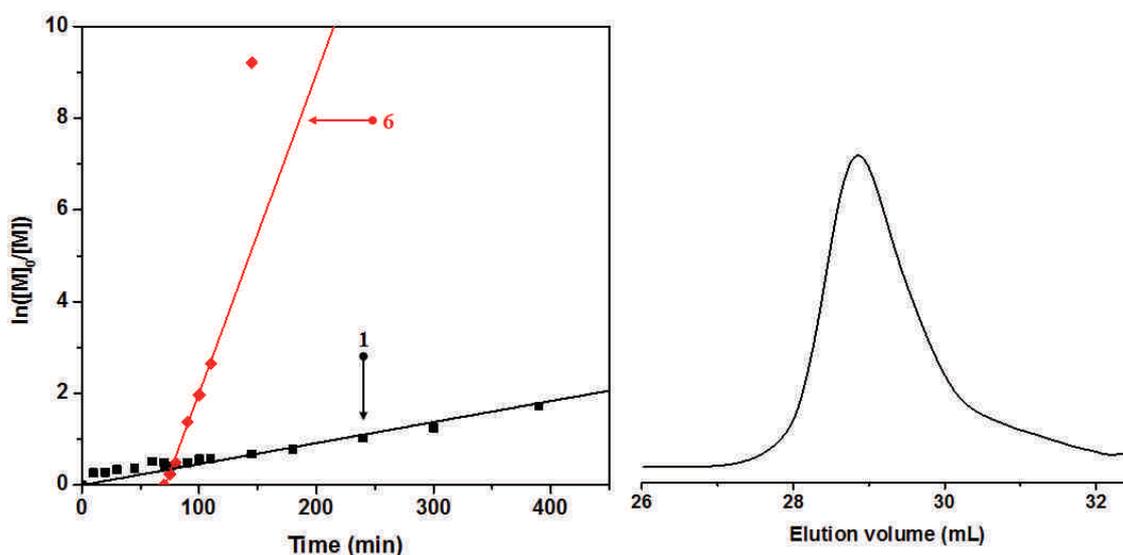

C14: White powder, 320 mg (38 %). ^{1}H NMR (400 MHz, CDCl$_3$, δ in ppm): 0.88 (t, -CH$_2$-C*H*$_3$), 0.50-2.06 (bm, -C*H*- and -C*H*$_2$- units of styrenic backbone + -C*H*- units of maleimide backbone + units of BlocBuilder® MA), 1.26 (bs, -Ar-CH$_2$-CH$_2$-(C*H*$_2$)$_{15}$-CH$_3$), 1.54 (bs, -Ar-CH$_2$-C*H*$_2$-(CH$_2$)$_{15}$-CH$_3$), 2.49 (bs, -Ar-C*H*$_2$-(CH$_2$)$_{16}$-CH$_3$), 6.08-7.17 (bm, -Ar-*H* of **1**), 7.47 and 7.90 (bs, Ar-*H* of **5**). DSC: T_m = 44.43 °C, T_c = 30.46 °C. SEC (THF): M_n = 14200 g·mol^{-1}, M_w /M_n = 1.14.


C15: White powder, 239 mg (36 %, precipitated twice). ^{1}H NMR (400 MHz, CDCl$_3$, δ in ppm): 0.88 (t, -CH$_2$- C*H*$_3$), 0.57-2.03 (bm, -C*H*- and -C*H*$_2$- units of styrenic backbone + -

C*H*- units of maleimide backbone + units of BlocBuilder® MA), 1.26 (bs, -Ar-CH$_2$-CH$_2$-(C*H$_2$*)$_{15}$-CH$_3$), 1.53 (bs, -Ar-CH$_2$-C*H$_2$*-(CH$_2$)$_{15}$-CH$_3$), 2.48 (bs, -Ar-C*H$_2$*-(CH$_2$)$_{16}$-CH$_3$), 6.06-7.18 (bm, -Ar-*H*), 7.47 and 7.90 (bs, Ar-*H* of **5**). DSC: T_m = 44.38 °C, T_c = 30.77 °C. SEC (THF): M_n = 10800 g·mol^{-1}, M_w /M_n = 1.31.


C16: yellow powder, 135 mg (21 %). ^{1}H NMR (400 MHz, CDCl$_3$, δ in ppm): 0.89 (t, -CH$_2$-C*H$_3$*), 0.60-2.07 (bm, -C*H*- and -C*H$_2$*- units of styrenic backbone + -C*H*- units of maleimide backbone + units of BlocBuilder® MA), 1.26 (bs, -Ar-CH$_2$-CH$_2$-(C*H$_2$*)$_{15}$-CH$_3$), 1.58 (bs, -Ar-CH$_2$-C*H$_2$*-(CH$_2$)$_{15}$-CH$_3$), 2.50 (bs, -Ar-C*H$_2$*-(CH$_2$)$_{16}$-CH$_3$), 6.09-7.24 (bm, -Ar-*H* of **1**), 7.88-8.30 (bm, Ar-*H* of **6**). DSC: T_m = 45.82 °C, T_c = 31.89 °C. SEC (THF): M_n = 10100 g·mol^{-1}, M_w /M_n = 1.33.
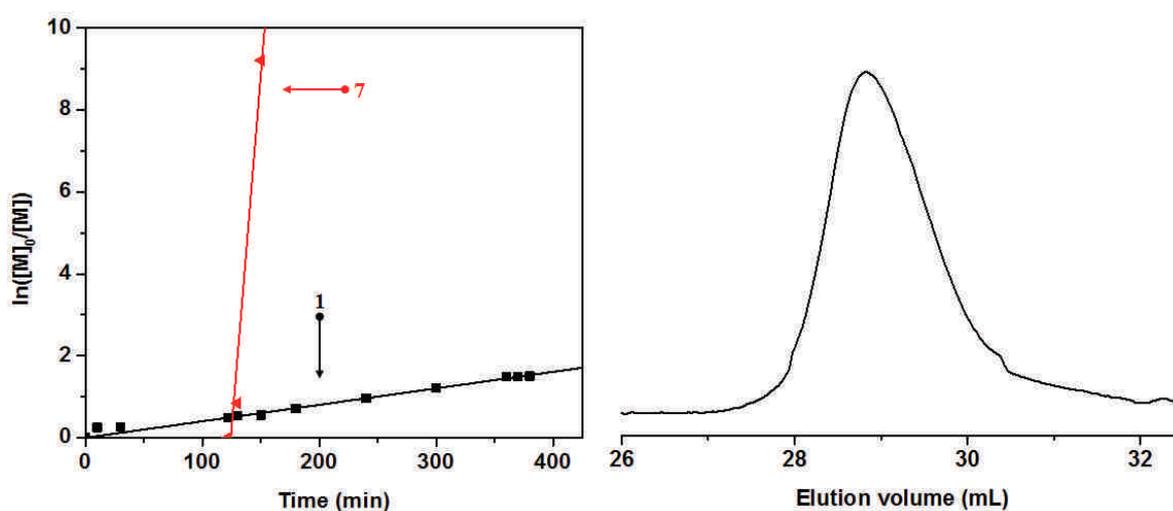
C17: white powder, 1.5 g (95 %). ^{1}H NMR (400 MHz, CDCl$_3$, δ in ppm): 0.88 (t, -CH_2-CH_3), 0.56-2.01 (bm, -CH- and -CH_2- units of styrenic backbone + -CH- units of maleimide backbone + units of BlocBuilder® MA), 1.27 (bs, -Ar-CH$_2$-CH$_2$-(CH_2)$_{15}$-CH$_3$), 1.58 (bs, -Ar-CH$_2$-CH_2-(CH$_2$)$_{15}$-CH$_3$), 1.85 (t, -O-(CH_3)$_3$ of **7**), 2.49 (bs, Ar-CH_2-(CH$_2$)$_{16}$-CH$_3$), 3.77 (t, -N-CH_2-CH$_2$-NH- of **7**), 6.10-7.07 (bm, -Ar-H). DSC: T_m = 44.66 °C, T_c = 32.77 °C. SEC (THF): M_n = 10600 g·mol^{-1}, M_w /M_n = 1.17.

V.5. Deprotection of *N*-Boc-amine in a copolymer
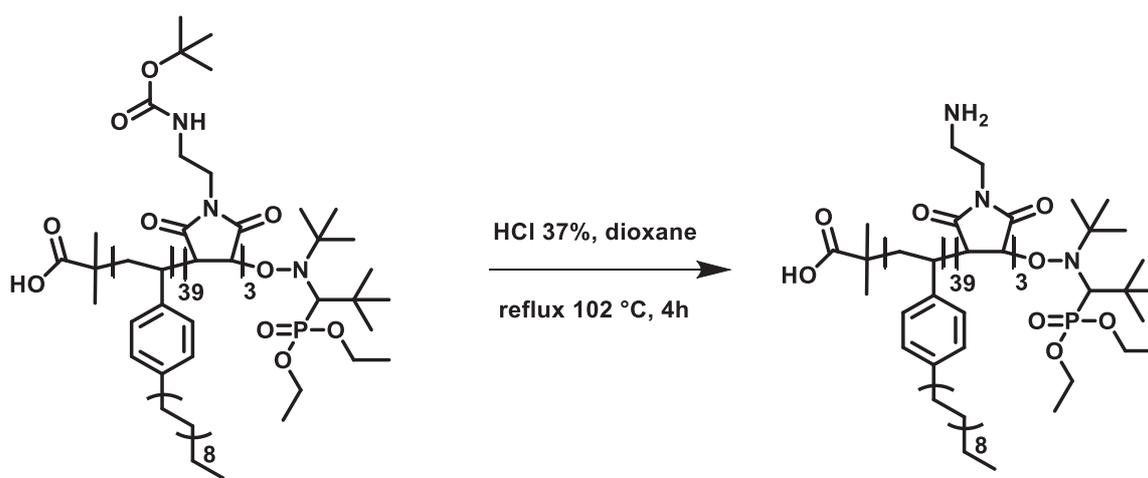
0.8 g of polymer (Entry **C17** in **Table 13**, M_n = 10600 g·mol^{-1}) was dissolved in 5 mL of dioxane in a 10 mL round bottom flask. Then, 0.11 mL of HCl (37%) was added and the flask was capped with a condenser. The reaction was refluxed for 4 h and subsequently cooled down to RT. The polymer was dissolved in THF and precipitated in an excess of cold methanol. The polymer was characterized by ^{1}H NMR, DSC and SEC. DSC curve was shown in **Figure 68**.

White powder, 250 mg (32 %). ^{1}H NMR (400 MHz, CDCl$_3$, δ in ppm): 0.88 (t, -CH$_2$- CH_3), 0.69-2.12 (bm, -CH- and -CH_2- units of styrenic backbone + -CH- units of maleimide backbone + units of BlocBuilder® MA), 1.25 (bs, -Ar-CH$_2$-CH$_2$-(CH_2)$_{15}$-CH$_3$), 1.43 (bs, -Ar-CH$_2$-CH_2-(CH$_2$)$_{15}$-CH$_3$), 2.51 (bs, -Ar-CH_2-(CH$_2$)$_{16}$-CH$_3$), 6.10-7.07 (bm, Ar-H of **1**). DSC: T_m = 46.34 °C, T_c = 32.60 °C. SEC (THF): M_n = 10600 g·mol^{-1}, M_w /M_n = 1.17.
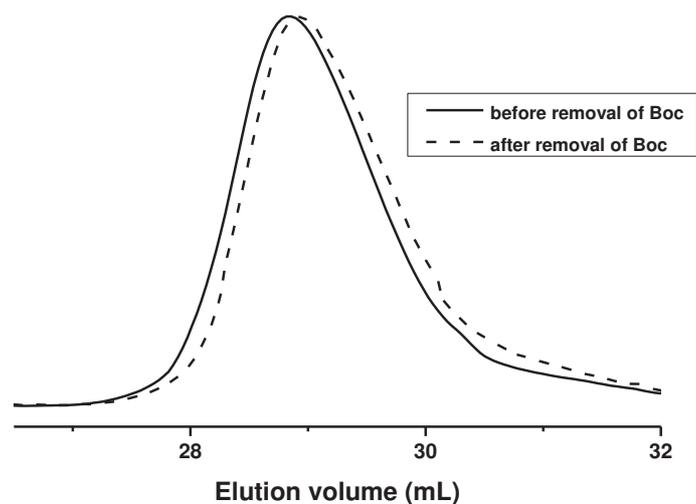
V.6. Post-modification of activated ester units in a copolymer
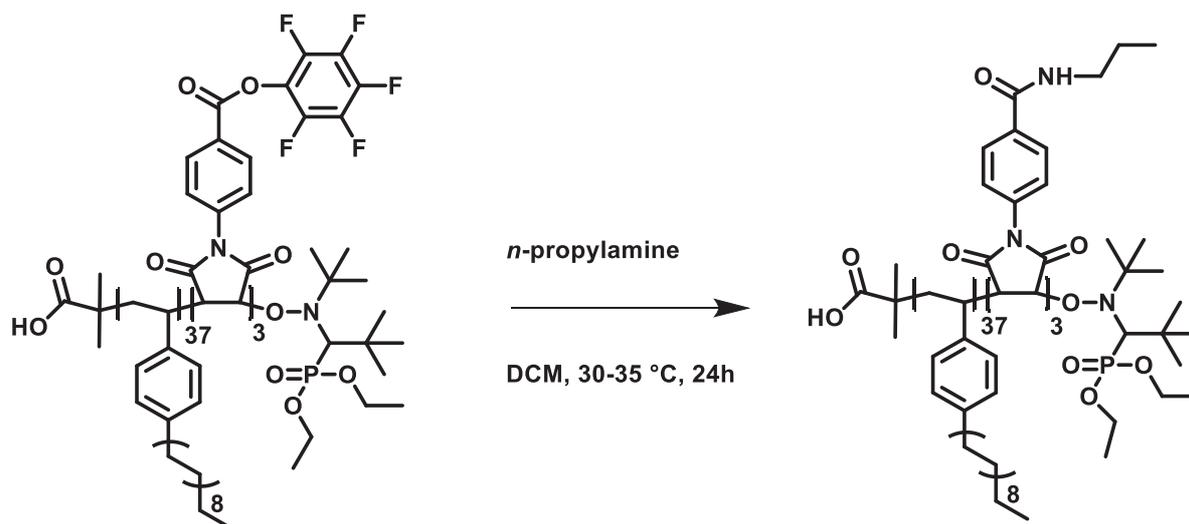
This present example corresponds to Entry **C9** in **Table 13.** 50 mg of copolymer containing activated-ester reactive units was dissolved in 2 mL of dichloromethane. The solution was degassed and 3 µL of propylamine in 1 mL dichloromethane were added. The mixture was heated at 35 °C for 1 day under argon atmosphere. After reaction, dichloromethane was removed by rotary evaporation. The polymer was dissolved in THF and precipitated in cold methanol. The modified copolymer was characterized by ^{1}H NMR, ^{19}F NMR, DSC and FT-IR.

White powder, 27.7 mg (60 %). ^{1}H NMR (400 MHz, CDCl$_3$, δ in ppm): 0.89 (t, -CH$_2$- CH_3), 0.54-2.14 (bm, -CH- and -CH_2- units of styrenic backbone + -CH- units of maleimide

backbone + units of BlocBuilder® MA), 1.27 (bs, -Ar-CH$_2$-CH$_2$-(CH$_2$)$_{15}$-CH$_3$), 1.55 (bs, -Ar-CH$_2$-CH$_2$-(CH$_2$)$_{15}$-CH$_3$), 2.49 (bs, -Ar-CH$_2$-(CH$_2$)$_{16}$-CH$_3$), 3.38 (bs, -NH-CH$_2$)-CH$_2$-CH$_3$, propylamide), 6.05-7.26 (bm, -Ar-H of **1**), 7.56-7.91 (bm, -Ar-H of phenyl propylamide). DSC: T_m = 42.43 °C, T_c = 31.66 °C.
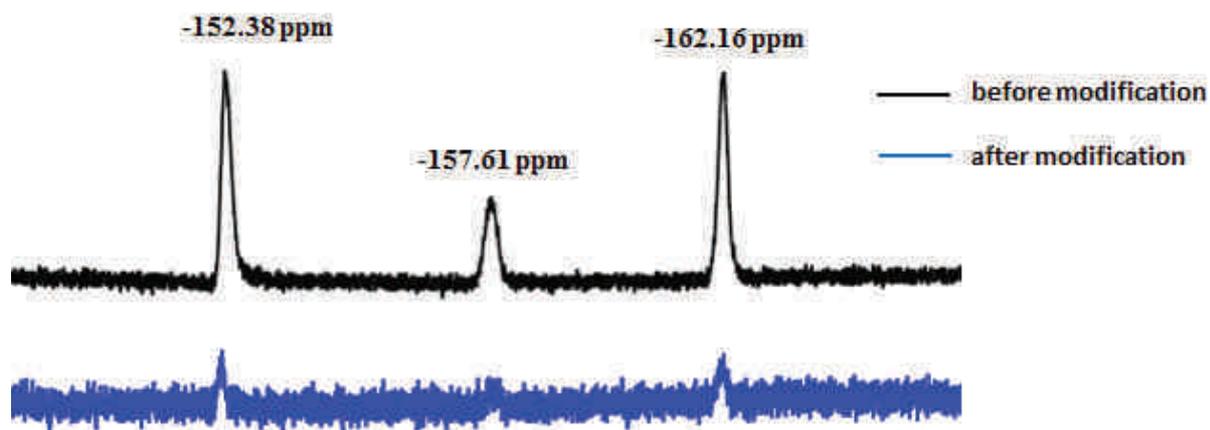
References

[1].   Bodtke, A.; Otto, H. H., *Int. J. Pharm. Sci.,* **2005**, *60*, 803-813.

[2].   Kakuchi, R.; Zamfir, M.; Lutz, J.-F.; Theato, P., *Macromol. Rapid Commun.,* **2012**, *33*, 54-60.

[3].   Fujita, S.; Reddy, P. Y.; Toru, T., Reacting an amino group-containing n-cyclic compound with maleic anhydride in acetic acid to obtain an n-cyclic maleamic acid, adding hexamethyldisilazane, cyclizing to form n-cyclic maleimide, use as a fluorescent dyes. US Patents, US5965746A.: **1999**.

[4].   Reddy, P. Y.; Kondo, S.; Toru, T.; Ueno, Y., *J. Org. Chem.,* **1997**, *62*, 2652-2654.

[5].   Schmidt, B. V. K. J.; Fechler, N.; Falkenhagen, J.; Lutz, J.-F., *Nat. Chem.,* **2011**, *3*, 234-238.

[6].   Kuo, S.-W.; Tung, P.-H.; Chang, F.-C., *Macromolecules,* **2006**, *39*, 9388-9395.

[7].   Lutz, J.-F.; Stiller, S.; Hoth, A.; Kaufner, L.; Pison, U.; Cartier, R., *Biomacromolecules,* **2006**, *7*, 3132-3138.

[8].   Lee, Y. J.; Jang, Y.; Cho, K.; Pyo, S.; Hwang, D. H.; Hong, S. C., *J. Nanosci. Nanotechnol.,* **2009**, *9*, 7161-7166.

[9].   Charreyre, M.-T.; Razafindrakoto, V.; Veron, L.; Delair, T.; Pichot, C., *Macromol. Chem. Phys.,* **1994**, *195*, 2141-2152.

[10].   Ohno, K.; Izu, Y.; Tsujii, Y.; Fukuda, T.; Kitano, H., *Eur. Polym. J.,* **2004**, *40*, 81-88.

[11].   Bertini, V.; Alfei, S.; Pocci, M.; Lucchesini, F.; Picci, N.; Iemma, F., *Tetrahedron,* **2004**, *60*, 11407-11414.

[12].   Zhao, B.; Li, D.; Hua, F.; Green, D. R., *Macromolecules,* **2005**, *38*, 9509-9517.

[13].   Ten Brummelhuis, N.; Weck, M., *ACS Macro Lett.,* **2012**, *1*, 1216-1218.

[14].   Lang, A. S.; Thelakkat, M., *Polym. Chem.,* **2011**, *2*, 2213-2221.

[15].   Fleischmann, S.; Komber, H.; Voit, B., *Macromolecules,* **2008**, *41*, 5255-5264.

[16].   Yeom, C.-E.; Kim, M. J.; Choi, W.; Kim, B. M., *Synlett,* **2008**, *2008*, 565-568.

[17].   Lutz, J.-F.; Börner, H. G.; Weichenhan, K., *Macromol. Rapid Commun.,* **2005**, *26*, 514-518.

[18].   Quirk, R. P.; Ok, M.-A., *Macromolecules,* **2004**, *37*, 3976-3982.

[19].   López-Carrasquero, F.; Giammanco, G.; Díaz, A.; Dávila, J.; Torres, C.; Laredo, E., *Polym. Bull.,* **2009**, *63*, 69-78.

Sansanee SRICHAN

Synthesis of sequence-controlled polymers by copolymerization of *para*-substituted styrenic derivatives and *N*-substituted maleimides

UNIVERSITÉ DE STRASBOURG

EDSC
École Doctorale des
Sciences Chimiques

Résumé en français

Dans ce travail, les copolymérisations radicalaires contrôlées de monomères donneurs (dérivés du styrène) et accepteurs (maleimides *N*-substitués) ont été effectuées afin de préparer des polymères à séquences contrôlées. Ces macromolécules ont été préparées par polymérisation radicalaire contrôlée par la voie des nitroxides en utilisant le SG1 comme agent de contrôle. Des polymères ayant des microstructures bien définies ont été obtenus par le contrôle du temps de l'addition d'une petite quantité de monomère accepteur au cours de la polymérisation d'un large excès de monomère de type donneur. Dans cette thèse, des nouveaux dérivés styréniques *para*-substitués ont été sélectionnés afin de préparer une variété de polymères fonctionnels à séquences contrôlées. Par exemple, des polyélectrolytes à base de poly(4-hydroxystyrène)s et poly(vinyl benzyle amine)s ont été obtenus par polymérisation de dérivés protégés du styrène (4-*tert*-butoxystyrène, 4-acetoxystyrène et *N*-(*p*-vinyl benzyl)phthalimide) avec une quantité non-stœchiométrique de maleimides *N*-substitués. Par ailleurs, des polymères PEGylés biocompatibles et solubles dans l'eau ont également été étudiés. Des polymères à séquences contrôlées portant des fonctions alcynes protégées sur chaque unité de styrène ont été dans un premier temps synthétisés. La suppression de ces groupes protecteurs a permis le greffage du α-méthoxy-ω-azido-PEG sur les fonctions alcynes libres en employant la chimie click de type CuAAC. Finalement, des polymères semi-cristallins à séquences contrôlées ont été élaborés en utilisant le styrène d'octadécyle comme monomère donneur. Les propriétés thermiques de ces polymères ont été étudiées afin d'évaluer l'influence de la microstructure sur le comportement de leur cristallisation.

Mots clés: Polymérisation radicalaire contrôlée, polymères à séquences contrôlées, monomères donneur-accepteur, PEGylation, chimie click, polymères semi-cristallins.

Résumé en anglais

In this work, controlled radical copolymerizations of donor (styrenic derivatives) and acceptor monomers (*N*-substituted maleimides, MIs) have been investigated in order to synthesize sequence-controlled polymers. These macromolecules were prepared by nitroxide mediated polymerization using the nitroxide SG1 as a control agent. Polymers with defined microstructures were obtained by time-controlled addition of small amounts of acceptor monomers during the polymerization of a large excess of donor monomer. In this thesis, new styrenic derivatives have been studied in order to design sequence-controlled polymers with functional backbones. For example, sequence-controlled polyelectrolytes based on poly(4-hydroxystyrene)s and poly(vinyl benzyl amine)s were obtained through the polymerization of protected styrenic derivatives (i.e. 4-*tert*-butoxystyrene, 4-acetoxystyrene and *N*-(*p*-vinyl benzyl)phthalimide) with non-stoichiometric quantities of *N*-substituted maleimides. Furthermore, the preparation of PEGylated biocompatible water-soluble polymers was also investigated. Sequence-controlled polymers bearing protected alkyne functional groups on each styrene units were first synthesized followed by the removal of their protecting groups allowing the grafting of α-methoxy-ω-azido-PEG on free alkyne moieties via CuAAC mediated click reaction. Finally, sequence-controlled semi-crystalline polymers were synthesized using octadecylstyrene as a donor monomer. The thermal properties of these polymers were studied to evaluate the influence of polymer microstructure on crystallization behavior.